MACHINING CHARACTERISTICS OF HASTELLOY C-2000 IN END MILLING USING ARTIFICIAL INTELLIGENCE APPROACH

NURUL HIDAYAH BINTI RAZAK

Thesis submitted in fulfilment of the requirements
for the award of the degree of
Master of Engineering (Mechanical)

FACULTY OF MECHANICAL ENGINEERING
UNIVERSITI MALAYSIA PAHANG

14 SEPTEMBER 2012

SUPERVISOR'S DECLARATION

I hereby declare that I have checked this thesis and in my opinion, this thesis is adequate in terms of scope and quality for the award of the degree of Master of Engineering (Mechanical).

Signature : .....

Name of Supervisor : DR. MD. MUSTAFIZUR RAHMAN

Position : ASSOCIATE PROFESSOR

Date : 14 SEPTEMBER 2012

STUDENT'S DECLARATION

I hereby declare that the work in this thesis is my own except for quotations and summaries which have been duly acknowledged. The thesis has not been accepted for any degree and is not concurrently submitted for award of other degree.

Signature : .....

Name : NURUL HIDAYAH BINTI RAZAK

ID Number : MMM10002

Date : 14 SEPTEMBER 2012

Dedicated, in thankful appreciation for support,

Encouragement and understanding,

To my beloved mother, Bonda Wan Rasnah Wan Idris

ACKNOWLEDGEMENTS

I would like to acknowledge and extend my heartfelt gratitude to my supervisor, Associate Professor Dr. Md Mustafizur Rahman, Faculty of Mechanical Engineering for his continues support, helpful advice and valuable guidance throughout my thesis. He has encouraged and guides me through the writing up thesis process by giving the best effort. I would also like to thank his for her effort in helping me to complete this project.

My sincere thanks go to all my labmates and members of the staff of the Mechanical Engineering Department, Universiti Malaysia Pahang, UMP, who helped me in many ways and made my stay at UMP pleasant and unforgettable. Many special thanks go to my colleagues in my section and other section who had been helping me all this while in doing the project. I would like to express my sincere gratitude to Universiti Malaysia Pahang (UMP) for granting me under Post Graduate Research Scheme and MyBrain 15 from Ministry of Higher Education Malaysia, without their support, my ambition to study abroad can hardly be realized.

Most importantly, I would like to thank my family especially my mother, Wan Rasnah Wan Idris, who have guided me throughout my life. She has always sacrifices their time and continuous support me to achieve my dreams and goals. I would like to thank for all her supports and encouragement for me.

ABSTRACT

This research work deals with the machining characteristics of Hastelloy C-2000 in the end milling operations. The mathematical model was developed through the response surface method (RSM) which basically focuses on machining characteristics such as surface roughness, tool life and cutting force using coated and uncoated carbide cutting inserts in wet conditions. The accuracy of this aforementioned technique and model was verified by ANOVA. The minimum and maximum of machining performance was presented followed by the confirmation test to validate the design variables. It is found that the models are able to predict the longitudinal component of the surface roughness, cutting force, and tool life close to those readings recorded experimentally with a 95% confident level. Artificial Neural network (ANN) prediction model was developed with back propagation algorithm with the use of multilayer perceptron and activation function of hyperbolic tangent. Feed rate is the most influential factor, followed by axial depth and cutting speed for surface roughness, tool life and cutting force. The mean absolute relative error for surface roughness of RSM models (first, second order) and ANN is 4.386 %, 2.324 % and 0.1790% for coated carbide inserts and 9.878 %, 6.681 % and 0.136 % for uncoated carbide inserts respectively. In addition, for tool life model, 8.3130 %, 4.8760 %, 0.2% for coated carbide inserts, 9.7880%, 7.6270 %, and 0.1580% for uncoated carbide inserts. Furthermore, for cutting force model 4.386 %, 2.324 % and 0.4181 % for coated carbide and 9.878 %, 6.681 % and 0.5% for uncoated carbide. The PVD coated-carbide cutting tools perform better than the uncoated-carbide in terms of the surface roughness, cutting force, and tool life. Surfaces finish and wear surfaces were characterized using an optical video measurement system, scanning electron microscope (SEM) and electron dispersive X-ray (EDX). The tool failures found in this research was flank wear, notching, and chipping. Adhesion and plastic lowering at cutting edge were the main tool wear mechanisms seen in the present work, which is clearly demonstrated by the adhered workpiece material and the formation of a built-up edge (BUE) on the tool flank. There have been a few chips found in this research and broadly they can be divided into two types. Type 1: unstable and type 2: critical. Due to the research done on the earlier models, RSM established prediction and optimization models. However, ANN serves more efficiency and accuracy because its error is very less compared to RSM. ANN has characteristics of predicting machining and they work far better when compares to mathematical modelling.

ABSTRAK

Laporan ini membentangkan proses pemesinan ciri Hastelloy C-2000 dalam prosess hujung penggilingan. Model matematik dibangunkan melalui kaedah tindakbalas permukaan oleh persamaan pertama dan kedua berdasarkan kekasaran permukaan, jangka hayat, dan daya pemotongan menggunakan mata alat bersalut dan tidak bersalut karbid dalam keaadan basah. Ketepatan model dianalisa oleh ANOVA. Peminimuman dan pengaksimunan pemesinan dibentangkan diikuti ujian pengesahan untuk kesahihan rekabentuk pembolehubah. Model rangkaian saraf buatan di formulasi dengan penyebaran belakang dengan penggunaan persepsi pelbagai lapisan dan fungsi pengaktifan garis lengkung. Kadar pemotongan adalah pengaruh faktor utama, diikuti kedalaman pemotongan dan kelajuan pemotongan untuk kekasaran permukaan, jangka hayat dan daya pemotongan. Purata mutlak relatif kesilapan untuk kekasaran permukaan bagi model pertama, kedua dan rangkaian saraf buatan adalah 4.386 %, 2.324 % dan 0.1790% untuk mata alat bersalut karbid dan 9.878 %, 6.681 % dan 0.136% untuk mata alat tidak bersalut karbid. Seterusnya, jangka hayat, 8.3130 %, 4.8760 %, 0.2% untuk mata alat bersalut karbid, 9.7880%, 7.6270 %, dan 0.1595 % untuk mata alat tidak bersalut karbid. Tambahan lagi, untuk model daya pemotongan 4.386 %, 2.324 % dan 0.4181% untuk mata alat bersalut karbid dan 9.878 %, 6.681 % dan 0.5% untuk mata alat tidak bersalut karbid. Mata alat bersalut PVD karbid berprestasi lebih baik berbanding mata alat tidak bersalut karbid dalam konteks kekasaran permukaan, jangka hayat dan daya pemotongan. Permukaan akhir dan kehausan permukaan dikategorikan menggunakan sistem pengukuran video optik, mikroskop penelitian elektron dan penyebaran elektron sinar X. Kegagalan mata alat yang ditemui dalam penyelidikan ini ialah kehausan rusuk, takik dan serpihan. Kelekatan dan kerendahan plastik pada hujung mata alat adalah kehausan utama dimana jelas di demonstrasikan oleh kelekatan bahan kerja dan pembentukan pembinaan hujung pada rusuk mata alat. Beberapa jenis serpihan telah dijumpai dan dibahagikan kepada jenis pertama: serpihan tidak stabil dan serpihan kedua: serpihan kritikal. Berdasarkan penyelidikan yang dibuat pada model-model, penganggaran dan peminimuman serta pengaksimuman telah didirikan melalui kaedah tindak balas permukaan. Walaubagaimanapun, rangkaian saraf buatan lebih efisien dan tepat kerana kesilapannya sangat sedikit dan berfungsi jauh lebih baik dari kaedah tindak balas permukaan.

TABLE OF CONTENTS

LIST OF TABLES

LIST OF FIGURES

LIST OF SYMBOLS

I/O	Input/output
X_i	Inputs
f_i	Non-linearity function
R_i	Signal
O_i	Output
R_a	Average surface roughness
L	Sampling length
Y	Ordinate of the profile curve
F_m	Feed rate in mm/min
R	Resultant force
F_c	Cutting force
F_t	Thrust force
F_s	Shear force
F_n	Normal force
F	Friction force
N	Normal force
f_r	Feet rates in mm/ rev
f_t	Feed rates in mm/tooth
f_r	Feed rate in mm/rev
n	number of teeth of the cutter
v	Cutting speed
D	Diameter in mm
N	Number of revolution

π	Mathematical constant
rpm	Revolution per minute
y	Response
$x_1, x_2,,, x_n,$	Input variables
ε	Experimental error
$\beta_1, \beta_2, \beta_3$	Model parameters
X_j^2, X_jXi	Squares and interaction terms of the input variables,
$B_0, B_j, B_{jj}, B_{ij},$	Second order regression coefficients
R^2	Coefficient of determination
xj	Signal
j	Input of synapse, number of neuron in the hidden layer
k	Neuron
wkj	Synaptic weight
V_k	Summing junction
wk0 = bk	Bias
Y_k	Output
W_m	Weighting matrix
$d_{k,p}$	Desired output
p_{th}	Pattern
n	Learning step, node
η	Learning rate
α	Momentum value, significant level
δ_{pj}	Error term
I_i^n	Input value

w_{ij}^{n}	connection of weight
H_{nj}^{n}	Hidden node
O_{j}^{n}	Output node
b_{i}^{n}	Threshold
f	Hidden node
H_{nij}^{n}, O_{j}^{n}	Output node activation function
x_0	Dummy variables
γ	Gamma prime
R_i	Average surface roughness
NR	Nose radius
V_c	Cutting speed
n	Constant
c	Constant
K_r	Radial constant
C_r	Helical and rake angle
t_c	Average thickness
P_r	Tool/workpiece material properties

LIST OF ABBREVIATIONS

BUE	Built up edge
RSM	Response surface method
ANN	Artificial neural network
SPRT	Self-propelled rotary tool
BUL	Built up layer
CBN	Cubic boron nitride
PVD	Physical vapour deposition
ANOVA	Analysis of variance
GA	Genetic algorithm
AI	Artificial intelligence
FL	Fuzzy logic
SA	Simulate annealing
MLP	Multi layer perceptron
SOFM	Self organizing feature map
RBFN	Radial basis function network
DOE	Design of experiment
CTW4615	Coated carbide cutting insert
CTP1235	Uncoated carbide cutting insert
CNC	Computer numerical control
BBD	Box behnken design
SEM	Scanning electron microscope
EDX	Energy dispersive x-ray
CD	Total cutting distance
F_R	Feed rate

A_D	Axial depth
C_S	Cutting speed
SR	Surface roughness
TL	Tool life
CF	Cutting force
S	Standard error of the regression
DF	Degree of freedom
SS	Total sum of squares
SSR	Regression sum of squares
SSE	Residual sum of squares
MAE	Mean absolute error
NP	Number of training pattern
N	Nodes
F	Fitness
TE	Training error
VE	Validation error
TE	Testing error
C	Correlation
R-S	R- square
SR	Stop reason
AID	All iteration done
T	Training
O	Overall
ARE	Absolute relative error

DF	Degree of freedom
SD	Standard deviation
FO RSM	First order RSM
SO RSM	Second order RSM

THESIS STATUS VALIDATION FORM

UNIVERSITI MALAYSIA PAHANG

DECLARATION OF THESIS AND COPYRIGHT

Author's full name : Nurul Hidayah Binti Razak
Date of Birth : 14-05-1986
Title : MACHINING CHARACTERISTICS OF HASTELLOY C-2000 IN END MILLING USING ARTIFICIAL INTELLIGENCE APPROACH
Academic Session : 2011/2012-II

I declare that this thesis is classified as :

☐	**CONFIDENTIAL**	(Contains confidential information under the Official Secret Act 1972)*
☐	**RESTRICTED**	(Contains restricted information as specified by the organisation where research was done)*
☑	**OPEN ACCESS**	I agree that my thesis to be published as online open access (Full text)

I acknowledge that Universiti Malaysia Pahang reserve the right as follows :

1. The Thesis is the Property of Universiti Malaysia Pahang
2. The Library of University Malaysia Pahang has the right to make copies for the purpose of research only
3. The Library has the right to make copies of the thesis for academic exchange.

Certified By :

(Student's Signature) (Signature of Supervisor)

(No IC/Passpord Number)
860514-33-5474
Date : 14/09/2012

(Name of supervisor)
Assoc. Prof. Dr. Md. Mustafizur Rahman
Date :14 /09/2012

NOTES : *if the thesis is CONFIDENTIAL or RESTICTED, please attach with the letter from the organisation with period and reasons for confidential or restriction.

CHAPTER 1

INTRODUCTION

1.1 INTRODUCTION

Given the advantages of nickel-based alloys, these are highly recommended in the industry over titanium-based alloys, aluminium and composites. According to M'Saoubi et al. (2008) and Wu (2007), nickel-based alloys are heat resistant which allows them to maintain their chemical and mechanical properties at high temperatures, high resistance corrosion, and high melting temperatures, resistance to shock, erosion, creep and thermal fatigue. According to Arunachalam et al. (2004), nickel-based alloys such as IN-718 are used in more than half of the materials made for aerospace industry and aeroengines. A typical Aerogas turbine's nickel-alloy weight percentage is given in Figure 1.1. According to Miller (1996), it can be observed that by the end of 20th century, the use of titanium and nickel-based alloys were used in the aerospace engines. UDIMET 720LI is a super alloy used in the aerospace industry which with the addition of Co-Ti can be made more useful for this industry as its strength and surface quality increases (Cui et al., 2005). Marine equipment, petrochemical plants, nuclear reactors, food processing equipment and other such applications undergo constant improvement in order to improve their surface integrity and strength. At high temperatures, they have better strength, wear resistance and chemical degradation. However, due to its poor thermal characteristics, good surface results are not obtained at high temperatures because of the friction and deformation induced heat and changes in micro structure ((Ezugwu et al., 2003).

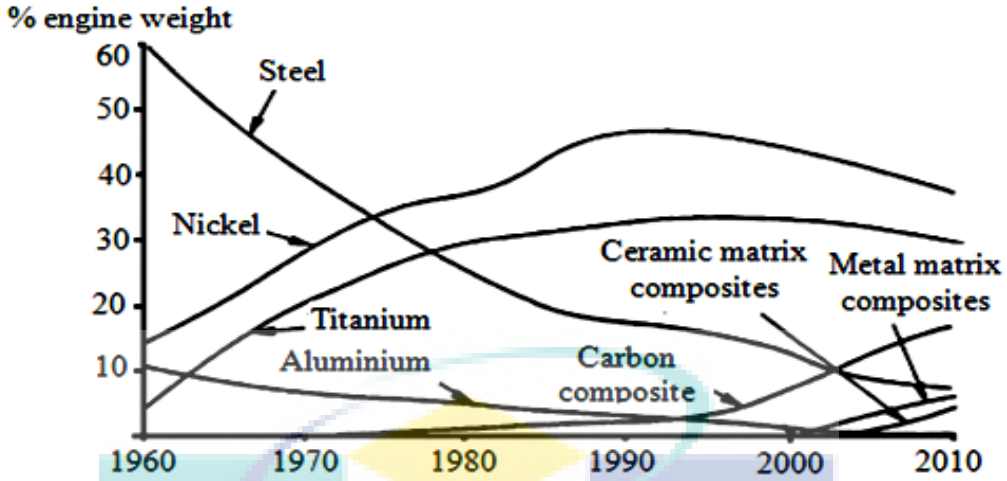

Figure 1.1: Evaluation of materials use in Aerogas turbines

Source: Miller (1996).

The main issue faced in the research is that heat-resistant nickel-based alloys have a low thermal conductivity as well as a high characteristic of adhesion which during the machining increases the effects of thermal and tool face parameters. The alloy can also contain carbides and abrasive particles that can create high tool wear. Thus, according to Axinte et al. (2006) the quality of the final products is low. Furthermore, the alloy has an austenitic matrix which makes the work hard during the process of machining. Besides this, the abrasive saw-toothed edges are produced because of localised shear in the chip making the handling of swarf difficult. In addition, the alloy can weld with the material of the tool during high temperature as a result of machining. This tendency to create built-up edge (BUE) during the process of machining and the abrasive carbides prevents any machinability. This is because of, according to Ezugwu et al. (1991), the high temperature (>1000°C) and stress (>3450 MPa) which accelerates the create ring, flank wear and notching.

Hastelloy C-2000 is the nickel-chromium-molybdenum (Ni-Cr-Mo) C-type alloy which is used in the aerospace, marine and food processing, chemical process industries. According to Shokrani et al. (2012), difficulties as well as high costs are expected in machining of this alloy because it is designed retain its strength at elevated temperatures. Thus, great efforts are being made to find an economical method of

machining these alloys to enhance its performance. As a result, the use of mathematical modelling is done to develop empirical equations for relating the cutting parameters to the tool life, surface roughness, tool wear and cutting force. A statistical method used to optimise the surface response is called response surface method (RSM). The RSM quantifies the relationship between response surfaces and input parameters (Montgomery, 1997; Kwak, 2005). The use of Artificial Neural Network (ANN) is done in modelling of different operations including drilling, turning and milling. The main characteristic of this network depends on three factors namely the dataset distribution, selection of the input/output system parameters and presentation format of the dataset for the network. In order to acquire the best results, activation function, hidden layers, training algorithms and neuron number are important.

In addition to being used as a mathematical model generator by RSM, the use of ANN is also taken in predicting the machining optimal conditions because it is considered as a powerful modelling method for performance characteristics prediction. The advantage of using ANN is that it can help solve processing issues which require interpretation and real-time encoding of variables and their relationship having high-dimensional space. According to Kartalopoulos (1996), ANN is a structure consisting of various interconnected elements. Each of these elements has the characteristics as an input/output which implements the local computation. The I/O characteristic determines the output of each element which is the interconnection to various other elements. This interconnected network creates an overall functionality by training forms. According to Skapura (1996), the unit of ANN is known as neuron which has an input set of X_i weighed before it reaches the main part of the processor. Furthermore, because of its bias terms, it has a threshold value which needs to be maintained in order to produce a signal by the neuron, which is non-linearity function (f_i) acting upon the signal produced (R_i) as well as output (O_i). This model is presented in Figure 1.2. According to Azlan et al. (2010), the sigmod activation function combined with the algorithm of feed forward back propagation is used in the end milling machining for predicting the roughness of the surface. Hao et al. (2006) has introduced a cutting force model using the artificial neural networks for the force prediction of self-propelled rotary tool (SPRT). In this present study focuses on best usage of machining Hastelloy C-2000 in

respect to the cutting force, tool life and surface roughness using the ANN approaches in the CNC milling machine.

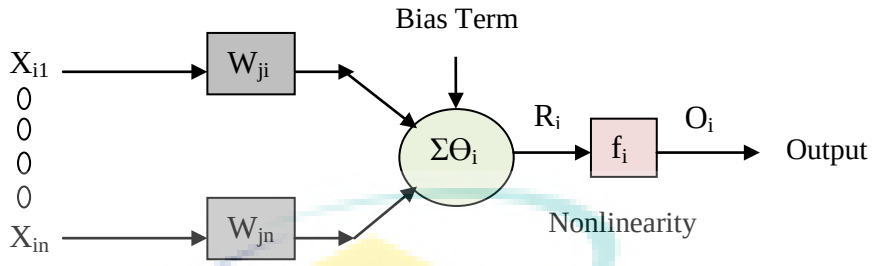

Figure 1.2: Basic model of artificial neural network

1.2 PROBLEM STATEMENT

A great challenge is presented to the manufacturers in the competitive marketplace because of the manufacturing environment, low costs, goals of high rates of production, and high quality. The accuracy of workpiece dimension, tool wear, surface finish, and tool life on the material removal rate and cutting tool have increased for enhancing the product performance in relation to the impact of the environment (Ulutan and Ozel, 2011). According to Li et al. (2006), Hastelloy C-2000 is considered because of its design to withstand high temperatures making the machining operations and cutting temperatures high. Furthermore, according to Ashtakhov (2006), the contact length of tool is short which produces high stress level at the tool-chip interface of the alloy. According to Kadirgama et al. (2011), the dominant features of tool failure are flank wear, cracking, catastrophic, notching, chipping, plastic lowering and the cutting edge and so on. The hardening of work is another issue which leads to high wear of tool at the flank face. It was reported by Outeiro et al. (2008) that the mechanical and thermal loads affect the tool's residual stress for instance the thermal load creates tensile stress for austenitic structure while it is suppressed by mechanical load. According to M'Saoubi et al. (2008), these loads are more dominant in high-temperature alloy machining that cause undesired tensile stress. According to Yahya (2007), it is important in manufacturing that the machining finishing process be of specified dimensions, surface finish, tolerances, type of surface generations and other behaviours. Given such demands of the manufacturing, it is imperative to examine the features of

the machining, chip formation and surface integrity. As such, the focus of this research is on the optimization of the Hastelloy C-2000 machining characteristics in regards to surface roughness, tool life, tool wear, and cutting force for acquiring high machinability. For this purpose, an artificial intelligent model and mathematical model are presented for finding a combination of independent variables of the end milling process of CNC (feed rate, axial depth, and cutting speed) for achieving the best machining behaviours.

1.3 OBJECTIVES OF STUDY

The objectives of this study are as follows:

1. To investigate the characteristics of the machining in the operation of end mill in terms of the surface roughness, surface integrity, tool life, and cutting force.
2. To develop a model of process optimization using the response surface method.
3. To establish a prediction model using artificial neural network based on the Hastelloy C-2000 machining characteristics.
4. To evaluate the mechanism of tool wear as well as formation of chips of the cutting tools when the machining Hastelloy C-2000.

1.4 SCOPES OF STUDY

The CNC milling machine conducts the experiments for different feed rate, axial depth and cutting speed. The two flutes and slotting process by the end milling are supposed to be cutting tool and machining operation. Cutting tool's diameter is 16 mm which is assumed to be constant while two cutting inserts are used namely uncoated carbide and coated carbide. The workpiece is machined in the wet cutting condition using fully synthetic lubricant type and experimental is conducted based on the Box-Behnken design. The characteristics of the machinability of the material are mentioned in respect of the surface roughness, surface integrity, tool life, tool wear, cutting force, and chip formation. The cutting force is measured online during the machining using dynamometer, where the surface roughness, tool life and tool wear is measured once the machining procedure has been completed. At the same time, the

integrity of the surface can be examine by using a scanning electron microscope (SEM), which helps in studying material and surface characteristics that may change because of work hardening of the Hastelloy C-2000 or elevated temperatures during the machining process. The chips are collected after machining process completed. The mathematical modelling based on first and second order of response surface methodology is developed as an aid in optimization of machining performance. The back propagation algorithm along with the artificial neural network can used to predict certain features of Hastelloy C-2000.

1.5 ORGANIZATION OF THESIS

The preparation of this thesis was made while aiming to provide adequate information regarding observations, facts, procedures and arguments which will help reach the determined goals. Other than the Introduction, four chapters were written in a way to show a logical progression of thought. The literature review discussed different theories relating to metal cutting, while in Chapter 2 discussed cutting force, tool wear and surface roughness. In addition, the artificial neural network and practical application of RSM were also discussed. In Chapter 3, the different tools and procedures used to analyze the data were discussed, along with information regarding data collection, evaluation of data and techniques used for analysis. Chapter 4 discusses the results obtained through meticulous analysis. Two sets of mathematical models based on response surface method were compared against the artificial neural network model. Other items in this chapter included how machining characteristics can be optimized. Chapter 5 contains the conclusions drawn along with recommendations. In addition, any areas of future research have been included in this chapter.

CHAPTER 2

LITERATURE REVIEW

2.1 INTRODUCTION

This chapter provides the review from previous research efforts related to milling process, CNC milling machine, cutting parameters in milling machine, and cutting tools. This chapter also involves a review some research studies like the statistical method and artificial neural network which are related to the mathematical modelling the present study. Substantial literature has been studied on machinability nickel based alloys which is covers on surface roughness, surface integrity, tool life, tool wear cutting force and chip formation. This review has been well elaborate to cover different dimensions of this research such as a discussion about the current content of the literature, the scope and the direction of current research. The review follows a chronological order to highlight how the outcomes of the previous research served as the basis for more work in this field this research is one such effort. To carry out this research, which had to undergo a considerable amount of literature but not enough information was available. The review is fairly detailed so that the present research effort can be properly tailored to add to the current body of the literature as well as to justify the scope and direction of present.

2.2 MILLING PROCESS

Milling is an extremely important process of removing material. When compared to other non-traditional machining processes milling is not just less costly but it can be used with a wised array of applications (Tang et al., 2009). The milling process

is a multipurpose material removal process. Machining of shapes that have close tolerances and are complicated can be done with the milling operations. Hence it can define milling as a machining operation where a work piece is inserted into a rotating cylindrical tool that has numerous cutting edges (Rao and Pawar, 2010). The axis of rotation of the tool is set at right angles to the direction of insertion. The tool that does this is known as the milling cutter and its cutting edges are known as the teeth. To perform the cutting action the work piece is inserted beside the rotating cutter. Only a proportionate arrangement of the process's parameters can lead to effective outcomes and the essential parameters of this process include the spindle speed, the table feed, the depth of cut, and the rotating direction of the cutter (Imani et al., 2012). Frequent use of milling happens to be as a secondary process used to enhance features on parts that were contrived with a different process. Since the milling process can provide surface finishes and high tolerances and surface finishes that is why it is deemed as the best way for adding precision features to a part whose basic shape has been formed previously (Dotcheva and Millward, 2005). There is multiple-axis of a milling machine used to machine byzantine surfaces. The example of milling process is illustrated in Figure 2.1.

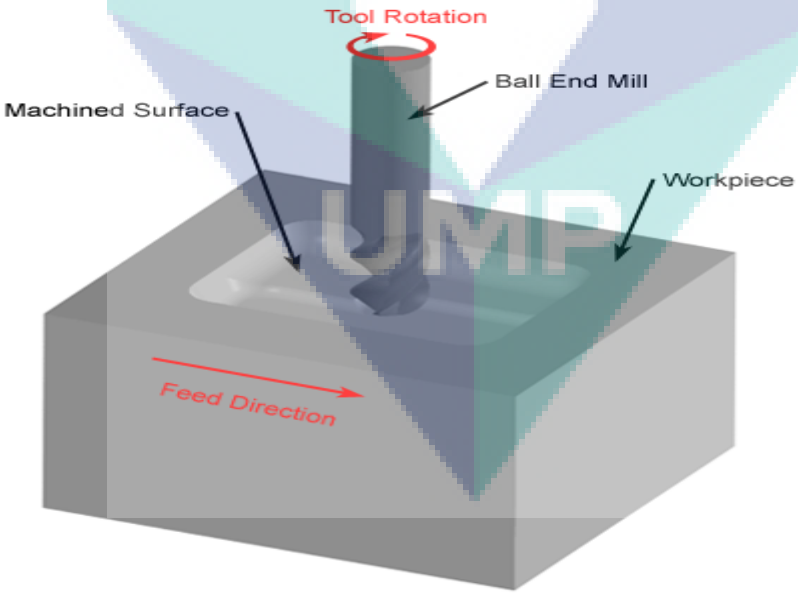

Figure 2.1: Typical example of milling process

Kang et al. (2007) conducted a study on the cutting conditions in micro-end milling. Peripheral milling operations are carried out by End milling, the peripheral

milling operations comprise of profiling and slotting operations. Bao and Tansel (2000) performed a study to understand the cutting force in the application of micro-end milling and conventional milling machine. The peripheral or slot cuts are made with an end mill the step-over distance through the work piece determine them to machine a definite feature, like a profile, slot, pocket, or even a complex surface contour. The type of end mill used most abundantly is 2- flute and 4-flute. A lot of aerospace components such as dies and moulds are commonly done by the machining processes of the flat end milling (Dang et al., 2001). There are many different quality specifications and styles of end milling cutting tools. However, Fontaine et al. (2007) did the exploration about the impact of tool workpiece inclination on cutting force by ball-end milling with slot tests. This study revealed that the trouble at low speed when slot end-milling is used due to the cutting temperature increases and strain hardens (Liao and Wang, 2008).

The machinery industry is ingested with the machine tools known as computer numerical control (CNC) milling (Yang and Lee, 2001). The higher productivity, integrity of workpiece machine and the maintenance of surface quality are all possible because of the CNC milling machine (Ertekin et al., 2003). Turning and drilling are the fundamental functions of CNC milling, the number of axes that they hold are used for their categorization. These axes are categorised as *X* and *Y* for horizontal movements, and *Z* for vertical movement. There are different ways of understanding the number of axes of a milling machine and it is often seen to be a casual "shop talk". The horizontal pivot serves as an extra axis for a five-axis CNC milling machine. It is used for milling head and leads to enhanced flexibility for machining with the end mill at an angle as per the given table (Shaw and Ou, 2008). There are a set of commands by the name of G-codes that are usually used for programming the CNC milling machines. Specific CNC functions written in alphanumeric format are denoted by G-codes (Omirou and Barouni, 2005). The selection of the size depends on the purpose, location of usage and the type of the material that ought to be cut the size of motor also changes the speed at which the materials are cut. The materials are difficult to cut and require more time and a stronger milling machine on the other hand materials such as plastic and wood are easy to cut. The higher the rigidity of the mill the more accurately it drills and cuts. When put CNC mills against the conventional mills, it can be seen that CNC mills have higher rigidity usually because they have superior and tougher engines (Mecomber et al., 2005).

2.3 CUTTING PARAMETERS IN MILLING MACHINE

The manufacturing engineers and researchers have now started to become conscious that efficient quantitative and predictive models that institute the relationship between a input independent parameters and output variables are required to enhance the economic performance of metal cutting operations for various manufacturing processes, cutting tools and engineering materials implied in the industry at the present point (Alberti et al., 2005). In order to improve the characteristics of machining input of cutting parameters in milling machine, four parameters are of paramount importance namely, feed rate (mm/tooth), axial depth (mm),cutting speed (m/min) and radial depth of cut (mm) where the value is kept constant (Arezoo et al, 2000). All these parameters are detailed below:

For machining cobalt based superalloy, the succeeding cutting parameters are used such as feed rate, axial depth and cutting speed (Aykut et al., 2007a). During the end milling of Inconel 718TM the authors had used different feed rates to improve the performance and life of the tool (Krain et al., 2007). The feed rate, axial depth and cutting speed were used as cutting parameters to describe and model for development of burr in micro-end milling (Lekkala et al., 2011). To inspect the chip load prediction of ball-end milling machine the feed rate is used as a fundamental parameter (Jung et al., 2001). The feed rate scheduling model allows traverse rupture strength of a tool 3D ball end-milling (Ko and Cho, 2004). The classification of common sensory topographies for the control of CNC milling operations in changeable cutting conditions is done by cutting parameters like feed rate, axial depth and cutting speed (Ertekin et al., 2003). Baek et al., (2001) used the surface roughness model for the enhancement of feed rate during a face milling operation. The CNC milling machine uses the parameter of feed rate to examine data fusion neural network for tool condition monitoring (Chen and Jen, 2000).

In the investigation of surface roughness AL20 14-T6 a slot end milling that comprises of cutting parameters such as axial depth, feed rate, cutting speed, concavity angle and axial relief angle (Wang and Chang, 2004). According to Lamikiz et al. (2004), the axial depth was used as a parameter in predicting the cutting force

sculptured surface milling. Axial depth was used as a variable for examining the influence of the cutting dynamics of small radial immersion milling operations on the machined surface roughness. When studied the hybrid adaptive control on the foundations of CNC end milling, the axial depth was used as a parameter (Yang and Lee, 2001). Kim et al., (2000) used *Z*-map in applying the axial depth for cutting input to study the cutting force in end-milling. When analysing the tool life and tool wear of Haynes-22HS by means of respond surface method the CNC milling machine parameters include axial depth, feed rate and cutting speed (Kadirgama et al., 2011).

The input parameter was used in the simulation of cutting forces in ball-end milling (Milfelner and Cus, 2003). The cutting speed, axial depth, radial depth, feed rate all are cutting parameters used in CNC milling machine when studying cutting force (Dang et al., 2010). For hardened steel the parameter for study of end milling is the cutting speed (Kita et al., 2001). When exploring the mechanistic modelling of the milling process for multi-axis machining of free surfaces cutting speed is applicable (Zhu et al., 2001). Force torque established online tool wear system assessment with different ranges of cutting speed, feed rate and depth of cut cutting conditions for CNC milling machine of Inconel 718 by means of neural networks (Kaya et al., 2011). As for a lengthy control scheme of cutting forces that normalise the tool life in end milling process as an input parameter various ranges of cutting speed were used (Ibaraki and Shimizu, 2010).

2.4 NICKEL BASED SUPERALLOYS

When compare Nickel-based superalloys (Ni-Co-Cr, Ni-Fe-Cr or Ni-Co-Fe) against titanium-based alloys, it can be seen that they have a plenty of advantages that is why they are widely prevalent in the industry (Shokrani et al., 2012). Even after these Nickel based alloys are exposed to extremely high temperatures for extensive time periods they still maintain most of their strength (Khidir and Mohamed, 2010) that is why when it comes to choose the material for turbine sections of the jet engines these Nickel based alloys are the ultimate choice. The strengths of the nickel-based alloys include: they have high melting temperatures, are heat-resistant, are high corrosion resistance, can maintain their high mechanical and chemical properties at high

temperatures, and are resistant to thermal fatigue, thermal shock, creep, and erosion (M'Saoubi et al., 2008; Wu, 2007). Nickel based alloys are normally use in the hot sections of mission critical apparatuses of jet engines or gas turbine engines are the commonly available forms of these alloys are wrought, forged, cast and in sintered (powder metallurgy) (Arunchalam et al., 2004). Cross section of a jet engine is shown in Figure 2.2.

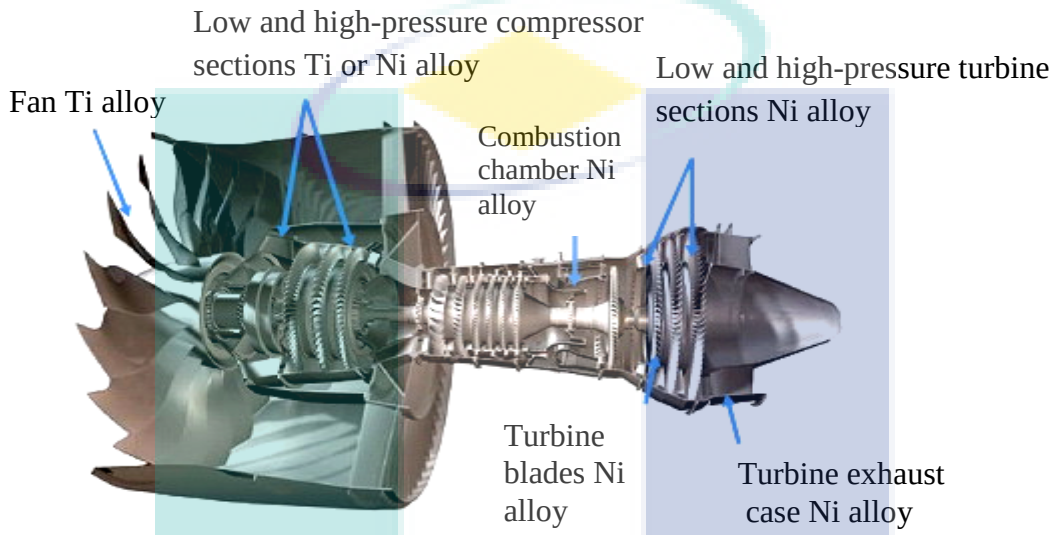

Figure 2.2: Cross section of a jet engine (courtesy of Pratt and Whitney).

The Ni-Fe-Cr alloy (Inconel-718 (IN-718)) is an alloy with properties like high strength and high temperature resistance that is why fifty percentage (50%) weight of a jet engine is made up of this alloy (Miller, 1996). Nevertheless these properties are have many setbacks such as decrease in the productivity and surface quality of surface machine (Ezugwu et al., 2003) and they cause low tool life for the tools used to machine them that is why it is deemed difficult to machine such alloys (Wu, 2007). They are not just able to resist all acids mainly hydrochloric, sulphuric, and hydrofluoric at high temperature ranges, but also resist the insidious types of attack prompted by chlorides and other halide solutions specially pitting, crevice attack, and stress corrosion cracking (HI, 2011). This material is used in the chemical process industry reactors like heat exchangers, columns, and piping (Ezugwu, 2005). On the contrary, the Inconel 100 (IN-100), Ni-Co-Cr superalloy is frequently applied to parts operating at intermediate temperature regimes, for components like disks, spacers and seals. The turbine and

compression blades in hot sections of jet engines also use cast nickel-based alloys (Ulutan and Ozel, 2011).

2.5 MACHINABILITY OF NICKEL BASED ALLOY

Machinability can be defined as “ability of being machined” or more logically as “ease of machining”. However the word ‘machinability’ refers to the development of work materials machining characteristics. The machining conditions determine what type of machining characteristics of the work materials are required (Hamann et al., 1996). The magnitude of the surface roughness, surface integrity, tool wear or tool life, cutting forces, and chip forms can all be used to evaluate the ease of machining of any tool-work pair (Ezugwu et al., 2003). Machinability is considered desirably high when cutting forces, temperature, surface roughness and tool wear are less, tool life is long and chips are ideally uniform and short enabling short chip-tool contact length and less friction (Trent, 1991). It is an ingrained fact that preformed components are fundamentally machined to deliver dimensional accuracy and surface finish so that the product can perform as intended and has a long service life. The easy removal of superfluous material and rapidly with lower power consumption, tool wear and surface deterioration have all been the efforts rendered to get machining done effectively, efficiently and economically (Aririola et al., 2011). Using the correct combination of cutting tools, cutting conditions and machine tool will considerably increase the machining productivity because it promotes high speed machining and does not compromise on the integrity and tolerance of the machined components. The economic machining of difficult-to-cut aero-engine alloys are the one in particular to benefit from it because their unusual characteristics usually damage machinability. Some properties of nickel-base super alloys generate poor machinability these properties are, an austenitic matrix that is why the work hardens quickly while machining those (Axinte et al., 2006). The nickel base alloys are deemed as difficult-to-machine materials because they possess high temperature strength, low thermal conductivity and high chemical affinity for tool materials which leads to lower machinability (Ezugwu et al., 2003). In addition, the abrasive saw-toothed edges which make swarf handling problematic are produced for the localization of shear in the chip (Aggrawal et al., 2008). The succeeding subtopic covers the machinability of nickel based alloy that depends on

surface roughness, surface integrity, tool life, tool wear, chip information, and cutting force.

2.5.1 Surface Roughness

The quality of a product is scrutinised by its surface roughness because it is a fundamental quality feature of end-milled product. If a higher surface roughness is required it is essential that before the process starts the setting of cutting parameters is done properly (Lou et al., 1999). The mechanical properties of work pieces that has to machined ,the rotational speed of the cutter, velocity of traverse and feed rate are all factors that yield the final surface however the machining process is responsible for the development of surface roughness (Benardos and Vosniakos, 2003). The BUE held by the tool flank face can deviate the tool from its original route they can also increase the roughness (Mantle and Aspinwall, 2001). In addition, the fact that the nickel based alloys is of highly ductile nature which also increases the surface roughness values. Because of this ductility they are more prone to develop a huge and unbalanced amount of BUE and can lead to lower surface roughness (Khidhir and Mohamed, 2010). The functional characteristic of products including their fatigue, friction, wearing, light reflection, heat transmission, and lubrication are all affected by the surface roughness (Ibraheem, 2008). When the product is exposed to extensive machining we may observe slight differences in surface roughness because of the on-going wear produced at the coated carbide cutting edge and the temperature reduction at the cutting by the coolant active all through machining Inconel 718 (Ezugwu et al., 2004).

There are certain parameters that influence the surface roughness of supermet 718 nickel-base super alloy and the feed-rate is the most dominant among those parameters (Darwish, 2000), the reason for this dominance is that higher feed rate leads to the lower surface roughness and the surface quality. When the feed rate is higher the surface becomes rougher (Ginting and Nuori, 2009; Joshi et al. 2008). According to the authors when machining IN-718 increasing the feed lowers the surface quality that is why feed rate is deemed as the most dominant parameter that can affect surface roughness (Ulutan and Ozel, 2011). The effects of spindle speed and feed rate on surface roughness were larger than depth of cut for milling operations (Zhang et al.,

2007). Arunachalam et al., (2004) documented that when the cutting speed of Inconel 718 is increased the surface roughness decreased. Moreover, Sharman et al. (2004) confirmed that in order to machine the nickel based alloys cutting speed is an important factor that increases the surface roughness value. Many researchers after studying the literature establish that the surface roughness of nickel bases alloy machine surface is negatively affected by feed rate and cutting speed, the surface roughness, however, rises linearly when the tool diameter and spindle speed are increased (Wang et al., 2005).

2.5.2 Surface Integrity

The condition of a surface produced in machining, this condition may be innate or else it is acquired but is measured by the mechanical, metallurgical, chemical and topological state of the surface is known as the surface integrity (Field and Kahles, 1971). The structural changes corrosion resistance, hardness variation, surface roughness, residual stress, etc. are all then used to measure these states (Jang et al., 1996). That is surface integrity is given so much importance during machining (Ulutan and Ozel, 2011). In the case where the fatigue life of a machined part is deemed central it is tried to achieve a smoothest possible surface (Novovic et al., 2004). The greater strength of nickel based alloys is due to elevated temperature, high ductility, high tendency to work hardening, etc. that is why heat treatment strengthens them further because of their sensitivity to microstructure change (Dudzinski et al., 2004). Another factor that can be essentially critical to the machined surfaces is the shape of the cutting tool. By feeding in the machine with round shape cutting insert the surface finish and minimum surface damage can be rectified (Arunachalam et al., 2004). The hardness of the surface layer and the machined surfaces are inversely proportional when exposed to extended machining (Ezugwu and Pashby, 1992) and (Ezugwu and Tang, 1992). The reason for this is high flank wear. As a result the component forces and cutting temperature increases because of higher contact area and relation motion between the flank land of the tool nose region and the freshly machined surface of the work piece (Che-Haron et al., 2007). The residual stresses, chemical change between the work piece and tool materials, micro cracking, tears, plastic deformation,

metallurgical transformations and changes in hardness of the surface layer are all declared as the foremost changes in the machined surface layer (Axinte et al., 2006).

Many researchers were seen certain flaws in a lot of different nickel- and titanium-alloys like NiCr20TiAl (Zou et al., 2009), IN-718 (Dudzinksi et al., 2004, Sharman et al., 2004), and Ti-64 (Che-Haron and Jawaid, 2005). It is known that while increasing the thermal softening of the material that compressive stresses also increase the machined surface becomes free of these flaws s that the work piece near- surface can rebuild itself easily (Pawade et al., 2007). Researchers like Ginting and Nouari, (2009) stated that materials and cutting conditions and the depth of cut cannot influence the surface roughness. The reported thermal and mechanical cycling, microstructural transformations, and mechanical and thermal deformations during machining processes all cause these impacts (Axinte and Dewes, 2002). Some other researchers also stated that increasing the depth of cut decreases the surface quality (Darwish, 2000).

Some interrelated topics like the residual stresses, metallurgical alterations, and alterations to mechanical properties of the work piece material can be used to study the integrity of surface (Liu. 1999). Itakura et al. (1999) studied Inconel 718 and established that it abides by the major cutting edge, and material to become a stable built-up-edge that keeps the rake face throughout incessant cutting at a cutting speed of 30 m/min. machining can make use of feed marks however the feed rate can be altered and enhanced to change their severity (Ginting and Nouari, 2009). These enhanced cutting speed values are capable of influencing the amount of microchip debris on the surface. Depth of cut along with parameters can impact material plucking, tearing, dragging, and smearing. It is extremely important to optimize the cutting conditions these issues can lead to difficulties while machining nickel and titanium alloys (Zou et al., 2009). There are crack locations that make the fatigue life of the material to decrease significantly because the nickel base alloy is opened to carbide cracking (Ranganath et al., 2009).

2.5.3 Tool Life

The tool life can be referred to as the span of cutting time of a tool. Moreover, tool life is the time before the cutting point tool fails to give satisfactory performance

(Onwubolu, 2006). It is to the credit of modern tools they do not fail too early because of mechanical breakage and rapid plastic deformation instead they wear down gradually as the machining time passes (Arsecularatne, 2004). When machining the nickel base alloys, the cutting tool is usually inserted so the tool is exposing to stark mechanical and thermal loads hence its tool life decreases because of fast tool wear (Xue and Chen, 2011). The machinability of nickel-based alloys is also damaged by a short tool life. It is because of this short tool life that the machining efficiency of these tools decreases (Kadirgama et al., 2011). Many studies focused on the tool materials and their wear mechanism (Costes et al., 2007; Devillez et al., 2007 and Ezugwu et al., 2005). Many studies have been carried out study on the topic of surface milling (Alaudin et al., 1998) and (Diniz and Filho, 1999), which reveal that increasing feed rate and cutting depth increase the cutting forces too. Therefore, there is a direct relation between the cutting forces and cutting speed. When the cutting speed during machining increases so does the temperature as a consequence hardness of the tool material decreases and abrasion and diffusion take place. The cutting speed is a core parameter that can impact the tool wear and tool life (Coromant, 1994).

Choudhurya et al. (1999) states that the when the effect of feed rate and cutting speed are compared it is observed that feed rate is more manifested whereas no matter what the feed velocity is the cutting speed has a dominant impact on tool life (Bermingham et al., 2011). Che-Haron (2001) detected that tool life increases as a result of lower feed rate the inserts and because of this temperature increases and the plastic is deformed. Ultimately the cutting tool materials tend towards failure. Moreover, inserting the cutting edge of the cutting tool at high temperature at the time when chemical reactivity is high will lead to lower tool life (Shokrani et al., 2012). As a result the microstructure of the material changes and prompts residual stress, micro cracks, micro hardness variation through to formation of white layer affecting the cutting tool's life (Dudzinski, 2004). It is also conceived that increasing the cutting speed and keeping the feed velocity constant will lead to an increased frequency of entry of every cutting edge into the work piece and the speed of friction between tool and work piece and between chip and tool will also increase. In the light of this testament we can say that machining with high cutting speed escalates the wear rate hence the tool life becomes short (Jawaid et al., 2001).

2.5.4 Tool Wear

It is extremely essential to pay attention to tool wear during all machining operations including mould and die wear in casting and metalworking. The elements such as tool life, the quality of the machined surface and its dimensional accuracy are all affected by the tool wear as a result the costs of cutting operations increase (Wanigarathne et al., 2005). The cutting tools undergo high localized stresses at the tip tool and high temperature at end to end of the rake face this glides the chip beside the rake face and the tool glides beside the newly cut work piece surface which is known as tool wear (Kalpakjian and Schmid, 2007). During the machining of nickel-based alloys the cutting tool materials are exposed to stark thermal and mechanical changes. The wear rate is also affected by the stresses and temperatures produced near the cutting edge. While machining nickel-based alloys notching at the tool nose and/or depth of cutting areas is a very frequent failure mode the amalgamation of high temperature, high work piece strength, work hardening, abrasive chips, etc. all cause this failure mode (Weinert et al., 2008). Other causes of tool failure mode during the machining of nickel-based alloys include flank wear, crater wear, adhesion wear, abrasion wear, oxidation wear, catastrophic failure, chipping, attrition wear, and built-up edges (Kadirgama et al., 2011). The notching wear results from the phenomenon like the fatigue loading on the tool, the work-hardened layer and the observance to work material on the notched area and following displacement (Krain et al., 2007). Notching can also be recognized as diffusion–attrition wear mechanisms (Kaya et al., 2011). The seizure and pulls out of the material machine also cause the notches (Olovsjo and Nyborg, 2012). The cemented carbide tools that are implied for machining nickel-based alloys are seen to do it at a speeds > 30 m/min but the effort remains futile because of the thermal softening of the cobalt binder phase and the later plastic distortion of the cutting edge (Kramer and Hartung, 1980). The relationship among the cutting tool and work piece such as contact stress and cutting temperature can dominantly impact the tool flank wear (Isik et al., 2007). During the process of machining with coated and uncoated carbide tools failure results because of the stark flank wear and notching at the tool nose and the depth of cut line (Che-Haron et al., 2007). When the carbide tools are used at an incredibly high cutting speed notching increases at a fast pace consequently a premature fracture of the entire insert edge takes place (Ezugwu et al., 1990).

Moreover, it has been observed that since the nickel-based alloys are high in strength they create high temperature and stress in the tool–chip contact area. Furthermore, the split-up of the edge of the chip from the work piece is a tearing process mainly (Niemi, 1971). High flank wear denotes short tool life (Thamizhmanii and Hassan, 2007). The flank wear is illustrated in Figure 2.3.

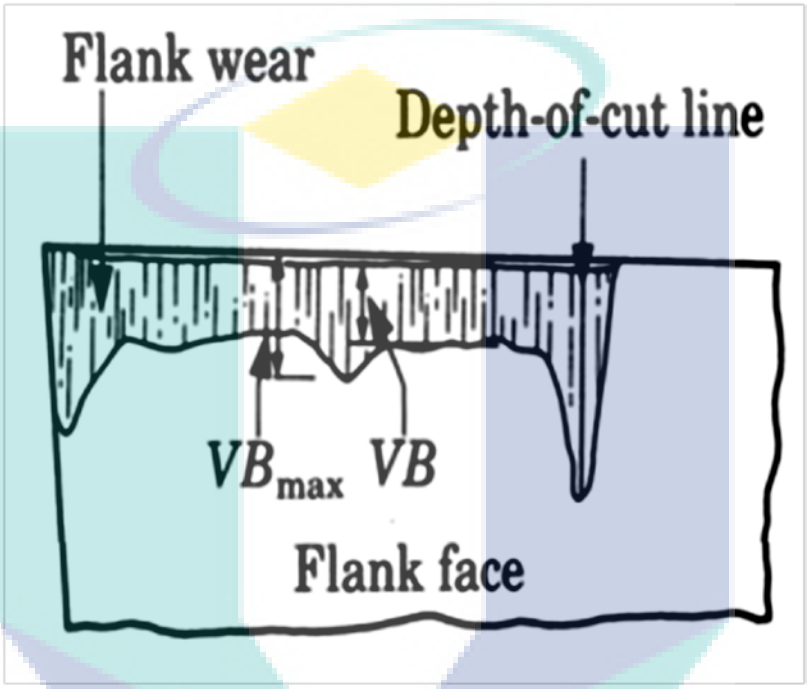

Figure 2.3: Flank wear

Source : Kalpakjian and Schmid (2007)

For tools chipping is also phenomenon like the tool wear. During chipping small pieces break and fall from the cutting edge of the tool the tools with brittle materials like ceramic usually undergo chipping (Zhao et al., 2010). When the machining was done at low cutting speed chipping was seen to grow fast into the tool flank than on the rake face (Jawaid et al., 2001). The abrasion wear mechanism is a result of the scoring action of hard carbide particles enclosed in the Inconel 718 alloy all through machining it is mechanical wear (Ezugwu et al., 2000). Pullouts at the depth of cut regions mostly were an outcome of the adhesion wear mechanism moreover abrasion took place on both the rake and flank faces because of the sharp ridges and grooves beside the chip flow and work piece travel directions (Bhatt et al., 2010).

The process of amputating grain or grains of in tool material by the work material is known as attrition wears but because of this process area of alloys becomes rough (Ezugwu et al., 2003). Tool fracture is a consequence of attrition wear and thermal cracking taking place at high temperature. The mechanical fatigue, fatigue induced by the serrated chip, the formation of cracks generated by thermal and/or irregular flow of the work material over the cutting edge of the tool, etc. all lead to the attrition wear of nickel base alloys (Zou et al., 2009). During the milling of Nimonic 75, the plucking of tool particles depends on attrition wear to a great extent (Aspinwall et al., 2007). In addition, the tool-side of the chip carries and dispenses the BUE and the remaining however, is deposited unsystematically on the work surface. Unless no effort is initiated the process of the formation and destruction of BUE will carry on and as a result built-up edge will form at the cutting edge and it deadens because of the alteration in its geometry. Dry turning tests of Inconel 718 were initiated by Devillez et al. (2007) to study the wear behaviour of coated carbide tools this study revealed that prevailing wear modes detected throughout dry cutting Inconel 718 were welding and hold of work piece material on top of the flank faces and the rake. The study also revealed that the material of the work piece that is sticking to the cutting edge causes a built-up-edge, and a built-up-layer (BUL) on the face of the tool. The character of the BUE and BUL varies as per the cutting conditions and the type of tool sometimes they are stable but they can be the pieces of work piece material that are later on removed. But a crater on rake face, a band of wear on flank face and a notching at the extremity of depth of cut may also be caused as a consequence of this process.

According to Liao and Shiue (1996) diffusion wear occurs when turning of Inconel 718 with K20 and P20 grades cemented carbide tools because Nickel (Ni) or Ferum (Fe) from work piece material gets spread on the grain boundaries of binder Co. The intermetallic phases between carbides and binder because of diffusion at high temperature. Since the affinity of carbides with Nickel (Ni) is high the intermetallic phases dissolve bringing about damage to the bonding between carbides and binder. The cutting temperature however is an essential element to control the extent of diffusion wear (Xue and Chen, 2011). Basically, diffusion wear is the process where the material from the tool at its rubbing surfaces, or the rake surface to be precise diffuses with the flowing chips in atom when the tool material has chemical affinity towards the work

material. When the temperature of the cutting zone raises so does the rate of tool wear (Olovsjo and Nyborg, 2012). Since the cutting velocity and strength of the work material are high at high temperature diffusion wear escalates (Kadirgama et al., 2011).

2.5.5 Cutting Forces

Upon increasing the feed rate, axial rate and the radial depth of cut the cutting forces increase (Liu et al., 2004). Because of the property of hardening possessed by nickel base alloy machining becomes difficult as soon as the milling cutter is used due because of the hardening property consequently the metal is not cut but pushed because the cutting edge is not very sharp. Ultimately the cutting force and temperature increase (Li et al., 2006). Traditionally, the softening of the work piece material increases cutting speed while decreasing cutting forces to the least (Krain et al., 2007). The relation between cutting force and the cutting speed is inversely proportional (Shunmugam et al., 2000). But when feed per tooth, axial depth of cut and radial depth of cut increase so does the cutting force (Liu et al., 2010). According to Fang and Wu (2009), when the cutting conditions are same as the cutting force and the thrust force in machining Inconel 718 are higher as compared to those in the machining of Ti–6Al–4V. Upon decreasing the cutting force, the thrust force, and the result force the cutting speed increases so does the force ratio for both materials. However, the coated carbide and uncoated carbide both have different cutting force the coating layer of coated carbide barricades heat owing to its high thermal conductivity and after this the heat in the chip is removed (MacGhinley and Monaghan, 2001). Nevertheless, numerous coating layers can expand wear resistance considerably as a point of fact the coated layer is not able to last longer because of the high rates of tool wear and short tool life. It is difficult to handle the increase in load and temperature. (Li et al., 2006). The cutting force decreases as the cutting speed increases (Shunmugam et al., 2000). On the contrary, the cutting force increases as the feed per tooth, axial depth of cut and radial depth of cut increase (Liu et al., 2010). The tool breaking is also affected the rake angle negatively that causes to the increases of cutting speed (Nalbant et al., 2007).

2.5.6 Chip Formation

The continuous chips, built-up edge, serrated or segmented and discontinuous are the most frequently used types of metal chips. The ductile materials that are machined at high cutting speed and high rake angle lead to the formation of continuous chips (Astakhov, 2006). The primary shear zone is constricted where the distortion of the material occurs. However, continuous chips are formed in a secondary shear zone as a result of high friction at the tool-tip interface. The high friction is produced subsequent to the thickening of the zone. When the cutting speed is below 50 m/min long and continuous chips of nickel based alloys are formed (Lorentzon et al., 2009). Chip formation is shown in Figure 2.4 (Kalpakjian and Schmid, 2007).

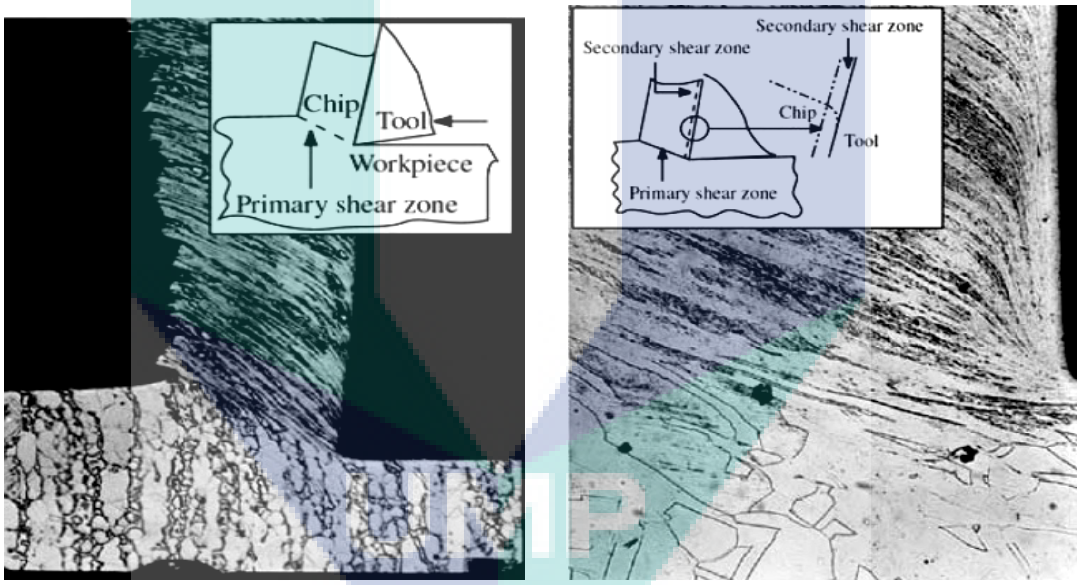

(a) (b)

Figure 2.4: The chip formation, (a) Continous chip with narrow, straight primary shear zone, (b) secondary shear zone at the chip tool

The built up edge is made up of layers of material of the work piece that are dumped on the tool tip bit by bit. The BUE becomes unstable and eventually breaks apart as a result. The succeeding ways can lead to lower BUE formation: increase the rake angle, increase the cutting speeds, decrease the depth of cut, and use the sharp tool and use cutting tool with chemical affinity for the work piece material. The BUE formation is illustrated in Figure 2.5 (Kalpakjian and Schmid, 2007).

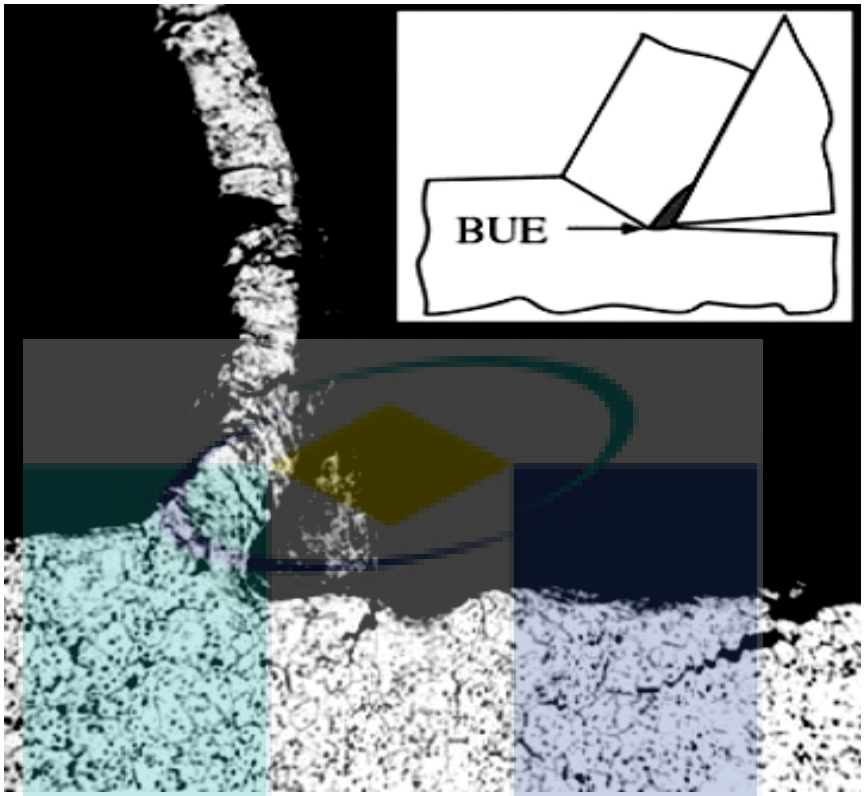

Figure 2.5: Built up edge

The chips look like teeth still no customary standard is available for the inception of saw-tooth chip formation (Trent and Wright, 2000; Thakur et al., 2009). The saw-tooth chip is made because of the adiabatic shearing and surface crack propagation (Guo and Yen David, 2004). Discontinuous chips are made up of firmly or loosely attached segments these chips develop due to the internal crack initiation and propagation in front of the cutting tool and above the cutting edge, the large depth of cut, low rake angle and deficiency of an operational cutting fluid (Guo and Yen David, 2004). Segmented chips are semi continuous chips and have large zones of low shear strain and small zones of high shear strain that result from the cutting speed of more than 100 m/min (Lorentzon et al., 2009). Shear localization is the name for small zones with high shear strain. Titanium has thermal softening which leads to low thermal conductivity and dulling strength that falls with temperature (Kalpakjian and Schmid, 2007). Figure 2.6 illustrates the segmented chip and discontinuous chip (Kalpakjian and Schmid, 2007).

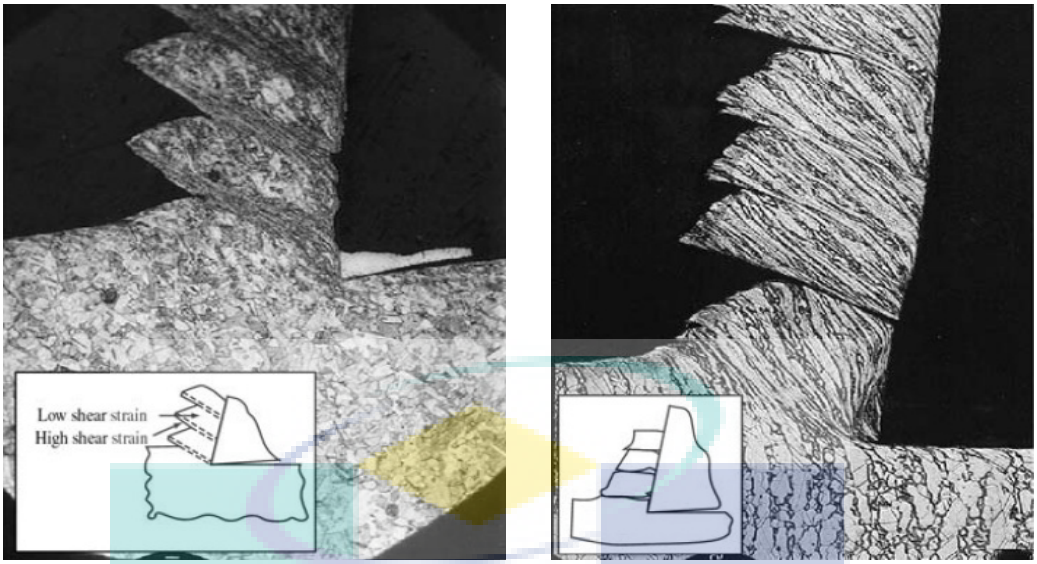

(a) (b)

Figure 2.6: (a) Serrated chips, (b) discontinuous chips

2.5.7 Cutting Tool Materials

The machining nickel based alloy is done at high temperatures produced at high speed hence the cutting tools used for this purpose must have tolerable hot hardness (Rahman et al., 2003), since a lot of tool materials drop their hardness under such conditions which leads to the wearying of the inter-particle bond strength and but the tool wear increases. The cutting tool materials when exposed to high thermal and mechanical stresses near the cutting edge and lead to poor machinability and plastic distortion. Since the machining of nickel based alloys has high performance requirements the machining is done at high speed with coated carbide tools, ceramics and cubic boron nitride (CBN) tools materials– because low speed machining is suitable only for tools with uncoated carbide (Ezugwu et al., 2003). During the machining of the super alloys, the ensuing factors are capable of impacting the performance of a cutting tool: chemical inertness, wear resistance, high hardness, and fracture toughness (Szeszulski et al., 1990).

The machining of the nickel-based super alloys applies cemented carbide tools (Subhas et al., 2000). The machining of nickel-based super alloys with these cemented

carbide tools are done within a speed range of 10–30 m/min (Warbuton, 1967). According to M'Saoubi et al., (1999), the uncoated tools have more strength during machining at high temperature than the coated tools. It is seen that for steel work pieces the coated carbide tools have lower maximum tool temperature, surface stresses, and smoother chip formation that is why white layer formation, residual stresses and thickness of the work-hardened zone is much better and 57% costs are saved than using carbide tools in the semi-finish turning of Inconel 718 (Baker, 2000). While machining with carbide tools stark flank wear and notching at the tool nose and the depth of cutline are the most prevailing failures (Xue and Chen, 2011). So for machining nickel base alloy up to 100 m/min the PVD TiAIN coated carbides are appropriate (Dudzinski et al., 2004; Li et al., 2002). The use of coated and uncoated WC cutting tools is seen to have control over the residual stress because the coated WC cutting tool enhances the residual field on the work piece machined to reduce cutting temperature when machining nickel base alloy (Outeiro et al., 2008). According to Sharman et al., (2001), TiAIN did well as compared to CrN because it is more hard and able to resist oxidation. When machining nickel based alloy at 76 m/min its multilayer leads to better performance than that of the TiAIN-monolayer and TiN and TiCN (Prengel et al., 2001). As per Jindal et al., (1999), TiN coating cannot do as well as TiAIN and TiCN.

When nonferrous metals and abrasive non-metallic materials have to be machined the diamond tools are best option (Prengel et al., 1998), because the single-crystal diamonds are high wear but low shock resistance. Tiny synthetic diamonds are bonded together with a suitable carbide substrate to form the contemporary diamond tools known as polycrystalline diamond (Stephenson and Agapiou, 1997). Machining with polycrystalline diamond (PCD) leads to higher wear, higher shock resistance and surface finish is improved too (Ulutan and Ozel, 2011). When charged with shock/wear resistance and high in edge life these tools are effective that is why they are suitable for machining high-temperature alloys and hardened ferrous alloys (Arsecularatne et al., 2006; Ashatakhov, 1999) These cutting tools form because of the bonding of a layer of polycrystalline cubic boron nitride to a cemented carbide substrate. The ceramic tools have their high hot hardness, high wear resistance and high chemical stability still they cannot effectively machine nickel-based alloys (Jianxin et al., 2005), this is because they are not able to resist thermal shock, have low fracture toughness/low resistance to

mechanical shock at high temperature (Nalbant et al., 2007). Severe notch is also formed by ceramic tools (Liao and Wang, 2008). When during cutting nickel based alloy notch wear speeded up on both rake and flank of ceramic tool because of water jet impingement (hydrodynamic) erosion (Ezugwu et al., 2005). Using the ceramic cutting tool prompts the tensile residual stresses that with cubic boron nitride (Arunachalam et al., 2004).

Other than diamond the Cubic boron nitride (CBN) is the hardest material however it is not natural (Farhat, 2003). The synthesis of polycrystalline CBN is made of approximately 50–90% CBN and ceramic binders including titanium carbide and titanium nitride. When cutting super alloys high CBN content is preferred (Ezugwu et al., 2003). CBN is a commonly used material in tools for cutting difficult-to-cut materials because it can perform better in high temperature stability, hot hardness and low affinity to iron (Lin et al., 2008). While machining nickel base alloy with CBN crater wear was seen at the rake face and flank wear at the edge of cutting edge (Ezugwu et al., 2003). While machining Inconel 718 adhesion, diffusion and abrasion are the prevalent forms of tool wear they result because of high temperature and stresses of work piece (Costes et al., 2007).

2.6 PERFORMANCE MODELLING

2.6.1 Regression Modelling

The response surface method (RSM) is used to optimize the responses (Montgomery, 1997), it is a mathematical and statistical method for modelling and analysing the engineering process. There are many parameters that are capable to cast an influence on the RSM. This method is proficient of optimizing when the desired response is being influenced by different factors (Tong et al., 2011). In order to understand the connection between explanatory and response variables in statistics used RSM (Box and Wilson, 1951). This method is practical, economical and comparatively easy to be applied to modelling of machining processes (Dabnun et al. 2005). A series of tests for acceptable and reliable measurement of response of interest is designed and a mathematical model of the response surface is developed to implement the RSM. And

expressing the direct and interactive effects of the process parameters over two and three dimensional plot and find the optimal set of experimental parameters that produce maximum and minimum value of response are essential for the RSM (Noordin et al., 2004). The Box Behnken design (BBD) of RSM was conceived when there were three levels of every factor with a "reasonable" number of experimental points instantaneously (Aslan and Cebeci, 2007). The Box-Behnken design was applied when cutting force in end milling of modified P20 tool steel with three levels of parameters were to be predicted (Abou-El-Hossien et al, 2007). For the time being, Box-Behnken design has become very popular and is widely used to study the possibility of homogeneous liquid-liquid solvent and also for finding lead from food samples (Khajeh, 2011). The optimization cutting condition for surface roughness leads to the development of linear and polynomial model (Oktem et al., 2005). Dicholkar et al. (2012) carried out modelling and optimizing of steam pyrolysis of dimethyl formamide by applying response surface method and Box-Behnken design. When turning AIS1 H11 steel with CBN tool, some authors have used RSM to determine the relationship between cutting parameters with surface roughness and cutting force (Aouici et al., 2012). The surface roughness model has been developed by response surface method (Sahin and Motorcu, 2008). The BBD was used for optimizing the process of foam cup moulding and for finding out the optimal moulding temperature (Wu et al., 2012). The optimal cutting parameters necessary for minimizing the cutting time while keeping up a satisfactory quality level is determined by the use of BBD design (Jeang, 2011).

A surface roughness model was devised by Mansour et al. (2002), for the end milling of a semi-free cutting carbon casehardened steel for this model a first-order equation covering the speed range 30–35 m/min and a second order generation equation covering the speed range 24–38 m/min was used. It was established as a result that if the feed or the axial depth of cut increases the surface roughness also increases whereas the surface roughness is decreased when the cutting speed increases. Choudhury and El-Baradie (1999) analysed the machinability of Inconel 718 also with the help of response surface methodology for as a result it was established that the dual response contours of tool life and surface roughness are extremely beneficial when it comes to finding the maximum attainable tool life for the same surface finish. Suresh et al. (2002) evaluated the process of machining mild steel by TiN-coated tungsten carbide (CNMG) cutting

tools to achieve a surface roughness prediction model with the help of RSM. Ozcelik and Bayramoglu (2006) used response surface methodology for creating a statistical model by for predicting surface roughness in high-speed flat end milling as a result it was established that the order of significance of the central variables is the total machining time, depth of cut, step-over, spindle speed and feed rate. Sahin and Motorcu, (2008) devised the first-order and second-order equations containing the independent variables are logarithmic transformations of speed, feed rate and depth of cut, by means of RSM for predicting surface roughness in machining the hardened steel. Finally, it was declared that the fundamental factor that influences the surface roughness is the feed rate. The prediction model for surface roughness in turning operation was devised by Kirby et al., (2004). The regression model was established by a single cutting parameter and vibrations along three axes served as in-process surface roughness prediction system. It was done by the means of multiple regression and Analysis of variance (ANOVA). The parameters including feed rate and vibration measured in three axes and the response that is the surface roughness share a strong linear relationship. It was further verified that it is not essential that spindle speed and depth should be fixed to create an operational surface roughness prediction model.

Doniavi et al., (2007) devised an empirical model to predict the surface roughness with the help of RSM to understand the optimum cutting condition in turning. The surface roughness was substantially seen to be affected by the feed rate. The authors determined that feed rate and surface roughness had a direct relationship cutting speed and surface roughness however share an indirect relationship. As compared to depth of cut, the feed and speed surface roughness have a stronger impact. The response surface methodology with an advanced genetic algorithm (GA) in the optimization of cutting conditions for surface roughness was used by Oktem et al. (2005). According to Sharif et al., (2006) applying factorial design along with response surface methodology to devise the surface roughness model as compare to the primary machining variables like cutting speed, feed, and radial rake angle. A methodology essential for attaining optimal process parameters for the prediction of surface roughness in Al turning was devised by Ahmed (2006). The nonlinear regression analysis with logarithmic data transformation was used for creating an empirical model. But there were some errors in the new model however other results

were reasonable. It was established that the low feed rate was beneficial for the development of reduced surface roughness. Moreover, high surface quality is an outcome of high speed.

Bouacha et al., (2010) conducted a statistical analysis of surface roughness and cutting force in hard turning of AISI 52100 that has steel with CBN tool with the help of RSM. The outcomes achieved by ANOVA table during the validation experiments are essential in particularised mathematical models for the predicting surface roughness parameters and cutting forces values with a 95% confident interval and high determination coefficient (greater than 96%). Shetty et al., (2008) discussed the use of Taguchi and response surface methodologies for minimizing the surface roughness in turning of discontinuously reinforced aluminium composites (DRACs) with the aluminium alloy 6061 as the matrix it comprises of 15 vol. % of silicon carbide particles of mean diameter 25 μm under pressured steam jet approach. The experiment shows that steam pressure and feed rate are important machining parameter for surface roughness. It was seen the predicted and measured values were almost same meaning that this model can be beneficial in predicting the surface roughness during the machining of DRACs.

2.6.2 Artificial Intelligence Approach

Artificial neural network (ANN) models are empirical as the solutions they offer are very nearly accurate and driven by occurrences which can only be explained by the experimental data and field observations (Basheer and Hajmeer, 2000). That is why it has been used ANN in this research. In order to solve mathematical problems traditional approaches are used because new models do not have enough autonomy and decision making ability to offer suitable solutions for uncertain artificial neural environments (Lin et al., 2003). Many artificial intelligence (AI) tools, techniques and paradigms like fuzzy logic (FL), neuro-fuzzy, simulate annealing (SA), artificial neural network (ANN) and many more have been used (Jawahir et al., 2003). Manufacturing of complex system is considered theoretically as being an integrated junction of complex interacting subsystem. The feedback manufacturing system is essential because part of society's total energy is taken as input which is then turned into the efficient product. Artificial

intelligence is very effective as for the development and application of this task the tool (Haber and Alique, 2003). Ever since the development of AI the researches have come across new openings and problems that are complex, uncertain difficulties and systems, which cannot be resolved with the help of traditional approaches (Clenaghan et al., 1999).

A lot of metal-cutting operations like turning, milling and drilling use ANN (Dimla and Lister, 2000). There are three factors comprising of the selection of the appropriate input/output parameters of the system, the distribution of the dataset, and the format of the presentation of the dataset to the network that influence the ability of the network (Eynard et al., 2011). It is essential to achieve the optimum performance that the neuron number, hidden layers, activation function and training algorithm are carefully selected. Automated manufacturing largely depends on the production of computer-based learning schemes to code operational knowledge (Uraikul et al., 2007). Machining processes are very complex to include the right analytical models. It is very common that analytical models are driven by basic assumptions which actually oppose each other (Correa et al., 2009). Alignment of all the above parameters of the aforementioned models is very difficult as a result; ANN is able to map the input/output relationships. There are some benefits of ANN in solving processing problems which need real-time encoding and interpretation of connections between variables of high-dimensional space (Ezugwu et al., 2005).

Tsai and Wang (2001) equated six types of neural network models and a neuro-fuzzy network in order to predict surface roughness the outcome was a multilayer feed-forward neural network with hyperbolic tangent-sigmoid transfer functions. Which are accomplished by feed-forward neural network models. Yilmaz et al. (2006) applied a user friendly fuzzy-based system to choose electro-discharge machining process parameters. Ho et al. (2002) devised a method with the help of adaptive neuro-fuzzy inference system to correctly institute the association amid the features of a surface image. This system is capable of predicting surface roughness with the help of cutting parameters.

A hyperbolic function was used as learning function by Erzurulmu et al. (2007) to predict surface quality of moulded parts for investigating the effect of cutting on

surface roughness in turning of free machining using ANN the same model was used (Davim et al., 2008). The feed forward back propagation algorithm that has sigmoid activation function was used to predict surface roughness in end milling machining (Mohd Zain et al., 2010). In the intervening time the activation function of hyperbolic tangent will develop the function of feed forward back propagation algorithm by Abeesh et al. (2008). As per Pal and Chakraborty (2005), the creation of back propagation neural network model for prediction of surface roughness in turning operation is used in mild steel work-pieces that have high speed steel in the lace of cutting tool to apply numerous experiments. A number of architectures of multilayer neural network with a back propagation training algorithm for drill wear monitoring were compared by Abu-Mahfouz (2003). Training data set was mined from the resulting vibration signal from an accelerometer connected to the work piece. The frequency domain features like the average harmonic wavelet coefficients, and the maximum entropy spectrum peaks are very useful in training the network as compared to the time-domain statistical moments. Őzel and Karpat (2005) feed forward neural networks models that predict precisely the surface roughness and tool flank wear both during finish dry hard turning. Using ANN with feed forward back propagation and tansig activation function subsists for the prediction of surface roughness in end milling machine (Oktem at al., 2006). For predicting the surface roughness in CNC lathe machine back propagation algorithm with sigmoidal function was suggested (Karayel et al., 2009).

Aykut et al. (2007b) applied ANN while modelling the properties of machinability on chip removal cutting parameters for face milling of satellite 6 in asymmetric milling processes. To do so a scaled conjugate gradient (SCG) feed forward back propagation algorithm and hyperbolic tangent sigmoid function was used. Propagation algorithm was also applied to model cutting tool stress of Inconel 718 (Kurt, 2009). Also with the help of back propagation algorithm of ANN with hybridization of genetic algorithm was used to craft a cutting force model for self-propelled rotary tool (SPRT) cutting force prediction (Hao et al., 2006). ANN with hyperbolic activation function as online model to tracking is used for the estimation of cutting condition on tool life for the creation of flank wear at the cutting edge during the machining of nickel based alloy (Kaya et al., 2011). Moreover, using ANN with back

propagation algorithm during hot machining of the output parameter of the research was tool life (Tosun and Ozler, 2002). The hybrid of artificial neural network was introduced in cutting force signal pattern in end milling recognition with the function multilayer perceptron (MLP) and with the back propagation algorithm and self-organizing feature map (SOFM) both (Seong et al., 2010). Tsao and Hocheng (2008) examined the thrust force in drilling composite material with the help of ANN. To do so the ANN was inputted with the feed rate, spindle speed and drill diameter whereas the radial basis function network (RBFN) and multi-variable regression analysis were used to scrutinise the data.

2.7 SUMMARY

This chapter has been summarized the literature review based on milling process, nickel based alloys, response surface method and artificial neural network. The surface roughness, surface integrity, tool life, tool wear, cutting force and chips formation has been selected to evaluate the machining performance of Hastelloy C-2000 since lack of research found conducted using this material based on machining characteristics listed. The experiment will be conducted using coated and uncoated carbide in order to indentify the effect of coating layer to the machining process in wet condition. The Box-Behnken design is selected to design the experiment procedure. The prediction and optimization will be developed through response surface method. The artificial neural network model will be used to predict the performance of machining characteristics. The experimental details and mathematical modeling will be further discussed in the next chapter.

CHAPTER 3

EXPERIMENTAL DETAILS AND MODELLING

3.1 INTRODUCTION

This chapter will present about the different methods and procedures used to develop this research. This includes the selection and properties of workpiece material, along with cutting inserts. The performance and cutting limits are included within the machining performances. Detailed information is also given for experiments conducted. This includes information regarding the design of experiment (DOE), physical equipment of the machine, workpiece preparation and experiment set up. In addition, the mathematical model based upon the first and secondary order response surface methodology and accompanying variance analysis are presented. The mathematical model in question aids in optimization of machining behaviour of Hastelloy C-2000 during the end milling processes. Other than the mathematical model, an artificial neural network is also to be completed so that predictions could be made regarding performance of the machining. Other items include multilayer perception, back propagation and training algorithms will be discussed.

3.2 MATERIALS

It can be seen from the previous research that more work has been done to examine the machining behaviour of nickel based alloys while focusing heavily on utilization of Ni-Cr20-Ti-Al, IN-100, Nimonic-75, IN-718, types and UDIMET 720 LI. However, a very little study has been performed on the Hastelloy C-2000 type. This is the reason behind the selection of the Hastelloy C-2000 superalloy so that it can study performance of machining within the end milling machinery by using various cutting

tool inserts. The following sub sections will discuss details regarding the mechanical and chemical characteristics of tool and workpiece resources.

3.2.1 Workpiece Materials

Hastelloy C-2000 has been used for many long years within the chemical process industry. It is a nickel-chromium-molybdenum (Ni-Cr-Mo) C-type alloy and is best known for its flexibility. This superalloy is capable of resisting acids (in particular sulphuric, hydrofluoric and hydrochloric acids) in a wide temperature range and able to withstand dangerous attacks caused by halide and chloride solutions. It can especially withstand crevice attacks, stress corrosion cracking and pitting (M'saoubi et al., 2008; Sharman et al., 2004). The scientific goal during the designing of this superalloy was to increase its already substantial flexibility (in comparison with other traditional Ni-Cr-Mo alloys) (HI, 2011). By using a small but precise amount of copper (1.6 wt.%) along with an elevated molybdenum content (16 wt.%) and elevated chromium content (23 wt.%), the above stated goal was achieved. It was found that copper helped improve the temperature capabilities within sulphuric acid, and also helped dilute the hydrochloric acid. The practical application of Hastelloy C-2000 is within the aerospace sector, where it is used primarily within gas turbines, and in the reactors used in the chemical process industry. Some examples of the reactors include columns, piping and heat exchanges (Nalbant et al., 2007; Arunachalam et al., 2004).

Other than these two sectors, Hastelloy C-2000 is also used in the pharmaceutical industry. It is used in flue gas desulfurization systems, reactors and dryers. During the experiments conducted, it made use of a test specimen with a 46 mm × 120 mm × 20 mm specification. Tables 3.1 and 3.2 show the physical and chemical characteristics of the Hastelloy C-2000 workpiece. It can be seen in Table 3.2 that the superalloy has poor thermal conductivity. This translates into a greater chance for adhesion on the cutting tool face and also, work hardening. Due to this, the surface quality can be affected, along with significant tool wear (Axinte et al., 2006). Figure 3.1 shows workpiece blocks and a small slot was etched onto the workpiece block to latch the workpiece to the force dynamometer. This was done to aid in measuring the cutting forces through the machining processes. In order to ensure that the workpiece could

easily fit into the scanning electron microscope, it was cut into 4 pieces. This helped study of surface integrity and surface texture.

Table 3.1: Chemical composition of workpiece material (Hastelloy C-2000)

Composition	Ni	Cr	Mo	Fe	Cu	Al	Mn	Si	C
Wt. (%)	Balance	23	16	3	1.60	0.50	0.50	0.08	0.01

Table 3.2: Physical properties of workpiece material (Hastelloy C-2000) at room temperature

Parameters and unit	**Value**
Density (g/cm^3)	8.5
Thermal conductivity (W/m°C)	9.1
Mean coefficient of thermal expansion (μm/m°C)	12.4
Thermal Diffusivity (cm^2/s)	0.025
Specific heat (J/kg°C)	428
Modulus of elasticity (GPa)	223

(a) (b)

Figure 3.1: (a) Workpiece blocks (Hastelloy C-2000); (b) Slot at workpiece

3.2.2 Cutting Tool Materials

The tool inserts are made by Ceratizit and its international standard organization (ISO) catalogue number is (CTP-1235, CTW-4615). CTW 4615 is a coated carbide grade with TiAlN coating PVD with grade designation P35 M50. Titanium-aluminium nitride (TiA1N) is used in the cutting of material like difficult -to- machine material (Dudzinski et al., 2004). Hard material layers cause a reduction of friction, heat, oxidation and diffusion. CTP-1235 is a carbide not covered with grade designation K15 (Ginting and Nouri, 2009). Only one input per experiment is allowed to rise on the cutter. Each of the cutters is a unique shape, axial rake 12.5 degree, radial rake angle 5 degree and sharp cutting edges. Highly positive position of the insert and the surface finish of the machined work piece can be improved by the positive axial and radial angle (Arunachalam et al., 2004). Cutting tool insert is shown in Figure 3.2 and the arrangement of the cutting tool insert for coated and uncoated carbide cutting inserts is signified in Table 3.3.

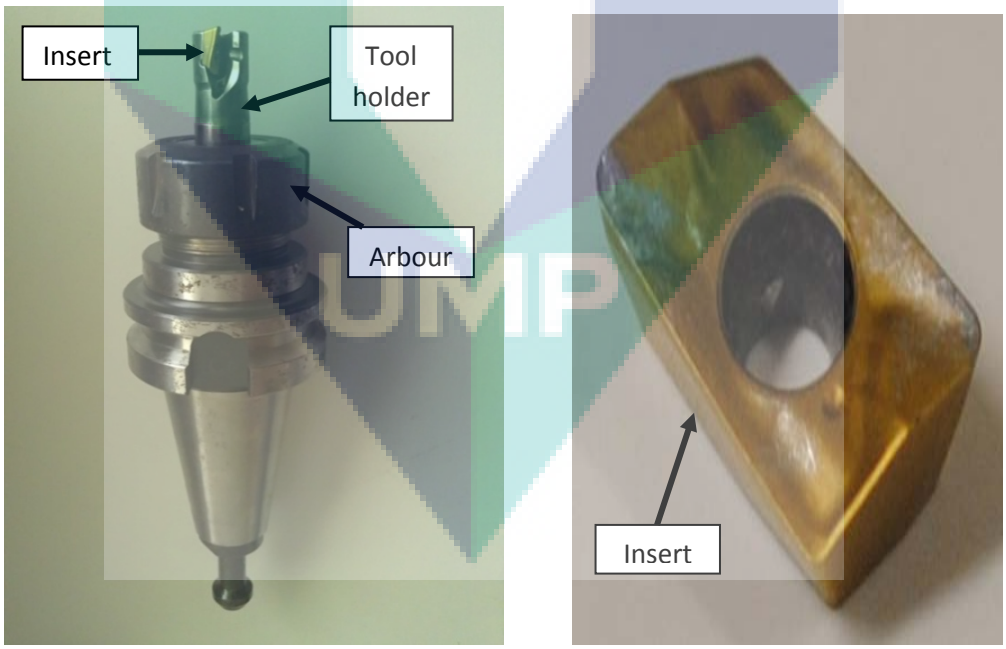

(a) (b)

Figure 3.2: (a) Tool holder and cutting tool insert, (b) cutting tool Insert

Table 3.3: Composition of the coated and uncoated carbide inserts

Type of carbide	Code name	Composition	Coating	Grain size
Coated carbide	CTW 4615	6 % of Co, 4 % carbide,90 % WC	PVD TiA1N, TiN	4µm
Uncoated carbide	CTP 1235	6 % Co, 94 % WC	-	1 µm

3.3 MACHINING PARAMETERS

The parameters of the machine can be sorted in two types; input parameters and output parameters. Table 3.4 shows the input and output parameters for machining Hastelloy C-2000.

Table 3.4: Input and output parameters

Input Parameters	Output Parameters
Feed rate	Surface roughness
Axial depth	Cutting force
Cutting speed	Tool wear
Radial depth of cut was kept (constant)	Tool life
	Chip formation

3.3.1 Performance Characteristics

The frequency features of the machine tool structure and the forces of the cutting process can define the performance of the machine. Surface integrity, tool wear, tool life, chip formation and cutting force can calculate the ability of machine in end milling processes (Joshi et al., 2008; Nurul-Amin et al., 2007; Sridhar et al., 2003; and Mantle and Aspinwall, 2001).

Surface Roughness: Substantial amount of random peaks and valleys cause surface roughness. The contact of two rough surfaces happens in a small area. This specific area is known as real area of contact. Real area of contact is a function of both surface topography and interfacial phenomena, for instance friction and wears (Bhushan, 1999). The participation of surface roughness is very vital in wear, affecting friction and

lubrication of contacting bodies that are what explained to Lee and Ren (1996). The area within the roughness profile and its centre-line called average roughness (R_a), also shown in Figure 3.3. R_a can be written as Eq. (3.1):

$$R_a = \frac{1}{L}\int_0^L |Y(x)|\,dx \tag{3.1}$$

Trapezoidal rule normally calculate integral, which can be described as Eq. (3.2).

$$R_a = \frac{1}{n}\sum_{i=1}^{n} |Yi| \tag{3.2}$$

In Eq. (3.2), R_a is the arithmetic average deviation from the mean line, Y symbolizes for alignment of the profile curve and L is sampling length.

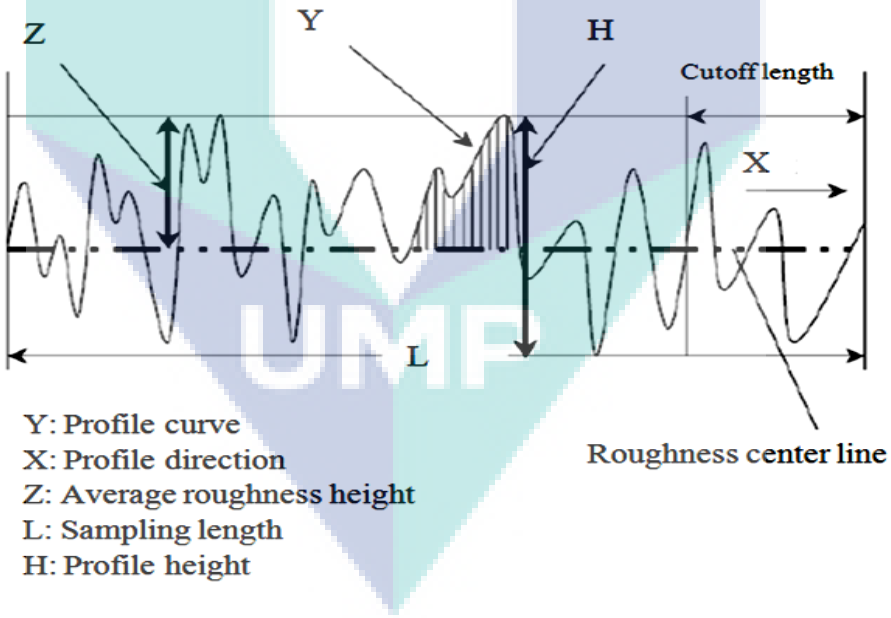

Figure 3.3: Surface roughness profile

Source: G¨o kkaya and Nalbant (2006)

The effect of nose radius and feed can be combined in an equation to predict the ideal average roughness for surface produced by single point tool which can be described in

Eq. (3.3). The equation assume that the nose radius is not zero and that the feed and nose radius will be the principal factors that determine the geometry of the surface.

$$R_i = \frac{f^2}{32NR} \tag{3.3}$$

where R_i is the theoretical arithmetic average surface roughness, mm; f is feed in mm and NR is the nose radius on the tool point. The greater the nose radius, the greater the degree of roundness at the tip. A zero degree nose creates a sharp point. The heat resistance of nickel based alloy accelerates tool wear of the nose radius cutting insert, thus affect the surface roughness of workpiece machined. A round insert with no sharp corner provides the strongest cutting edge, but the work-hardening common of nickel based alloy leads to progressive insert notching.

Surface Integrity: The natural or improved form of workpiece surface machine by machining process is called the surface integrity (Field and Kahlas, 1964). Surface integrity can be sorted as frictional and wear performance at the edge of bodies when they are in contact, efficiency and control of lubrication through machining process, emergence and function of surface in successive surface finishing processes (cleaning, coating, or surface treating), initiation of surface cracks and residual stresses that influence fatigue life and corrosion properties (Ghanem et al., 2002) The usual transformation of the surface were recognized as plastic deformation, micro cracking, phase changes, hardness variations, tears and laps of BUE development and (Ulutan and Ozel, 2011).

Tool Life: It refers to the duration of work till which a new tool can work earlier to achieving the definite limit of tool deterioration. For the end milling application, the wear characteristic is determined based on ISO 8688-2:1989 (E) while ISO Geneva, 1993 has placed a suggested a standard of 0.3 mm for uniform wear criterion, maximum criterion of 0.6 mm and severe flaking or chipping greater than 0.4 of the width takes place at the time in end milling (Kadirgama et al., 2011). The variables upon which the tool life is dependent include work material, machine tool, cutting conditions, tool material and geometry (Arsecularatne and Montross, 2006).

Mathematically, tool life can be described by Taylor equation as Eq. (3.4).

$$V_c T^n = C \tag{3.4}$$

where V_c is the cutting speed, T is tool life, n and c is constant maybe found in specific workpiece and tool material and feed, f, either by experiment or from published data. This equation is applicable normally for turning process.

In end milling process, the formulation used for tool life is as Eq. (3.5).

$$\text{Toollife} = \frac{CD}{F_m} \tag{3.5}$$

where,

CD = the overall distance required for cutting tool to reach flank wear (0.3mm) according ISO 8688-2:1989(E) and F_m is the combination of feed rate and cutting speed from RPM to mm/min.

In the mathematical model based on response surface method, tool life can be modelled as Eq. (3.6).

$$TL = CV^k d^l f^m \tag{3.6}$$

where C is the constant, V is the cutting speed (m/min), d is the depth of cut (mm) and f is the feed rate (mm/tooth) and k, l and m are model parameters. The above function Eq. (3.7) can be represented in linear mathematical form as follows.

$$In\ TL = In\ C + k\ In\ V + i\ In\ d + m\ In\ f \tag{3.7}$$

Equation (3.8) can be written as a linear form:

$$y = \beta_0 x_0 + \beta_1 x_1 + \beta_2 x_2 + \beta_3 x_3 + \varepsilon \tag{3.8}$$

Where, y is the estimated response based on first-order equation and y is the measured tool life on a logarithmic scale, x_0 = 1 (dummy variable), x_1, x_2, x_3 are logarithmic transformations of cutting speed, depth of cut and feed respectively. The parameters β_0, β_1, β_2, and β_3 are to be estimated where ε the experimental error. Y is the estimated response based on the first-order model. Analysis of variance (ANOVA) is used to verify and validate the model.

Tool Wear: The basic processes involving wear and friction are called tool machining. The wear of a tool takes place while the procedures of cutting are in the process. This minimises the working span of the cutting tool and also results in enhanced roughness of the surface of the machine (Zhang et al., 2001). The optimum machining processes can be achieved through the aim of maximum material removal rate and minimum tool wear of the tool in the adequate cutting environment (Li et al., 1999). The surface on which the work is being performed gets changed due to the formation tool deterioration which is largely caused by feed rate (Liew and Ding, 2008). Gu et al. (1999) is of the view that the erosion and deterioration takes place because of the presence of unbalanced built up edge on the flank of the tool.

Cutting Force: It is important to be aware of the significance of cutting force while carry out a machining process. Appropriate designing of the machine tools can help reduce faults in parts of machine, assist in choosing proper holders for tools and work holding devices and to sustain the required dimensional correctness of the machined component. Apart from this, the workpiece has the capacity to endure these forces without getting highly distorted. The forces which act in the orthogonal are displayed in Figure 3.4 (Kalpakjian and Schmid, 2007). The resultant force (R) comprises of two component namely the thrust force (F_t) and the cutting force (F_c). The F_c has the same direction as the tool travel and controls the volume of completed work while F_t is not working. Nevertheless, two of these forces cause the tool to bend. The ensuing force, too, contains two constituents on the surface where wear is taking place. The friction force (F) and the normal force (N) are the constituent forces existing on the surface of the tool. The acting forces can be viewed in the orthogonal in Figure 3.4.

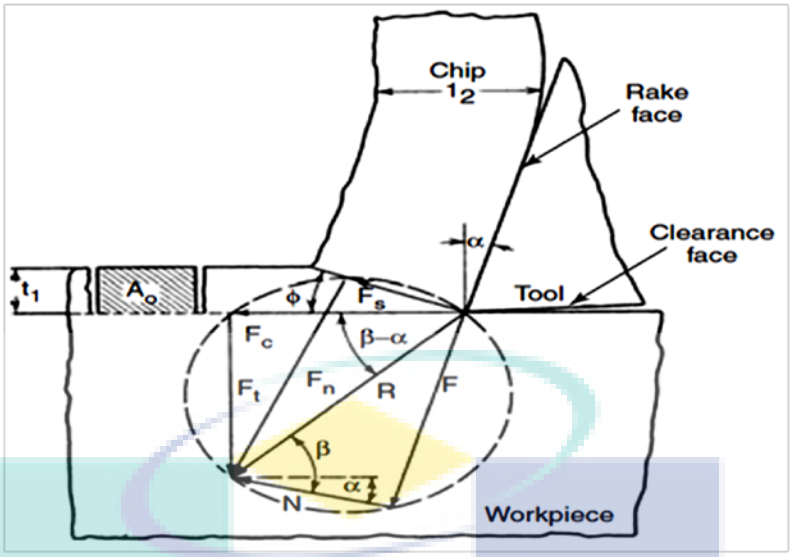

Figure 3.4: Force acting in orthogonal

The figure shows that the direction of shear force and the thrust force F_t is opposite. This takes place when the rake angle together with the depth of cut is large and the resistance is less.The impact of the depth of cut is quite evident because as the depth of cut escalates, the ensuing energy also escalates bringing about an increase in the cutting force too. A surplus amount of force is provided by this action, which is needed to eliminate the surplus material generated by the escalating depth of cut (Astakhov, 1999; Ostwald and Munoz, 2002). The cutting force is also influenced by the speed of cutting. The cutting force is reduced when the cutting speed increases. The reason is that the work material becomes soft around the cutting area and brings about a positive modification in the contact between chip and tool (Fang and Wu, 2009). Kline et al. (1982) developed mechanistic discrete models of cutting force for end milling in which cutter is treated as an aggregation of discretized thin disk cutters along the cutter axis. At any angular position, chip load of each disk cutter can be computed as the product of chip thickness and disk thickness and can be determined by Eq. (3.9).

$$K_r = C_r(\bar{t_c})\, p_r \tag{3.9}$$

where k_r is the radial cutting constant, Cr is the helical and rake angle, t_c is the average chip thickness and p_r is the tool/workpiece material properties. In this research, the

cutting force is measured by cutting force dynamometer. The force dynamometer is clamped on the table of CNC machining, and the workpiece is attached on the cutting force dynamometer. The force dynamometer will record the cutting force during the machining process and the data is send to the charge amplifier for data acquisition. The cutting component of (F_y), radial thrust force is measured where the cutting component of F_z and F_x are neglected due to the small values of them. Chen (2008), during the finishing operation of hardened steel, the radial thrust force (*Fy*) becomes the largest amongst the three cutting force components and it is very sensitive to the changes of cutting edge chamfer, tool nose radius and flank wear.

Chip formation: Chip formation in primary and secondary deformation zones is known as chip formation. The cutting forces and contact processes at the tool-chip interface are among the basic points of consideration in kinematic relationship. Cutting speed and use of difficult methods in the development of materials of the machine are among factors that causing an increase in the number of broken chips (Astakhov, 2006). The crack often spreads from the tool tip of the chip to the free surface of the deformed chip in the share zone. This is because of different stress states near the tool tip of chip. The discontinuous and segregated continuous morphology of the chip is because of variation in crack and considered the basic reason (Hua and Shivpuri, 2004). The negative effect of strength occurs because of change in local temperature, which can be equivalent to or greater than the positive effect of strain hardening, the whole phenomenon is described as catastrophic shear that lead the formation of serrated chips used in machining difficult-to-machine material (Recht, 1964).

3.3.2 Process Parameters

Feed rate, axial depth and cutting speed are process parameters of CNC end milling machine (Mohd Zain et al. 2010; Ozcelik and Bayramoglu 2006; Yin-fong and Min-der, 2005). The details of these process parameters are as follows:

Feed Rate: The rate at which cutter is raised against work piece is defined as feed. The higher value of feed rate, increases the cutting force thus affects the surface finish of workpice machined (Korkut and Donertas, 2007). However, the calculation for single

point cutting machine is relatively direct and can be obtained from work done on a single point of willing machine which is equipped with multi-tipped cutting tools. Thereafter the number of teeth on the cutter and the desired volume of material of each tooth required during cutting are desired to produce anticipated feed rate. Therefore, feed rate is described as mm/rev (f_r), mm/min (f_m), or mm/tooth (f_t) by the vendors of milling machine. Feed rate described in mm/tooth are used for specific cutter of the machine whereas feed rate described in terms of mm/ tooth are desirable for general use. However, the feed rate mm/rev can be represented as follows in Eq. (3.10):

$$f_r = f_t \times n \times v \tag{3.10}$$

where,

f_r = Feed rate in mm/rev; f_t = Feed rate in mm/tooth

n = Number of the teeth of cutter; v = Cutting speed

Axial depth: The distance at which tools digs in metal at the time of working is used to measure the axial depth of cut. There are two types of cut: the axial depth of cut and the radial depth of cut. The former is measured by the depth of the cut along its axis during the time of cutting workpiece. Lower feed rate is useful to get large axial depth of cut and help to maintain fewer loads on the tool and results to maximize the life of the tool. Thus, when tool moves through each pass it will generate passes at several stages and moves the tool along specific axial depth of cut. However, the depth of tool along the radius of workpiece is the radial depth of cut, which is less than the radius of the tool and partially used to make peripheral cut in the work piece. The surface roughness of workpiece machined is affected mainly by radial depth of cut (Vivancos et al., 2005).

Cutting speed: Cutting speed is the speed at the outside edge of the milling cutter as it is rotating. It can also be defined as how fast the metal comes into contact with the tool at the cutting point. There are multiple variables which affect the machinist's decisions to fix the speed of the tool. It is equally valid for drilling, grinding, milling and turning (lathe). The decreases in the cutting speed enhance the machinability without using lubricant (Diniz and Micaroni, 2002). It can help improve productivity and streamline the cutting process. The cutting speed in the context of milling cutter is defined as the

speed which allows cutting tip to pass the work. It is measured in m/min. When the cutter is moving at the *N* rpm and its diameter is *D* (measured in mm), the distance covered by cutting edge in *N* revolution. The formula of cutting speed is mentioned in Eq. (3.11).

$$v = \pi DN \tag{3.11}$$

The intensity of the heat source is an important measure in the cutting system. It is affected by cutting speed which in turn determines the energy distribution level. When the cutting speed is increases, plastic deformation in the chip formation zone reduces. This inverse relationship leads to low level of conversion from applied mechanical energy to heat. As a result, the chip is born at the less hot level (Ashtakhov, 2006).

3.4 EXPERIMENT DETAILS

3.4.1 Parameters Selection

Findings from the literature review by the previous researchers and the preliminary experiment were the bases of selecting the parameters. The process parameters such as the axial depth, feed rate and cutting speed were considered in the end milling process (Palanisamy et al., 2009). Earlier considered factors of nickel based alloys are depicted in Table 3.5

Table 3.5: Factors considered in previous studies of Nickel based alloys

Material	Variables	Author (years)
IN-718	Feed rate (0.03 mm/rev) Axial depth (1.2 mm) Cutting speed (30 m/min)	Li et al. (2006)
IN-718	Feed rate (0.04 mm/rev) Axial depth (0.5 mm) Cutting speed (16, 200 m/min)	Derrien and Vigneau (2004)
IN-718	Feed rate (0.08 mm/rev) Axial depth (0.2 mm) Cutting speed (18,200 m/min)	Guerville and Vigneau (2002)

3.4.2 Design of Experiments

The procedure of choosing the optimum level of cutting tools, machines and cutting parameters and condition is very long and costly (Kincl et al., 2005). An experiment was performed with diverse cutting tools for various parameters, then it is concluded that the best technique which can be used to cut different things is Design of Experiment (DOE). The Box-Behnken design used to optimize the experiment of judging effects of important parameters by using RSM (Zhao et al., 2006). This design is also used in practicing some discontinuous experiments but for only once. As you can see the Figure 3.5, which illustrated the Box-behnken design of three different variables, (Ferreira et al., 2007). Because of the advantages of using Box-Behnken design in different studies, it is finally concluded that this design has few points to remember and very much cheaper in conducting experiments (Chopra et al., 2007). Thus, it is preferable than the other central composite designs (Li et al., 2010). To check the feasibility and authenticity, three cutting levels parameters were used to observe the machinability and features of this trustworthy design. As you can see this model in Table 3.6, that shows the coated and uncoated carbide. The output value of the experiment is entered under the coated and uncoated columns in Table 3.7.

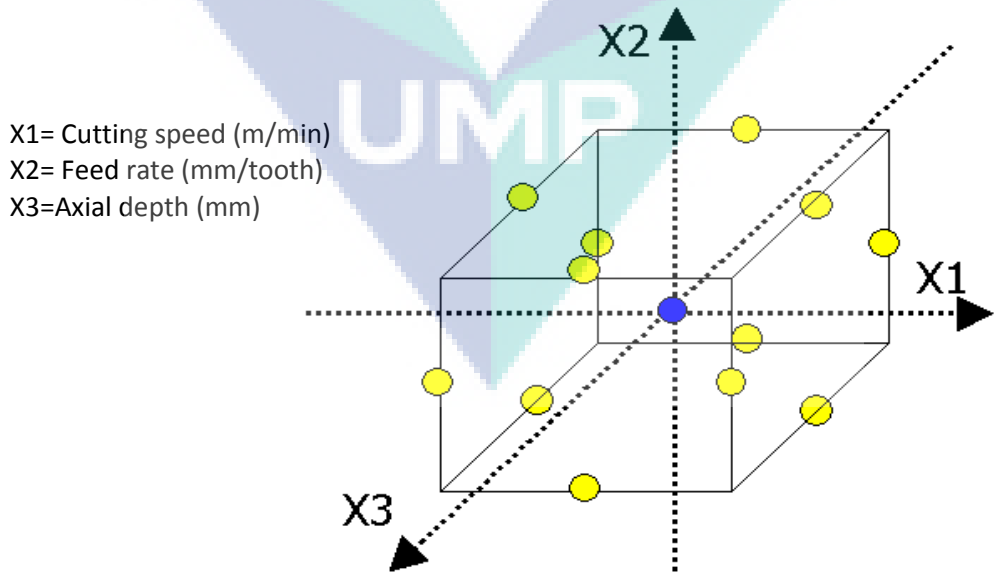

Figure 3.5: Typical example of BBD with three variables

Table 3.6: Machining parameters and their levels for coated and uncoated carbide cutting tool inserts.

Process Parameters	Level		
	-1	0	1
Feed rate (mm/tooth)	0.1	0.15	0.2
Axial depth (mm)	0.4	0.7	1
Cutting speed (mm/min)	15	23	31

Radial depth was kept constant at 16mm

The radial depth of cut plays an important role in milling forces because as the radial depth of cut is increased, the "contact area" increases in the rotational direction, and the forces becomes larger. In this research, the machining is conducted in end milling machining and its is fully engaged, the radial depth of cut is equal to the diameter of cutting tool which is 16 mm, where the value is constant.

Table 3.7: Design values of experiment for coated and uncoated carbide inserts

Experiment No.	Feed rate (mm/tooth)	Axial Depth (mm)	Cutting speed (m/min)
1	0.15	0.4	31
2	0.15	1	15
3	0.1	0.7	15
4	0.2	1	23
5	0.2	0.7	31
6	0.15	0.7	23
7	0.15	0.7	23
8	0.2	0.7	15
9	0.1	0.4	23
10	0.15	1	31
11	0.15	0.4	15
12	0.1	0.7	31
13	0.1	1	23
14	0.15	0.7	23
15	0.2	0.4	23

3.4.3 Workpiece Preparation

A moist cloth and sand paper were used on the surface of the Hastelloy C-2000 blocks (dimension of 46 mm x 120 mm x 20 mm) to make it more smooth and clean.

Sometimes the sticking dust makes the block very rough, so it is very beneficial to clean it before processing further. After cleaning up, the top surface is removed from the block and further uses it in the workpiece. After that, the dynamometer is attached with the slot and then clamped it with the block.

3.4.4 Experimental Setup

For the experimental setup, the Hastelloy C-2000 machine is used to test the design of the cutting technique. A wet cutting condition is made to test the effectiveness of the result of the CNC milling machine, HAAS TM-2 (See, Figure 3.6). This machine is equipped with 5.6 KW motor drive, 400 rpm spindle speed and 5.1 m/min feed rate (the complete specification is also shown in Table 3.8). The quality of the cutting tool for the cutting machine is very important. Therefore, coated carbide (CTW 4615) and uncoated carbide (CTP 1235) are used in the cutting tool. For each 15 different experiments, a new set of cutting tool is used every time to get authentic data.

Table 3.8: The specification of the CNC milling machine HAAS TM2

Part	Specification
X- axis	40"
Y- axis	16"
Z- axis	16"
Table surface to spindle nose	4" to 20"
Column to spindle centre	22.05"
Table working surface	57.75" x 10.5"
Table load capacity	1000 lb
Spindle speed RPM	4000 to 6000 rpm
Spindle taper size	40 Taper
Drive system	Direct speed, belt drive
Maximum torque	33 ft-lb@ 1200 rpm
Maximum thrust rating	2000 lb
Cutting feed	200 to 400 ipm
Tool storage capacity	20 Tools
Max tool diameter with adjacent tools	5.31"
Max tool weight	12 lb
Tool-to-Tool (avg)	5.7 sec
Spindle drive	5.7 sec

Along with the dynamometer, a workpiece block is fastened on the table of CNC milling. It is very important to know that the dynamometer is used to measure the force of cutting a thing with the machine. On the other side, a CNC program is applied to cut the block in 120 mm of length. MarSurf PS (a portable tester used to calculate the roughness on a surface) is used on the surface of the block of the workpiece from different locations before going further. After this, a Scanning Electron Microscope is used to categorize the integrity of the surface. An advanced optical video computing system is used to evaluate the effectiveness of the cutting tool. The tool holder is removed from the panel of the testing machine, during the measurement of the operation. Flank wear is tested by using it on cutting 120 mm long block. After the first half, the tool wear at the face of the flank is measured to get the accurate result. The frequency of the tool wear is depended upon the rate of growth when the wear. After it, the final parameter of the tool wear is called the optimal tool wear. The actual life of the tool is calculated by the total time of the cutting the cutting-part to get a specific tool life. During the milling operation, the Kistler charge Amplifier model 5070 and Kistler dynamometer model 1679A5 are used to measure the cutting force. These tools save the data of the critical forces into the computer for future analysis. At the end of this experiment, the chips are examined to know the mechanism of them. The method which is used to collect data from these chips describes as follows:

Figure 3.6: CNC milling machine HAAS TM-2

Measuring Surface Roughness: For removing the coolness and oiling of machine while measuring the roughness of the surface the workpiece was dipped in an ultrasonic bath. To measure the surface roughness, a tester was used of model Marsurf PS1 whose value is represented as R_a. For calculating the mean surface roughness, 6 readings were taken: 2 from a space of 30 mm, 2 at the centre and 2 from the distance measuring 90 mm. SEM is used to measure the surface integrity of model Hastelloy C-2000. The cutting pieces of the workpiece are then go through the process of polishing and grinding to clear the dirt and coolant as the workpiece was fixed by a certain fixing methodology. A mixture of epoxy and hardener was poured in a little container of size 30 mm in diameter. Before the next stage, the specimens were kept to dry out and get hardened. Then with a Cameo Platinum with a wheeler having speed of 150 rpm was used to grind the fixed workpiece. Following this process, polishing starts with a Cameo silver disc of 6 micron having a speed of 150 rpm, then again a Cameo White FAS Disc of 3 micron with a diamond mixture, along with the diamond mixture of 1 micron and red cloth plus a micro extender of speed 200 rpm. Before the last process of giving the ultrasonic bath to get rid of the coolant and residue, polishing was done with colloidal silica of 0.05 micron along with imperial cloth and water having a wheeler speed of 150 rpm. The ultra sonic bath was given by Aqua Regia-Glycerol an etching compound, and before this specimen was cleaned with an ultrasonic cleaner.

Measuring Flank Wear: During the machining while last milling operation a flank wear inserted on the mill was determined after each pass on the specimen i.e. workpiece with an ISO 8688-2:1989 (E) tool with a constant wear criterion of 0.3 mm. This tool flank was chosen by looking at the different modes of failure predicted accordingly. It continues recording of each pass during the cutting till the insert collide its end criterion.

Tool Life Measurement: The complete cutting duration of the cutting session at a particular tool-life principle is termed as tool life. It is defined as a calculated value of particular types of tool wear as per recommendations. During the machining of steel while end milling a recommended ISO 8688-2:1989 (E) tool of uniform wear of 3.3 mm along with the maximum wear criterion of about 0.5 mm is used. The process implemented during the trial is: highest flank wear = 0.3 mm, fracture or catastrophic

and also maximum wear standard = 0.5 mm. The trial stops immediately on reaching any of the mentioned criterions.

Cutting Force Measurement: Kistler Force Dynamometer is utilized to measure the cutting force throughout the machining session going on.

Chip Collection and Measurement: As illustrated in Figure 3.7, the chips were trapped by using a net while the machining session going on. This method is considered easier than others. Before the examination done by scanning of electron microscope, the chips were grinded and polished just like it is done for the surface integrity.

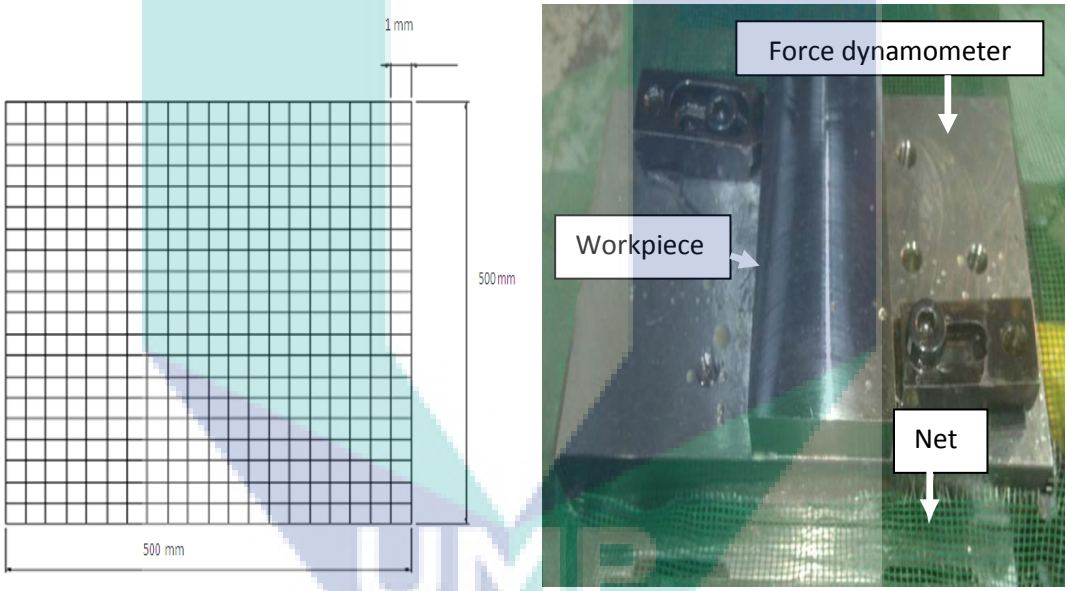

Figure 3.7: (a) Dimension of the net (b) Workpiece covered with net to collect the chips.

3.4.5 Cutting Fluid

The mineral oil is a rough classification of cutting fluids which is further differentiated as mixtures and emulsions. It posses characteristics like they are vastly combustible, inefficient at elevated cutting paces, greasy and are found at relatively high prices. A homogenous mixture is formed by the composition of mineral oils and emulsifiers. A stumpy surface layer is produced with the help of stabilizers including chlorine, sulphur and phosphor, detergents, rust controllers, foam controlling agents, as

well as steam controlling agents so as to diminish the friction (Nachtman, 1995). Mineral oils are not present in the solution which is soluble in water. The mineral oil was restored by synthesized hydrocarbons, forming synthetic fluids. When emulsified oil is mixed in this fluid, it forms semi-synthetic fluid possessing mutual properties. X-Ten C 30 is the cutting fluid which is used as a synthetic brand in the overall research and literature. It is a synthetic fluid which can be used on different alloys and metals. It protects the alloys and metals used in the machines against corrosion and have the ability to cool the objects. It generally increases the years of life of the tools used for cutting through its coolant property as well as anti corrosion ability. The suggested strength and ratio of the coolant is around 1:10 to 1:20 and is used in a range of manoeuvres like drilling, grinding and milling.

3.4.6 Physical Equipments

The operations that particularly required cutting off pieces of work, a vertical milling machine was used namely HAAS TM2 for such operations and this machine can be viewed in Figure 3.6 above section. This is also known as a CNC milling machine commonly. This machine is firm for its operations and is perfect for end milling; it is a highly accurate machine. The machine center is driven by a 5.6 kW stepless motor which provides high torque. The experimental setup can be viewed in Figure 3.8.

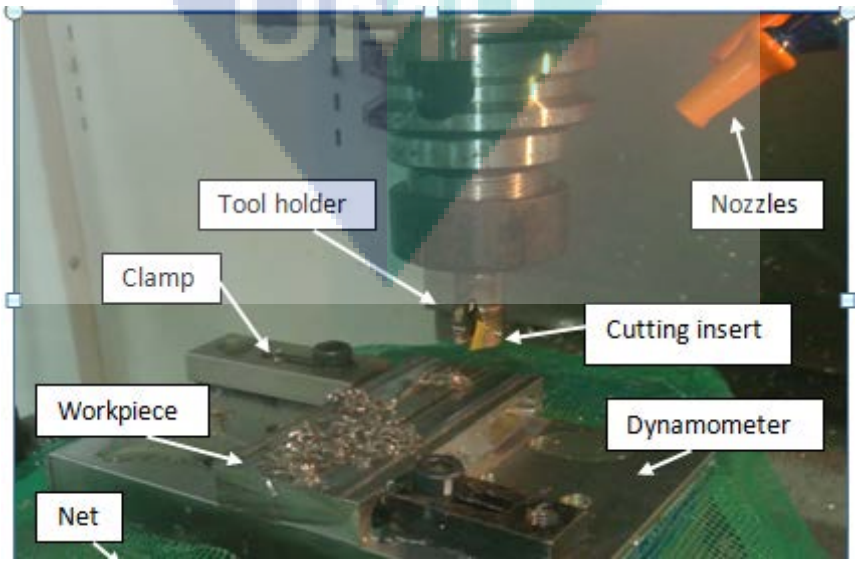

Figure 3.8: Experimental set up

Surface Roughness Tester: Figure 3.9 shows a portable roughness tester model MarSurf PS1, which measures the arithmetic average roughness of a surface (R_a). Basically, the purpose of this model is to measure the roughness of the machined surface which occurs during an experiment.

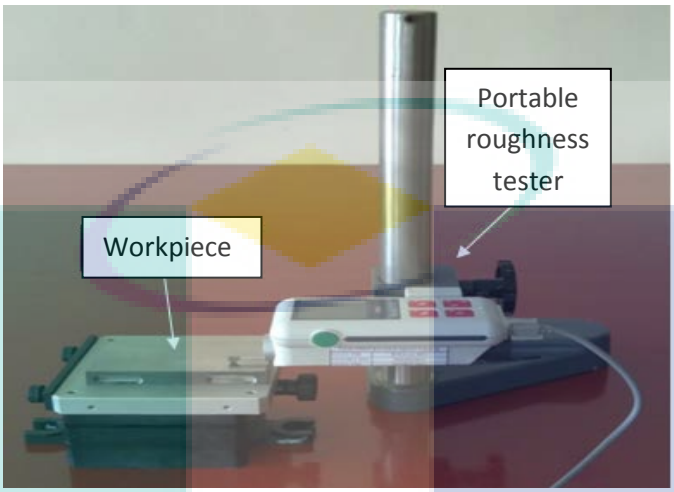

Figure 3.9: Portable roughness tester, MarSurf PS1

Optical Video Measuring System: For capturing the wear progress at the edge where cutting has taken place, from the period when first pass takes place to the end of tool's life, an optical video measuring system model SOV-2010 (N/A) is used as shown in Figure 3.10.

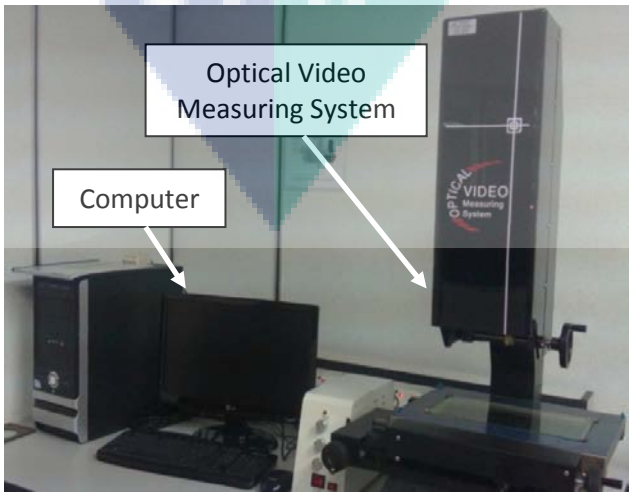

Figure 3.10: Optical video measuring system

Scanning Electron Microscope: SEM observes the microstructures of the tools very closely and then measures the damage or the defects present on it. By doing this, it has played a very significant role, and has helped to a great extent in this study. Figure 3.11 shows the picture of a Scanning electron microscope model XL 40. This model is outfitted with EDAX *X*-ray system. SEM consists of a filament, which is just 40 to 50 μm. This filament has the capability to magnify the image up to 50,000*X*. On *X* and *Y*-axis the movement range is about 150 mm, and the unusual working distance is 10 mm.

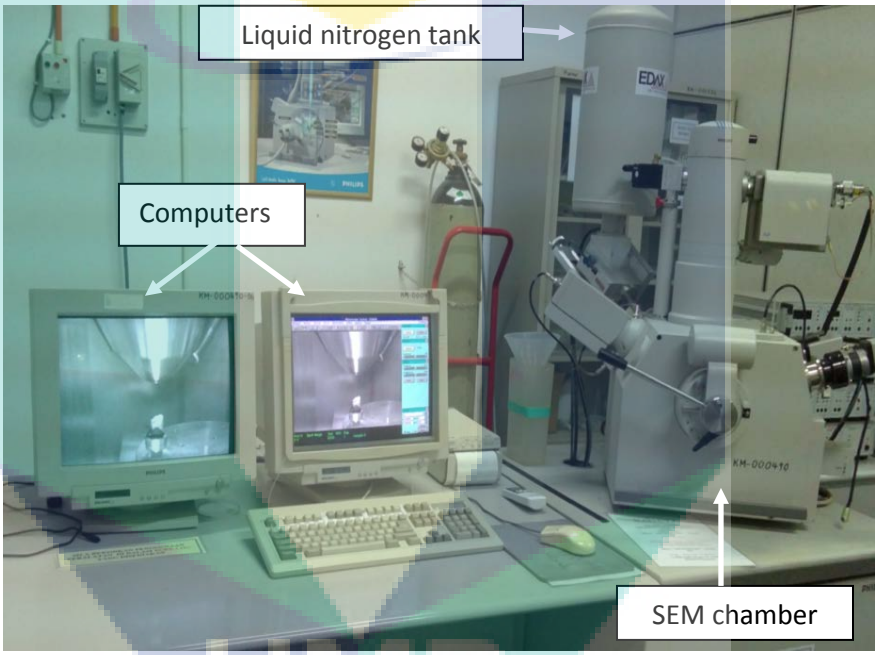

Figure 3.11: Scanning electronic microscope (SEM) model XL40

Force Dynamometer and Charge Amplifier: Figure 3.12(a) shows a Kistler force dynamometer model 1679A5 for the purpose of recoding the force of cutting during the milling operations. The output signals of dynamometer are changed into voltage signals by the Kister dual mode charge amplifier, model 5070 as in Figure 3.12 (b). This change is done for the acquisition system and this is demonstrated in Figure 3.12(c). As per the sensitivity of the output force of the dynamometer the sensitivity of the charge amplifier is set. Dynamometer is rigid and gives a high natural frequency. Due to the high resolution of the dynamometer even the slightest changes in outsized forces are measures easily.

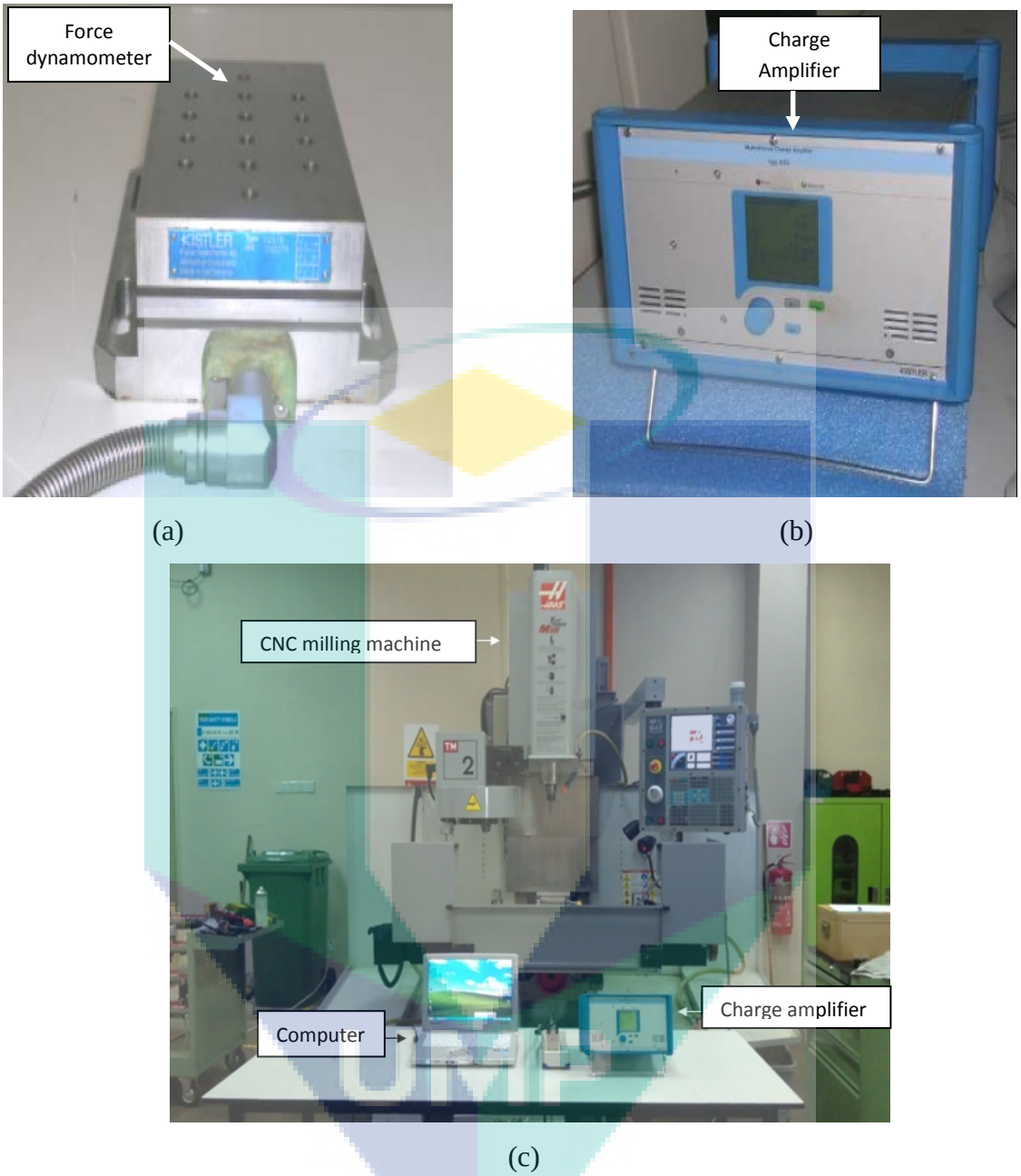

Figure 3.12: (a) Force dynamometer; (b) Model 5070 of Kistler dual mode charge amplifier; (c) The setting of force dynamometer and charge amplifier at CNC milling machine

Grinding and Polishing Machine: The purpose of this machine is to prepare the workpiece along with the tools that are to be used for cutting. It prepares the tools by providing polish and grinding them. The tools pass through this machine before they undergo they undergo the surface integrity investigation test by the scanning electron microscope. Once the workpiece has gone through the machine, they are given an ultrasonic bath. Ultrasonic bath removes the presence of any residue or coolant.

Chemicals along with cloths are used in this mechanism of polishing and grinding. Cloth, grinding machine, ultrasonic bath and chemicals are shown in Figure 3.13.

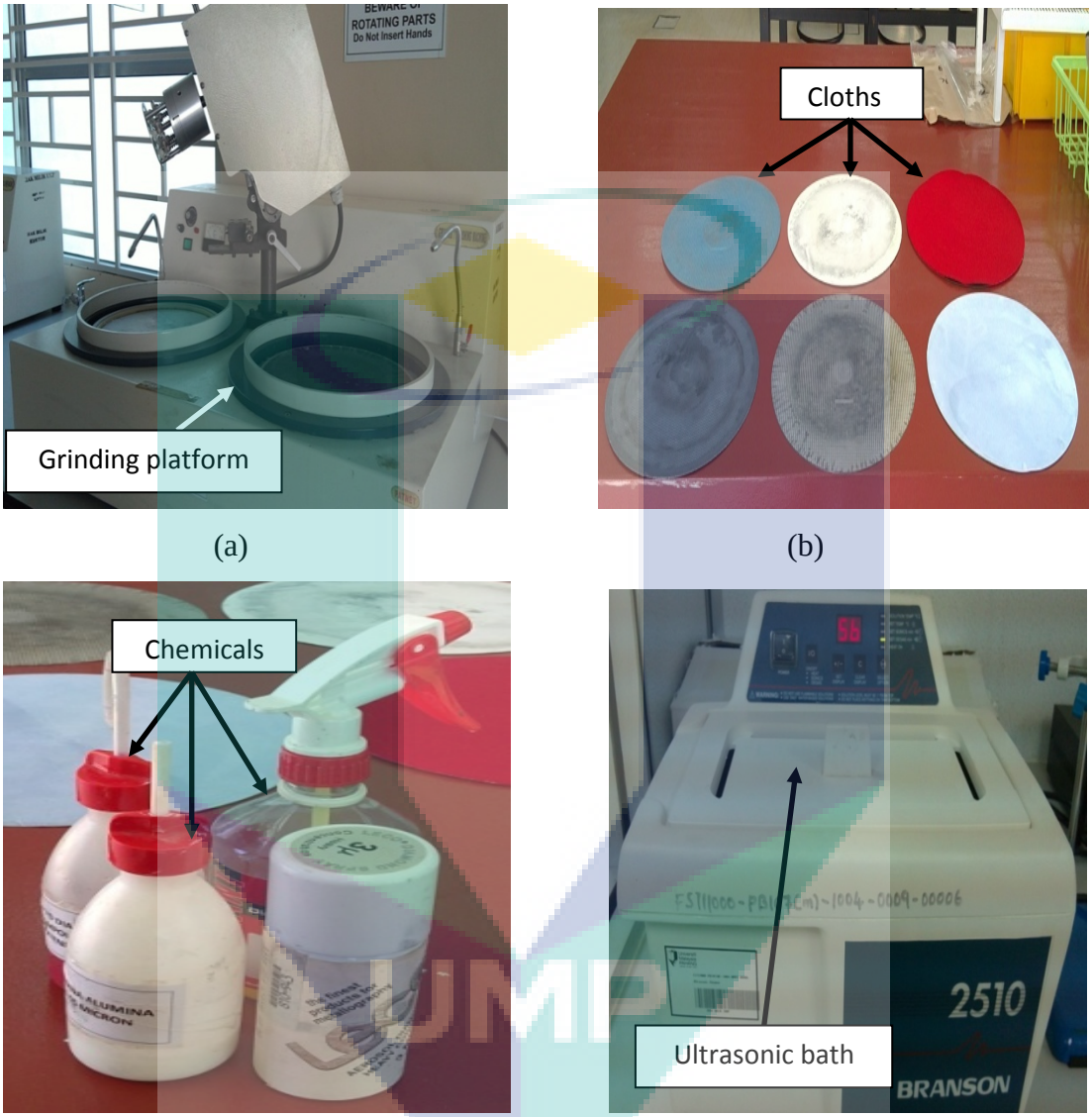

Figure 3.13: (a) Grinding machine, (b) Cloths, (c) Chemicals, (d) Ultrasonic bath

3.5 MATHEMATICAL MODELLING

3.5.1 Response Surface Method

RSM is basically a statistical and mathematical approach which is used by the researchers, it makes the solutions of engineering processes easy (Gayton et al., 2003).

RSM can also be regarded as a technique which is aimed to optimize the response that is being influenced by many factors (Montgomery, 2005). RSM came into existence to develop model experimental responses (Box and Draper, 1987). It is assumed that the output y is dependent on input $x_1, x_2, \ldots, x_n$, (Myers, 1971).

The problems that arise in RSM deal with both these models. All the factors of these models are independent of each other. For achieving the best possible results for approximation polynomials, the data are collected by using proper experimental designs. Best understanding about the RSM could be attained by knowing the topography of responses (local maximum, local minimum, ridge lines) and also by finding out the place where optimal response takes place. The target of RSM is to move with efficacy along the path to attain maximum or minimum responses, for getting optimized response (Kwak, 2005). RSM builds relationship between different cutting factors and characteristics of machines. The factors include; axial depth, feed rate, cutting speed, while the machine characters comprise of the tool life, surface roughness and cutting force. Eq. (3.12) gives the mathematical expression:

$$Y = f(X_1, X_2, X_3) + \varepsilon \tag{3.12}$$

where Y is a dependent variable and is a function of X_1, X_2, X_3. Experimental error is denoted by ε. All other variations, which are not considered by f, are taken in by the error term along with any other measurement error that occurs on a response. This error is a statistical one and is distributed with variance, s^2 and zero mean. Within this work, it will be taking X_1, X_2, X_3 as feed rate (F_R) and axial depth would be taken as A_D. C_S would be denoting cutting speed, and Y takes place of responses. Responses are tool life (TL), surface roughness (SR) and cutting force (CF). Therefore, Equation (3.8) can also be written as Eq. (3.13).

$$Y = f(F_R, A_D, C_S) + \varepsilon \tag{3.13}$$

In terms of SR, TL and CK, the equations can be written as, Eq. (3.14), Eq. (3.15) and Eq. (3.16) respectively.

$$SR = f(F_R, A_D, C_S) + \varepsilon \tag{3.14}$$

$$TL = f(F_R, A_D, C_S) + \varepsilon \tag{3.15}$$

$$CF = f(F_R, A_D, C_S) + \varepsilon \tag{3.16}$$

3.5.2 First-Order Model

The function *f* is not known in most of the problems of RSM. Experimenter must commence his work with a low order polynomial within a few small regions, like this they can achieve a better understanding for *f*. When linear function of independent variables is used to define the response, then the first order model is applied for approximating function. Eq. (3.17) gives an illustration of the first order model along with two variables, which are independent.

$$y = \beta_0 + \beta_1 x_1 + \beta_2 x_2 + \beta_3 x_3 + \varepsilon \tag{3.17}$$

The three further equations have been formed by taking the responses as endogenous variables *SR*, *TL* and *CF* and the input parameters as exogenous variables F_R, A_D, and C_S. Eq. (3.17) can be formulated further as Eq. (3.18), Eq. (3.19) and Eq. (3.20) respectively by neglecting error term ε.

$$SR = \beta_0 + \beta_{S\,R1} F_R + \beta_{SR2} A_D + \beta_{SR3} C_S \tag{3.20}$$

$$TL = \beta 1 + \beta_{TL1} F_R + \beta_{TL2} A_D + \beta_{TL3} C_S \tag{3.21}$$

$$CF = \beta 2 + \beta_{CF1} F_R + \beta_{CF2} A_D + \beta_{CF3} C_S \tag{3.22}$$

where, β_0 is the intercept coefficient and the other coefficients β_1, β_2,and β_3 are the model parameters which describe the linear effect of the connecting factor.

3.5.3 Second-Order Model

The approximating function by constituting two variables is called a second-order model as shown in Eq. (3.23).

$$Y = \beta_o + \sum_{j=1}^{k} \beta_j X_j + \sum_{j=1}^{k} \beta_{jj} X_j{}^2 + \sum_{i<j} \sum_{j=2}^{k} \beta_{ji} X_j X_i + \varepsilon \tag{3.24}$$

where Y represent the corresponding responses such as *SR*, *TL*, *CF*, that yield by the several variables. X_j represents the input variables such as F_R, A_D and C_S; $X_j{}^2$ is square of the input variables, and X_jXi is multiplication term of the input variables. The estimators β_0, β_j, β_{jj} and β_{ij} are the second order regression coefficients. Equation (3.24) can be written as Eq. (3.25):

$$y = \beta_0 + \beta_1 x_1 + \beta_2 x_2 + \beta_3 x_3 + \beta_{11} x_1^2 + \beta_{22} x_2^2 + \beta_{33} x_3^2 + \beta_{12} x_1 x_2 + \beta_{13} x_1 x_3 + \beta_{23} x_2 x_3 + \varepsilon \tag{3.25}$$

where x_1, x_2, x_3 are feed rates (measured in mm/tooth), axial depth (measured in mm) and cutting speed (measured in m/min) respectively. The three further equations of the fitted model by taking *SR*, *TL* and *CF* as endogenous variable are indicated in Eq. (3.26), Eq. (3.27) and Eq. (3.28) respectively

$$SR = \beta_0 + \beta_1 F_R + \beta_2 A_X + \beta_3 C_S + \beta_{11} F_R^2 + \beta_{22} A_X^2 + \beta_{33} C_S^2 + \beta_{12} F_R A_X + \beta_{13} F_R C_S + \beta_{23} A_X C_S + \varepsilon \tag{3.26}$$

$$TL = \beta 1 + \beta_1 F_R + \beta_2 A_X + \beta_3 C_S + \beta_{11} F_R^2 + \beta_{22} A_X^2 + \beta_{33} C_S^2 + \beta_{12} F_R A_X + \beta_{13} F_R C_S + \beta_{23} A_X C_S + \varepsilon \tag{3.27}$$

$$CF = \beta_2 + \beta_1 F_R + \beta_2 A_X + \beta_3 C_S + \beta_{11} F_R^2 + \beta_{22} A_X^2 + \beta_{33} C_S^2 + \beta_{12} F_R A_X + \beta_{13} F_R C_S + \beta_{23} A_X C_S + \varepsilon \tag{3.28}$$

All above three equations represent the second-order polynomial models, which measure the relationship between the machining characteristics of Hastelloy C-2000 (*SR*, *TL* and *CF*) and the process parameters (F_R, A_X and C_S). The first- and second-order RSM were established on the basis of the experimental results. In order to estimate the proposed responses, it is essential to determine the relationship through the designed mathematical models. Therefore, the different statistical tools were carried out to measure for the linear and polynomial models to estimate the adequacy of the fitted model, such as analysis of variance.

3.5.4 Analysis of Variance

Analysis of variance (ANOVA) is a collection of statistical technique that represents a set of models that can be fit to data, and also a set of methods that can be used to summarize an existing fitted model (Gelman, 2005). It is the smart method of comparing the mean values from more than two samples. ANOVA has been considered to be vital in order to determine which factors have a significant effect on the response (*SR*, *TL* and *CF*), and how much of the variability in the response variable (*SR*, *TL* and *CF*) is attributable to each factor. The ANOVA technique measures the coefficient of determination (R^2), *F*-ratio, *P*-value, the standard error of the regression (*S*), and adjusted R^2 of the model. The estimated results of ANOVA include other terms, like: sources of variance, their degree of freedom (*DF*), the total sum of squares, and the mean squares. The coefficient of determination of R^2 can be determined as Eq. (3.29).

$$R^2 = \frac{\text{Regression sum of squares (RSS)}}{\text{Total sum of squares (TSS)}} \tag{3.29}$$

where, the total sum of squares (TSS) is equal to the sum of regression sum of squares (RSS) and the residual sum of squares (SSE).

R^2 is the coefficient of determination is defined as the ratio of the sum of squares explained by a regression model and the "total" sum of squares around the mean. R^2 measures the proportion of the total variation that is explained by the sample regression equation. The value of R^2 lies in between 0 and 1. A high R^2 value indicates that much of the variation in the regression and is explained by the sample regression equation (by the regressors), which in a regression framework means that model the data well. The value of R^2 also suggests that very little of the variance is explained by the random error term. Mean square error (MSE) is the ratio of the sum of square of residuals (SSE) to the degree of freedom. The *F*-ratio is a useful test statistics that is associated with ANOVA, which determine whether the variances in the two independent data sets are equal. It also defined as how different the means are relative to the variability within each sample. When the variances between two data sets are equal, then the value of the *F*-test is equal to 1. A large *F*-ratio value is an indication of significant differences

between the data sets. A large *F*-value shows that the average treatment (between) variation is larger than the error (within) deviation. The *P*-value is the probability of obtaining a test statistic, given that the samples are of the same population. Therefore, for large *P*-value, it is likely that the samples are part of the same population. The hypothesis that the samples are of the same population is known as the null hypothesis (H_0)**.** Furthermore, for a *P*-value greater than the significance level (larger than 0.05, in general), analysis would be said to not reject the null**.** The *P*-values less than the significance level, suggest that the null hypothesis is false and the results is said to be statistically significant.

3.6 ARTIFICIAL NEURAL NETWORK

3.6.1 Introduction

Artificial neural network (ANN) has been defined by Luo and Unbehauen (1998), as "a model of reasoning based on the human brain". According to them, the human brain comprises of a densely interconnected set of nerve cells, or basic information-processing unit, called neurons. Furthermore, ANN is basically a computational model at human brain than assumes that computational is distributed over several interconnection processing element called neurons. The brain can perform its functions much faster than the fastest computer by using these multiple neurons simultaneously. Although, the structure of each neuron is very simple, like an army of such elements constitutes a tremendous processing power. A neuron comprises of a cell body, soma, a lot number of fibres which is called as dendrites, and a single long fibre called the axon. While dendrites branch into a network around the soma, the axon stretches out to the dendrites and somas of other neurons. A schematic drawing of a biology neural network is depicted in Figure 3.14 (Negnevitsky, 2004).

By the complex electrochemical reactions, the different types of signals are broadcasted from one neuron to another. In this process, the chemical substances released from the synapses cause a change in the electrical potential of the cell body. When the potential reaches its threshold level, an electrical pulse, action potential is sent down through the axon. The pulse spreads out and eventually reaches synapses, causing

them to increase or decrease their potential. Conversely, the most intriguing discovery is that a neural network shows plasticity. The strength of the connections of neurons is modified for a long-standing time period as a reaction to the stimulation pattern. Neurons also have the ability to develop new links with other neurons. The neuron is a recipient to information from many other neurons at the synapses. Approximately, one neuron may be a recipient to stimuli from around 10 000 neurons. Even whole groups of neurons may relocate from one region to another. These mechanisms make up the foundation of learning in the brain. A neuron is basically an information-processing element that is essential for a neural network to work properly. The three core elements of a neuron model can be identified. The non-linear model of a neuron is illustrated in Figure 3.15.

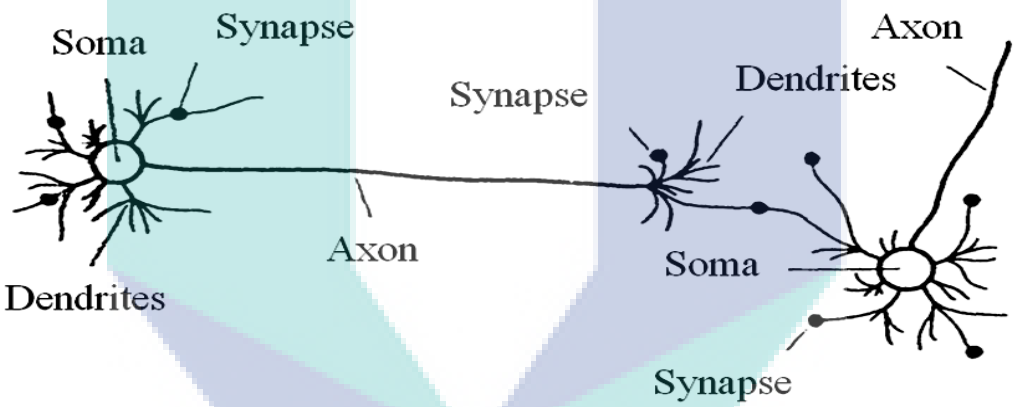

Figure 3.14: Schematic drawing of biology neural network

Their own force distinguishes a collection of synapses. Distinctively, the presence of a signal x_j at the input of synapse j linked with neuron k is multiplied by the weight of the synapse W_{kj}. It is significant to pay attention to the way the subscripts W_{kj}, representing the synaptic weight, are written. The neuron in question is represented by the first subscript, and the second subscript represents the input side of the synapse, which the weight represents. The weight W_{kj} becomes positive when the linked synapse is excitatory in nature. However, when the synapse is inhibitory in nature, then the weight W_{kj} is negative. This is basically an activation function to decrease the amplitude of the output of a neuron. It has also been called as the squashing function in the previous literature, since it squashes (reduces) the allowable amplitude range of the

output signal produced by a neuron to a finite value. Usually, the regulated amplitude range of the output signal generated by a neuron is scribed as the closed unit interval [0, 1] or otherwise [-1, 1]. The neuron model consists of an outwardly applied bias (threshold) $w_{k0} = b_k$ that influences the activation function by decreasing or escalating its net input. Mathematically, this pair of Eq. (3.30), Eq. (3.31) and Eq. (3.32) respectively, may be used to explain a neuron *k*.

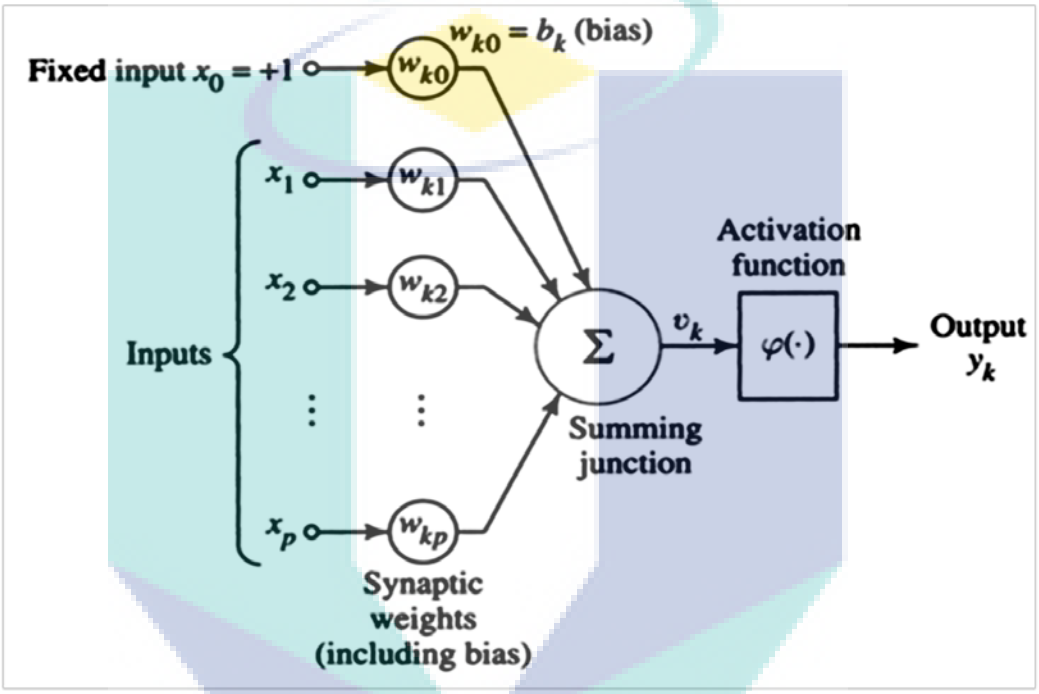

Figure 3.15: Non-linear model of a neuron

$$V_k = \sum_{j=1}^{p} W_{kj} X_j \tag{3.30}$$

$$Y_k = \phi(V_k) \tag{3.31}$$

And

$$V_k = \begin{bmatrix} W_{k0} & W_{k2} & \ldots W_{kp} \end{bmatrix} \begin{bmatrix} X_0 \\ X_1 \\ . \\ . \\ . \\ X_p \end{bmatrix} = W_K^T X \tag{3.32}$$

3.6.2 Training Algorithm

Artificial neural systems are made on the basis of the simplified version of the human brain's biological roles. As a result, these systems are very competent with respect to computational systems where complicated factual world issues are represented (Svozil et al., 1997). Neural systems can be categorized into two types. Feed forward with respect to their activation period, and as supervised and unsupervised with respect to the learning period. Feed forward systems only permit one-way journey of signal from input to output. No feedback is present. No layer is influenced in any way by its own output the data dispensing can be expanded to include several units (Marini et al., 2007). The supervised training requires input and output information in the training procedure like Recurrent Cascade Correlation, Boltzman Machine, and Back propagation (Maren et al., 1990). A vital constituent of the supervised is the easy accessibility of an outside guide that is able to give the neural system a target reaction. The joint effect of the training vector and the error signal adjusts the system boundaries. The regulation is done on a step-by-step basis, with the objective of making the neural system imitate the trainer in due time. This type of supervised learning is actually error-connection learning, as has been previously explained. Figure 3.16 illustrates supervised learning.

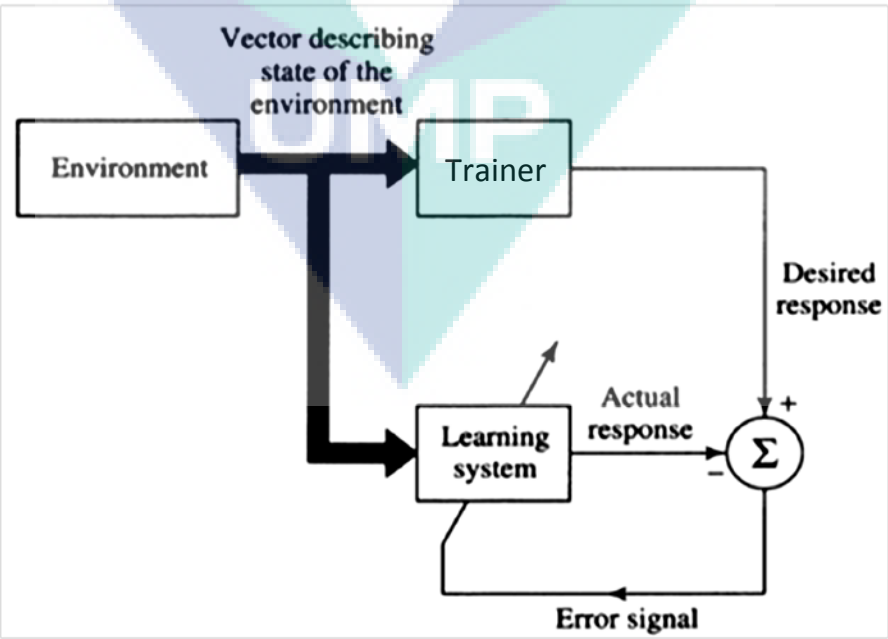

Figure 3.16: Typical example of supervised learning

Supervised learning is needed for pattern matching, and one of the most widely accepted supervised learning methods is back propagation. The back propagation archetype modifies the linkage weights to decrease the output error. In the opening condition, the system contains an arbitrary set of linkage weights. When a network begins with all linkage weights equivalent, the system initiates a type of domestic optimum, and will not unite with a world-wide answer. For the system to learn, a collection of inputs is given to the network, and a group of outputs are deliberated. The disparity between the real outputs and the preferred outputs is deliberated, and the linkage weights are adjusted to decrease this disparity. The current researches have the aim to utilize the supervised system with perceptrons consisting of many layers, and train using the back propagation algorithm (with momentum). The input outline contains the control variables, which are utilized in the machining process (feed rate, axial depth and cutting speed), while the constituents of the output outline show the replies from sensors (surface roughness, tool life, and cutting force). The nodes found in the concealed level are mandatory to put into practice the nonlinear mapping between the input and output outlines.

3.6.3 Multilayer Feed Forward Network

Multilayer feed forward neural system, also known as multilayer perceptron (MLP), is very renowned, and is utilized more than the other neural system type for a large variety of deeds (Kumar and Yadav, 2011). Multilayer feed forward neural system understands using the back propagation algorithm, and is made on the basis of supervised process. The system builds a representation, which has roots in examples of information with recognized output. It has constructed the representation exclusively from the examples given, which are said to innately hold the data essential to building a link. An MLP is a potent system, usually proficient in constructing complicated connections among variables (Mohd Zain et al., 2010). It permits the forecast of output object for a presented input object. The infrastructure of MLP is a feed forward neural system consisting of various levels, in which the non-linear constituents (neurons) are assembled layer-by-layer, and the data flow is one-way from the input level to output level, via concealed level(s). The more the amount of levels, the more time required for training, and unsteady networks are produced (Radhakrishnan and Mohamed, 2000),

and train excessively (Yue et al., 1998); however, it generates improved results (Crowther and Cooper, 2001).

A MLP containing only one incognito level can learn to estimate basically any task to any extent of accuracy. Due to this reason, MLPs are termed as universal approximates, and can be utilized even when it only has a slight amount of previous knowledge of the connection between input and goal. One incognito level is enough, given that ample amount of information is provided. Figure 3.17 illustrates a MLP with one incognito level, having X_1, X_2, X_3, ..., X_m as input parameters, W_m as the weighting matrix for the incognito layer, and R as the exterior parameters for the reaction.

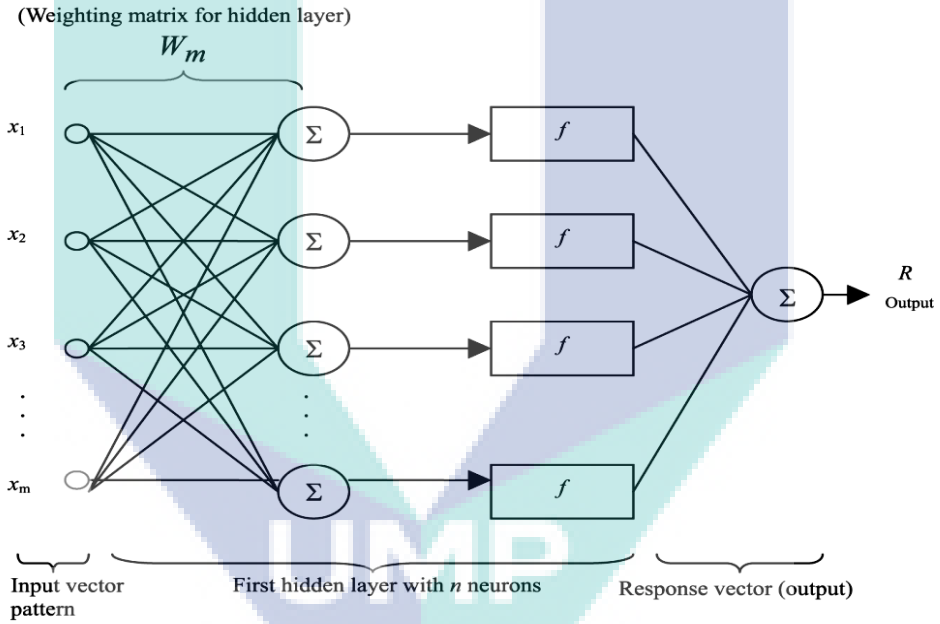

Figure 3.17: MLP with one hidden layer

The neurons found in between the levels are joined by the links, which have synaptic weights. The error back propagation training algorithm is made on the basis of weight updates, so that the sum of squared error for k amount of output neurons is decreased. As shown in Eq. (3.33)

$$E = \frac{1}{2}\sum_{k=1}^{k}(d_{k,p} - o_{k,p})^2 \tag{3.33}$$

where $d_{k,p}$ = the desired output for p_{th} pattern.

The weights of link are updated as Eq. (3.34).

$$w_{ji}(n+1) = w_{j_i}(n) + \eta\delta_{pj}o_{pi} + \alpha\Delta w_{ji}(n) \tag{3.34}$$

where n is the learning step, η is the learning rate and α is the momentum constant and δ_{pj} is the error term. Then it followed by Eq. (3.35) and Eq. (3.36).

$$\text{For output layer} = \delta_{pk} = (d_{kp} - o_{kp})(1 - o_{kp}) \qquad k = 1 \ldots\ldots k \tag{3.35}$$

$$\text{For input layer} = \delta_{pj} = o_{p_j}(1 - o_{pj})\sum \delta_{pk} w_{kj} \qquad j = 1 \ldots\ldots j \tag{3.36}$$

where, j denotes the number of neurons present in the hidden layer. When small values of weight are randomly assigned to all the links, then only the training process is commenced. The patterns of input and output come along one by one and keep on updating the weights. At the end of each period, the mean absolute error (MAE) is computed as per Eq. (3.37).

$$MAE = \frac{1}{NP}\sum_{P}^{NP}\sum_{k=1}^{k}(d_{kp} - o_{kp})^2 \tag{3.37}$$

In this equation, *NP* gives the number of training patterns. When the target is achieved then the training process will come to an end.

3.6.4 Back Propagation Algorithm

Back propagation is the most well known example of supervised learning, which is provided to train the MLP network (Nalbant et al., 2009; Abeesh et al., 2008; Erzurumlu and Oktem, 2007; and Cus and Zuperl, 2006). Back propagation aims to achieve very less errors in the prediction of the training set, and it achieves this objective by making adjustments to the threshold and the weight. Figure 3.18 gives an illustration of a typical example of back propagation ANN. The figure shows that for every node, i is the input value, I_i^n is the layer, while n is linked with each node j, via a weight of w_{ij}^n. It can be seen in Equations (3.38), (3.39) and (3.40) that when

multiplication of input and weight values takes places unfairly then the outputs received are H_{nj}^{n} (hidden node) and O_j^{n} (output node) (Takashi, 2000). Artificial neural networks of back propagation are shown in Figure 3.18.

$$H_{ij}^{1} = f\left(\sum_{i=1}^{m} I_i \, w_{ij}^{1} + b_{ij}^{1}\right) \tag{3.38}$$

$$O_j = f\left(\sum_{i=1}^{m} H_{ij}^{1} w_{ij}^{2} + b_{ij}^{2}\right) \tag{3.39}$$

And

$$O_j = f\left(\sum_{j=1}^{m} f\left(\sum_{j=1}^{m} I_i \, w_{ij}^{1} + b_{ij}^{1}\right) w_{ij}^{2} + b_i^{2}\right) \tag{3.40}$$

With the layer *n*, b_i^{n} is the threshold and neuron is denote by *i*th. Here, *n* is equal to 1, and the function *f* is given the name of hidden node and output node activation function for H_{nij}^{n} and O_j^{n}.

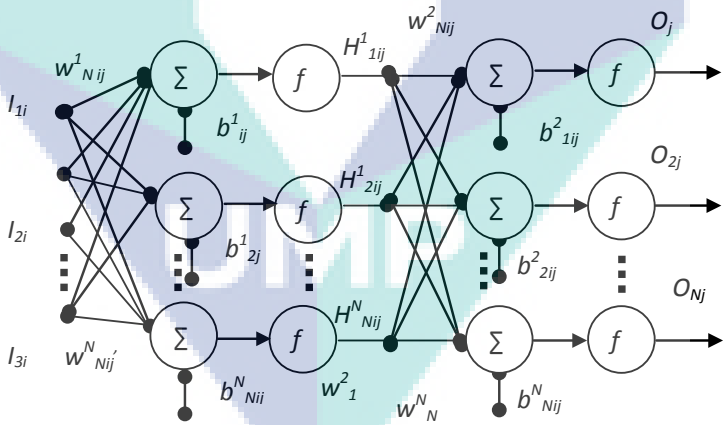

Figure 3.18: Back propagation algorithm artificial neural networks

Source: Demuth and Beale (1998)

In back propagation, three types of activation function are used, namely; linear (purelin), tangent hyperbolic (Tansig) and sigmoid. When moving from input to hidden node, non linear functions are used. Tansig and sigmoid are the non-linear functions. As "*S*" shaped curve is produced by sigmoid and Tansig function. The output of the

sigmoid function varies in between [0, 1], while the output of tanh varies between [-1, 1]. For getting an output node from the hidden node, a purelin function is used. Non-linear function is also known as hyperbolic tangent function, and is written just as Eq. (3.41) is written (Abeesh et al., 2008; Al-Ahmari, 2007; Oktem et al., 2006; Ezugwu, 2005). Figure 3.19 shows the hyperbolic tangent activation function.

$$\tanh(x) = \frac{\sinh(x)}{\cosh(x)} = \frac{e^{x} - e^{-x}}{e^{x} + e^{x}} \tag{3.41}$$

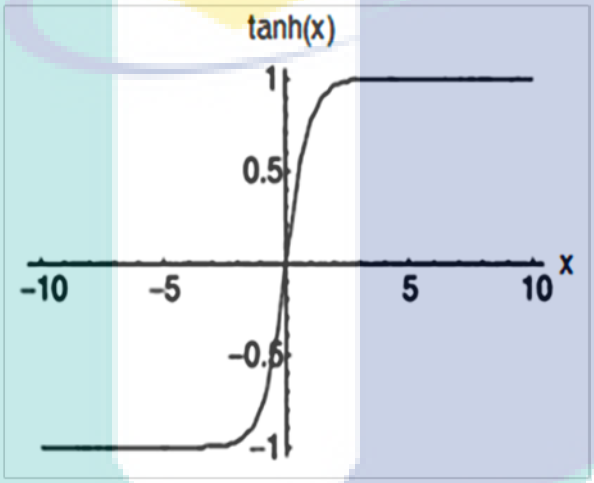

Figure 3.19: Hyperbolic tangent activation function

For giving appropriate results, ANN learns through the input data and then the adjustment is made to the weight. During the training session, the data are collected, and on the basis of collected data, the number of hidden layers are determined, states Maren et al. (1990). Training involves a greater time period when the number of hidden layers is more, and this results in unstable networks as well (Radhakrishnan and Mohamed, 2000). At times over training (Yue et al., 1998) also takes place under this situation, to give much better results (Crowther and Cooper, 2001). Training is provided to an extent that the chances of errors are minimized to the least. When the errors are less in number then very few adjustments would also be required. Weights are figured out on the basis of input data, which corresponds with the output data. While ANN process takes place, the weights are adjusted in a random manner. This research work has used back propagation algorithm along with training provided at the hands of artificial neural

network. This algorithm makes use of supervised training mechanism in situations where network weights are initialized in a random manner, just at the commencement of the training period. In order to fit in the hyperbolic function model, patterns are normalized appropriately between 0 and 1 (Grabec and Kuljanic, 1994). As the iteration numbers increase and reach up to a limit of 10000, the number of errors decreases. Error criterion is considered along with the number of iteration. An experiment was performed on the trial and error basis (Mohd Zain et al., 2010). Under this experiment, training session was stopped after 10000 iterations. Three inputs, namely; feed rate, axial depth and cutting speed were used, while the output parameters were; the surface roughness, tool life, and cutting force. The hidden layers along with the neurons were functioned to suit the complication of the dilemma. For activation of the hidden layer, the sigmoid function is used. For output and hidden layer, the learning rule function of back propagation was preferred. The MAE was 10^{-6}, while the number totalled to 10000. The heuristic technique grounded on the correlation of the values of coefficient and R^2 determines the finest network structure. The design of ANN for uncoated and coated cutting attachments is shown in Figure 3.20.

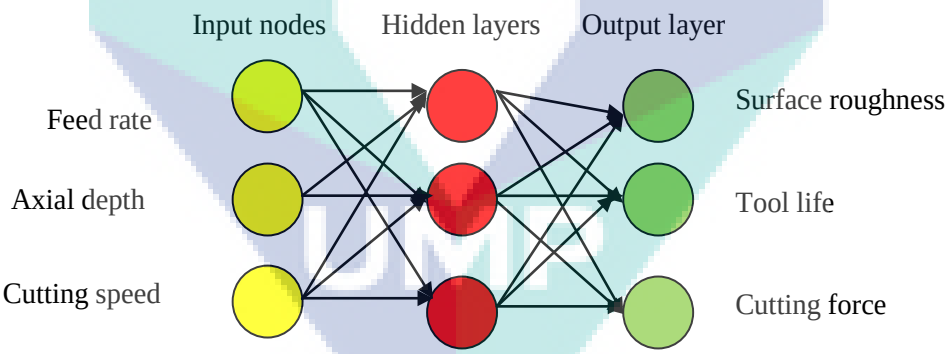

Figure 3.20: Design of ANN for uncoated and coated cutting attachments

3.7 SUMMARY

The chapter explained the technique by Hastelloy C-2000 employed by end milling processes. The chapter elucidated the features of uncoated and coated carbide cutting attachments and Hastelloy C-2000. The tentative arrangement, appropriate choice of cutting structures and the choice of Box-behnken architecture of the

experiment is clearly discussed. Techniques to examine the working of the machining process through the use of calculated modelling and mock neural network has been established. The way these approaches will work will be explained in the upcoming chapter.

CHAPTER 4

RESULTS AND DISCUSSION

4.1 INTRODUCTION

The purpose of this report is to develop a mathematical model by making use of the response surface method. The process would take place when machining Hastelloy C-2000 using coated and uncoated carbide in the end milling processes. The mathematical model would help to establish a relationship between the input variable like feed rate, axial depth, and cutting speed with the cutting responses which are the surface roughness, tool life and cutting force. Regression models have been used to carry out the optimization of the machine characteristics and the prediction of these characteristics is done by the artificial neural network (ANN). In order to extract efficient results it is essential to use the hidden layers, neuron number, training algorithm and activation functions. To make sure the best performance is achieved, the ANN and RSM are compared to the most appropriate models. The chip formation and tool wear mechanism have also been stated as part of the report.

4.2 SURFACE ROUGHNESS

4.2.1 Development of Mathematical Model

RSM has been used to develop the mathematical modelling and to optimize the machining parameters when machining Hastelloy C-2000 by using coated carbide (CTW4615) and uncoated carbide (CTP 1235). First order and second order of RSM model has been developed based on surface roughness results. Using the RSM model it is possible to find those factors which have the ability to influence the surface

roughness. This is basically done to enhance the efficiency levels of the response surface which is found to be influenced by the different parameters. The RSM also provides a quantifiable relationship with the response surfaces and the input parameters (Montgomery, 1997 and Kwak, 2005). The following eq. (4.1) is a linear model which consists of independent variables and responses correlation in order to perform the task.

$$y = a \times \text{Feed rate} + b \times \text{Axial depth} + c \times \text{Cutting speed} + d \tag{4.1}$$

where *a*, *b*, *c* and *d* are the constants and *y* is the response.

This Equation (4.1) can also be written as Eq. (4.2):

$$y = \beta_0 x_0 + \beta_1 x_1 + \beta_2 x_2 + \beta_3 x_3 \tag{4.2}$$

where, *y* is the response, x_0 = 1(dummy variable), x_1=feed rate, x_2 =axial depth, and x_3 = cutting speed. β_0 = D and β_1, β_2, and β_3, are the model parameters.

Equation (4.3) is the presentation of the second-order model:

$$y'' = \beta_0 x_0 + \beta_1 x_1 + \beta_2 x_2 + \beta_3 x_3 + \beta_{11} x^2{}_1 + \beta_{22} x^2{}_2 + \beta_{33} x^2{}_3 + \beta_{11} x_1 x_2 + \beta_{12} x_1 x_3 + \beta_{13} x_2 x_3 \tag{4.3}$$

First Order Model

To predict the surface roughness, the first order linear equation has been expressed as eq. (4.4) and (4.5) for coated and uncoated carbide inserts respectively:

For coated carbide inserts (CTW 4615):

$$y' = 0.415933 + 0.072250\ x_1 + 0.017250\ x_2 - 0.008750\ x_3 \tag{4.4}$$

For uncoated carbide inserts (CTP 1235):

$$y' = 1.3786 + 0.5939x_1 + 0.3654x_2 - 0.2170x_3 \quad (4.5)$$

Table 4.1 presents the results of the analysis of the variances of the coated and the uncoated carbide cutting inserts. The ANOVA has provided the level of adequacy of the first order model at a confidence level of 95%. According to the table 4.1, both models have *P*-values of linear source which are less than α-value (0.05) stating that they are significant as well as adequate. The values for coated and uncoated carbide of 0.301 and 0.205 respectively have been found to be unfit and insignificant since they are higher than the α-level (0.05). Hence, it is found that the effectiveness of the model which is built in the value of the surface roughness prediction date can be observed using an indicator, as the models are considered appropriate. The appropriateness of the Regression model can be judged by using the co-efficient R^2 (Davidson et al., 2008).The value of the uncoated carbide is higher than that of the coated carbide since it has been observed that coated carbide is 86.32 % and uncoated carbide is 93.57 %. Therefore, by making use of the models it is possible to extract an accurate prediction of the surface roughness which lies within the level of ±10% (Sahin and Motorcu, 2008).

Table 4.1: Variance analysis for the first order model of the surface roughness for coated and uncoated carbide

Source	**DF**	**Coated inserts**	**Carbide**	**Uncoated inserts**	**carbide**
		F-value	**P-value**	**F-value**	**P-value**
Regression	3	3.61	0.049	53.32	0.000
Linear	3	3.61	0.049	53.32	0.000
Residual Error	11				
Lack of Fit	9	2.69	0.301	4.25	0.205
Pure Error	2				
Total	14				

Note: DF= Degree of freedom

Figure 4.1 shows the contour plot of surface roughness for the coated and uncoated carbide cutting inserts. They have been compared to the feed rate, axial depth and cutting speed and the linear models has been used to develop the linear line. Hence,

with the help of this table it has been possible to note that there exists a direct relationship between the surface roughness and the axial depth and feed rate.

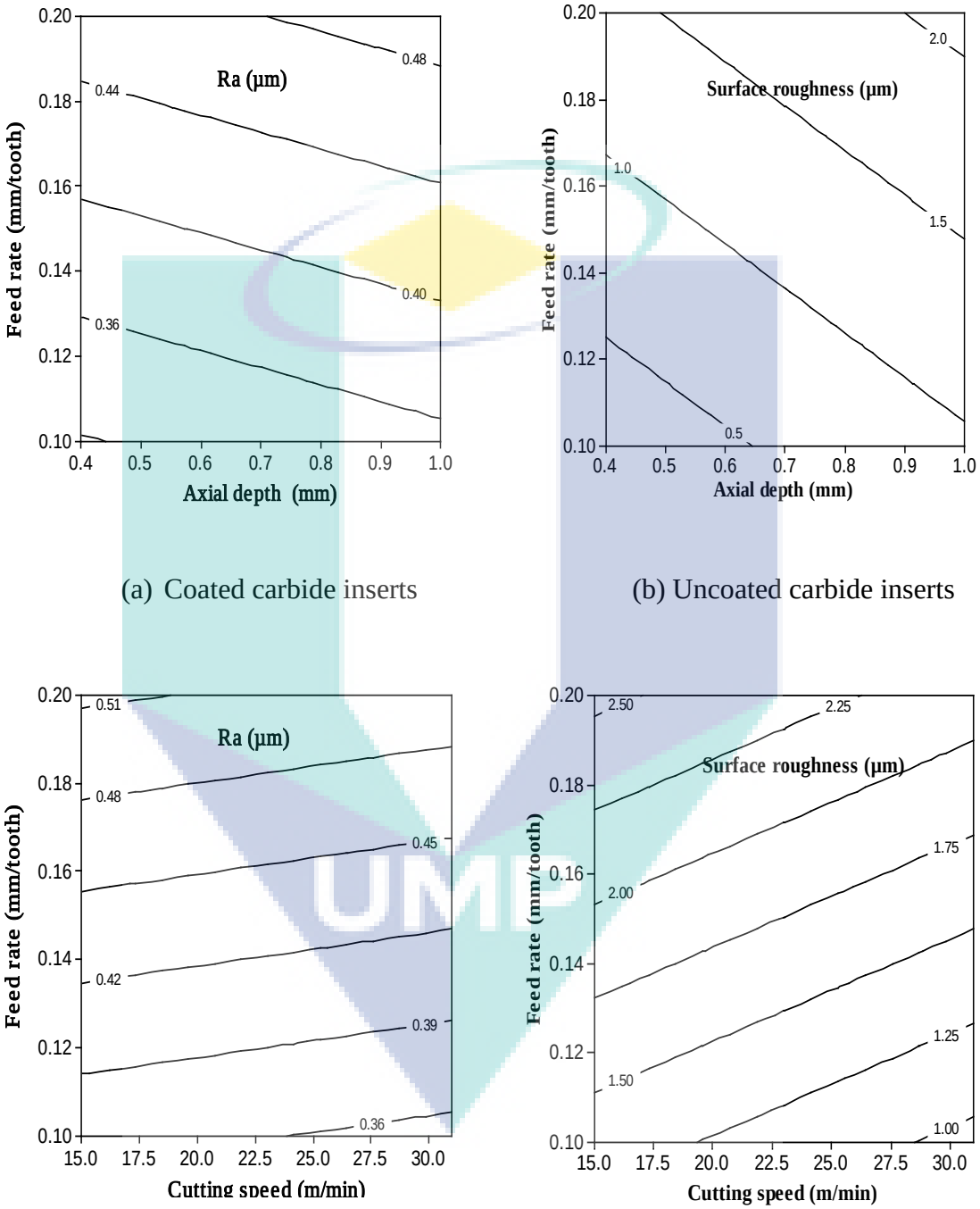

(a) Coated carbide inserts

(b) Uncoated carbide inserts

(c) Coated carbide inserts

(d) Uncoated carbide inserts

Figure 4.1: The surface roughness first order RSM contour plot versus feed rate and axial depth for (a) coated; (b) uncoated carbide inserts and feed rate as well as cutting speed for (c) coated and (d) uncoated carbide inserts

In the cutting condition, if the slow feed rate is being used then it is observed that the surface roughness value is also lower. The outer surface has been uniformed by a slow feed rate causing the surface roughness to be low and the machined work piece surface finish increases (Davidson et al., 2008). The surface roughness was found to be affected by the feed rate the most and because of this rate increased the surface quality lowered (Darwish, 2000; Ezugwu et al., 1999; Joshi et al., 2008). Keeping the axial depth low, the cutting speed had a sensitive effect over the surface roughness, since the roughness would decrease as the cutting speed increased (Doniavi et al., 2007). All these activities take place during the machining process due to the thermal and mechanical cycling, microstructural transformations, and mechanical and thermal deformations (Axinte and Dewes, 2002).

Table 4.2: Experimental results and the first order RSM predicted values for coated and uncoated carbide

No	Exp.Cutting Condition			Experimental result		Predicted result		Absolute Error (%)	
	FR	AD	CS	CTW 4615	CTP 1235	CTW 4615	CTP 1245	CTW 4615	CTP 1235
1	0.15	0.4	31	0.378	0.710	0.3899	0.7962	3.157	12.141
2	0.15	1	15	0.412	2.100	0.4419	1.9610	7.266	6.619
3	0.1	0.7	15	0.318	0.950	0.3524	1.0017	10.827	5.442
4	0.2	1	23	0.500	2.310	0.5054	2.3379	1.087	1.208
5	0.2	0.7	31	0.456	1.993	0.4794	1.7555	5.139	8.906
6	0.15	0.7	23	0.422	1.271	0.4153	1.3786	1.438	8.466
7	0.15	0.7	23	0.427	1.200	0.4159	1.3786	2.592	14.883
8	0.2	0.7	15	0.518	2.175	0.4969	2.1895	4.067	0.667
9	0.1	0.4	23	0.334	0.520	0.3264	0.4194	2.266	19.346
10	0.15	1	31	0.461	1.386	0.4244	1.5270	5.995	10.173
11	0.15	0.4	15	0.442	1.250	0.4074	1.2302	7.821	1.584
12	0.1	0.7	31	0.325	0.650	0.3349	0.5677	3.056	12.662
13	0.1	1	23	0.365	1.335	0.3609	1.1501	1.114	13.850
14	0.15	0.7	23	0.435	1.101	0.4159	1.3786	4.383	25.213
15	0.2	0.4	23	0.446	1.728	0.4709	1.6071	5.590	6.997

Note: FR= Feed rate (mm/tooth), AD=Axial depth (mm), CS=Cutting speed(m/min),CTW 4615= Coated carbide, CTP 1235= Uncoated carbide

Figure 4.1(b) shows that as the cutting speed is increased the surface roughness reduces. If there is a decrease in the feed rate and an increase in the cutting speed, the contour plot of surface roughness has been observed to reduce (Davim et al., 2007). The uncoated carbide cutting tools have a higher surface roughness than the coated carbide.

With a minimum axial depth, higher cutting speed and lower feed rate it is possible to obtain a low surface roughness. Table 4.2 shows the experimental result and the first order RSM with percentage of absolute relative error for coated and uncoated carbide. The minimum errors have been observed as 1.087 % for coated and 0.667 % for uncoated carbide and the maximum errors 10.827 % and 25.13 % are coated and uncoated carbide cutting inserts respectively.

Second Order Model

The first order model had been considered efficient for use; however, due to some extended variable it was essential to develop the second-order model. This model would be able to form the relationship between the machining independent variables and the surface roughness (Kwak et al., 2005). Hence, the second order model for coated and uncoated carbide cutting tool inserts have been expressed in the linear equation as eq. (4.6) and eq. (4.7).

For coated carbide inserts (CTW 4615):

$$y'' = 0.428000 + 0.72250x_1 + 0.17250x_2 - 0.008750x_3 - 0.017875{x_1}^2 + 0.001125{x_2}^2 - 0.005875{x_3}^2 + 0.005750x_1x_2 + 0.028250x_1x_3 - 0.017250x_2x_3 \quad (4.6)$$

For coated carbide inserts (CTP 1235):

$$y'' = 1.19067 + 0.59387x_1 + 0.36538x_2 - 0.21700x_3 + 0.18154{x_1}^2 - 0.10104{x_2}^2 + 0.06979{x_3}^2 - 0.05825x_1x_2 + 0.02950x_1x_3 - 0.04350\,x_2x_3 \quad (4.7)$$

At 95% confidence level of the ANOVA results, the adequacy of the second order model has been checked. It is observed from Table 4.3 that the *P* values of lack-of-fit are 0.098 and 0.193 for coated and uncoated carbide cutting tool inserts respectively , which shows that they are insignificant and the model is adequate. Hence, an indicator has been found that shows the fitness of both the models as well as their effectiveness. The R^2 is 90.80 % and 97.59 % for coated and uncoated carbide and by comparing this R^2 for RSM first and the second order it can be said that the RSM

second order model is significant and adequate in order to determine the surface roughness.

Table 4.3: Variance analysis for second order model surface roughness for coated and uncoated carbide

Source	DOF	Coated carbide insert		Uncoated carbide insert	
		F-value	P-value	F-value	P-value
Regression	9	21.67	0.002	22.54	0.002
Linear	3	57.55	0.000	64.82	0.000
Square	3	1.65	0.291	2.42	0.182
Interaction	3	5.81	0.044	0.37	0.776
Residual Error	5				
Lack of Fit	3	9.38	0.098	4.53	0.193
Pure Error	2				
Total	14				

Note: DF= Degree of freedom

Figure 4.2 shows the contour plot for the second order RSM model. Non-linear trends in the surface roughness had been fund with the help of the contour plot. When the axial depth and feed rate are high and combined for coated and uncoated carbide cutting tool inserts, the value of the surface roughness is also greater. It is due to the elastic deformation caused by a high feed rate that the surface roughness is negatively influenced. In this case, the tool profile also becomes prominent to the surface of the work piece (Karayel, 2009). However, when the cutting speed is increased, the surface roughness had been found to be low and this fact can be observed in Figure 4.2(b). The higher cutting speed generates high temperature which is attributed to the softening of the workpiece machined as well as increase the surface finish (Arunachalam et al., 2004). The maximum and minimum feed rate for experimental number 3 and 8 can be observed in Table 4.4. Experimental 8 has a surface roughness of 0.518 µm for coated carbide and is 2.175 µm for uncoated carbide when using a maximum feed rate of 0.2 mm/tooth. When maximum feed rate is present, the surface roughness is found to be high for both the cutting tools. Keeping the feed rate at 0.1 mm/tooth, the surface roughness value declines to a great extent. The coated carbide insert has a surface roughness of 0.318 µm and the uncoated carbide insert has a roughness of 0.950 µm; hence proving that the feed rate has the highest ability to affect the values of the

roughness (Ginting and Nouari, 2009). When feed rate increases, the roughness value increases. The roughness has also been affected by the coating layers in terms of efficiency since the coated carbide insert performs much better than the uncoated carbide insert.

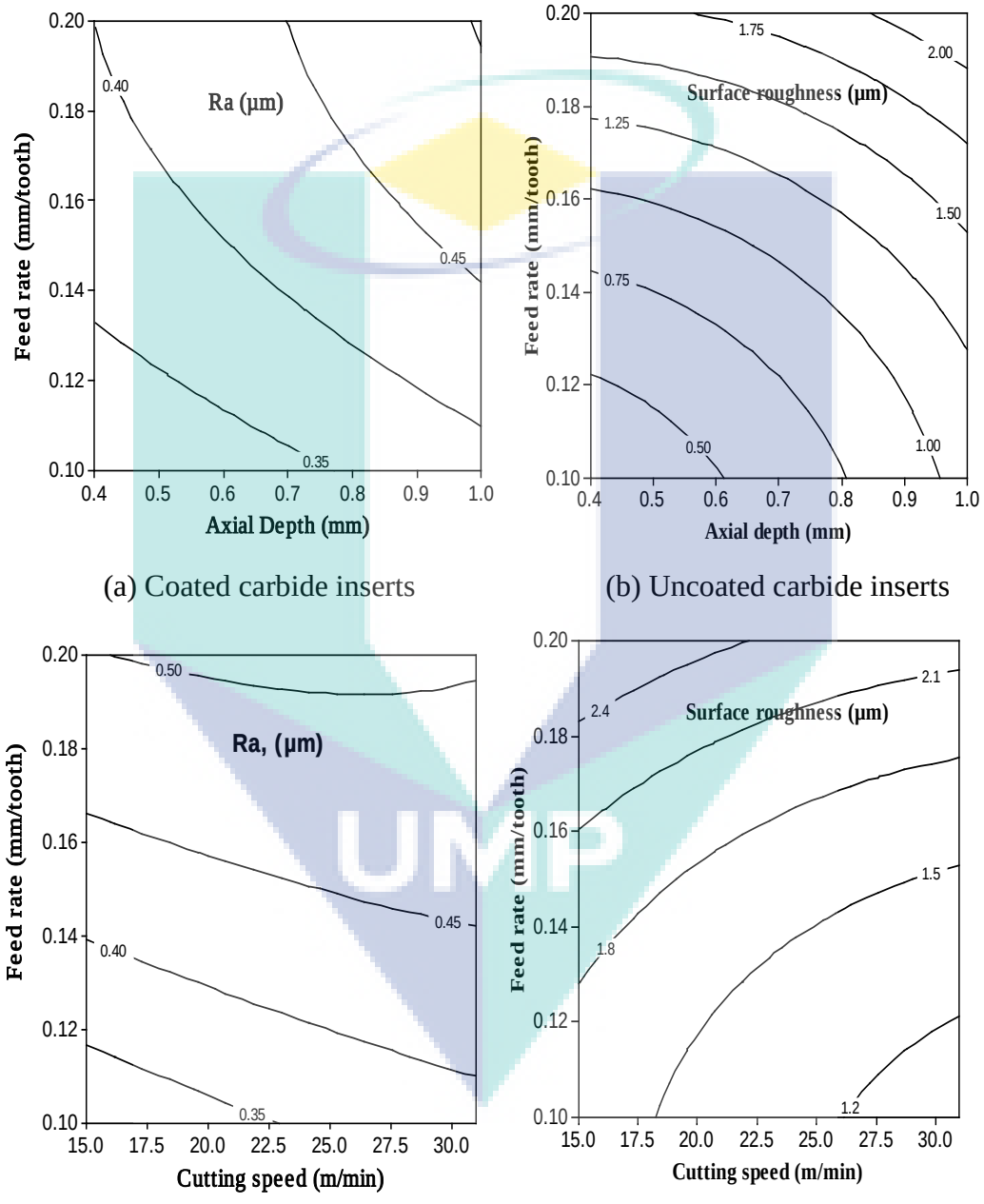

(a) Coated carbide inserts (b) Uncoated carbide inserts

(c) Coated carbide inserts (d) Uncoated carbide inserts

Figure 4.2: The surface roughness second order RSM contour plot versus feed rate and axial depth for (a) coated; (b) uncoated carbide inserts and feed rate as well as cutting speed for (c) coated and (d) uncoated carbide inserts

Table 4.4: Result of surface roughness values for coated and uncoated inserts

Experimental no.	Feed rate (mm/tooth)	Axial depth (mm)	Cutting speed (m/min)	Surface roughness (µm)	
				Coated carbide	Uncoated carbide
8	0.2	0.7	15	0.518	2.175
3	0.1	0.7	15	0.318	0.950

According to the contour plot, the feed rate has the highest ability to affect the characteristics of the surface roughness. The uncoated carbide is compared to the values of coated carbide cutting insert lower surface roughness. There is toughness, abrasion resistance, good heat transmission and hardness observed in the behaviour of the coating layer of the PVD-coated which provides a work material with a good surface finish (Jindal et al., 1999). The thermal softening of the material is increased thus compressive stresses increases and such surface flaws clear out of the machined surface, as well as enabling the workpiece near- surface to reconstruct itself easily (Pawade et al., 2007).

Table 4.5 shows the percentage of the absolute relative error of the experimental result along with the second order RSM model for coated and uncoated carbide. The first order RSM has a higher absolute relative error than the second order. The coated and uncoated carbides have minimum and maximum errors of 6.754 % and 0.226 % and 15.859 % and 0.775 % respectively. Hence, observing these values it is found that the second order RSM should be chosen as the roughness model. The first and the second order RSM predicted values have been compared to the experimental results for coated and uncoated cutting inserts in Figure 4.3. The first order RSM shows that the mean absolute relative errors for coated and uncoated carbide are 4.386 % and 9.878 % respectively. The second order RSM has mean absolute relate error of 2.324 % and 6.681 % for coated and uncoated carbide. The second order values are closer to the results of the experiment than the first order that is why the second order is found to be more significant to be used in the model of surface roughness.

Table 4.5: Experimental results and second order RSM predicted values for coated and uncoated carbide

No	Exp.Cutting Condition			Experimental result		Predicted result		Absolute Relative Error (%)	
	FR	AD	CS	CTW 4615	CTP 1235	CTW 4615	CTP 1245	CTW 4615	CTP 1235
1	0.15	0.4	31	0.378	0.710	0.369	0.8226	2.381	15.859
2	0.15	1	15	0.412	2.100	0.421	1.9874	2.143	5.362
3	0.1	0.7	15	0.318	0.950	0.323	1.0946	1.730	15.221
4	0.2	1	23	0.500	2.310	0.506	2.3743	1.300	2.784
5	0.2	0.7	31	0.456	1.993	0.506	1.8484	1.206	7.255
6	0.15	0.7	23	0.422	1.271	0.428	1.1907	6.754	6.318
7	0.15	0.7	23	0.427	1.200	0.428	1.1907	0.370	0.775
8	0.2	0.7	15	0.518	2.175	0.502	2.2234	2.993	2.225
9	0.1	0.4	23	0.334	0.520	0.327	0.4558	1.950	12.346
10	0.15	1	31	0.461	1.386	0.460	1.4664	0.217	5.801
11	0.15	0.4	15	0.442	1.250	0.443	1.1696	0.226	6.432
12	0.1	0.7	31	0.325	0.650	0.340	0.6016	4.769	7.446
13	0.1	1	23	0.365	1.335	0.350	1.303	3.973	2.391
14	0.15	0.7	23	0.435	1.101	0.4280	1.1907	1.609	8.147
15	0.2	0.4	23	0.446	1.728	0.4605	1.7600	3.251	1.852

Note: FR= Feed rate (mm/tooth), AD=Axial depth (mm), CS=Cutting speed(m/min),CTW 4615= Coated carbide, CTP 1235= Uncoated carbide

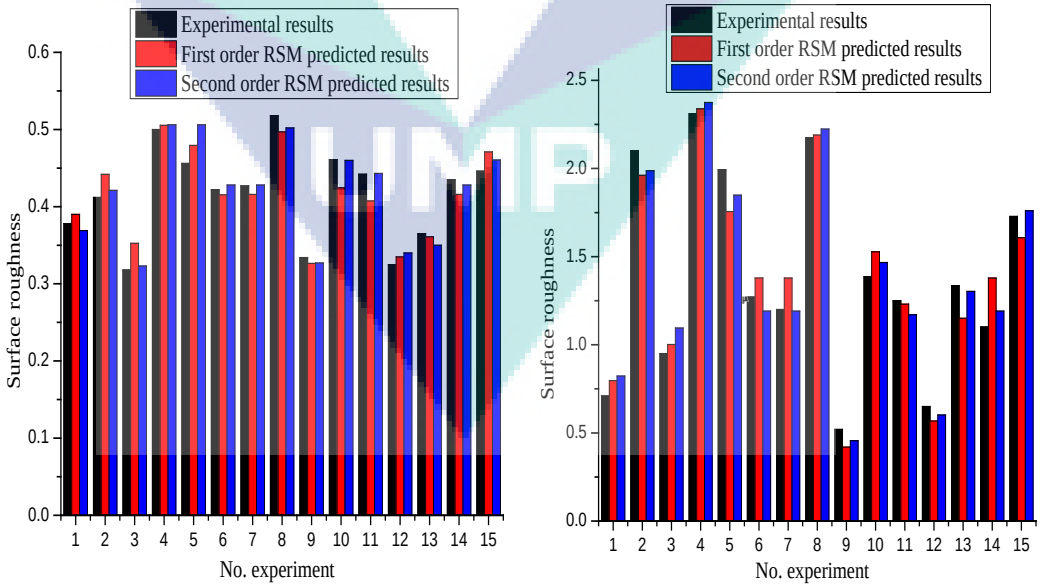

(a) Coated carbide inserts (b) Uncoated carbide inserts

Figure 4.3: Comparison between experimental result, first order and second order RSM for different cutting tool.

4.2.2 Artificial Neural Network Model

In order to carry out non-linear mapping between the input and the output variables a multi-layer perception (MLP) network has been used (Mohd Azlan et al., 2010). The back-propagation algorithm helped train the artificial neural network which was developed using the different iteration numbers (Abeesh et al., 2008 and Cus and Zuperl, 2006). During the training phase, the algorithm uses the supervised training technique and initializes the network weights and biases randomly. Till the iteration number reaches 10,000 the sum squared errors are found to decrease; however in this case they became constant. The error criterion was also developed when the number reached 10,000 and this error criterion was considered with the iteration number. No specific rule has been developed to extract the numbers or neurons of the hidden layers Due to this fact a trial-and-error process was applied (Mohd Zain et al., 2010) where the algorithm training was stopped at 10,000 iterations. The experimental test consisted of 3 inputs namely feed rate, axial depth of cut and cutting speed and one surface roughness input parameter. Depending on the problem complexity and data set, the hidden layer number and neurons have been set in each of the layers. The ratio between training and testing is selected as 70% : 30%, (Mohd Zain et al., 2010).

A single hidden layer along with a set of neurons was used as selection for the initial network. The hyperbolic function was used as the activation function for the hidden layer (Al-Ahmari, 2007 and Oktem et al., 2006). Several other networks along with topologies needed to be examined, since the ANN model was not accurate enough with a single hidden layer. In order to improve the performance of ANN a subsequent network development process was managed. The learning rule function of back-propagation was used for the output layer and hidden layers (Nalbant et al., 2009). The MSE was kept at 10^{-6} and the total number of epoch was 10,000. In Table 4.6 it has been observed that the heuristic method was used with the R^2 evaluation to extract the hidden layer. This table also states that the coated carbide inserts have an ANN structure of no 4 with 15 hidden layers. The correlation coefficient is 0.996368 and R^2 for the architecture is 0.990377 along with ID no 5 with 17 hidden layers being the best kind of hidden layer for the uncoated carbide cutting tool inserts. In this case the correlation of coefficient is 0.998914 and R^2 for the structure is 0.997092.

Table 4.6: Heuristic search for coated and uncoated carbide inserts

ID	N	F	TE	VE	TE	C	R-S	SR
Coated carbide inserts (CTW4615)								
1	18	113.5572	0.00578	0.00310	0.00880	0.992108	0.979777	AID
2	11	114.0107	0.00365	0.00193	0.00877	0.995310	0.990297	AID
3	7	113.2086	0.00610	0.00541	0.00883	0.99620	0.989341	AID
4	15	112.3259	0.00356	0.00489	0.00203	0.996368	0.990377	AID
5	13	116.4575	0.00781	0.00781	0.00821	0.992368	0.989891	AID
6	14	118.5072	0.00478	0.00455	0.00778	0.99499	0.976351	AID
7	21	115.0708	0.00784	0.00168	0.00678	0.993391	0.991221	AID
8	12	111.2085	0.00654	0.00689	0.00606	0.994332	0.988762	AID
9	10	113.1313	0.00567	0.00789	0.00716	0.992134	0.986854	AID
Uncoated carbide inserts (CTP1235)								
1	2	0.553658	0.50243	0.24992	0.46641	0.19124	0.053658	AID
2	25	0.944337	0.13029	0.34413	0.37670	0.974537	0.943373	AID
3	16	0.968333	0.09510	0.30622	0.32446	0.987614	0.968331	AID
4	10	0.996678	0.02647	0.35519	0.35519	0.998765	0.996678	AID
5	17	0.997092	0.02379	0.45225	0.49123	0.998914	0.997092	AID
6	8	0.08516	0.46635	0.32875	0.44589	0.9594834	0.911507	AID
7	4	0.911507	0.46635	0.16748	0.34413	0.957838	0.821450	AID
8	18	0.932114	0.60570	1.00221	0.80101	0.98874	0.758339	AID
9	14	0.463519	1.677203	1.86953	0.99340	0.863745	0.756340	AID

Note: N= Neurons, F= Fitness, TE= Training error, VE= Validation error, TE= Testing error, C= Correlation, R-S= R-square, SR= Stop reason AID = All iterations done

Table 4.7: Summary training and testing best network for coated and uncoated carbide inserts

	Target		Output		Absolute Error		ARE	
	TR	TE	TR	TE	TR	TE	TR	TE
Coated Carbide cutting tool inserts CTW 4615 with NN model of 3-15-1								
Mean	0.407	0.430	0.4060	0.4230	0.0013	0.00070	0.186	0.164
SD	0.411	0.434	0.4100	0.4340	0.0057	1.01250	0.261	0.228
Min	0.318	0.325	0.3186	0.3250	0.0007	0.00009	0.032	0.027
Max	0.518	0.500	0.5176	0.5009	0.0071	0.0021	0.151	0.454
Uncoated Carbide cutting tool inserts CTP 1235 with NN model of 3-17-1								
Mean	1.425	1.286	1.427	1.286	0.0019	0.0013	0.149	0.116
SD	1.524	1.402	1.526	1.404	0.0035	0.0014	0.202	0.137
Min	0.520	2.310	0.522	2.312	0.0008	0.0009	0.007	0.003
Max	2.175	2.310	2.1748	2.312	0.0102	0.0024	0.485	0.249

Note: TR=Training, TE=Testing, ARE= Absolute relative error, SD: Standard Deviation

Table 4.7 highlights the summary of the training and testing of the coated and uncoated carbide cutting tool inserts. The absolute relative errors of the training and testing for coated are averaged out to be 0.186 % and 0.164 % meanwhile for uncoated are 0.149% and 0.116%. Table 4.8 and Table 4.9 show the training and testing of artificial neural network for coated and uncoated carbide cutting insert. Keeping in mind the coated carbide inserts the coefficient of correlation is 0.981 824 and R^2 is 0.989 8658. The testing shows the values of 0.999 851 and 0.999 956. For training uncoated carbide inserts, the coefficient of correlation is 0.999 985 and R^2 is 0.998 822. The testing values are 0.999 999 and 0.999 065. Table 4.10 shows the validation for coated and uncoated carbide. The absolute error for validation for coated carbide and uncoated carbide is within 1% to 4% of error accuracy.

Table 4.8: The training, testing of artificial neural network for coated carbide inserts

No	Exp. Cutting condition			Experimental result	Predicted ANN	Absolute Relative Error (%)
	FR	AD	CS			
Training, R^2= 0.989 8658, C=0.981 824						
1	0.15	0.4	31	0.37800	0.37621	0.47354
2	0.15	1	15	0.41200	0.41187	0.03155
3	0.1	0.7	15	0.31800	0.31830	0.19811
6	0.15	0.7	23	0.42200	0.42136	0.15166
8	0.2	0.7	15	0.51800	0.51760	0.07720
9	0.1	0.4	23	0.33400	0.44159	0.09270
11	0.15	0.4	15	0.44200	0.366443	0.15616
13	0.1	1	23	0.36500	0.43521	0.04827
14	0.15	0.7	23	0.43500	0.44583	0.03810
15	0.2	0.4	23	0.44600	0.33201	0.59580
Testing, R^2=0.999 956, C=0.999 851						
4	0.2	1	23	0.50000	0.50091	0.18200
5	0.2	0.7	31	0.45600	0.45640	0.08771
7	0.15	0.7	23	0.42700	0.42730	0.07025
10	0.15	1	31	0.46100	0.43999	0.45475
12	0.1	0.7	31	0.32500	ho0.32509	0.02769

Note: FR= Feed rate (mm/tooth), AD=Axial depth (mm), CS=Cutting speed (m/min), R^2=R square, C= Correlation coefficient

Table 4.9: The training, testing and validation of artificial neural network for uncoated carbide inserts

No	Exp. Cutting condition			Experimental result	Predicted ANN	Absolute Relative Error (%)
	FR	AD	CS			
Training, R^2=0.998 822, C=0.999 985						
1	0.15	0.4	31	0.71000	0.71110	0.15493
2	0.15	1	15	2.10000	2.11020	0.48571
5	0.2	0.7	31	1.93300	1.99286	0.00702
7	0.15	0.7	23	1.20000	1.2012	0.10000
8	0.2	0.7	15	2.17500	2.17482	0.08276
9	0.1	0.4	23	0.52000	0.52119	0.22885
10	0.15	1	31	1.38600	1.38720	0.08650
13	0.1	1	23	1.33500	1.33420	0.05993
14	0.15	0.7	23	1.10100	1.10393	0.26612
15	0.2	0.4	23	1.72800	1.72835	0.02023
Testing, R^2=0.999 065, C=0.999 998						
3	0.1	0.7	15	0.95000	0.94890	0.11579
4	0.2	1	23	2.31000	2.31241	0.10433
6	0.15	0.7	23	1.27100	1.27147	0.00369
11	0.15	0.4	15	1.25000	1.25094	0.07520
12	0.1	0.7	31	0.65000	0.64838	0.24923

Note: FR= Feed rate (mm/tooth), AD=Axial depth (mm), CS=Cutting speed (m/min), R^2=R square, C= Correlation coefficient

Table 4.10: Validation of artificial neural network for coated and uncoated carbide inserts

No	Exp. Cutting condition			Experimental result	Predicted ANN	Absolute Relative Error (%)
	FR	AD	CS			
Coated carbide cutting insert						
1	0.15	0.4	31	0.38200	0.37621	1.5157
9	0.1	0.4	23	0.44900	0.44159	1.6503
12	0.1	0.7	31	0.31620	0.32509	2.8115
Uncoated carbide cutting insert						
5	0.2	0.7	31	2.0231	1.99286	1.4947
3	0.1	0.7	15	0.9828	0.94890	3.4493
4	0.2	1	23	2.2218	2.31241	4.0782

The coated carbide cutting tool has an ANN structure with 15 hidden layers which is found in Figure 4.4.

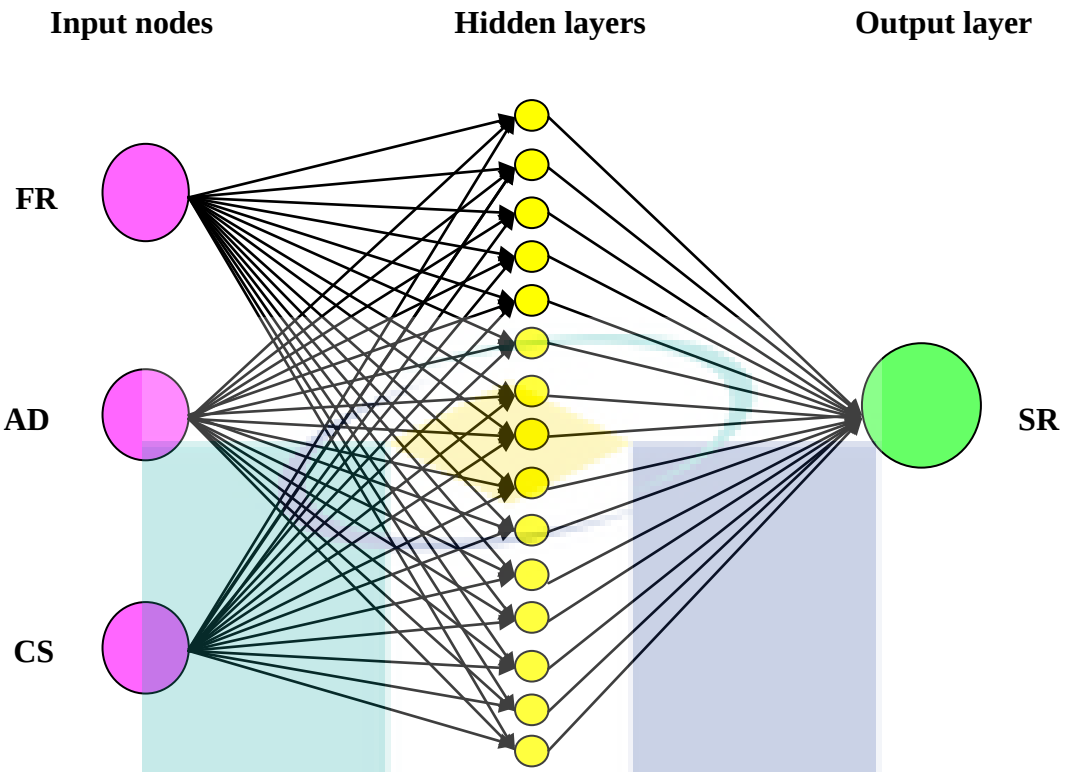

Figure 4.4: The best network for Coated carbide insert, 3-15-1

The experimental values have a level of conformity with the ANN prediction since the results are 99% similar with the actual results. The coated cutting inserts have a maximum absolute relative error of 0.186 % and for uncoated is 0.164 %. On the other hand the minimum coated cutting inserts absolute relative errors are 0.149 % and uncoated is 0.116 %. Hence, it is found that the statistical models are not as accurate in terms of surface roughness prediction as the ANN model with back propagation algorithm (Feng and Wang, 2003).The experimental and ANN predicted results can be found in Figure 4.5 for the coated and uncoated carbide inserts. This table will help determine how much closer the ANN is able to predict the values. The experimental results are also found to be the same for coated and uncoated carbide. Hence the feed forward multilayer with the hyperbolic activation function can perform in an efficient manner and have the ability to predict the values for surface roughness (Davim et al., 2008; Tsai and Wang, 2001).In Table 4.11, the models with the error analyses are recorded. Through this analysis it is observed that the ANN model has been able to perform better than the regression models (Ozel and Karpat, 2005). The first and second order RSM predicted results for both inserts show that the error analysis is small for the

ANN model. Therefore, the surface roughness of Hastelloy C-2000 can be predicted by using the ANN and the following Figure 4.6 has provided the comparison of the surface roughness of ANN and experimental results for the different kinds of cutting tools.

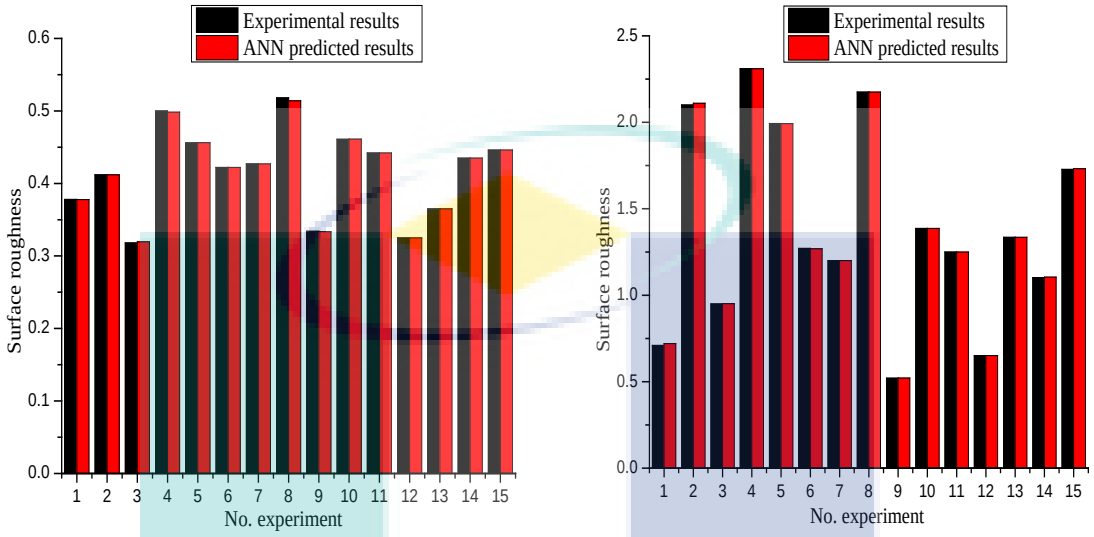

(a) Coated carbide inserts (b) uncoated carbide inserts

Figure 4.5: Comparison between experimental results versus ANN predicted for coated and uncoated carbide inserts

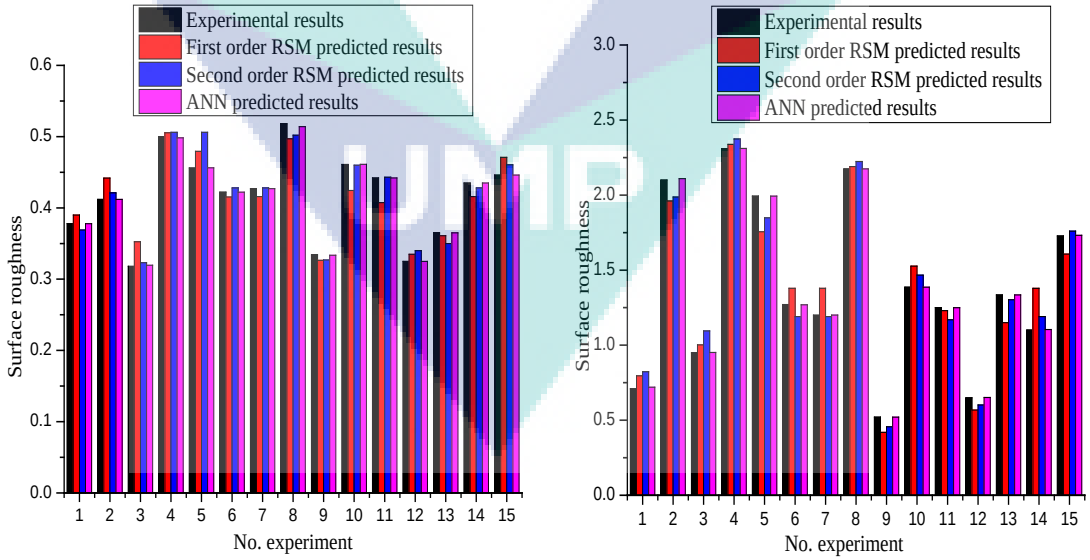

(a) Coated carbide inserts (b) Uncoated carbide inserts

Figure 4.6: Comparison between experimental results, first order RSM predicted, second order RSM predicted and ANN predicted.

The first and the second order have an absolute error of 4.386 % and 2.324 % respectively for coated carbide insert and of 0.1790 % for the ANN model. In the case of the uncoated carbide the mean absolute error for ANN, first order and second order RSM are 0.136 %, 9.878 % and 6.681 %. Hence, it is found that ANN significant for use as the model for surface roughness prediction and provides a less error than the statistical model. The absolute errors are able to provide a much more accurate ANN prediction than the regression models.

Table 4.11: The error analysis of surface roughness model for coated and uncoated carbide inserts

Model	Minimum error (%)		Maximum error (%)		Mean error (%)	
	CTW4615	CTP1235	CTW4615	CTP1235	CTW4615	CTP1235
FO RSM	1.0870	0.6670	10.827	25.130	4.386	9.878
SO RSM	0.2260	0.0750	6.7540	15.890	2.324	6.681
ANN	0.0277	0.0070	0.5958	0.4850	0.1790	0.136

Note: CTW4615= Coated carbide, CTP1235= Uncoated carbide, FO RSM = First order RSM, SO RSM = Second order RSM

4.2.3 The Minimization of Surface Roughness

The basic aim of this research is to use appropriate variables in order to minimize and maximize the characteristics of the machining Hastelloy C-2000. By applying the optimization approach using the statistical analysis it would be possible to achieve this aim. Desirability functions would be used to convert each response and the weight would be able to define the desirability function shape for each of the responses. Using any weight from 0.1 to 10 for each of the responses the target can be emphasized or de-emphasized. When a weight:

i) Below 1 and above 0.1 is chosen then there is less emphasis on the target
ii) If it is equal to one then there is equal importance to the bounds and the target
iii) Higher than 1 and below 10 then there is more emphasis on the target

In Table 4.10, the design variables for the coated and uncoated carbide inserts are corresponding to the minimum cutting conditions of surface roughness. Confirmation experiments have also been carried out upon the optimum machining

parameter combinations which show that there exists an efficient response for the surface model predictions. When the optimum design values are applied the surface roughness of the machined work piece is much lower. The coated and uncoated carbide inserts conditions have an error value for validation test to be 2.533 % and 2.88 % as shown in Table 4.12. Hence it is possible to use for minimize of surface roughness value. Many issues may be observed even though the models are considered accurate. These issues include high accuracy machining where the surface roughness is required to be efficient should be well observed since the cutting tool deflection or thermal condition are the future models for the creation of surface roughness. Another kind of application which could be efficient is that the existing models could be provided a general advisory system that can be used with a machine tool.

Table 4.12: The minimum cutting conditions of surface roughness for coated and uncoated carbide inserts

Cutting insert	Feed rate (mm/tooth)	Axial depth (mm)	Cutting speed (m/min)	Target (min)	Experimental (min)	Error (%)
Coated carbide	0.1	0.4	31	0.333	0.3415	2.553
Uncoated carbide	0.1	0.4	31	1.25	1.286	2.880

4.2.4 Surface Integrity

Deviation from the nominal surface of the third level till the sixth order is the concept of surface roughness. Order of deviation is defined in international standards (DIN 4760). Circularity, flatness and waviness refer to the first- and second-order deviations. These deviations are usually caused by the erroneous setups, workpiece material inhomogenities, machine tool errors, deformation of the workpiece and clamping. Chip formation, process kinematics, cracks, dilapidations and periodic grooves are the Third-and fourth-order deviations. The Fifth- and sixth-order deviations are the lattice scale like oxidation, residual stress, slip, diffusion etc and the workpiece material structure like physical–chemical mechanisms acting on a grain. When a nickel base alloy is machined there are many surface defects which are found. Magnifications for the coated and uncoated carbide inserts can be observed in Figure 4.7 since it shows

the images of scanning electron microscope (SEM). A feed rate of 0.2 mm/tooth, axial depth 0.7 mm and cutting speed 15 m/min has been used for the images that are taken and a surface defect has been found due to the low cutting speed.

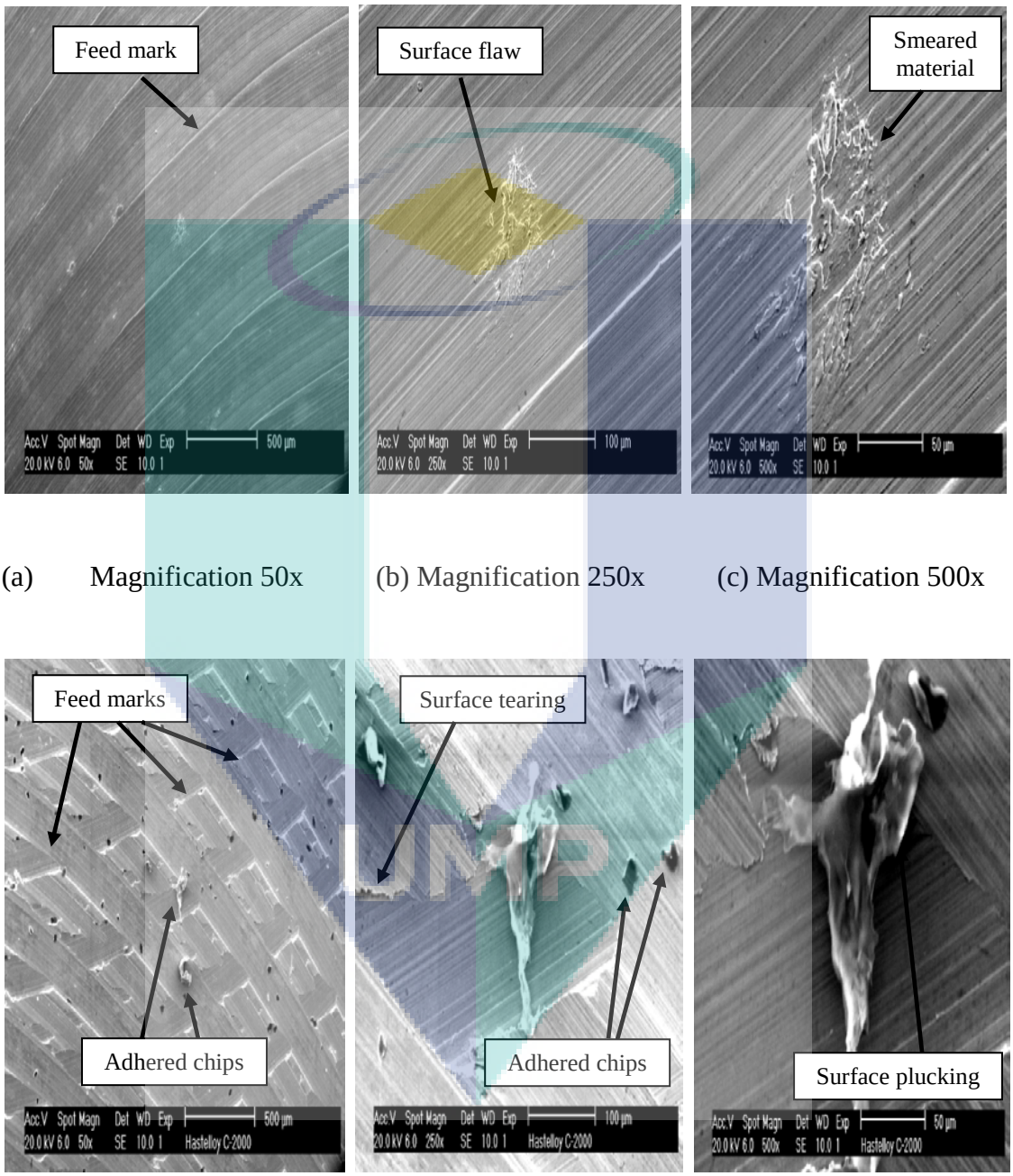

(a) Magnification 50x (b) Magnification 250x (c) Magnification 500x

(d) Magnification 50x (e) Magnification 250x (f) Magnification 500x

Figure 4.7: SEM viewing of Hastelloy C-2000 texture at certain magnification using different cutting tools (a-c) coated carbide, (d-f) uncoated carbide inserts.

During the machining of the workpiece of the coated carbide cutting insert, there are several kinds of surface defects which occur. Out of these few the surface flaw, feed marks and chip redeposition are the most common kinds of defects that occur. The severity of a feed mark can be changed by optimizing the feed rate or than varying it in order to carry out effective machining process (Ginting and Nouri, 2009). Furthermore, plucking of particles from the surface and their redeposition to the surface create two different defects. The particles have the ability to cause tearing and dragging effect on the surface of the next pass (Soo et al., 2011). In the case of uncoated carbide, the same kind of surface plucking and tearing would take place. The uncoated carbide has a very different surface texture from the coated carbide which is mainly because the coating layer helps make the tool harder and tougher with a good surface finish. The residual stress which is present on the surface machine is improved along with reducing the cutting temperature and enhancing of the machine surface with the help of the coating layer (Outeiro et al., 2008). The depth of the cut can affect the cutting speed which in return affects the material plucking, tearing, smearing and the microchip debris on the surface (Ginting and Nouri, 2009). If there is a low cutting speed then the surface condition is also poor since the contact time between the work piece and cutting tool is increased (Soo et al., 2011). It is observed that the compressive stresses increases when increase of the thermal softening of the material and such surface flaws clear out of the machined surface and enabling the workpiece near- surface to reconstruct itself easily (Pawade, 2007).

Prolonged machining tends to increase the hardness of surface layer and also deteriorates the surface finish of machined workpiece. This is due to the fact that the contact area and motion that exists between the tool, flank area and workpiece machine surface is increased hence causing surface defect, increase component cutting forces and temperature and flank wear. When there is presence of nickel based alloys, many issues arise since the cutting parameters affect the defects to an extent. To avoid these problems the cutting condition optimization is essential. The machining processes have been observed to have many defects in the surface specifically in the micron precisions. It is not possible to entirely remove the cutting parameters or even adjust them to an extent. There are carbide particles in the structure of nickel based work piece materials along with coating inserts material with carbide particles. There is often detachment of

the carbide particles with the machine surface or the tool inserts when the work piece is machined or stuck on the work piece surface. Such a process is referred to as carbide cracking and may cause an increase in the level of stress when the cutting takes place due to plucking in the surface cavities (Zou et al., 2009). Figure 4.8 shows the carbide cracking formation.

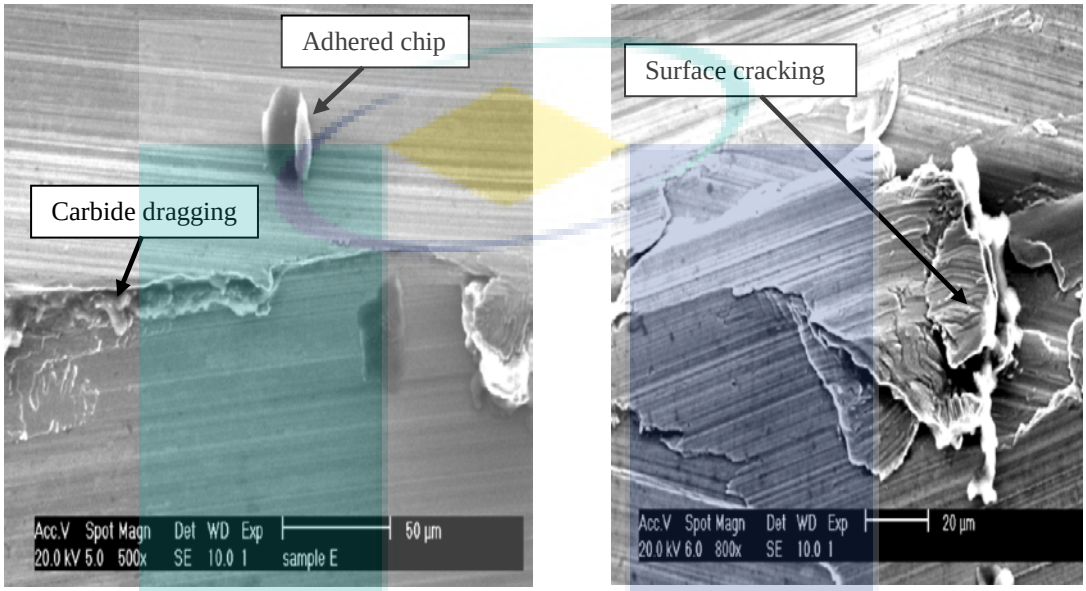

(a) Magnification, 500x (b) Magnification, 800x

Figure 4.8: SEM viewing of experimental no 3 with two different magnifications for uncoated carbide insert.

Keeping a feed rate 0.2 mm/tooth, axial depth of 1.0 mm and cutting speed 23 m/min of the uncoated carbide machine process the phenomenon took place in the third experiment. Residual cavities and cracks occur in the machine surface which may cause several issues in terms of the micro-scale surface integrity. Much importance is given to the carbide cracking and end surface product when the feed values and axial depth are lower and the carbide particle sizes are too close to the level which is concerned. Energy dispersive energy (EDX) tests have been carried out after maintaining cutting parameters of work piece feed rate 0.2 mm/tooth, axial depth 0.7 mm and cutting speed 15 m/min. These tests help to investigate the chemical composition of the material when machining takes place of the coated and uncoated carbide tool inserts. Cobalt has been formed in the EDX test when checking the texture of the machined surface; hence proving that adhesion mechanism does take place. All these activities have been

observed in Figure 4.9. This Cobalt, Co is a new element of the Hastelloy C-2000 which is present due to the high temperature of machining and the chemical change that takes place between the cutting tool insert and the work piece (Axinte et al., 2006).

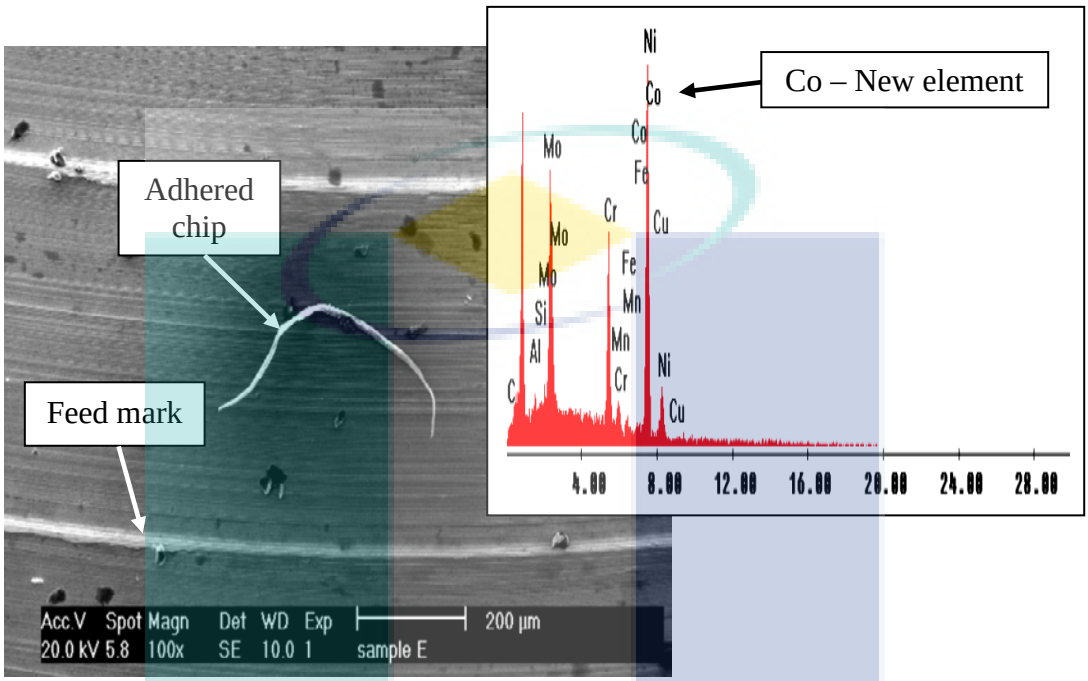

Figure 4.9: Adhesion and diffusion base on EDX result at magnification 100x at coated carbide cutting tool.

The formation of cobalt happened due to adhesive mechanism during the machining where the coated carbide itself contains the component of cobalt. The rake face is protected with the help of the adhering element (Co) as it became a stable built-up-edge (Itakura et al. 1999). Diffusion took place which is why there was a vast increase or decrease in the elements of Carbon (C), Aluminum (Al) and Molybdenum (Mo). Due to this mechanism the atom present in the metallic crystal lattice changes from the higher atomic concentration to the lower concentration level. As the temperature increases the rate of diffusion also increases. The machining process of the coated and uncoated carbide caused by the chemical composition can be observed in Table 4.13. The diffusion mechanism also took place in these coated and uncoated cutting inserts. The weight elements of the several materials also changes due to the diffusion mechanism. The aluminum (Al), silicon (Si), ferum (Fe), chromium (Cr), manganese (Mn), copper (Cu) and Nickel (Ni) are found to decrease. On the other hand

carbon (C), and molybdenum (Mo) are found to increase for the coated carbide cutting tool insert. 1.01% contribution to the chemical element is provided by the new element as shown in the table. The EDX based diffusion at uncoated carbide base can be observed in magnification of 100x in Figure 4.10.

Table 4.13: Chemical composition (%) of material (Hastelloy C-2000), before and after machining for coated and uncoated carbide inserts

Cutting insert	**Chemical element before machining**									
	Ni	**Cr**	**Mo**	**Fe**	**Cu**	**Al**	**Mn**	**Si**	**C**	Co
	55.31	23	16	3	1.60	0.50	0.50	0.08	0.01	-
	Chemical element after machining									
Coated carbide	54	12.83	24.53	1.05	2.16	1.2	0.57	0.76	1.89	1.01
Uncoated carbide	54.22	15.28	24.84	0.45	1.25	0.58	0.29	0.71	2.38	-

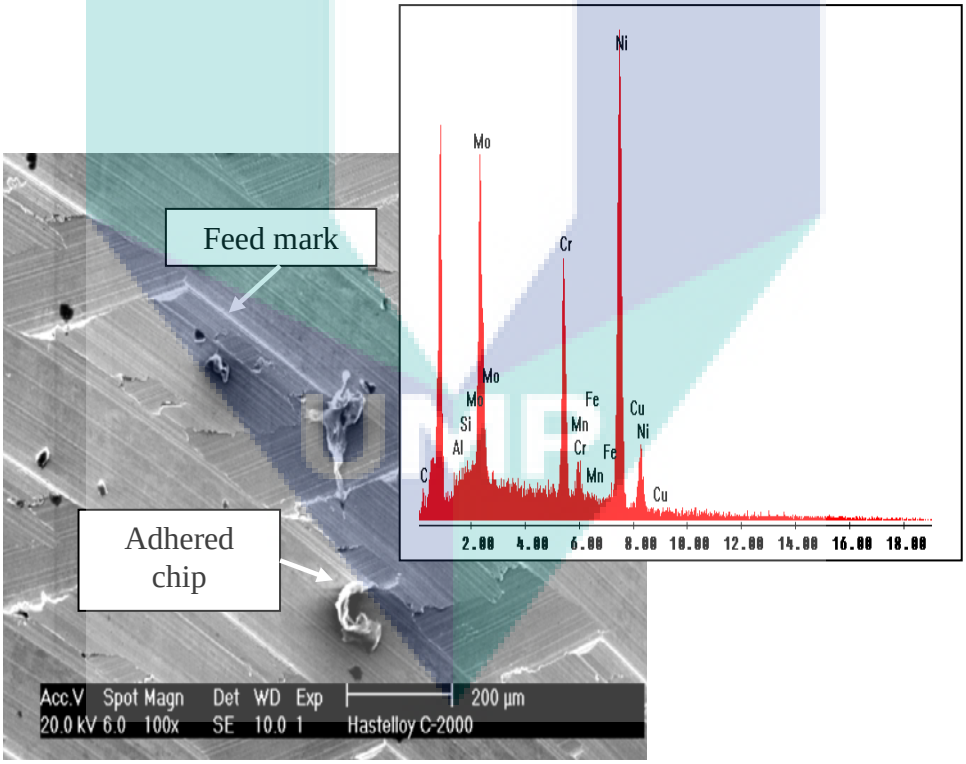

Figure 4.10: The diffusion based on EDX result at magnification 100x for uncoated carbide insert.

The case of diffusion occurs when applying uncoated carbide, however, with no adhesion formation found as happened in coated carbide. It take place during cutting

condition of feed rate of 0.2 mm/tooth, axial depth 1.0 mm and cutting speed 23 m/min. Here, decrease is found in composition of chromium (Cr), manganese (Mn), copper (Cu), ferum (Fe) and Nickel (Ni) and increase is observed in molybdenum (Mo), aluminum (Al), silicon (Si), and carbon (C).

4.3 TOOL LIFE

A specific length of cutting time is managed by a tool which is referred to as the tool life (Onwubolu, 2006). Till the time the criterion value of the flank wear is achieved, there exists a usable time which is referred to as the tool life (Bouzid, 2005). In order to manage designs for the materials of cutting tools, the contributions of various wear mechanism should be predicted in an efficient manner (Gupta, 2005). The following Eq. (4.8) can be used to express tool life:

$$\text{Tool life} = \frac{CD}{F_m} \tag{4.8}$$

CD = the overall distance required for cutting tool to reach flank wear (0.3mm) according ISO 8688-2:1989(E) and F_m is the combination of feed rate and cutting speed from RPM to mm/min.

The machine efficiency is limited and the nickel based alloy machinability is also harmed due to the short tool life (Kadirgama et al., 2011). In this section, the tool life, the mathematical models have been developed to predict and optimize the machining characteristics for the first and second order RSM.

4.3.1 Mathematical Model

First Order Model

The coated and uncoated carbide cutting tools inserts have the following Eq. (4.9) and Eq. (4.10) as their first order linear equations to predict the tool life.

First order equation for coated carbide cutting tool inserts:

$$y' = 1.17867 - 0.79363\,x_1 - 0.17475\,x_2 - 0.02738\,x_3 \quad (4.9)$$

First order equation for uncoated carbide cutting tool inserts:

$$y' = 0.565933 - 0.320750x_1 - 0.104375\,x_2 - 0.007125\,x_3 \quad (4.10)$$

The tool life is highly influenced by the equations (Eq. (4.9) and Eq. (4.10)) along with the feed rate, axial depth and cutting speed. If the feed rate, axial depth, and cutting speed increase then the life of the tool decreases. If these three things are kept at a minimal level then a longer tool life can be obtained. Table 4.14 provides an analysis of the variance of the coated and uncoated carbide. The adequacy of first order model is verified by ANNOVA results. It has been found that the *P*-values of linear terms of both models are less than α-value (0.05), for coated carbide, 0.000 and uncoated carbide, 0.000 which is why they are considered significant and the model is adequate. The *P*-values for lack of fit are 0.353 and 0.009 for coated and uncoated carbide respectively are insignificant since they are higher than α-level (0.05). Hence, this shows that the model is adequate and fit for use since there is an indicator to measure the effectiveness of this model based on the surface roughness data. The value of the uncoated carbide R^2 is higher than that of the coated carbide since it is 98.97 % and the coated carbide is 94.03 %. Therefore, the models which have been established are able to provide a much accurate prediction of the surface roughness.

Table 4.14: Variance analysis for first tool life model for coated and uncoated carbide

Source	DOF	Coated Carbide inserts		Uncoated carbide inserts	
		F-value	**P-value**	**F-value**	**P-value**
Regression	3	353.43	0.000	57.70	0.000
Linear	3	353.43	0.000	57.70	0.000
Residual Error	11				
Lack of Fit	9	2.18	0.353	110.00	0.009
Pure Error	2				
Total	14				

Figure 4.11 shows the contour plot of tool life versus feed rate, axial depth cutting speed for coated and uncoated carbide cutting inserts. The cutting speed has a lower effect than the feed rate on the life of the tool. If the feed rate is low, the tool life is better rather than when the feed rate is high. A high feed rate can cause the cutting tool inserts to break (Kadirgama et al., 2011). This significant change attributed to the increase of temperature and plastic deformation which weaken the cutting tool materials (Shokrani et al., 2012). This increase in temperature causes the micro cracks and micro hardness by establishing a white layer and reducing the tool life of the cutting tool insert (Dudzinkski et al., 2004). The tool life of coated carbide is found to be longer than that of the uncoated carbide when the contour plot is observed of the axial depth versus the feed rate. If the axial depth and feed rate are increased then the tool life for the coated carbide reduces to 0.5 minutes and if it is maintained at low levels then the timings are 2 minutes. The experimental results for the RSM predicted coated and uncoated carbide inserts can be found in Table 4.15. For coated and uncoated carbide the maximum errors are 29.90 % and 17.931 % respectively and the minimum errors are 0.0167 % and 0.599 % respectively.

Table 4.15: Experimental result and first order RSM predicted for coated and uncoated carbide inserts

No	Exp. Cutting Condition			Experimental result		Predicted result		Absolute Relative Error (%)	
	FR	AD	CS	CTW 4615	CTP 1235	CTW 4615	CTP 1245	CTW 4615	CTP 1235
1	0.15	0.4	31	1.278	0.667	1.3260	0.6632	3.759	0.599
2	0.15	1	15	0.980	0.450	1.0312	0.4687	5.233	4.222
3	0.1	0.7	15	2.000	0.830	1.9997	0.8938	0.017	7.590
4	0.2	1	23	0.300	0.200	0.2103	0.1408	29.900	29.500
5	0.2	0.7	31	0.450	0.290	0.3577	0.2381	28.149	17.931
6	0.15	0.7	23	1.100	0.530	1.1787	0.5659	7.152	6.792
7	0.15	0.7	23	1.140	0.520	1.1787	0.5659	3.392	8.846
8	0.2	0.7	15	0.350	0.267	0.4124	0.2523	17.833	5.618
9	0.1	0.4	23	2.166	1.122	2.1470	0.9911	0.875	11.676
10	0.15	1	31	0.933	0.400	0.9765	0.4544	4.667	13.500
11	0.15	0.4	15	1.500	0.667	1.3808	0.6774	7.947	1.499
12	0.1	0.7	31	1.950	0.800	1.9450	0.8796	0.261	9.875
13	0.1	1	23	1.833	0.901	1.7975	0.7823	1.934	13.208
14	0.15	0.7	23	1.200	0.515	1.1787	0.5659	1.778	9.903
15	0.2	0.4	23	0.500	0.330	0.5597	0.3496	11.800	6.061

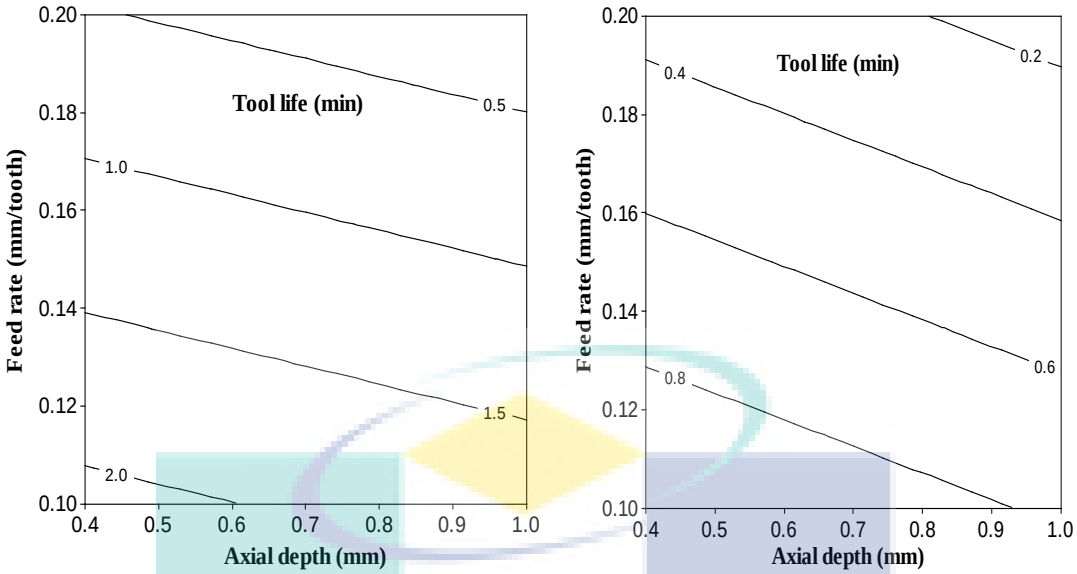

(a) Coated carbide inserts

(b) Uncoated carbide inserts

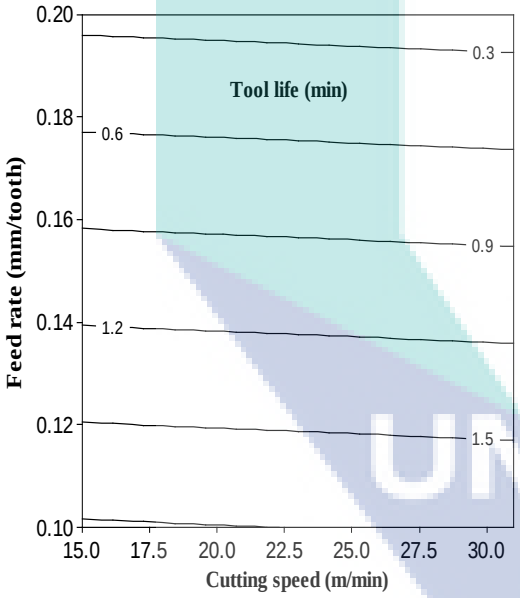

(c) Coated carbide inserts

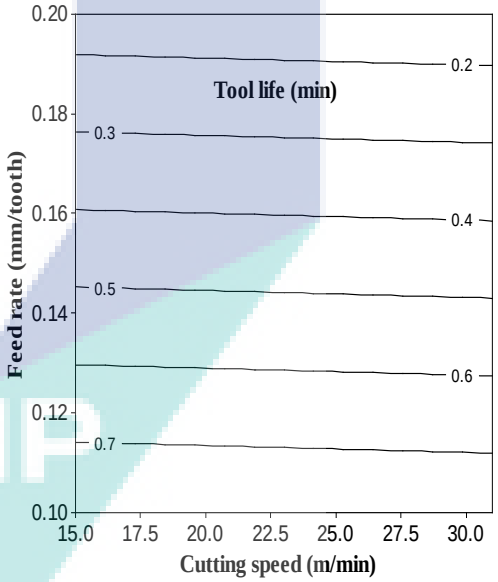

(d) Uncoated carbide inserts

Figure 4.11: The tool life first order RSM contour plot versus feed rate and axial depth for (a) coated; (b) uncoated carbide inserts and feed rate as well as cutting speed for (c) coated and (d) uncoated carbide inserts

Second Order Model

The second order of the tool life for coated and uncoated carbide inserts can be expressed by the following equations Eq. (4.11) and Eq. (4.12).
For coated carbide cutting tool inserts:

$$y'' = 1.14667 - 0.79363x_1 - 00.17475x_2 - 0.02738x_3 + 0.03392{x_1}^2 + 0.01917{x_2}^2 + 0.00692{x_3}^2 + 0.03325x_1x_2 - 0.03750x_1x_3 + 0.04375x_2x_3 \quad (4.11)$$

For uncoated carbide cutting tool inserts:

$$y'' = 0.521667 - 0.320750x_1 - 0.104375x_2 + 0.007125x_3 + 0.058667{x_1}^2 + 0.057917{x_2}^2 - 0.033583{x_3}^2 + 0.022750x_1x_2 + 0.013250x_1x_3 - 0.012500x_2x_3 \quad (4.12)$$

The ANOVA results have helped understand the adequacy of the second order model at a level of 95%. The *P*-value for lack of fit have been considered insignificant since they are 0.229 and 0.007 for coated and uncoated carbide cutting tool inserts which states that the model is adequate. The *P*-value of regression for coated carbide is 0.000 and uncoated carbide, 0.002 which are significant. These values are present in Table 4.16 and the model is fit for use. An indicator has been identified for the model effectiveness and both of the models are considered acceptable. The coated and uncoated carbides have R^2 of 99.40 % and 97.46 % respectively and based on the *P*-value and R^2 it is clear that the second order model of RSM is much more adequate and significant in order to predict the tool life. Besides these effects, an increase in cutting speed increases the frequency of tool edge entrance into the workpiece (increasing the number of shocks per minute) and in addition the energy of the shock between the cutting edge and the workpiece. This makes cutting speed even more important to the end of tool life. High temperature is generated when the cutting speed is high and there is a long period contact between the cutting tool and the workpiece. This high temperature causes the tool life to reduce (Vivancos et al., 2005). The tool life may be induced with the help of the high chemical affinity of the chemicals being used for the cutting tool materials attributes to the increases of diffusion wear (Sharman et al.,

2001). Cutting tool insert always experiences the severe mechanical and thermal load and enhances the tool wear in addition to reduce the tool life (Xue and Chen, 2011). When there is high cutting speed and feed rate, the inserts break which is why it is not possible to maintain a long tool life of the uncoated carbide inserts. The coating causing a high level of resistance and till the time it is still in shape, the tool wear rate is very low.

The substrate of the tool and the work piece come into direct contact after a certain period of time due to the machine wear which removes the coating. Hence, the tool wear rate increases to a great extent and the tool life shows a large decline. Maximum cutting speed and feed rate values can be observed in Table 4.17 and in Figure 4.12 the graphs for different feed rate values and maximum cutting speed for the cutting tool in different cutting conditions can be observed.

Table 4.16: Variance analysis for second order tool life model for coated and uncoated carbide inserts

Source	DOF	Coated carbide insert		Uncoated carbide insert	
		F-value	P-value	F-value	P-value
Regression	9	92.61	0.000	21.31	0.002
Linear	3	276.64	0.000	61.67	0.000
Square	3	0.28	0.840	2.02	0.229
Interaction	3	0.93	0.493	0.23	0.872
Residual Error	5				
Lack of Fit	3	3.53	0.229	139.96	0.070
Pure Error	2				
Total	14				

Note: DF= Degree of freedom

Table 4.17: Cutting parameters when using the maximum cutting speed for coated and uncoated carbide

Exp. no	Feed rate (mm/tooth)	Axial depth(mm)	Cutting speed (m/min)
1	0.15	0.4	31
5	0.2	0.7	31
10	0.15	1.0	31
12	0.10	0.7	31

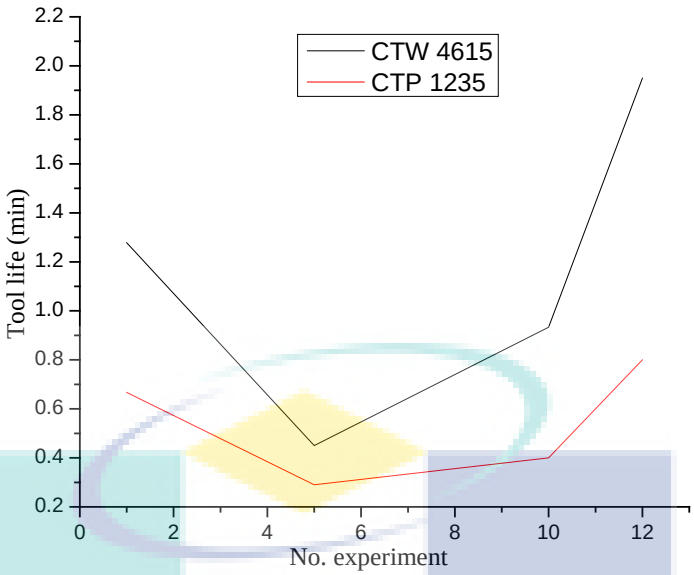

Figure 4.12: Tool life with different values of feed rate and maximum cutting speed

Figure 4.13 shows the contour plot of tool life versus feed rate, axial depth and cutting speed for coated and uncoated carbide inserts. Here, the uncoated carbide is much more superior to the coated carbide tool life. The heat that was generated by the high feed rate was able to decrease the tool life and the hardness of the cutting tool material (Venugopal et al., 2007). Based on the contour plot of feed rate versus cutting speed, if the machine cutting speed is increased, the temperature increases which in return decreases the tool material hardness and leading to diffusion and abrasion (Coromant, 1994). In both the cases of coated and uncoated carbide inserts it is found that the tool life declines from 0.1 mm/tooth to 0.2 mm/tooth as shown in Experiment 12 and 5 respectively. If the feed rate is at minimum level then the tool life is much higher and with a high cutting speed there is tool wear and short life of the tool is experienced (Jawaid et al., 2001). A low feed rate is able to provide a much longer tool life than a feed rate which is high (Che Haron, 2001 and Kadirgama et al., 2011). Table 4.18 shows the experimental results of second RSM predicted model for coated and uncoated carbide inserts. In uncoated carbide the maximum absolute error is 11.792 % and 20.909 % and minimum absolute error is 0.166 % and 0.385 % for coated and uncoated carbide respectively. The experimental results and the first and second order RSM are being compared in Figure 4.14. The coated and uncoated carbide mean absolute error for the first order RSM are 8.313 % and 9.788 % respectively and the

second order RSM are 4.876 % and 7.627 %. The experimental values and the second order RSM are found to be much closer than the first order. Hence, for the surface roughness model, the second order model of RSM is considered significant.

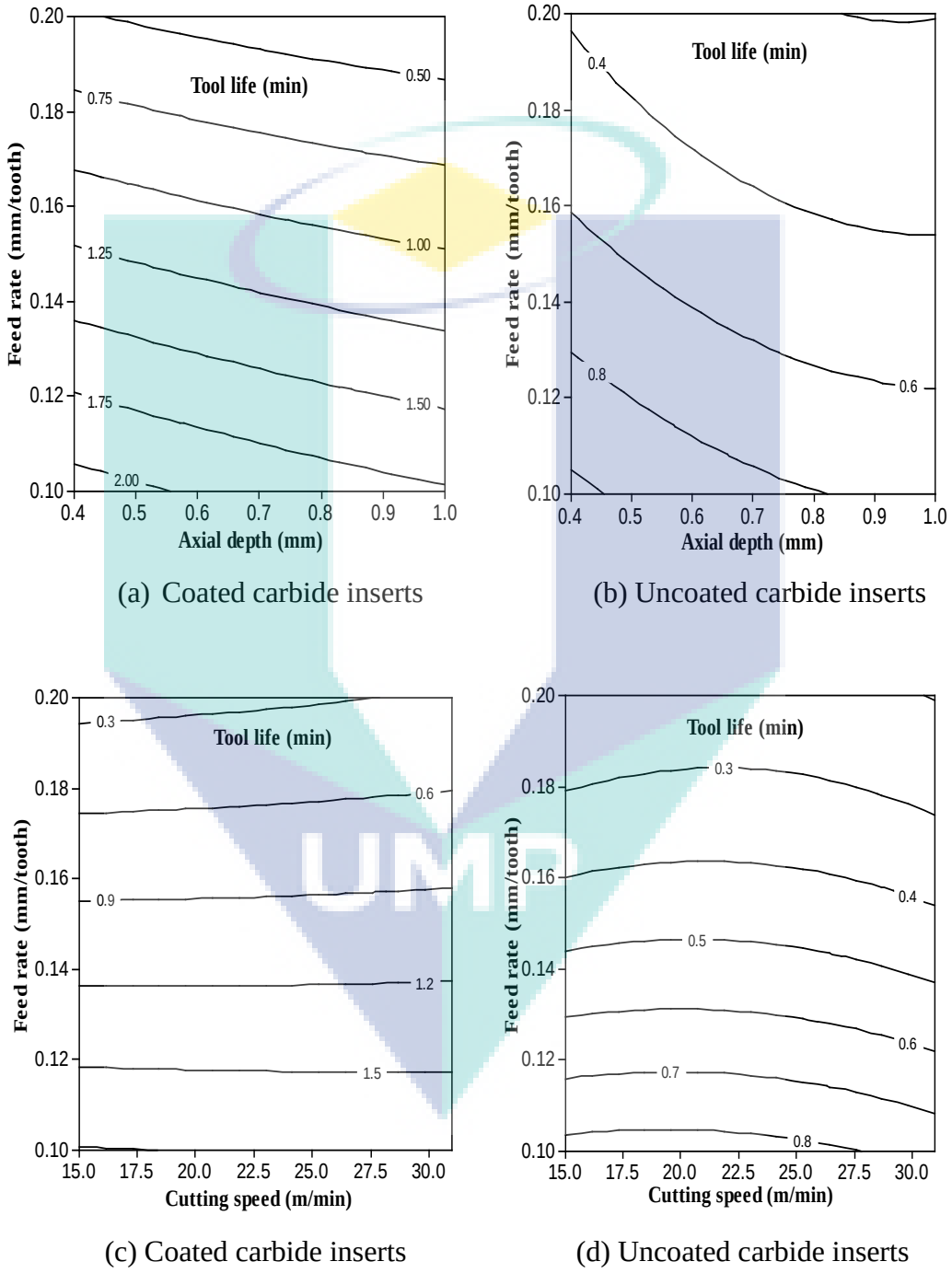

Figure 4.13: The tool life second order RSM contour plot versus feed rate and axial depth for (a) coated; (b) uncoated carbide inserts and feed rate as well as cutting speed for (c) coated and (d) uncoated carbide inserts

Table 4.18: Experimental, second order RSM predicted results and absolute error for coated and uncoated carbide inserts

No	Exp. Cutting Condition			Experimental result		Predicted result		Absolute Error (%)	
	FR	AD	CS	CTW 4615	CTP 1235	CTW 4615	CTP 1245	CTW 4615	CTP 1235
1	0.15	0.4	31	1.278	0.667	1.2764	0.6558	0.127	1.649
2	0.15	1	15	0.980	0.450	0.9817	0.4613	0.166	2.444
3	0.1	0.7	15	2.000	0.830	2.0460	0.8879	2.300	6.988
4	0.2	1	23	0.300	0.200	0.2646	0.2359	11.792	16.000
5	0.2	0.7	31	0.450	0.290	0.4040	0.2321	10.222	20.000
6	0.15	0.7	23	1.100	0.530	1.1467	0.5217	4.240	1.538
7	0.15	0.7	23	1.140	0.520	1.1467	0.5217	0.585	0.385
8	0.2	0.7	15	0.350	0.267	0.3838	0.2199	9.643	17.603
9	0.1	0.4	23	2.166	1.122	2.2014	1.0861	1.633	3.209
10	0.15	1	31	0.933	0.400	1.1014	0.4220	8.713	5.500
11	0.15	0.4	15	1.500	0.667	1.4186	0.6450	5.425	3.298
12	0.1	0.7	31	1.950	0.800	1.9163	0.8471	1.731	5.875
13	0.1	1	23	1.833	0.901	1.7854	0.8319	2.598	7.658
14	0.15	0.7	23	1.200	0.515	1.1467	0.5217	4.444	1.309
15	0.2	0.4	23	0.500	0.330	0.5476	0.3991	9.525	20.909

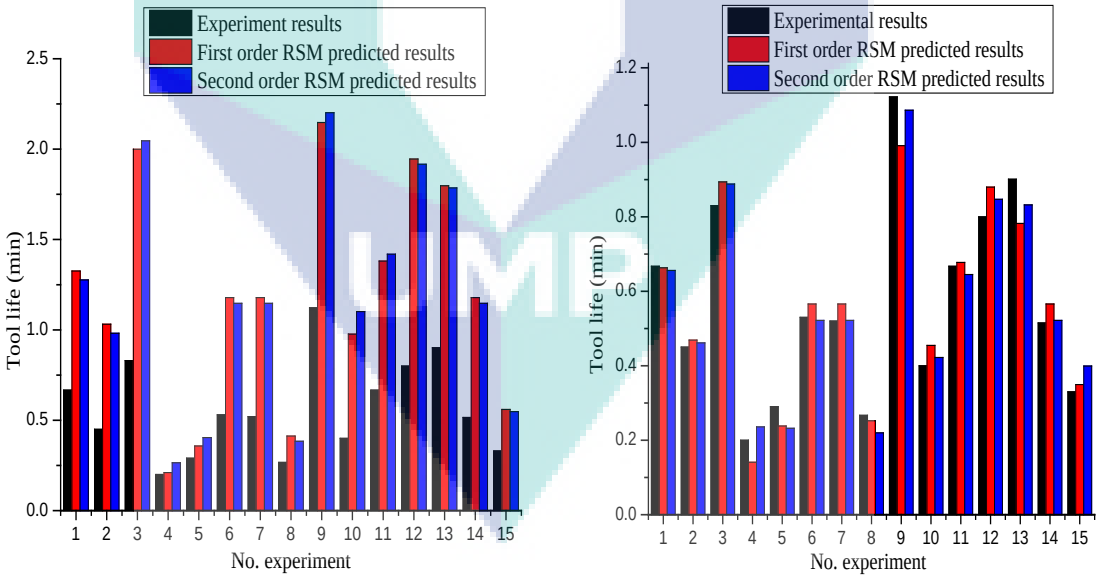

(a) Coated carbide inserts (b) Uncoated carbide inserts

Figure 4.14: Comparison between experimental results, first order RSM, second order RSM model

4.3.2 Development of Artificial Neural Network Model

In the case of a coated carbide cutting tool, the best kind of ANN structure consists of three inputs, twenty five hidden layers and one output layer; (3-25-1). Table 4.19 clearly shows the heuristic search for the best kind of hidden layer. In the case of uncoated carbide cutting tool, the ANN structure which is considered best is three inputs, seven teen hidden layers, and one output (3-17-1) with ID number 7. Using the correlation coefficient value and the R-square value, it is possible to choose the best criterion. The correlation of coefficient is 0.996991 and R^2 for the structure (3-25-1) is 0.991946 for coated carbide as shown in Table 4.17. The hidden layers structure provides a lower value as compared to this structure. In the case of uncoated carbide cutting tool the correlation of coefficient is 0.998218 and the R^2 for combination (3-17-1) is 0.997695.

Table 4.19: Heuristic search for coated and uncoated carbide inserts

ID	N	F	TE	VE	TE	C	R-S	SR
Coated carbide inserts (CTW4615)								
1	16	4.33121	0.0561	0.4331	0.2660	0.977891	0.990123	AID
2	10	7.00241	0.0678	0.4412	0.3450	0.969678	0.98321	AID
3	21	6.69124	0.3001	0.3911	0.0188	0.992100	0.972128	AID
4	25	7.44175	0.0448	0.3876	0.1347	0.996991	0.991946	AID
5	19	3.34456	0.0607	0.6210	0.3821	0.994387	0.990014	AID
6	23	4.03299	0.0522	0.6770	0.2236	0.987622	0.989991	AID
7	22	8.09211	0.0489	0.4241	0.2467	0.99100	0.97956	AID
8	12	7.13760	0.0789	0.5150	0.2981	0.978945	0.956712	AID
9	17	3.00310	0.0056	0.4789	0.3364	0.995002	0.957781	AID
Uncoated carbide inserts (CTP1235)								
1	25	9.6667	0.0178	0.0196	0.1034	0.996826	0.992725	AID
2	16	10.0104	0.0228	0.0143	0.0998	0.995133	0.992725	AID
3	10	6.15251	0.0378	0.0257	0.1625	0.989431	0.972564	AID
4	21	8.69578	0.0115	0.0201	0.1149	0.998238	0.996302	AID
5	13	6.49981	0.0322	0.0180	0.1538	0.998238	0.996302	AID
6	19	6.96342	0.0223	0.0189	0.1436	0.995218	0.988567	AID
7	17	13.1721	0.0144	0.0148	0.0759	0.997695	0.998218	AID
8	16	10.9123	0.7718	0.3245	0.8214	0.9899011	0.977895	AID
9	20	8.9126	0.0337	0.2323	0.0895	0.9956781	0.997213	AID

Note: N= Neurons, F= Fitness, TE= Training error, VE= Validation error, TE= Testing error, C= Correlation, R-S= R-square, SR= Stop reason AID = All iterations done

Table 4.20: Summary training and testing for coated and uncoated carbide

	Target		Output		Absolute Error		ARE	
	TR	**TE**	**TR**	**TE**	**TR**	**TE**	**TR**	**TE**
Coated Carbide cutting tool inserts CTW 4615 with NN model of 3-15-1								
Mean	1.247	1.382	1.246	1.381	0.0017	0.0020	0.1596	0.5663
SD	1.410	1.428	1.409	1.426	0.0028	0.0022	0.2444	0.1728
Min	0.350	0.933	0.348	0.934	0.0009	0.0032	0.0261	0.0570
Max	2.166	2.000	2.168	1.998	0.0085	0.0032	0.5857	0.2633
Uncoated Carbide cutting tool inserts CTP 1235 with NN model of 3-17-1								
Mean	0.604	0.524	0.603	0.524	0.00080	0.0016	0.1803	0.2397
SD	0.658	0.563	0.657	0.563	1.04520	0.0013	0.2728	0.3224
Min	0.200	0.290	0.198	0.524	0.00009	0.0002	0.0021	0.0440
Max	1.122	0.901	1.226	0.899	0.00180	0.021	0.7000	0.5862

Note: T=Training, O=Overall, ARE= Absolute relative error, SD: Standard Deviation

Table 4.21: The training and testing of artificial neural network for coated carbide cutting inserts.

No	**Exp. Cutting condition**			**Experimental result**	**Predicted ANN**	**Absolute Relative Error (%)**
	FR	AD	CS			
				Training, R^2= 0.999 981, C=0.999 991		
2	0.15	1	15	0.98000	0.98091	0.09286
4	0.2	1	23	2.00000	1.99793	0.10350
5	0.2	0.7	31	0.45000	0.44963	0.08222
6	0.15	0.7	23	1.00000	1.10032	0.02910
7	0.15	0.7	23	1.14000	1.14044	0.03860
8	0.2	0.7	15	0.35000	0.34795	0.58571
9	0.1	0.4	23	2.16600	2.16674	0.03410
12	0.1	0.7	31	1.95000	1.95051	0.02615
13	0.1	1	23	1.83300	1.82450	0.46372
15	0.2	0.4	23	0.50000	0.50070	0.14000
				Testing, R^2=0.999 960, C=0.999 990		
1	0.15	0.4	31	1.27800	1.27678	0.09550
3	0.1	0.7	15	2.00000	1.99886	0.05700
10	0.15	1	31	0.93300	0.93436	0.14577
11	0.15	0.4	15	1.50000	1.49677	0.21533
14	0.15	0.7	23	1.20000	1.19684	0.26333

Note: FR= Feed rate (mm/tooth), AD=Axial depth (mm), CS=Cutting speed (m/min), R^2=R square, C= Correlation coefficient

Table 4.22: The training and testing and of artificial neural network for uncoated carbide cutting inserts.

No	Exp. Cutting condition			Experimental result	Predicted ANN	Absolute Relative Error (%)
	FR	AD	CS			
Training, R^2=0.999 983, C=0.999 954						
1	0.15	0.4	31	0.66700	0.66512	0.28186
2	0.15	1	15	0.45000	0.44838	0.36000
3	0.1	0.7	15	0.83000	0.82877	0.14819
4	0.2	1	23	0.20000	0.19860	0.70000
7	0.15	0.7	23	0.52000	0.51989	0.02115
8	0.2	0.7	15	0.26700	0.26691	0.03370
9	0.1	0.4	23	1.12200	1.12261	0.05437
11	0.15	0.4	15	0.66700	0.66620	0.11994
12	0.1	0.7	31	0.80000	0.80050	0.06250
14	0.15	0.7	23	0.51500	0.51489	0.02136
Testing, R^2=0.999 959, C=0.999 980						
5	0.2	0.7	31	0.29000	0.28830	0.586210
6	0.15	0.7	23	0.53000	0.53310	0.396226
10	0.15	1	31	0.40000	0.40020	0.05000
13	0.1	1	23	0.90100	0.89990	0.12209
15	0.2	0.4	23	0.50000	0.49978	0.04400

Note: FR= Feed rate (mm/tooth), AD=Axial depth (mm), CS=Cutting speed (m/min), R^2=R square, C= Correlation coefficient

Table 4.20 shows the summary of the training and testing of the coated and uncoated carbide cutting tool inserts. The absolute relative errors of the training and testing for coated are averaged out to be 0.1596% and 0.5663%. Meanwhile for uncoated are 0.1803% and 0.2397%. Table 4.21 and Table 4.22 show the training and testing of artificial neural network for coated and uncoated carbide cutting insert. Keeping in mind the coated carbide inserts the coefficient of correlation is 0.999 991 and R^2 is 0.999 983. The testing shows the values of 0.999 990 and 0.999 960. For training uncoated carbide inserts, the coefficient of correlation is 0.999 954 and R^2 is 0.999 983. The testing values are 0.999 980 and 0.999 959. Table 4.23 shows the validation for coated and uncoated carbide. The absolute error for validation for coated carbide and uncoated carbide is within 3% to 1%. Figure 4.15 shows the prediction of ANN values compare to the actual values from the experimental. The coated and uncoated carbide cutting inserts have a maximum absolute relative error of 0.58621 % and 0.58571 % respectively and the minimum absolute relative errors are 0.02136 % and 0.02615 % respectively. Results state that the ANN values are much closer to the experimental

values and provide a good correlation level. Hence, the ANN models are able to provide better results than the regression method. Fewer errors are observed in the training of back propagation in predicting tool life than using the polynomial regression models. Table 4.24 can provide the error analyses of the tool life for coated and uncoated carbide inserts models. With the help of this table it is found that the first order RSM and second order RSM for coated carbide and uncoated carbide cutting insert have a higher error than those found by the ANN predictions. Hence, it is required that the ANN predicted results be used for the Hastelloy C-2000 tool life prediction

Table 4.23: Validation of artificial neural network for coated and uncoated carbide inserts

No	Exp. Cutting condition			Experimental result	Predicted ANN	Absolute Relative Error (%)
	FR	AD	CS			
Coated carbide cutting insert						
8	0.2	0.7	15	0.34795	0.34795	2.4530
12	0.1	0.7	31	2.0042	1.95051	2.6788
1	0.15	0.4	31	1.3220	1.27678	3.3948
Uncoated carbide cutting insert						
3	0.1	0.7	15	0.8415	0.82877	1.5128
8	0.2	0.7	15	0.2598	0.26691	2.7370
15	0.2	0.4	23	0.5115	0.49978	2.2913

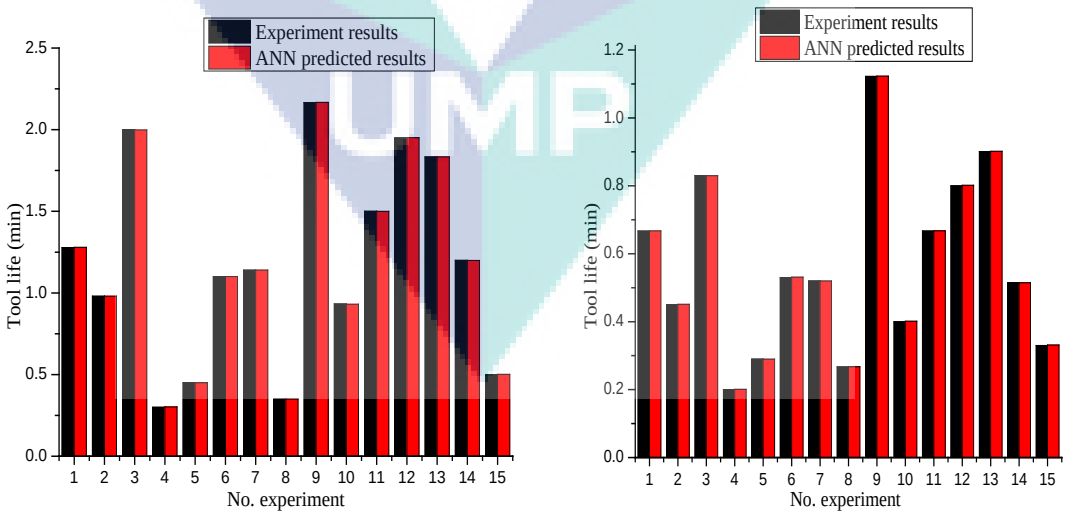

(a) Coated carbide inserts (b) Uncoated carbide inserts

Figure 4.15: Experimental result versus ANN predicted for tool life values

Table 4.24: The error analysis of tool life for coated and uncoated carbide inserts

Model	Minimum relative error (%)		Maximum relative error (%)		Mean relative error (%)	
	CTW4615	**CTP1235**	**CTW4615**	**CTP1235**	**CTW4615**	**CTP1235**
FO RSM	0.0167	0.5990	29.9000	17.9310	8.3130	9.7880
SO RSM	0.1660	0.3850	11.9200	20.9090	4.8760	7.6270
ANN	0.02136	0.0262	0.58621	0.58571	0.2000	0.1580

Note: CTW4615= Coated carbide, CTP1235= Uncoated carbide, FO RSM = First order RSM, SO RSM = Second order RSM

It is found that the absolute relative error for ANN model, first order and second order carbide cutting inserts are 0.2 %, 8.3130 % and 4.8760 % respectively. In the case of uncoated carbide absolute relative error for ANN model, first order and second order carbide cutting inserts are for ANN, first order and second order, 0.1580 %, 9.7880% and 7.6270 % respectively. Both cutting tool inserts show that the error of ANN is smaller than the two orders. The statistical and ANN predicted results can be observed in Figure 4.16. The ANN predicted results provide a better prediction that those extracted from statistical analysis in the case of coated and uncoated carbide.

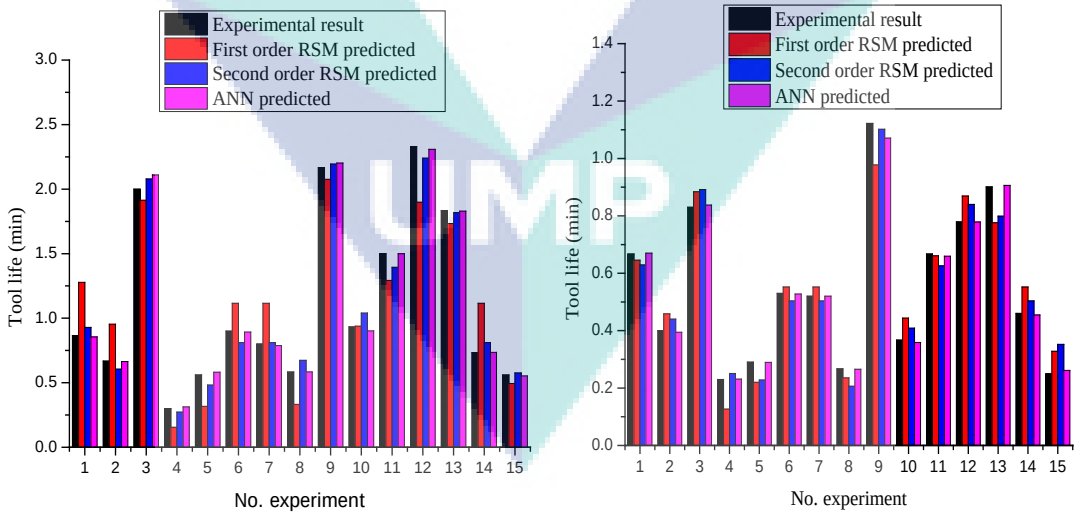

(a) Coated carbide inserts (b) Uncoated carbide inserts

Figure 4.16: Comparison between experimental results, first order RSM predicted, second order RSM and ANN predicted results

4.3.3 The Maximization of Tool Life

Table 4.25 shows the maximum value of the tool life with correspondence to design variable. The error percentage and the design variables have been used to calculate the validation process. Using the set of design for the experimental results provides both the tool with a longer tool life.

Table 4.25: The maximum value for tool life for coated and uncoated carbide

Cutting Insert	Feed rate (mm/tooth)	Axial depth (mm)	Cutting speed (m/min)	Target (min)	Experimental (min)	Error (%)
Coated carbide	0.10	0.4	15	2.3	2.28	1.593
Uncoated carbide	0.10	0.4	15	1.086	1.050	3.368

4.4 TOOL WEAR

The cutting tool is subjected to stress at the tool tip and this is how the tool wear is actually classified. The rake face is able to generate high temperature which then slides the new cut of the work piece (Kalpakjian and Schmid, 2007). Oxidation wear, fatigue wear, adhesive wear, abrasive wear and diffusion wear are some of the wear mechanisms which may take place during the machining process (Gu et al., 1999). Machining processes such as drilling and turning causes the tool life to last longer as compared to the milling process which causes the tool life to deteriorate due to cracks, chipping and edge breakage. Milling is an interrupted operation since the entry and exit of the tool cutting edge takes place in the work piece at many instances per second (Diniz and Filho, 1999). Chipping can be observed if the cutting edge is found to be jagged or then there are cavities present. Small chips break off from the tool cutting edge on account of mechanical impact, transient thermal stresses due to cycled heating and cooling in intermittent machining operations, chatter and flank wear. Figure 4.17 Figure 4.17 shows the value of flank wear is 0.4199 mm after first pass for uncoated carbide at feed rate 0.15 mm/tooth, axial depth 0.7 mm and cutting speed 23 m/min

measured by optical video measuring system. The ISO 8688-2:1989 (E) end milling specification has provided the criterion for the classification of flank.

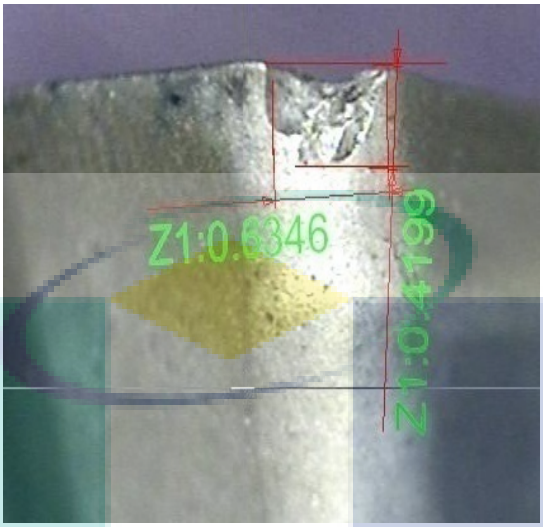

(a) Uncoated carbide insert

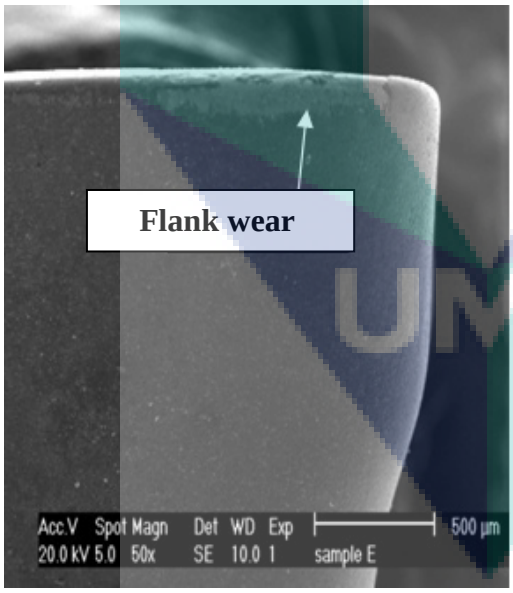

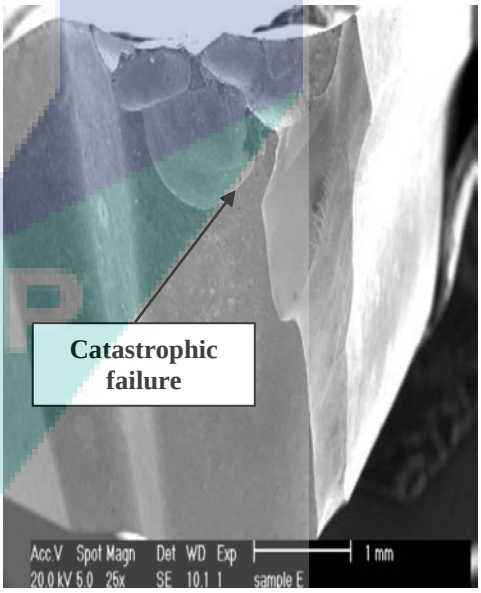

(a) Coated carbide insert (c) Uncoated carbide insert

Figure 4.17: (a) Value of flank (b) Flank wear at coated carbide insert, (c) catastrophic failure at uncoated carbide insert

The flank wear of the coated and uncoated carbide cutting inserts can be found in Figure 4.17 which also shows the catastrophic failures happened at uncoated carbide inserts. In the case of nickel-based alloys there is possibility of tool rejection which is caused by disastrous break downs; chipping and flank wear (Kadirgama et al., 2011). Table 4.26 shows the cutting parameters by keeping a maximum cutting speed of (31 m/min) for coated and uncoated carbide cutting inserts. Figure 4.18 shows the progress of flank wear during the machining process at maximum cutting speed (31 m/min) which (a) coated carbide and (b) uncoated carbide.

Table 4.26: Cutting parameters when using the maximum cutting speed for coated and uncoated carbide inserts

Exp. No	Feed rate (mm/tooth)	Axial depth(mm)	Cutting speed (m/min)
	Maximum cutting speed		
1	0.15	0.4	31
5	0.2	0.7	31
10	0.15	1.0	31
12	0.10	0.7	31

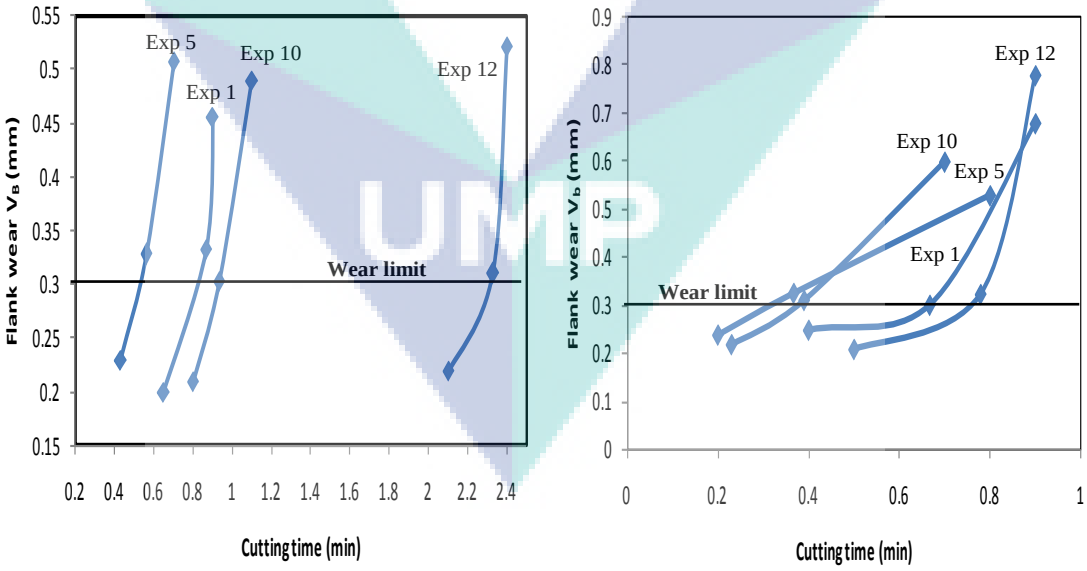

(a) Coated carbide inserts (b) Uncoated carbide inserts

Figure 4.18: Progress of flank wear (a) coated carbide, (b) uncoated carbide

Figure 4.18 shows that the uncoated carbide takes 0.3 minutes to wear out as compared to the coated carbide which takes 0.5 minutes. The tool life of the cutting insert and the flank wear values are affected by the increase in cutting speed and the feed rate. The tool life is shorter if the flank wear is greater (Thamizhmanii and Hassan, 2007). The interaction between workpiece machined and high cutting temperature has influences the tool flank wear (Isik, 2007). Severe flank wear may also be caused due to the high tool tip temperature which is caused by compressive stress since it weakens the machining characteristics and leads to plastic deformation at the cutting edge (Ezugwu and Bonney, 2004). In a coated carbide, the coated layers helps act as a protecting agent for the cutting inserts which is why it takes a longer time to wear. Whereas the uncoated carbide takes a shorter time period to wear due to the absence of the coating layer.

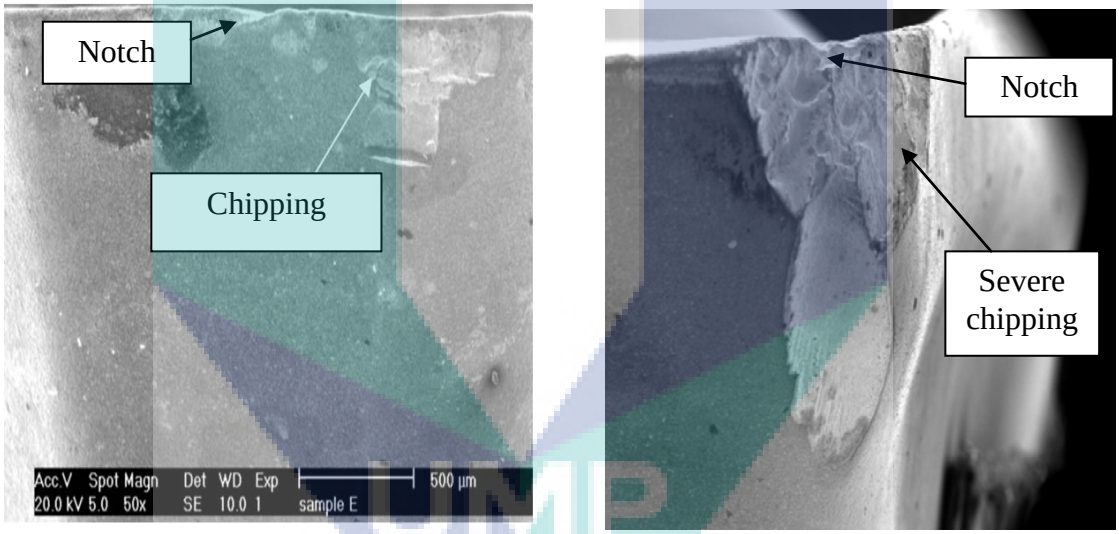

(a) Coated carbide insert (b) Uncoated carbide insert

Figure 4.19: Chipping (a) Coated carbide insert (b) Uncoated carbide insert

Figure 4.19 shows the chipping found to develop particularly at cutting speed of 15 m/min, feed rate of 0.2 mm/tooth, axial depth 0.7 mm and cutting speed 15 m/min after 120 mm cutting length. Both coated and uncoated carbide experience chipping but the severe chipping occurs for uncoated carbide compared to coated carbide inserts at the same cutting condition due to no protecting layers present to protect it. If there is unfavourable chip removal then the cutting area is affected by chip impact and edge chipping occurs. This chip removal is accompanied with high temperature as well as the

tool rake face adhesion. The high strain hardening of nickel based alloys also leading to severe chipping to the cutting tool insert (Ezugwu et al., 2005). If the cutting tool insert has been affected by chipping, the geometry is changed as more heat is created and the force increase which is present become higher causing the surface finish to be a poor process. The adherence of the work material, the work hardened layer of nickel base alloy and fatigue loading are responsible for the occurrence of the notch (Krain et al., 2007). The notching of in machining nickel base alloy is very much affected by the work hardening (Ezugwu et al., 1998). Diffusion-attrition wear may also be held responsible for the formation of notching (Kaya et al., 2011). The coated and uncoated carbide are machined during which the notching of the tool takes place (Che-Haron et al., 2007). The uncoated carbide is subjected to stronger notch wear than the coated carbide even though both categories are affected. Physical vapour deposition of TiA1N coated layers act as a thermal barriers and protecting layers to enhance the performance levels of the tool. This helps in the machining process of the substrate softening since it prevents the temperature form rising high (Krain et al., 2007). The tool flank of the cutting tool insert consists of the development of built-up edge (BUE) and adhered workpiece material which is mainly attributed to the adhesion and attrition mechanisms. The high chemical affinities between cutting tool insert and workpiece machined along with a high temperature causes the pressure to rise resulting in BUE (Krain et al., 2007). Figure 4.20 shows the formation of built-up edge (BUE) for coated carbide on the tool flank due to the attrition wear where the workpiece was machined at cutting speed 15 m/min, feed rate 0.1 mm/tooth and axial depth 0.7 mm after second pass due to the attrition wear.

The analysis of EDX shows the existence of new elements such as Manganese (Mn), Ferum (Fe), Molybdenum (Mo), Nickel (Ni) at the coated carbide insert. These elements were found due to adhesive of the workpiece during the machining process, which is subjected to high heat concentration. Adhesion wear is a removal of grains of tool material due to intermittent adhesion between the tool and the workpiece, as a result of the irregular chip flow and the breaking of a partially stable BUE. The rake face of the cutting insert can be protected if the BUE is stable which is why only flank wear is found and rake wear can be avoided. Coating peeling or delamination takes place due to BUE in a coated carbide cutting insert. In the case of nickel based alloys,

when high stress is applied to the cutting edge the breakdown of the cutting edge of the cutting tools takes place. The serrated chip causes fatigue which is why the adhesion mechanism takes place and this fatigue is also held responsible for the cracks that are formed.

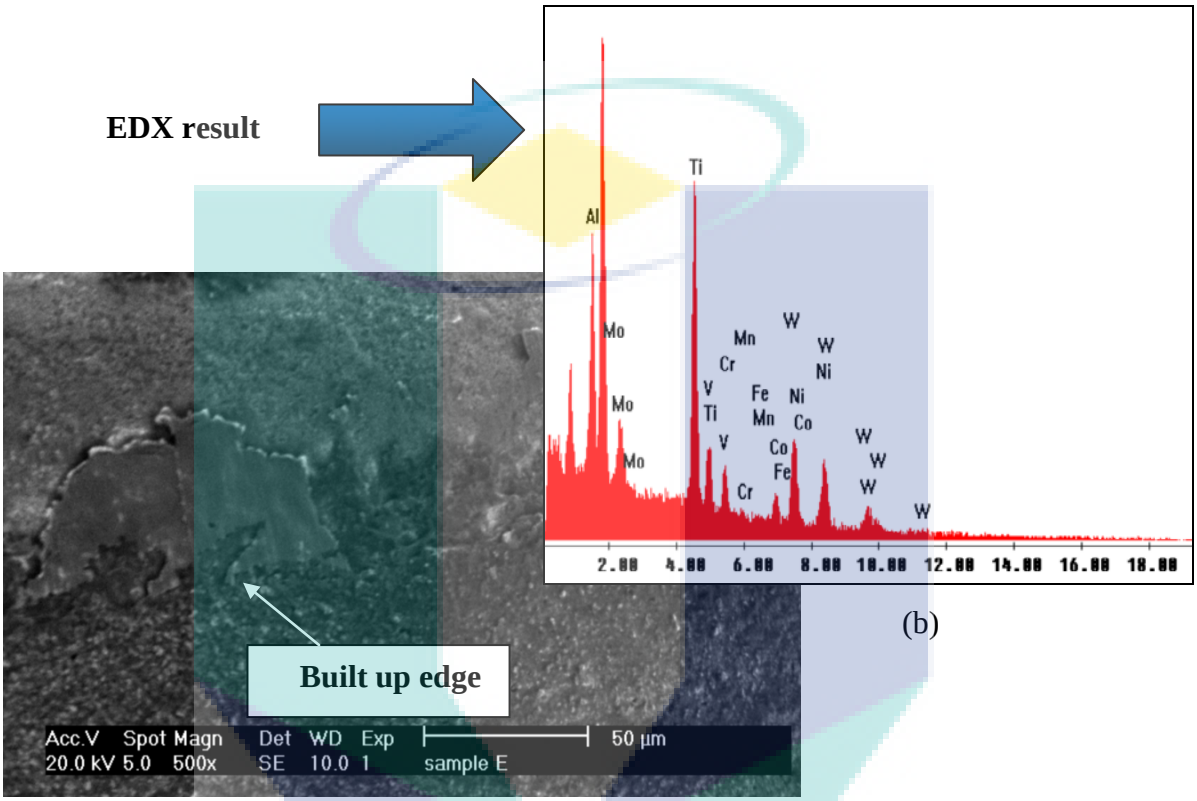

Figure 4.20: (a) BUE formation at coated carbide, (b) EDX result

Figure 4.21 shows the formation of adhering layer at uncoated carbide cutting insert. Thermal softening, strain rate and work hardening have been found to have a unique and complex relationship due to the passing of the workpiece material along the rake face. Such parameters are physical in nature which is why they are able to affect the dynamic flow strength of the material (Wright and Chow, 1982). A high temperature gradient would be able to create a difference amongst the tool–layer interface and the workpiece–layer interface. This temperature has also been referred to as the transient temperature since it has the ability to form a layer of hard base and top face which is soft (Qi and Mills, 2000).

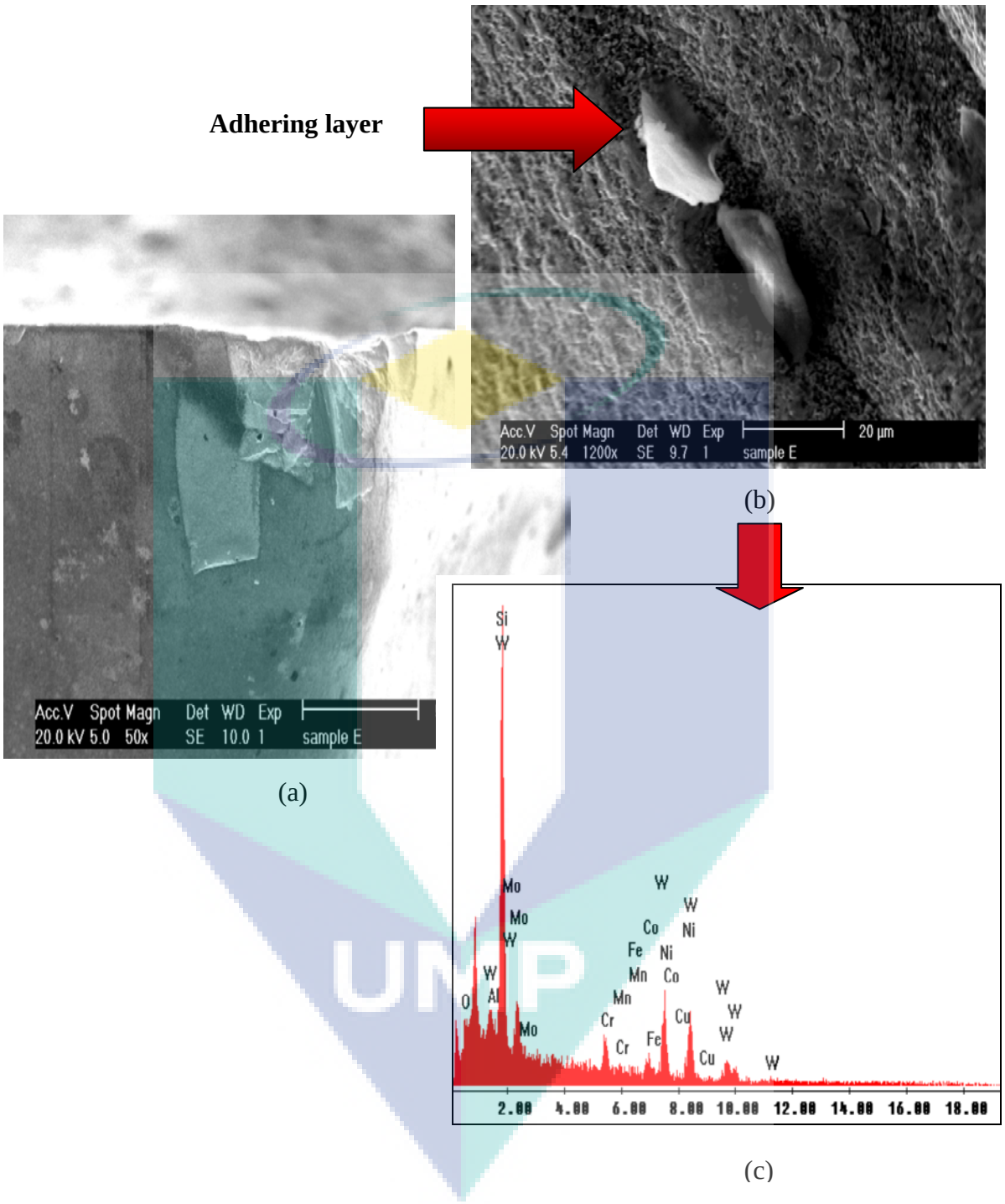

Figure 4.21: (a) adhesion wear at uncoated carbide at magnification 50x, (b) adhering layer at magnification 1200x, (c) EDX test.

It can be inferred that under the proper conditions of temperature, shear strain rate, and work hardening, the wear of adhered layer and the stacking of the layer attained a balance, leaving a relatively stable layer on the interface. The increasing stacking of layer contributed to an irregular, unstable layer, which was force fully

plucked away by the action of chip flow or workpiece travel. Thus, When the tool materials were removed, certain pullouts were formed which were inside the unstable layer. Figure 4.22 shows the plucking formation at coated carbide cutting tool insert.

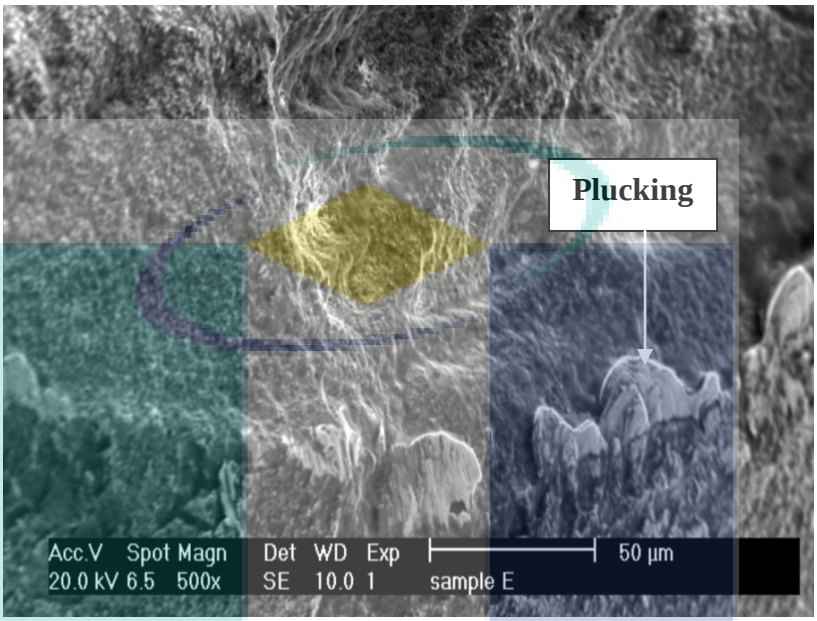

Figure 4.22: Plucking at coated carbide inserts

Figure 4.23 shows the adhesion and diffusion mechanism for coated and uncoated cutting inserts. A new adhering layer has been formed over the area which was exposed due to the pullouts that occurred over the tool. A process by the name of formation–stacking–plucking took place in the adhering layer at the depth of the cut regions. When this process repeated, it was possible to form a notch at the cut line depth (Xue and Chen, 2011). Attrition wear may be held responsible for the plucking activity that has taken place (Aspinwall et al., 2007). Aggregates or removal individual cutting tool inserts take place in the workpiece which is why a rough area is formed over the cutting insert (Ezugwu et al., 2003). During the machining process there has been a localized form of tensile stress by the intermittent chip flow which causes the mechanism to take place. The tensile stress took place due to the chip detachment which occurred at the time of tool exit and then an instant ejection took place which stuck the chip on to the next entry (Jawaid et al., 2001). Attrition wear has also been caused by the irregular flow of the material of the cutting edge of cutting inserts and the cracks which formed at the time of the elevated temperature (Zou et al., 2009). The changes in

strains and stress have been held responsible for the adhesion wear process which is also intermittent. There is also presence of periodic attachment and detachment of workpiece material on the tool surface. Hence, the adhesion wear mechanism has been held responsible for the formation of notching in the depth of the cut line.

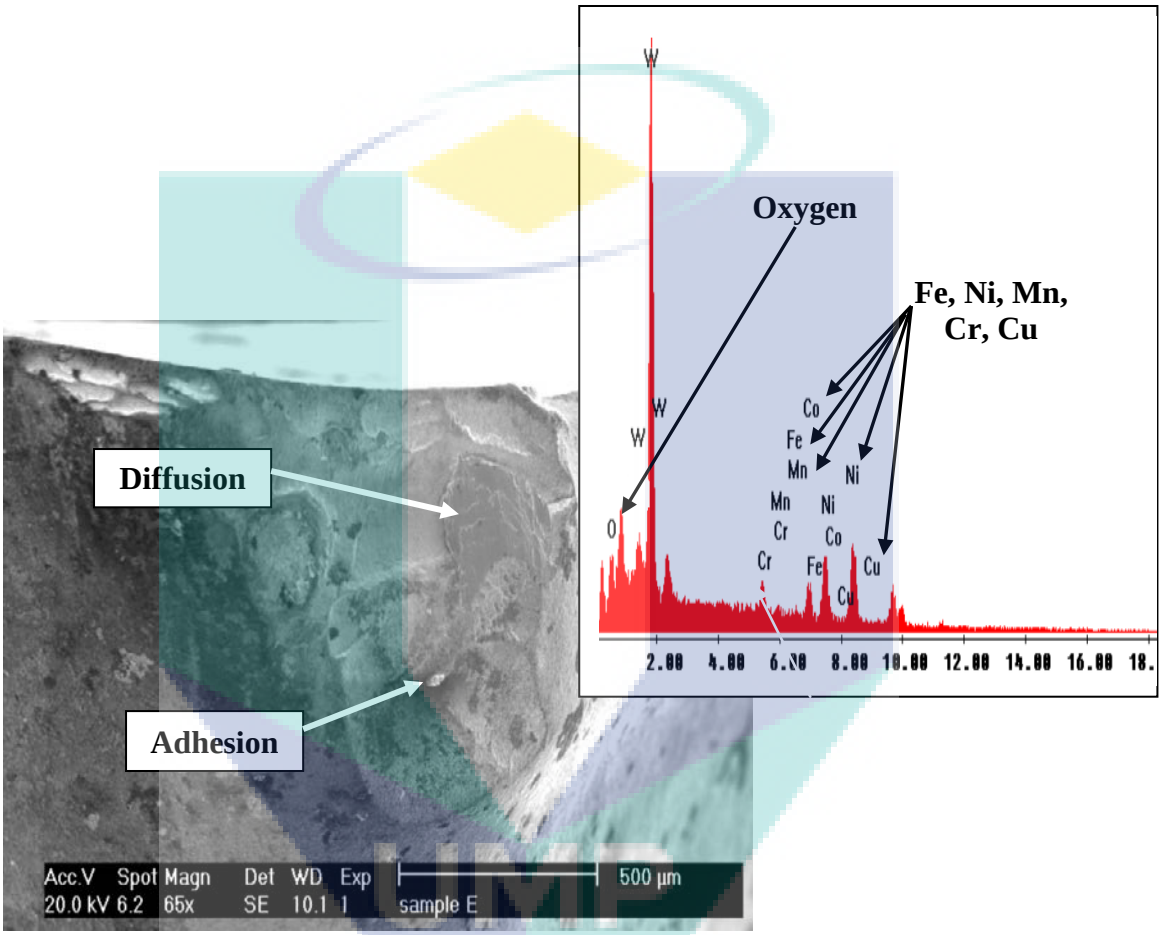

Figure 4.23: Adhesion and diffusion wear at uncoated carbide

Ferum (Fe), Nickel (Ni), Manganese (Mn), Cromium (Cr), Copper (Cu) have been found at the feed rate 0.1 mm/tooth, axial depth 0.4 mm, and cutting speed 23 m/min using CTP 1235 (uncoated carbide) in the EDX analysis. This clearly shows that the diffusion mechanism has taken place. The material have been diffused into the cutting tool at the time of the machining process. High cutting temperature and intimate contact between the tool and the workpiece during machining were considered as the prerequisites for the occurrence of diffusion (Xue and Chen, 2011). If there is a high

temperature of cutting diffusion would occur and a metallic crystal lattice would move from high concentration to low concentration levels.

The high temperatures increase the rate of diffusion which is why the cutting temperature has been regarded as the main characteristic to determine the rate of diffusion (Olovsjo and Nyborg, 2012). With the help of complete seizure at the tool layer along with high cutting temperatures, an environment is created where the tool material atoms are diffused from a high to a low concentration level (Itakura et al., 1999). There exists strong contact between the cutting tool and workpiece and the atoms move from the workpiece to the cutting insert when a high temperature is maintained at the machining. Between two materials, an interface takes place which is within a narrow reaction zone hence causing the surface structure of the tool to weaken. Diffused into the grain boundaries of binder Co are the elements Nickel (Ni) and Ferum (Fe) from workpiece material. The high temperature causes the intermetallic phases between carbides and binder by ways of grain boundary diffusion. There exists high affinity of carbides with Nickel (Ni) which causes the intermetallic phases to dissolve which then disrupts the binder and carbide bonding (Liao and Shiue, 1996). As observed in Figure 4.23 shows process adhesion, diffusion and oxidation take place. There exists oxidizing temperature and higher levels of hardness in the PVD- coated carbide with TiA1N coating layers. The aluminum coating film oxides are subjected to a high temperature which forms a very thin layer of amorphous aluminum oxide and stops any more of oxidation to take place (Yamada et al., 1996). Hence, the coated carbide is found to have no mechanism of oxidization. The water soluble coolant is able to create the mechanism (Kadirgama et al., 2011). The pull out, oxidation mechanism and increased level of seizure has the ability to increase the level of depth of cut notching (Machado et al., 1998). Co has lower levels of oxidation growth that W when the cutting temperature increases (Warren et al., 1996). Figure 4.24 shows the mapping wear of coated and uncoated carbide. For coated and uncoated carbide the Hastelloy C-2000 machining has the ability to carry out chipping, notching and flank wear. Only uncoated carbide carries out catastrophic wear and the failure, notching and chipping takes place due to adhesion, BUE and mechanism of attrition. Both flank wear for cutting tools mainly attributes to BUE and adhesion however, it also happens due to diffusion and oxidation mechanism for uncoated carbide cutting tool.

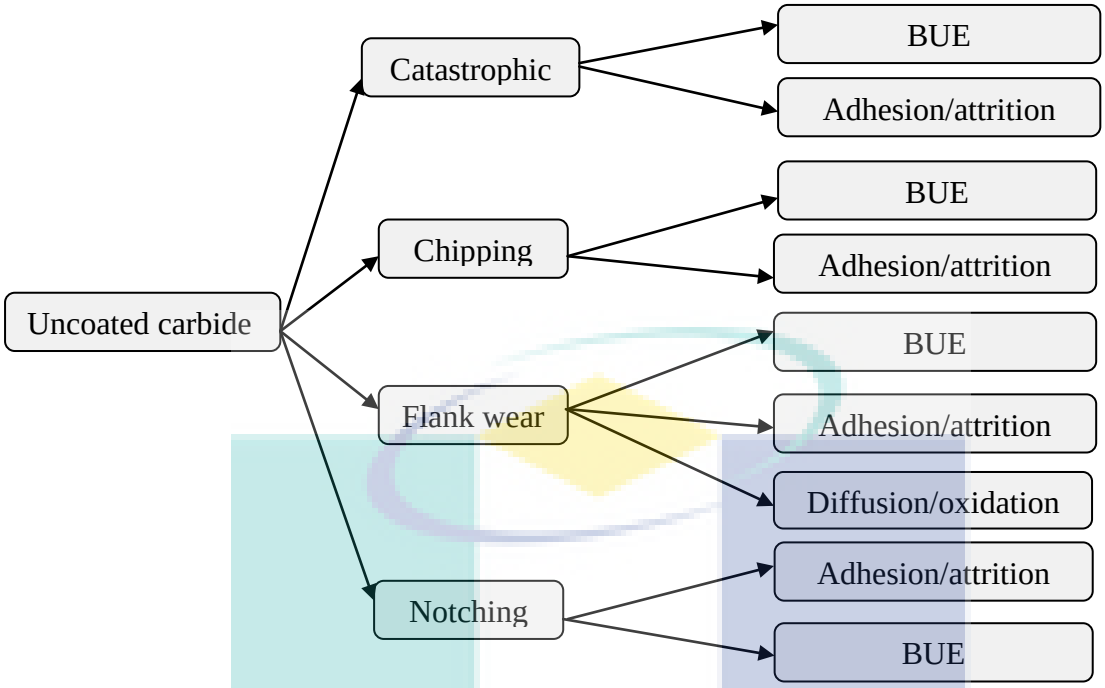

(a) Uncoated carbide cutting insert

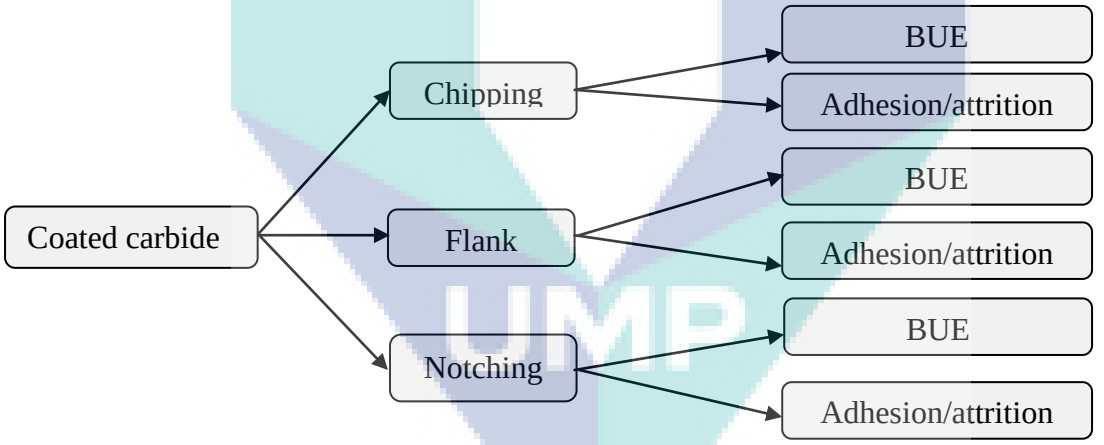

(b) Coated carbide cutting insert

Figure 4.24: Mapping of wear for different cutting tools

4.5 CUTTING FORCE

In a metal cutting theory, the main issue that has been observed is the modelling process of the cutting forces. There are several kinds of parameters like rake angles,

clearance angle, nose radius etc which are all held responsible for the issues which arise in developing an appropriate model. Many of the machining handbooks are available but they only stress upon the relation between the cutting parameters along with fixing other parameters. Using existing machining data it is required that proper mechanisms be developed for general models. Using the first and second order RSM, an approach for the model cutting forces will be developed in the section along with an analysis of the chip formation of Hastelloy C-2000.

4.5.1 Mathematical modelling

Development of Linear Model

When experimental miller operations take place, a Kistler force dynamometer model 1679A5 is used to record cutting force. Each pass is equal to 120 mm length and after managing the first pass of 15 cutting experiments, the cutting force readings have been used to figure out the parameters in the linear order model Eq. 4.13 and Eq. 4.14 for coated and uncoated carbide inserts.

For coated carbide cutting tool inserts:

$$F_y = 442.56 + 107.66x_1 + 76.67x_2 - 58.52x_3 \quad (4.13)$$

For uncoated carbide cutting tool inserts:

$$F_y = 508.79 + 115.47x_1 + 71.76x_2 - -61.41x_3 \quad (4.14)$$

The feed rate has the highest level of effect on the cutting force which is then followed by the axial depth and the cutting speed for all the models. This aspect can be observed in equation (4.13-4.14). The cutting force consisted of the feed rate as the strongest cutting force which was also followed by the axial depth, radial depth and the cutting speed (Ibraheem et al., 2008). If the feed rate decreased or then the cutting speed increased, there is possibility that the cutting force would decrease overall. This aspect

has also been presented by the researcher Fang and Wu (2009). Table 4.27 displays the variance analyses for cutting tools of both categories. ANOVA has presented the level of adequacy for the linear order model at a 95% confidence level. The *P*-values of linear terms for both the models are 0.000 for coated carbide and 0.000 for uncoated carbide that are less than the α-value (0.05) which is why the model is considered adequate and statistically significant. There are vast effects on the responses by the terms which are chosen in the model. The *P*-values of lack of fit for coated and uncoated carbide which are higher than the α-level (0.05) are 0.296 and 0.072 respectively are considered insignificant. Therefore the model has been observed as adequate and acceptable with an indicator to measure the effectiveness of the levels. In order to decide whether the linear model is appropriate, the co-efficient R^2 has been used which also helps decide the best response model when it reaches unity (Bouacha et al., 2010). The uncoated carbide has a greater value of R^2 which is 89.25 % than the coated carbide which is 86.90 %.

Table 4.27: Variance analysis for linear order cutting force model for coated and uncoated carbide inserts

Source	**DF**	**Coated Carbide inserts**		**Uncoated carbide inserts**	
		F-value	**P-value**	**F-value**	**P-value**
Regression	3	24.33	0.000	30.43	0.000
Linear	3	24.33	0.000	30.43	0.000
Residual Error	11				
Lack of Fit	9	2.74	0.296	13.31	0.072
Pure Error	2				
Total	14				

Note: DF= Degree of freedom

Figure 4.25 (a-b) shows the relationship of cutting force with feed rate and axial depth for coated and uncoated carbide. For both cutting inserts, the cutting force is high when the axial depth and feed rate are high, hence proving that they have a directly proportionate relationship. The uncoated carbide had a higher cutting force than the coated carbide. The force concentration was reduced during the machining process since the coated carbide layering did not allow easy cutting.

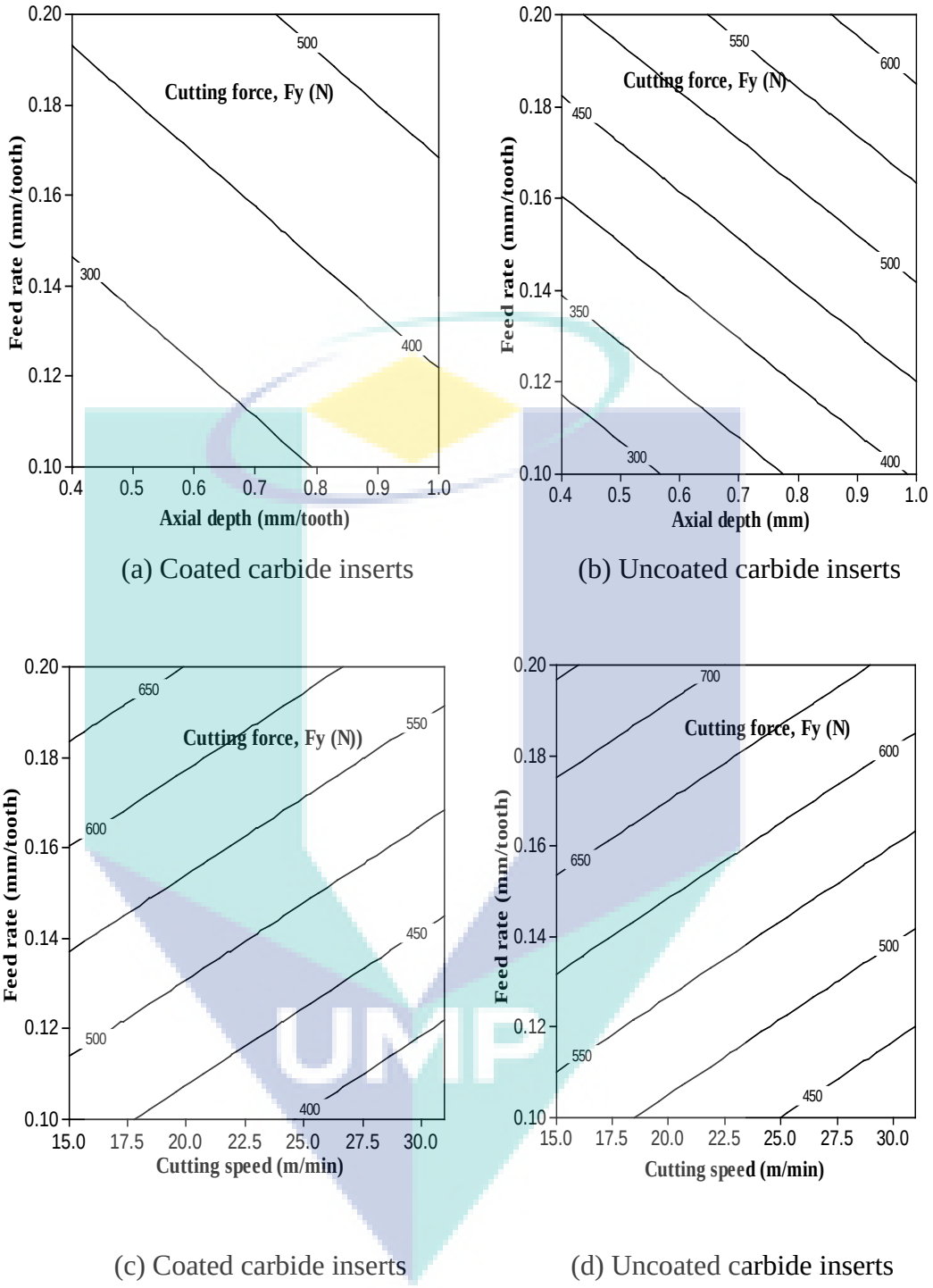

Figure 4.25: The cutting force first order RSM contour plot versus feed rate and axial depth for (a) coated; (b) uncoated carbide inserts and feed rate as well as cutting speed for (c) coated and (d) uncoated carbide inserts

Table 4.28: Experimental result and linear models predicted values for coated and uncoated carbide inserts

No	Exp. Cutting Condition			Experimental result		Predicted RSM		Absolute Error (%)	
	FR	AD	CS	CTW 4615	CTP 1235	CTW 4615	CTP 1245	CTW 4615	CTP 1235
1	0.15	0.4	31	280.901	350.223	307.3663	375.6227	9.422	7.252
2	0.15	1	15	552.332	570.896	577.7496	641.9605	4.602	12.448
3	0.1	0.7	15	350.220	450.290	393.4257	454.7351	12.337	0.987
4	0.2	1	23	650.308	680.440	626.8818	696.0170	3.613	2.289
5	0.2	0.7	31	423.020	500.110	491.6902	562.8481	16.233	12.544
6	0.15	0.7	23	420.186	530.240	442.5579	508.7916	5.324	4.045
7	0.15	0.7	23	460.525	550.801	442.5579	508.7916	3.901	7.627
8	0.2	0.7	15	550.222	720.880	608.7399	685.6709	10.636	4.884
9	0.1	0.4	23	239.706	326.995	258.2341	321.5662	7.730	1.66
10	0.15	1	31	500.222	561.424	460.6998	519.1377	7.882	7.532
11	0.15	0.4	15	480.330	461.433	424.4161	498.4455	11.64	8.021
12	0.1	0.7	31	260.860	300.451	276.3759	331.9124	5.950	10.471
13	0.1	1	23	450.309	500.831	411.5676	465.0812	8.603	7.138
14	0.15	0.7	23	480.524	525.831	442.5579	508.7916	7.901	3.267
15	0.2	0.4	23	538.802	600.880	473.5483	552.5020	12.11	8.051

The cutting tools of both categories have a cutting speed and feed rate relationship with the cutting force which is found in 4.36 (b). Feed rate and cutting force are directly proportional but the cutting force and cutting speed are found to be inversely proportional to each other. If there is high feed rate and a low level of cutting speed then the cutting force of the Hastelloy C-2000 would increase. The cutting force tends to reduce when applying high cutting speed because it can to contributes to elevated temperature and softening the workpiece (Chen, 2001). The use of low cutting speed, decreases the shear angle which giving a long shear plane that contributes to the increases of shear force required for stress deformation. The friction of efficient also increases, thus the cutting force is increases (Alauddin et al., 1999). If the axial depth and the feed rate increase then the cutting force increases (Liu et al., 2010). Since nickel alloys work harden rapidly, once the milling cutter starts cutting, it will become more and more difficult for further machining due to the hardening effect. Hence, at one point the cutting does not occur and the metal is pushed as the edges are not sharp enough resulting in higher temperature and higher cutting force (Li et al. 2006). Table 4.28 shows the experimental results for the coated and uncoated carbide inserts. The coated and uncoated carbide maximum absolute relative error is 16.233 % and 12.544 %

respectively and the minimum absolute relative error is 3.613 % and 0.987 % respectively.

Development of Quadratic Model

To find the desired region target and help extract the optimal condition of the machine processing, a quadratic model of response function is used. This function does not only provide help with the input and output of the responses (Bouacha et al., 2010). The end milling cutting forces can be predicted by using the quadratic models (Kadirgama and Abou-El-Hossien, 2005). Eq. 4.15 and Eq. 4.16 can be used for the quadratic model equation to predict the cutting force for coated and uncoated carbide cutting inserts.

For coated carbide cutting tool inserts:

$$453.745 + 107.657x_1 + 76.657x_2 - 58.525x_3 - 20.653x_1^{\,2} - 20.653 - 36.689x_2^{\,2} - 37.012x_3^{\,2} - 24.774x_1x_2 - 9.460x_1x_3 + 36.806x_2x_3 \quad (4.15)$$

For coated carbide cutting tool inserts:

$$535.674 + 115.468\,x_1 + 71.757\,x_2 - 61.411x_3 - 0.724x_1^{\,2} + 7.663\,x_2^{\,2} - 42.017\,x_3^{\,2} - 23.569x_1x_2 - 17.733x_1x_3 + 25.434x_2x_3 \quad (4.16)$$

Table 4.29 shows the variance analysis for quadratic model of cutting force model for coated and uncoated carbide inserts. The adequacy of the second-order model is verified using ANOVA results. At a level of confidence of 95%, the models are checked for its adequacy. The *P* values of lack-of-fit are 0.557 in the case of coated and 0.060 for uncoated carbides stating that they are insignificant and that the model is adequate. The *P* values for regression models are 0.001 and 0.007 for coated and uncoated carbide respectively and considered significant. Both models have been considered efficient and there is a measure to check the effectiveness of the model. Meanwhile F-value for the model is for 0.920 coated carbide and 15.91 for uncoated

carbide model implies the lack of fit is not significant relative to the pure error (Lajis et al., 2008).The coated and uncoated carbide R^2 are 97.66 % and 95.61 % respectively. When the R^2 and the *P*-values are compared it is found that between the linear and the quadratic models, the quadratic is much more efficient. This is specifically in the case of Hastelloy C-2000 as the cutting force of the machining.

Table 4.29: Variance analysis for quadratic model of cutting force model for coated and uncoated carbide inserts

Source	DF	Coated carbide insert		Uncoated carbide insert	
		F-value	P-value	F-value	P-value
Regression	9	23.16	0.001	12.09	0.007
Linear	3	61.82	0.000	33.87	0.001
Square	3	4.610	0.067	1.26	0.382
Interaction	3	3.040	0.131	1.15	0.413
Residual Error	5				
Lack of Fit	3	0.920	0.557	15.91	0.060
Pure Error	2				
Total	14				

Note: DF= Degree of freedom

In Figure 4.26, the contour plot for the coated and uncoated carbide quadratic model RSM can be found. A parabolic line is provided by the quadratic models for both the carbides. The cutting force relation between the axial depth and the feed rate can be found in Figure 4.26 (a-b). The cutting force increases in both types of tools when the axial depth and the feed rate are increased. This increase occurs in the same proportion and the uncoated carbide is found to apply a higher cutting force than the coated carbide. There exists lack of protection in the uncoated tool which is why this scenario occurs. However, for the coated cutting tool, the cutting force is lower because mainly the decreased friction between the chip and tool, chip and workpiece and also the effect of the coatings acting as a thermal barrier. This barrier prevents heat from entering the tool due to its high thermal conductivity and hence most of the heat is removed in the hip (MacGhinley and Monaghan, 2001). For the coated carbide insert, the multiple coating layers can improve wear resistance significantly. It is hard to bear the high load impacts and high temperature. Actually, the coated layer cannot stand for long before it is worn. This causes in severe tool wear and short tool life (Li et al., 2006).

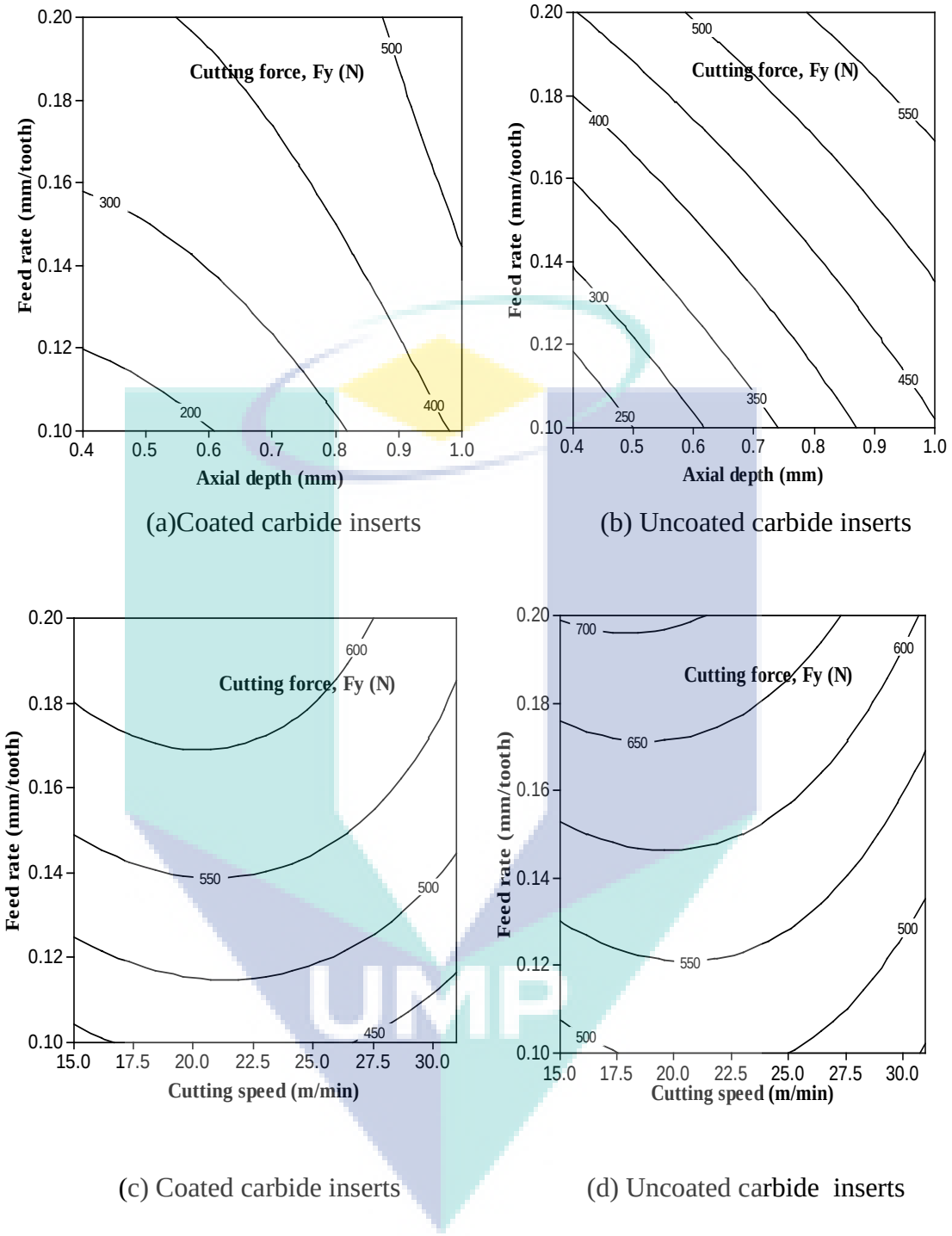

(a)Coated carbide inserts

(b) Uncoated carbide inserts

(c) Coated carbide inserts

(d) Uncoated carbide inserts

Figure 4.26: The cutting force second order RSM contour plot versus feed rate and axial depth for (a) coated; (b) uncoated carbide inserts and feed rate as well as cutting speed for (c) coated and (d) uncoated carbide inserts

Figure 4.26 (c-d) shows the contour plot of cutting force with the relation of feed rate and cutting speed (Shunmugam et al., 2000). When the cutting speed is increased then the cutting force decreases due to the increase in feed rate which more material will

have to be cut per tooth per revolution; as a consequence more energy is required (Reddy and Rao, 2006). Side surface, crater, notch wear, tool breakage and plastic deformation are all caused by the high cutting speed. To supply energy, the cutting force is working towards the cutting direction. As the depth of the cut increases, the cutting force also increases due to the resultant forces. The depth of the cut in increased and the extra material is removed by the additional energy that has been provided (Astakhov, 1999; Ostwald and Munoz, 2002). The coated and uncoated carbide inserts experimental results of quadratic models are present in Table 4.30. The minimum absolute relative errors for coated and uncoated carbide are 0.0095 % and 0.97 % respectively and the maximum absolute relative errors are 8.751 % and 11.095 % respectively.

Table 4.30: Experimental result and quadratic models predicted values for coated and uncoated carbide inserts

No	Exp.Cutting Condition			Experimental result		Predicted RSM		Absolute Error (%)	
	FR	AD	CS	CTW 4615	CTP 1235	CTW 4615	CTP 1245	CTW 4615	CTP 1235
1	0.15	0.4	31	280.901	350.223	281.4249	327.3906	0.186	6.519
2	0.15	1	15	552.332	570.896	551.8081	593.7284	0.001	3.999
3	0.1	0.7	15	350.220	450.290	337.4878	421.1435	3.635	6.472
4	0.2	1	23	650.308	680.440	629.3309	690.9429	3.226	1.544
5	0.2	0.7	31	423.020	500.110	435.7523	529.2565	3.010	5.828
6	0.15	0.7	23	420.186	530.240	453.7450	535.6737	7.987	0.970
7	0.15	0.7	23	460.525	550.801	453.7450	535.6737	1.472	2.746
8	0.2	0.7	15	550.222	720.880	571.7230	687.5448	3.908	4.624
9	0.1	0.4	23	239.706	326.995	260.6831	316.4921	8.751	3.212
10	0.15	1	31	500.222	561.424	508.3689	521.7746	1.649	7.062
11	0.15	0.4	15	480.330	461.433	472.0851	501.0824	1.717	9.243
12	0.1	0.7	31	260.860	300.451	239.3590	333.7863	8.242	11.095
13	0.1	1	23	450.309	500.831	463.5651	507.1451	2.944	1.261
14	0.15	0.7	23	480.524	525.831	453.7450	535.6737	5.573	1.936
15	0.2	0.4	23	538.802	600.880	525.5459	594.5659	2.460	1.000

The experimental results for the coated and uncoated carbides are compared to the linear and quadratic RSM model in Figure 4.27. The quadratic RSM model shows the coated and uncoated carbide to be 3.651 % and 4.5 % respectively and the linear order RSM is 8.526 % and 6.547 % respectively. Hence the quadratic results are closer to the experimental results which states that the quadratic RSM is significant to the roughness model.

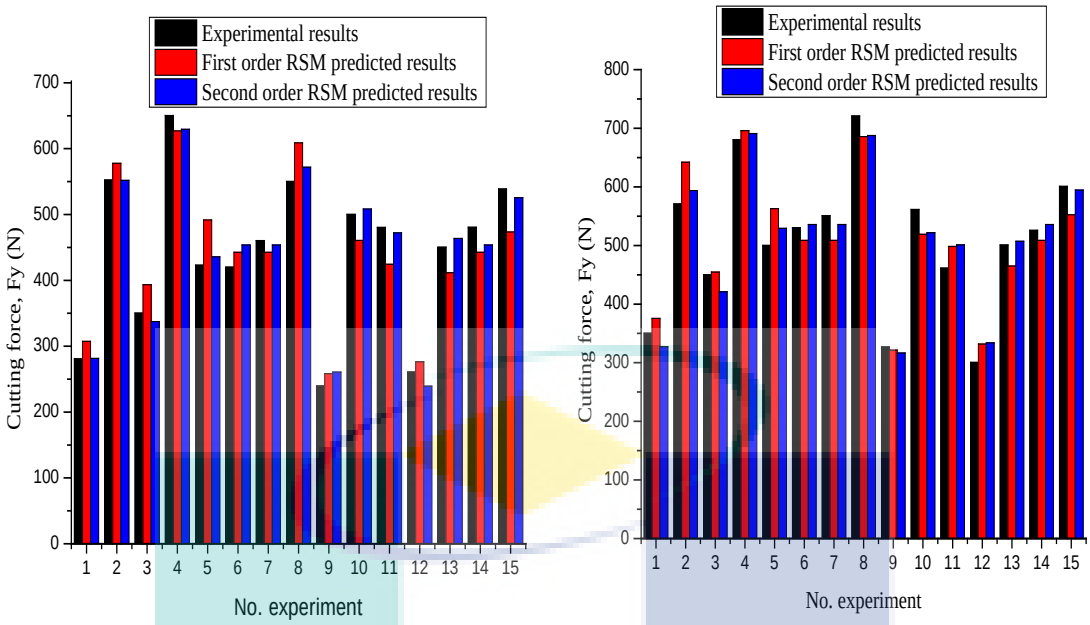

(a) Coated carbide inserts (b) Uncoated carbide inserts

Figure 4.27: Comparison between experimental results, first order RSM, second order RSM for coated and uncoated carbide inserts

4.5.3 Artificial Neural Network Model

The Artificial Neural Network comprises of three inputs, twenty five concealed levels and one output level; (3-25-1). The paramount blend of the ANN system is ID number two used for cutting tool coated carbide. Table 4.31 shows the analytical exploration towards the finest hidden levels. In the meantime, the finest ANN's formation for uncoated carbide is at ID number seven which is three inputs, fourteen hidden levels and one output (3-14-1). The The best criterions are automatically chosen by the software based R-square values and correlation coefficient values. The value of R^2 for coated carbide is 0.999871 and correlation of coefficient is 0.999718. The best criterions are selected based on R-square values and correlation coefficient value. Moreover, 0.997284 is the R^2 for uncoated carbide cutting tool and 0.998767 is the correlation of coefficient. The best architecture is trained using bath back propagation algorithm.

Table 4.31: Heuristic search for coated and uncoated carbide inserts

ID	N	F	TE	VE	TE	C	R-S	SR
Coated carbide inserts (CTW4615)								
1	2	0.1650	18.037	15.9413	60.5873	0.974298	0.943840	AID
2	25	0.0194	1.9316	19.5725	51.2844	0.999718	0.999871	AID
3	16	0.0181	0.3880	22.6253	55.0630	0.999967	0.99870	AID
4	10	0.0157	0.6445	39.9913	63.6887	0.999556	0.99828	AID
5	21	0.0175	1.0775	19.9626	56.8750	0.999331	0.999415	AID
6	13	0.0088	0.4316	59.0196	112.441	0.999421	0.999841	AID
7	19	0.0123	0.4156	56.7643	78.7603	0.999231	0.999233	AID
8	17	0.0243	0.5897	40.2128	61.4343	0.999610	0.99940	AID
9	22	0.0192	0.6342	16.7921	62.2748	0.999570	0.999011	AID
Uncoated carbide inserts (CTP1235)								
1	9	0.0040	123.31	43.0506	249.877	0.449329	0.181491	AID
2	10	0.0176	6.4446	9.85683	56.6367	0.998971	0.997693	AID
3	21	0.0044	140.272	15.0904	224.0021	0.386889	0.790624	AID
4	13	0.0072	69.0799	34.8271	137.0080	0.93609	0.903399	AID
5	19	0.0139	45.2312	53.5528	71.6309	0.980390	0.992264	AID
6	14	0.1636	6.2861	34.5556	6.1113	0.998767	0.997284	AID
7	17	0.0235	11.3348	11.3348	42.4054	0.996595	0.982144	AID
8	16	0.4321	8.4321	30.4789	20.2148	0.98764	0.982144	AID
9	23	0.0339	7.2219	16.4789	13.2284	0.99021	0.990210	AID

Note: ID= Identity number, N= Neurons, F= Fitness, TE= Training error, VE= Validation error, TE= Testing error, C= Correlation, R-S= R-square, SR= Stop reason
AID = All iterations done

Table 4.32 highlights the summary of the training and testing of the coated and uncoated carbide cutting tool inserts. The absolute relative errors of the training and testing for coated are averaged out to be 0.354 % and 0.794 %. Meanwhile for uncoated are 0.367 % and 0.519 %. Table 4.33 and Table 4.34 show the training and testing of artificial neural network for coated and uncoated carbide cutting insert. Keeping in mind the coated carbide inserts the coefficient of correlation is 0.999 899 and R^2 is 0.999 793. The testing shows the values of 0.999 968 and 0.998 570. For training uncoated carbide inserts, the coefficient of correlation is 0.999 955 and R^2 is 0.999763. The testing values are 0.999 968 and 0.998 570. Table 4.35 shows the validation for coated and uncoated carbide. The absolute error for validation for coated carbide and uncoated carbide is within 3% to 1%. Based on the training and testing, ANN gives near prediction to the experimental value and the validation test gives the error accuracy 1.5%-3.7% to the predicted value and considered in acceptable range.

Table 4.32: Summary training and testing for coated and uncoated carbide inserts

	Target		Output		Absolute Error		ARE	
	TR	**TE**	**TR**	**TE**	**TR**	**TE**	**TR**	**TE**
Coated Carbide cutting tool inserts CTW 4615 with NN model of 3-15-1								
Mean	400.697	442.261	442.401	444.264	1.470	3.513	0.354	0.794
SD	457.863	454.732	457.495	457.615	1.786	3.989	0.446	0.852
Min	260.860	239.706	263.241	234.429	0.034	1.869	0.007	0.389
Max	650.308	550.222	651.284	557.348	3.377	7.127	0.913	1.295
Uncoated Carbide cutting tool inserts CTP 1235 with NN model of 3-17-1								
Mean	502.802	508.948	502.206	510.016	1.822	2.616	0.367	0.519
SD	519.997	511.397	520.138	511.599	0.206	2.913	0.407	0.594
Min	300.451	450.290	299.443	454.889	0.619	0.554	0.118	0.497
Max	720.880	570.896	724.432	568.224	3.552	4.599	0.638	1.021

Note: TR=Training, TE=Overall, ARE= Absolute relative error, SD: Standard Deviation

Table 4.33: The training and testing of artificial neural network for coated carbide

No	**Exp. Cutting condition**			**Experimental result**	**Predicted ANN**	**Absolute Relative Error (%)**
	FR	AD	CS			
Training, R^2=0.999 793, C=0.999 899						
1	0.15	0.4	31	280.9010	280.9220	0.0074
2	0.15	1	15	552.3320	552.2985	0.0060
3	0.1	0.7	15	350.2200	351.0000	0.2223
4	0.2	1	23	650.3080	651.2845	0.1501
5	0.2	0.7	31	423.0200	424.6371	0.3823
6	0.15	0.7	23	420.1860	417.7848	0.5715
10	0.15	1	31	500.2220	498.6261	0.3190
12	0.1	0.7	31	260.8600	263.2411	0.9128
13	0.1	1	23	450.3090	448.7873	0.3379
15	0.2	0.4	23	538.8020	535.4248	0.6268
Testing, R^2=0.998 570, C=0.999 968						
7	0.15	0.7	23	460.5250	463.2816	0.5986
8	0.2	0.7	15	550.2220	557.3486	1.2952
9	0.1	0.4	23	239.7060	234.4293	0.9498
11	0.15	0.4	15	480.3300	483.8691	0.7368
14	0.15	0.7	23	480.5240	482.3922	0.3887

Note: FR= Feed rate (mm/tooth), AD=Axial depth (mm), CS=Cutting speed (m/min), R^2=R square, C= Correlation coefficient

Table 4.34: The training and testing of artificial neural network for uncoated carbide

No	Exp. Cutting condition			Experimental result	Predicted ANN	Absolute Relative Error (%)
	FR	AD	CS			
Training, R^2=0.999 763, C=0.999 955						
1	0.15	0.4	31	350.2230	347.9872	0.6384
4	0.2	1	23	680.4400	683.7643	0.4886
5	0.2	0.7	31	500.1100	497.2360	0.5748
6	0.15	0.7	23	530.2400	531.1111	0.1642
7	0.15	0.7	23	550.8010	549.6734	0.2047
8	0.2	0.7	15	720.8800	724.4322	0.4928
9	0.1	0.4	23	326.9950	325.5651	0.4373
12	0.1	0.7	31	300.4510	299.4429	0.3355
14	0.15	0.7	23	525.8310	525.2111	0.1179
15	0.2	0.4	23	538.8020	1.1807	0.2191
Testing, R^2= 0.998 570, C=0.999 968						
2	0.15	1	15	570.8960	568.2245	0.4679
3	0.1	0.7	15	450.2900	454.8890	1.0213
10	0.15	1	31	561.4240	558.6592	0.4925
11	0.15	0.4	15	461.4330	461.9874	0.1201
13	0.1	1	23	500.8310	503.3210	0.4972

Note: FR= Feed rate (mm/tooth), AD=Axial depth (mm), CS=Cutting speed (m/min), R^2=R square, C= Correlation coefficient

Table 4.35: Validation of artificial neural network for coated and uncoated carbide inserts

No	Exp. Cutting condition			Experimental result	Predicted ANN	Absolute Relative Error (%)
	FR	AD	CS			
Coated carbide cutting insert						
4	0.2	1	23	357.5420	351.000	1.8297
15	0.2	0.4	23	522.6168	299.4429	2.4507
11	0.15	0.4	15	492.3214	558.6592	1.7168
Uncoated carbide cutting insert						
5	0.2	0.7	31	484.2339	497.2360	2.6851
12	0.1	0.7	31	310.9031	299.4429	3.6861
10	0.15	1	31	568.4240	558.6592	1.7178

Figure 4.28 shows the graph of experimental and ANN predicted results. This graph is constructed to indicate how well ANN can predict the cutting force result. The prediction results fall just near to the actual experimental results. The networks applied the feed-forward back-propagation algorithm. Results for the values predicted by ANN

were very close to experimental values. Feed forward multilayer ANN along with back propagation algorithm is applied to model cutting force for simulation.

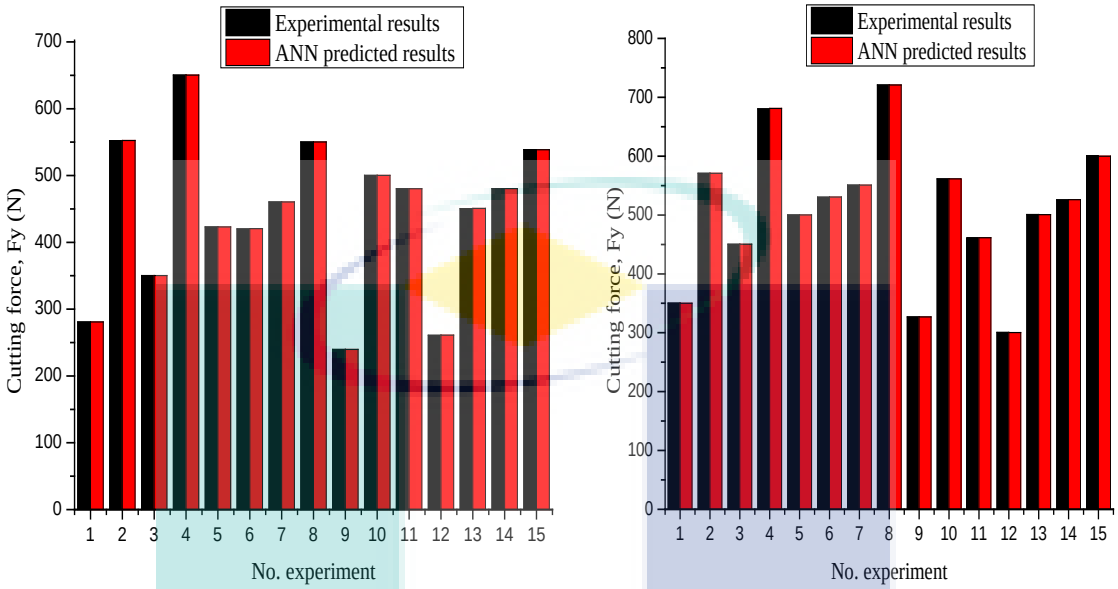

(a) Coated carbide inserts (b) Uncoated carbide inserts

Figure 4.28: Experimental result versus ANN predicted for cutting force, Fy (N) values for coated and uncoated carbide inserts.

A good performance was acquired by applying the feed forward back propagation algorithm to forecast the cutting forces by tangent sigmoid activation function. Figure 4.29 illustrates the combination of linear, quadratic RSM model, ANN and speculative values. It is apparent that the ANN predicted model provides with high precision in predicting the cutting force values as in contrast to the linear and quadratic RSM model. Table 4.36 illustrates the analysis error of statistical and ANN model in which the ANN model shows minor errors in comparison to the other models for coated and uncoated carbide. As a result it can be said that the ANN can be applied as a successful tool towards predicting the cutting force in machining Hastelloy C-2000. The mean absolute error for ANN model is 0.4181 %, for linear is 8.5260% and 3.6510% for quadratic model for coated carbide insert. In cases of uncoated carbide, the mean relative mistakes for ANN is 0.5 %, for linear is 6.5470% and for quadratic model is 4.5000%. Regarding the errors, the ANN shows a better predict with fewer errors as compared to the statistical models. It is important to apply the ANN as the prediction

model of cutting force. Table 4.36 shows the error analysis of cutting force for coated and uncoated carbide inserts.

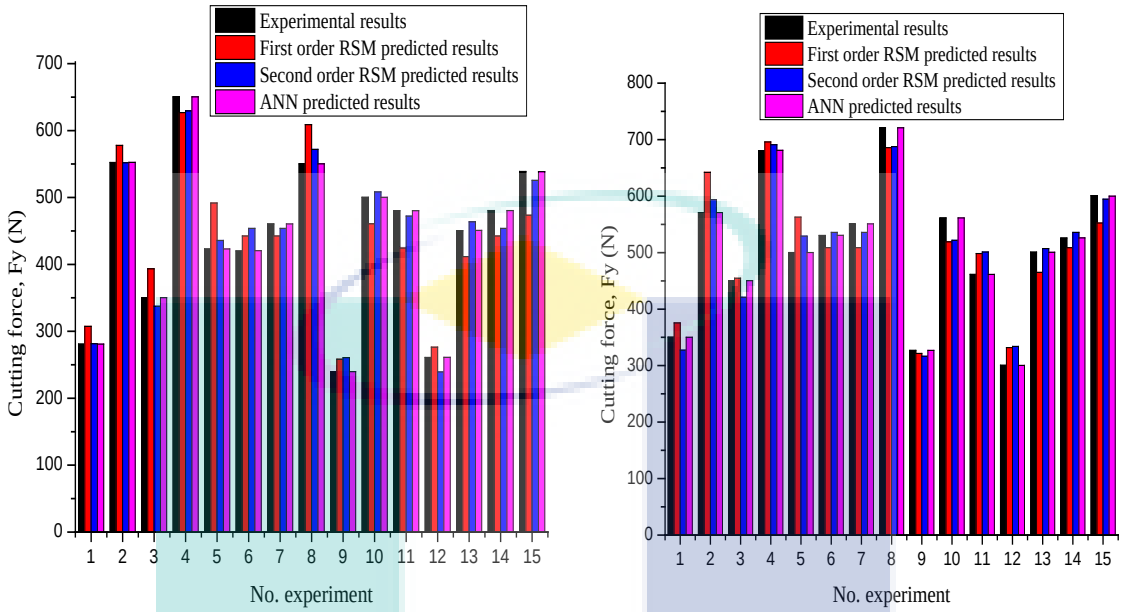

(a) Coated carbide inserts (b) Uncoated carbide inserts

Figure 4.29: Comparison between experimental result, first order RSM, second order RSM for different cutting tools.

Table 4.36: The error analysis of cutting force for coated and uncoated carbide inserts

Model	Minimum relative error (%)		Maximum relative error (%)		Mean absolute relative error (%)	
	CTW4615	CTP1235	CTW4615	CTP1235	CTW4615	CTP1235
FO RSM	3.6130	0.9870	16.2330	12.5440	8.5260	6.5470
SO RSM	0.0095	0.9700	8.7510	11.0950	3.6510	4.5000
ANN	0.0074	0.1179	1.2952	0.63840	0.4181	0.5000

Note: CTW4615= Coated carbide, CTP1235= Uncoated carbide, FO RSM = First order RSM, SO RSM = Second order RSM

4.5.4 The Minimization of Cutting Force

An attempt is fulfilled to estimate the minimum value of cutting force within the experimental constraints. Table 4.37 shows the minimum values of parameters that were achieved. The validation test was performed based on the design variables and percentage of error was calculated. The outcome that was achieved from the validation test gave an up close reading to aim for minimizing the value of cutting force. In order

to accurately minimum and maximum the machining aspects is by bearing in mind the machinability principle the rates of production and outstanding output that such as low cutting forces, surface finish, high tool life, power utilization and dimensional accurateness.

Table 4.37: The minimum value of cutting force for coated and uncoated carbide insert

Cutting insert	Feed rate (mm/tooth)	Axial depth (mm)	Cutting speed (m/min)	Target (min)	Experimental (min)	Error (%)
Coated carbide	0.10	0.4	31	450	460	2.222
Uncoated carbide	0.10	0.4	31	550	563.4	2.444

4.6 CHIP FORMATION

Chip formation pertains to the formation of the chip in the primary and secondary deformation zones. Primary attention was established towards the kinematic relationships, cutting force and the contact process at the tool-tip interface. According to Astakhov (2006) the dilemma of chip-breaking became tremendously significant with growing cutting speed and the establishment of novel difficult-to-machine materials. According to Aykut el al. (2007a) chip formation relies upon the outcome of the workpiece and cutting tool materials, feed rate, cutting speed and the cutting tool geometry. According to Nakayama et al. (1992), the contemporary meaning of this expression implies the chip that has immediately left the tool-chip interface is to be broken. The chips produced during machining rely upon the materials being machined, the tools and the cutting condition. The mechanism of chip formation and separation is due to the extreme strain rate that occurs during the machining process. In case of the cutting of Hastelloy C-2000 due to the lower thermal conductivity characteristics of the material, temperature can be very high locally in some areas of the workpiece, resulting in thermal softening which reduces the material strain hardening capacity and therefore, the shear instability takes place in a narrow band of chips. Figure 4.30 shows the shape of chip and surface texture at feed rate 0.2 mm/tooth, axial depth 0.7 mm and cutting

speed 31 m/min for coated carbide inserts. This type of chip shows a lot of waving. The types of chip formation can be organized into two groups that is unstable and critical chip, depending on its waviness. The unstable chip points towards the adiabatic shear taking place in the work material. According to Yuan Ning et al (2001) chatter acts as a cause of uneven surface roughness and the completed surface will comprise of alternate unburnished (dull) and burnished (shiny) areas. This mechanism of chip formation differs significantly from that of stable cutting. When chattering is developed fully, the cutting edge is no longer moving in the way as that in stable cutting, but vibrates while it is rotating.

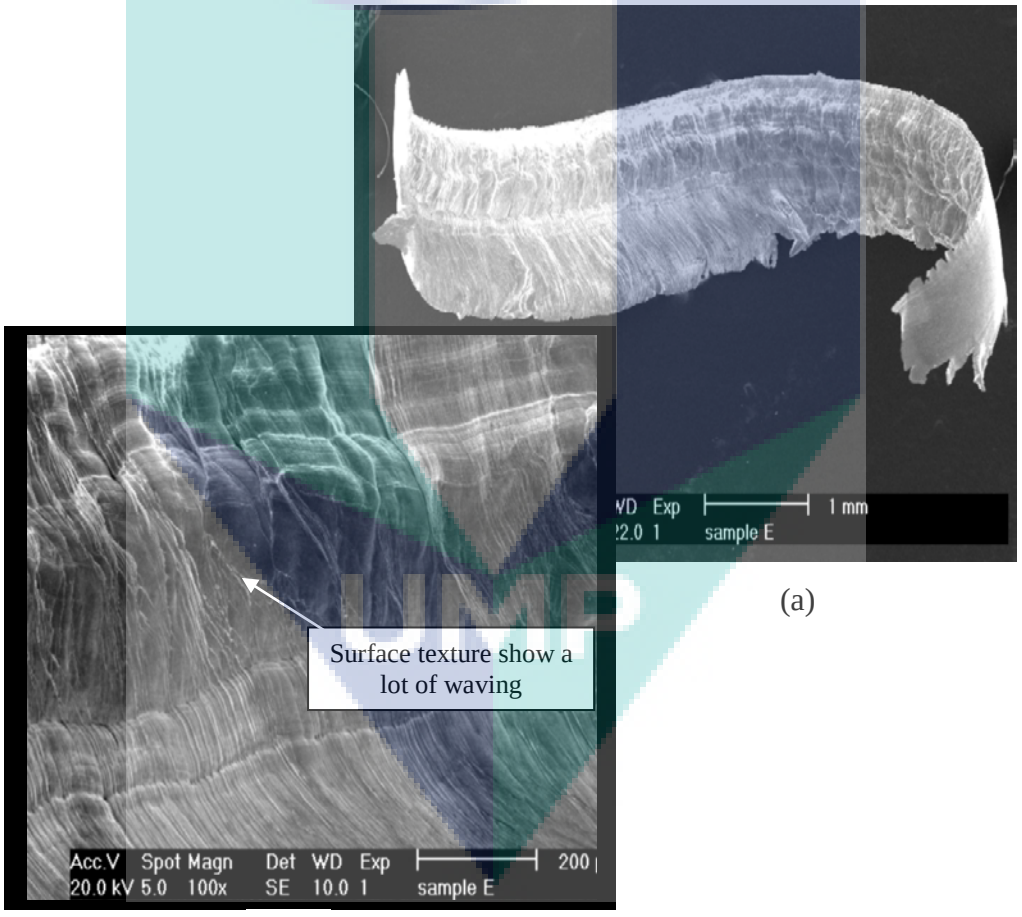

(a)

(b)

Figure 4.30: (a) Shape of chip, (b) Unstable chip – Coated carbide insert

It has been illustrated in Figure 4.31 the figure of the chip with uncoated carbide at cutting machining feed rate 0.2 mm/tooth, depth of cut 0.7 mm and cutting speed 31 m/min. The structure of the critical chip created when machining applying uncoated

carbide because of the chatter marks is dissimilar as in comparison to the unstable chips. Due to the lower thermal conductivity features of the Hastelloy C-2000, there can be a rise in temperature locally in a few areas of the workpiece which may result in thermal softening, that decreases the material strain hardening capability. As a result the shear unsteadiness takes place in a narrow band of chips. No harsh plastic deformation can be seen in the area of adjacent cracks produced between the constituents of the chip.

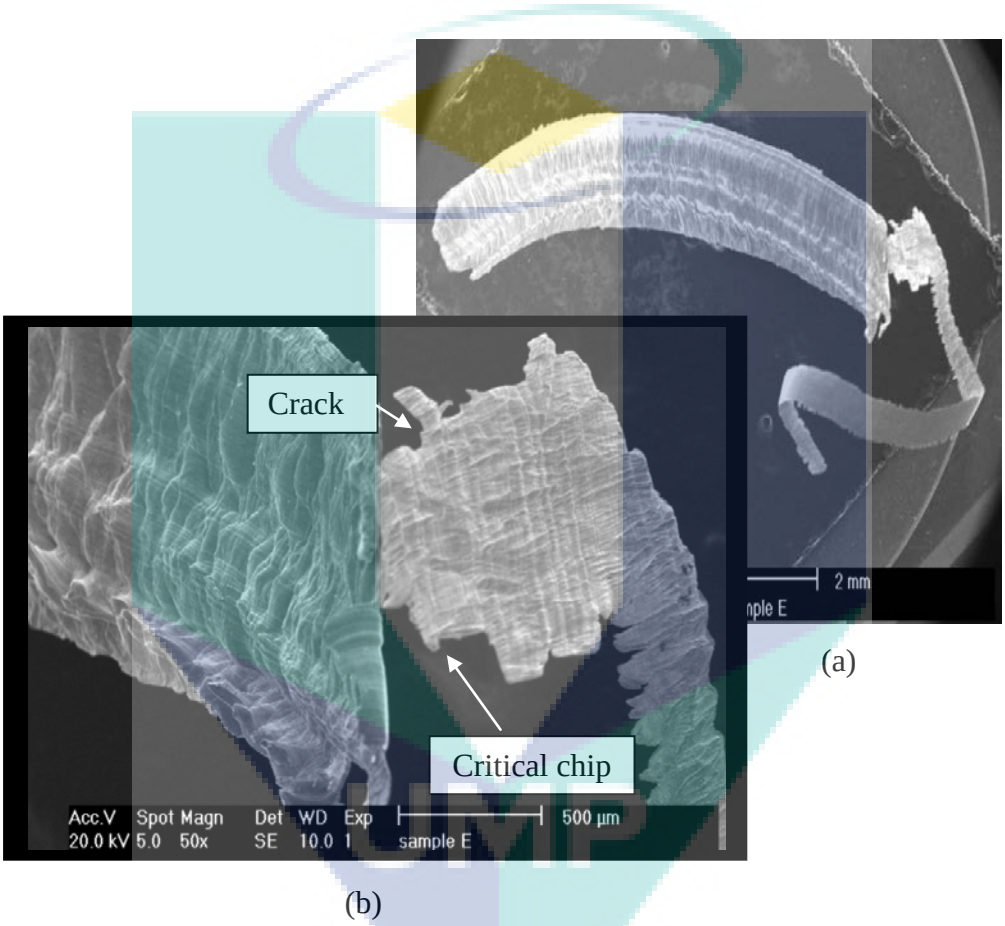

Figure 4.31: (a) Shape of chip, (b) Critical chip – Uncoated carbide insert

It was determined that a work material that cracks at a very low cutting speed would not crack at a higher cutting speed as compared to the chip formation at a low cutting speed. The crack increases without any obvious deformation of the worrkpiece free surface at a low cutting speed. A compressive stress ahead of the cutting edge was the reason towards the formation of the cracks at the free surface creating the brittleness of the workpiece (Kishawy and Elbestawi, 1999). According to Ekinovic et al. (2002) the cracks produced during the formation of chips cannot be entirely repaired by plastic

deformation. Therefore, their tips can be perceived at high magnification. According to Mason et al. (2007) the crack mechanism commenced through gross periodic fractures taking place from the workpiece free surface to the cutting tool tip and in the mean while the fracture initiated at the workpiece surface and prolongs down along the tool tip until the compressive stress established from the tool tip have a huge propensity to prevent the crack.

Figure 4.32 show the saw-toothed edge chip. The deformation of chip is normally known to be inconsistent and deformation is very high in a narrow band between the segments. Abrasive saw toothed edges are generated from the localization of shear in the chip. The chip is a constant kind at low speed cutting and when the speed is enhanced it changes into a saw-tooth kind. It demonstrates that the higher the cutting speed, the saw-tooth chips are more visible. According to Trent and Wright (2000); Thakur et al. (2009) the mechanism engaged in the creation of saw-tooth chip is very intricate and is known to be accredited to the adiabatic shear on the shear plane and cycle cracks at the free surface of the chip. There is no regular principle to forecast the onset of saw-tooth chip formation. According to Guo and Yen David (2004) the creation of saw tooth attributes from the adiabatic shearing and surface crack propagation. According to Davies et al. (1997) and Vyas and Shaw (1999) the saw-tooth creation also contributes by catastrophic strain localization and fracture or crack generation. During the examination of the chip by applying the SEM and EDX test, adhesion mechanism has been detected on the chip when in the process of machining with uncoated carbide at machining parameters of feed rate 0.1 mm/tooth, axial depth 0.7 mm and cutting speed 15 m/min. Figure 4.33 shows adhesion mechanism at uncoated carbide. The chemical element from the cutting tool such as cobalt (Co) and tungsten (W) were found at the magnification 500x on the chip of workpiece machined by EDX. The reason behind this is that the adhesion mechanism, which accredited towards the irregular flow of work material towards the cutting edge of the tool, fatigue produced by the serrated chip and creation of cracks produced by thermal/mechanical fatigue. According to Ezugwu and Wang (1996) and Dearnly and Gearson, (1986) the attrition wear is the elimination of grains, or agglomerates, of tool material because of irregular adhesion between the tool and the workpiece, consequently the uneven chip flow and the breaking of a moderately steady BUE takes place.

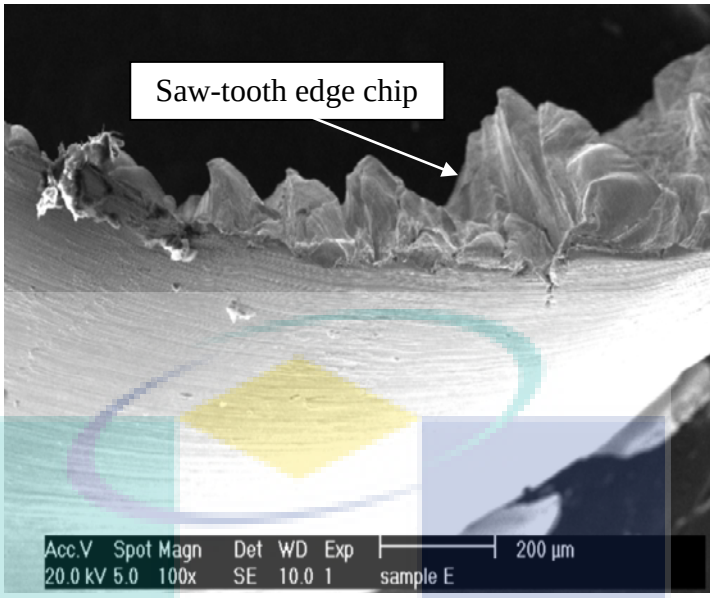

Figure 4.32: Saw-tooth edge chip

Figure 4.34 illustrates that a little quantity of chip flows out of the cutting zone throughout machining with coated carbide at machining parameters, feed rate 0.15 mm/tooth, axial depth 1.0 mm and cutting speed 31 m/min. Many chips are pressed to the sides of the slot, and they are piece-wisely piled up. The chips welded on both the sides of the slot slow down the flow of the chip and cutting temperature rises due to the heat produced cannot be dissipated with the chips. Simultaneously, the cutting force increases quickly. Each and every chip is welded on the sides of the slot, and there is no authorization of chip disposal and generating cutting force over 620.77 N. Regarding the earlier discussions, it is established that the cutting temperature and chip disposal are very significant and concurrent factors that affect slot milling of Hastelloy C-2000 since the cutting temperature is associated to the cutting speed. The cutting temperature will be less than the softening point of gamma prime (γ) when the speed is low. High cutting speed is disadvantageous as it produces harsh strain hardening of the work material. The work material is softened during a high cutting speed but the cutting temperature will also be too high for the cutting tool to survive. Due to these circumstances, the welding of the chips on the work surface becomes grave and it is highly improper.

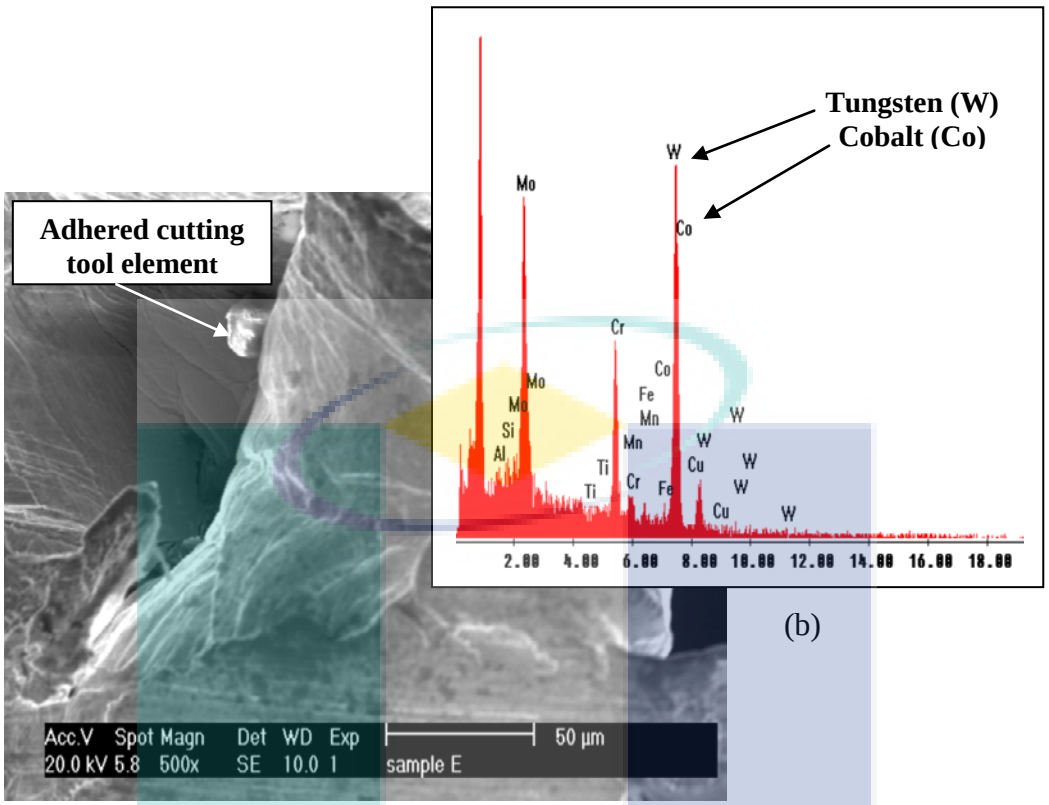

(b)

(a)

Figure 4.33: The adhesion mechanism at uncoated carbide insert

Figure 4.34: Welded chip at the slot machining for coated carbide insert.

4.7 SUMMARY

Using the RSM on machine characteristics like surface roughness, tool life, and cutting force, the mathematical model for Hastelloy C-2000 had been developed. ANOVA helped to check the accuracy levels of the model. The design variables have all been validated using the confirmation test in order to optimize the performance of the machine. Hyperbolic activation function and multilayer perceptron with back propagation algorithm are present in the ANN model to predict the performance of the machine. The machining of Hastelloy C-2000 with coated carbide and uncoated carbide tools the BUE, diffusion, adhesion and oxidation mechanism occur due to the dominant tool failure modes attributes such as , chipping, catastrophic failures, flank wear and notching. In the case of tool life, the PVD coated is found to provide much better performance than the uncoated carbide. The feed rate has the most effect over the cutting force which is then followed by the axial depth and the cutting speed for all kinds of models. As the cutting speed increases, the cutting force decreases. There are two kinds of chips found as part of this study. The Type I: unstable chip and type II: critical chip. The next section will focus on the findings, recommendation and suggestion for the future workings.

CHAPTER 5

CONCLUSIONS AND RECOMMENDATIONS

5.1 INTRODUCTION

The chapter abridges the significant results of the efforts made in this research. This study has tried to come up with several models to predict the performance characteristics of machining Hastelloy C-2000 employed by end milling processes by means of uncoated and coated carbide cutting inserts. Some recommendations and suggestions are also provided so that further research can be carried out in this field.

5.2 CONCLUSIONS

In this thesis, an ample amount of dominant methods and new techniques have been thoroughly scrutinized to instate an improved model for optimization with the help of a response surface methodology, to devise a prediction model centred at machining characteristics by means of artificial neural network, and to investigate the contrivance of tool wear and development of chips of cutting tools during machining Hastelloy C-2000 in end milling. The machining characteristics such as the surface roughness, surface integrity, tool life, tool wear and cutting force in end milling operation were all investigated to accomplish the aforementioned objectives of the thesis.

5.2.1 Mathematical Modelling

The coated carbide and uncoated carbide in wet cutting environment was implied to this research initiated to devise first order and second order mathematical models that predict cutting parameters for Hastelloy C-2000. The experimental results and the

prediction models were used to formulate these mathematical models with the help of first and second order model. With these newly developed models optimization parameters such as the surface roughness, tool life and cutting force were calculated. ANOVA was applied for the process of analyzing data and to test the importance of the statistical models. When both the first and second order models for cutting inserts were compared it was seen that the second order models were more significant to be applied in the modelling of the machining. The RSM shows that surface roughness is considerably affected by the feed rate, axial depth and cutting speed for all the models this is owed to the fact that lower feed rate leads to lowers cutting forces. Lower axial depth means surface roughness will be decidedly subtle to cutting speed and increase in cutting speed significantly reduces the surface roughness. The surface roughness however, increases with increasing of feed rate and axial depth. Lower impact of cutting force decreases the vibration which ultimately improves the surface finish. Contrarily, the surface roughness and cutting force will be increased with the decrease in cutting speed. Nevertheless, the feed rate 0.1 mm/tooth, axial depth 0.4 mm and cutting speed 31 m/min for coated carbide and feed rate 0.1 mm/tooth, axial depth 0.4 mm and cutting speed 31 m/min for coated carbide make up the optimum cutting conditions for surface roughness. It is seen that a majority of uncoated carbide inserts do not have a long tool life when exposed to high cutting speed, and feed rate leading to breakage of the inserts. Tall this takes place because the tool was coated and as long as the coating is unharmed, the tool wear rate is very low because wear resistance of the coating is still high. In terms of effect on tool life the feed rate is most influential then comes the axial depth and cutting speed. Higher cutting speed, feed rate and axial depth indicate lower tool life. The optimum value for tool life for both types of cutting insert parallel to design variables are, feed rate 0.1 mm/tooth, axial depth 0.4 mm and cutting speed 15 m/min. The tool life of coated carbide is 30-50 % higher compare to the uncoated carbide cutting insert to their toughness and hardness of coating layer.The feed rate is most influential factor affecting the cutting force and followed by axial depth and cutting speed for both coated and uncoated carbide models. The cutting force decreases as the cutting speed increases. Since nickel alloys work harden rapidly, once the milling cutter starts cutting, it will become more and more difficult for further machining due to the hardening effect. In a situation when cutting edge is insufficiently sharp the metal is pushed instead of being cut creating an increase in cutting force and temperature. The cutting conditions optimum for cutting force are as follows; feed rate 0.14 mm/tooth,

axial depth 0.4 mm and cutting speed 31 m/min for coated carbide and feed rate 0.1 mm/tooth, axial depth 0.4 mm and cutting speed 31 m/min for uncoated carbide.

5.2.2 Artificial Neural Network

The foundations of the best network our laid on the feed forward multilayer perceptron, back propagation algorithm and hyperbolic activation function. The artificial neural network prediction models however, are devised on the grounds laid by the experimental results with the feed rate, axial depth and cutting speed used as the input parameters. And the output of the parameters comprised of surface roughness, tool life and cutting force. The mean absolute relative error is 0.1790 % and 0.136 % for coated and uncoated carbide for surface roughness models in that order these mean absolute relative error are an evidence to prove the accuracy of ANN network. The mean absolute relative error for tool life is 0.2 % and 0.1580 % for coated and uncoated carbide, which is tailed by 0.4181 % and 0.500 % for cutting force models. On the basis of these outcomes we can say that ANN can yield much better results than mathematical modelling in predicting the machining characteristics. The trial and error method was applied here in order to find the efficient network for prediction model.

5.2.3 Tool Wear

For coated and uncoated carbide both during the machining Hastelloy the acquired tool wear included flank wear, chipping, and notching. But only the use of uncoated carbide resulted in very severe chipping because there was no protecting layer of carbide cutting insert that is why in the course of machining breakage becomes obvious. These protective layers are made up of PVD coated carbide with TiA1N coating layers their purpose is to increase the tool performance by acting as thermal barrier thus prevent the elevated temperature generating during the machining process from softening the substrate. Therefore coated carbide inserts perform better compare to the uncoated carbide. The flank wear for cutting tools mostly is an aspect of BUE, adhesion or attrition, diffusion and oxidation mechanism for uncoated carbide cutting tool. The BUE and adhesion/attrition mechanism cause the catastrophic failure, chipping, and notching.

5.2.4 Chip Formation

In the course of this research, the chips formed were stable and unstable chip. The formation of the unstable chip is due to the adiabatic taking place in the work material. It is this adiabatic shear on the shear plane and or cyclic cracks at the free surface of the chip and catastrophic strain localization that leads to the formation of saw-tooth edge chip. The crack also found occurs at the chip because of compressive stresses in front of the cutting edge. It is also formed in the formation of chip cannot be completely healed by plastic deformation. When the work material is irregularly flowing over the cutting edge of the tool, the fatigue brought by the saw-toothed chip and development of cracks by thermal/mechanical fatigue all lead to adhesion mechanism.

6.2 RECOMMENDATIONS FOR FUTURE RESEARCH

This study presents a wider scope in making the model more reliable and useful and to display an improved understanding of the end milling processes taking into account every individual constraint which influences the working features. Several fields of research are described in this section.

- Further cutting variables like vibration, distinct coated cutting tools and distinct angle of cutting tool could be used to forecast the cutting constraints of various alloys involving nickel.
- Apart from that, the research on the cutting temperature must be emphasised upon. The experiment must be carried out in high feed rate, axial depth and cutting speed so that greater values of an assortment are covered.
- The minimum quantity lubricant (MQL) and nano-fluids coolant can be apply in order to compare the machining characteristics when using conventional lubricant.
- Furthermore, part swarm optimization, colony fuzzy logic, protein optimization and fuzzy logic can be used to examine the findings.
- A distinct type of ANN having distinct learning principles as well transfer roles can be assimilated.

REFERENCES

Abeesh, B.C., Dabade, U.A., Joshi, S.S., Bhanuprasad, V.V. and Gadre, V.M. 2008. Modeling of surface roughness in precision machining of metal matrix composites using ANN. *Journal of Material Processing Technology*, **197**: 439–444.

Abu-Mahfouz, I. 2003. Drilling wear detection and classification using vibration signals and artificial neural network. *International Journal of Machine Tools and Manufacture*, **43**: 707–720.

Aggarwal, A., Singh, H., Kumar, P. and Singh, M. 2008. Optimization of multiple quality characteristics for CNC turning under cryogenic cutting environment using desirability function. *Journal of Materials Processing Technology*, **205**: 42–50.

Ahmed, S.G. 2006. Development of a prediction model for surface roughness in finish turning of aluminium. *Sudan Engineering Society Journal*, **52**(45): 1-5.

Al-Ahmari, A.M.A. 2007. Predictive machinability models for a selected hard material in turning operation. *Journal of Material Processing Technology*, **190**: 305–311.

Alauddin, M., Mazid, M.A., Baradi M.A. El. and Hashmi, M.S.J. 1998. Cutting forces in the end milling of Inconel 718. *Journal of Material Processing Technology*, **77**: 153–159.

Alberti, M., Ciurana, J. and Casadesús, M. 2005. A system for optimising cutting parameters when planning milling operations in high-speed machining. *Journal of Materials Processing Technology*, **168**(1): 25–35.

Aouici, H., Chaoui, M.A.Y.K., Mabrouki, T. and Rigal, J.F. 2012. Analysis of surface roughness and cutting force components in hard turning with CBN tool: Prediction model and cutting conditions optimization. *Measurement*, **45**(3): 344–353.

Arezoo, B., Ridgway, K. and Al-Ahmari, A.M.A. 2000. Selection of cutting tools and conditions of machining operations using an expert system. *Computer Industry*, **42**(1): 43–58.

Arriola, I., Whitenton, E., Heigel, J. and Arrazola, P.J. 2011.Relationship between machinability index and in-process parameters during orthogonal cutting of steels. *CIRP Annals - Manufacturing Technology*, **60**(1): 93–96.

Arsecularatne , J.A., Zhang, L.C. and Montross, C. 2006. Wear and tool life of tungsten carbide, PCBN and PCD cutting tools. *International Journal of Machine Tools and Manufacture*, **46(**5): 482–491.

Arsecularatne, J.A. 2004. Prediction of tool life for restricted contact and grooved tools based on equivalent feed. *International Journal of Machine Tools and Manufacture*, **44**: 1271–1282.

Arunachalam, R.M., Mannan, M.A. and Spowage, A.C. 2004. Residual stress and surface roughness when facing age hardened Inconel 718 with CBN and ceramic cutting tools. *International Journal of Machine Tools and Manufacture*, **44:** 879–887.

Aslan, N. and Cebeci, Y. 2007. Application of Box–Behnken design and response surface methodology for modeling of some Turkish coals. *Fuel*, **86**(1–2): 90–97.

Aspinwall, D.K., Dewes, R.C., Ng, E.G., Sage, C. and Soo, S.L. 2007. The influence of cutter orientation and workpiece angle on machinability when high-speed milling Inconel 718 under finishing conditions. *International Journal of Machine Tools and Manufacture*, **47:** 1839–1846.

Astakhov , V. P. 1999. Metal cutting mechanics. USA: CRC press.

Astakhov,V.P. 2006. Tribology of metal cutting. London: Elsevier Science.

Axinte, D.A. and Dewes, R.C. 2002. Surface integrity of hot work tool steel after high speed milling—experimental data and empirical models. *Journal of Materials Processing Technology*, **127**: 325–33.

Axinte, D.A., Andrews, P., Li, W., Gindy, N. and Withers, P.J. 2006.Turning of advanced Ni based alloys obtained via powder metallurgy route. *Annals of the CIRP*, **55**(1): 117-120.

Aykut, Ş., Aykut, E.B., K.O. and Yazıcıoğlu, K.O. 2007a. Experimental observation of tool wear, cutting forces and chip morphology in face milling of cobalt based super-alloy with physical vapour deposition coated and uncoated tool. *Materials & Design*, **28**(6): 1880–1888.

Aykut, Ş., Gölcü, M., Semiz, S., Ergür, H.S. 2007b. Modeling of cutting forces as function of cutting parameters for face milling of satellite 6 using an artificial neural network. *Journal of Materials Processing Technology*, **190**(1–3): 199-203.

Baek, D.K., Ko, T.J. and Kim, H.S. 2001. Optimization of feedrate in a face milling operation using a surface roughness model. *International Journal of Machine Tools and Manufacture*, **41**: 451–462.

Baker, R.D. 2000. A new world of high and performance. *Carbide Tool Journal*, **12**: 10–18.

Bao, W.Y. and Tansel, I.N. 2000. Modeling micro-end-milling operations. Part I: Analytical cutting force model. *International Journal of Machine Tools and Manufacture,* **40**: 2155–2173.

Basheer, I.A. and Hajmeer, M. 2000. Artificial neural networks: fundamentals, computing, design, and application. *Journal of Microbiological Methods,* **43(**1): 3–31.

Benardos, P.G. and Vosniakos, G.C. 2003. Predicting surface roughness in machining: a review. *International Journal of Machine Tools and Manufacture,* **43**(8):833–84.

Bermingham, M.J., Kirsch, J., Sun, S., Palanisamy, S. and Dargusch, M.S. 2011. New observations on tool life, cutting forces and chip morphology in cryogenic machining Ti-6Al-4V. *International Journal of Machine Tools and Manufacture,* **51(**6): 500–511.

Bhatt, A., Attia, R.H. and Vargas, V. 2010. Thomson Wear mechanisms of WC coated and uncoated tools in finish turning of Inconel 718. *Tribology International*, **43**: 1113–1121.

Bhushan, B. 1999. *Handbook of Micro-Nano Tribology*. USA: CRC Press.

Bouacha, K., Yallese, M.A. and Mabrouki, T. 2010. Statistical analysis of surface roughness and cutting forces using response surface methodology in hard turning of AISI 52100 bearing steel with CBN tool. *International Journal Refractory Metals Hard Material,* **28**: 349–361.

Bouzid, W. 2005. Cutting parameter optimization to minimize production time in high speed turning. *Journal of Materials Processing Technology,* **161**: 388–395.

Box, G.E.P. and Draper, N.R. 1987. Empirical model-building and response surface. New York: John Wiley and Sons, Inc.

Box, G.E.P. and Wilson, K.B. 1951. On the experimental attainment of optimum conditions. *Journal of Royal Statistical Society*, **13**: 1–12.

Che Haron C.H. 2001. Tool life and surface integrity in turning titanium alloy. *Journal of Materials Processing Technology,* **118:** 231–237.

Che Haron, C.H., Ghani, J.A., Ibrahim, G.A., Husin, K. and Yong. T.S. 2007. Performance of coated and uncoated carbide tools in turning AISI D2. Faculty of Engineering, Deparment of Mechanical Engineering, National University of Malaysia.

Che-Haron, C.H., and Jawaid, A. 2005. The Effect of Machining on Surface Integrity of Titanium Alloy Ti–6% Al–4% V. *Journal of Materials Processing Technology,* **166** (2): 188–192.

Che-Haron, C.H., Ginting, A. and Arshad, H. 2007. Performance of alloyed uncoated and CVD-coated carbide tools in dry milling of titanium alloy Ti-6242S. *Journal of Materials Processing Technology*, **185**: 77–82.

Chen , S.L. and Jen, Y.W. 2000. Data fusion neural network for tool condition monitoring in CNC milling machining. *International Journal of Machine Tools and Manufacture*, **40**(3): 381–400.

Chen, J.C. and Savage, M. 2001. Fuzzy-net-based multilevel in-process surface roughness recognition system in milling operations. *International Journal of Advanced Manufacturing Technology*, **17**: 670–676.

Chen, W. 2002. Cutting forces and surface finish when machining medium hardness steel using CBN tools. *International Journal of Machine tools and Manufacture*, **40**: 455-466.

Chopra, S., Motwani, S.K., Iqbal, Z., Talegaonkar, S., Ahmad, F.J. and Khar, R.K. 2007. Optimisation of polyherbal gels for vaginal drug delivery by Box-Behnken statistical design. *European Journal of Pharmaceutics and Biopharmaceutics*, **67(**1): 120–13.

Choudhury, I.A. and El-Baradie, M.A. 1998. Machinability of nickel base superalloys: a general review. *Journal of Materials Processing Technology*, **77 (**1–3): 278–284.

Choudhurya, I.A. and El-Baradie, M.A. 1999. Machinability assessment of Inconel 718 by factorial design of experiment coupled with response surface methodology. *Journal of Materials Processing Technology*, **95**: 30–39.

Clenaghan, M.K., Kelly, K. and Byrne, G. 1999. Tool condition monitoring—a new algorithm for breakage detection. In: Proceedings of 2nd. International Workshop on Intelligent Manufacturing Systems, Leuven, Belgium, pp. 825–833.

Coromant, S. 1994. Modern metal cutting: a practical handbook. Sweden: Tofters Tryckeri.

Correa, M., Bielza, C. and Pamies-Teixeira, J. 2009. Comparison of Bayesian networks and artificial neural networks for quality detection in a machining process. *Expert Systems with Applications*, **36(**3): 7270–7279.

Costes, J.P., Guillet, Y., Poulachon, G. and Dessoly, M. 2007. Tool-life and wear mechanism of CBN tools in machining of Inconel 718. *International Journal of Machine Tools and Manufacture*, **47**: 1081–1087.

Crowther, W.J. and Cooper, J.E. 2001. Flight test flutter prediction using neural network. *Journal of Aerospace Engineering*, **215**(1): 37-47.

Cui, C., Gu, Y., Harada H. and Sato, A. 2005. Microstructure and yield strength of UDIMET 720LI alloyed with Co-16.9 Wt Pct Ti. *Metallurgical and Materials Transactions A*, **36A**: 2921–2927.

Cus, F. and Zuperl, U. 2006. Approach to optimization of cutting conditions by using artificial neural networks. *Journal of Material Processing Technology*, **173**: 281–290.

Dabnun, M.A., Hashmi, M.S.J. and El-Baradie, M.A. 2005. Surface roughness prediction model by design of experiments for turning machinable glass–ceramic (Macor). *Journal of Materials Processing Technology*, **164–165**: 1289–1293.

Dang, J.W., Zhang, W.H., Yang, Y. and Wan, M. 2010. Cutting force modeling for flat end milling including bottom edge cutting effect. *International Journal of Machine Tools and Manufacture*, **50**: 986–997.

Darwish, S.M. 2000. The impact of tool material and the cutting parameters on surface roughness of supermet 718 nickel superalloy. *Journal of Materials Processing Technology*, **97**: 10–18.

Davidson, M.J., Balasubramanian, K. and Tagore, G.R.N. 2008. Surface roughness prediction of flow-formed AA6061 alloy by design of experiments. *Journal of Materials Processing Technology*, **1-3**: 41-46.

Davies, M.A., Burns, T.J. and Evans, C.J. 1997. On the dynamics of chip formation in machining hard metals. *Annals of the CIRP*, **45**: 25-30.

Davim, J.P. and Figueira, L. 2007. Machinability evaluation in hard turning of cold work tool steel (D2) with ceramic tools using statistical techniques. *Materials Design*, **28**: 1186–1191.

Davim, J.P., Gaitonde, V.N. and Karmik, S.R. 2008. Investigations into the effect of cutting conditions on surface roughness in turning of free machining steel by ANN models. *Journal of Material Processing Technology*, **205**: 16–23.

Dearnley, P.A. and Grearson, A.N. 1986. Evolution of principal wear mechanisms of cemented carbides and ceramics used for machining titanium alloys, IMI 318. M*aterial Science and Technology*, **2**: 47–58.

Demuth, H. And Beale, M. 1998. *Neural Network Toolbox for Use with MATLAB.* USA: The MathWorth, Inc.

Devillez, A., Schneider, F., Dominiak, S., Dudzinski, D. and Larrouquere, D. 2007. Cutting forces and wear in dry machining of Inconel 718 with coated carbide tools. *Wear*, **262**: 931–942.

Dicholkar, D.D., Gaikar, V.G. and Natarajan, S.K.R. 2012. Modeling and optimizing of steam pyrolysis of dimethyl formamide by using response surface methodology

coupled with Box-Behnken design. *Journal of Analytical and Applied Pyrolysis,* **96**: 6-15.

Dimla,D.E. and Lister, P.M. 2000. On-line metal cutting tool condition monitoring. II: tool state classification using multi-layer perception neural network. *International Journal of Machine Tools and Manufacture,* **40**: 769–781.

Diniz, A.E. and Filho, J.C. 1999. Influence of the relative positions of tool and workpiece on tool life, tool wear and surface in the face milling process. *Wear,* **232**: 67–75.

Diniz, A.E. and Micaroni, R. 2002. Cutting condition for finish turning process aiming the use of dry cutting. *International Journal of Machine Tools and Manufacture,* **42**: 899–904.

Doniavi, A., Eskanderzade, M. and Tahmsebian, M. 2007. Empirical modeling of surface roughness in turning process of 1060 steel using factorial design methodology. *Journal of Applied Sciences,* **7**(17): 2509-2513.

Dotcheva, M. and Millward, H. 2005. The application of tolerance analysis to the theoretical and experimental evaluation of a CNC corner-milling operation. *Journal of Materials Processing Technology,* **170**(1–2): 284–297.

Dudzinski, D., Devillez, A., Moufki, A., Larrouquere, D., Zerrouki, V. and Vigneau, J. 2004. A review of developments towards dry and high speed machining of Inconel 718 alloy. *International Journal of Machine Tools and Manufacture,* **44**: 439–456.

Ekinovic, S., Dolinsek, S., Brdarevic,S. and Kopac, J. 2002. Chip formation process and some particularities of high-speed milling of steel materials. *In Trends in the Development of Machinery and Associated Technology, TMT 2002, B&H, Neum.*

Ertakin, Y.M., Kwon, Y. and Tseng, T.L. 2003. Identification of common sensory features for the control of CNC milling operations under varying cutting conditions. *International Journal of Machine Tools and Manufacture,* **43**(9): 897–904.

Erzurumlu, T. and Oktem, H. 2007. Comparison of response surface model with neural network in determining the surface quality of moulded parts. *Materials & Design*, **28**: 459–465.

Eynard, J., Grieu, S. and Polit, M. 2011. Wavelet-based multi-resolution analysis and artificial neural networks for forecasting temperature and thermal power consumption. *Engineering Applications of Artificial Intelligence,* **24**(3): 501–516.

Ezugwu, E.O., Bonney J. and Yamane, Y. 2003. An overview of the machinability of aeroengine alloys. *Journal of Materials Processing Technology***, 134**: 233–253.

Ezugwu, E.A., Machado, A.R., Pashby, I.R. and Wallbank, J. 1991. The effect of high-pressure coolant supply when machining a heat-resistant nickel-based superalloy. *Journal Social Tribologists Lubrication Engineering*, **47** (9): 751–757.

Ezugwu, E.O. 2005. Key improvements in the machining of difficult-to-cut aerospace superalloys. *International Journal of Machine Tools and Manufacture*, **45:**1353–1367.

Ezugwu, E.O. Machado, A.R., Pashby, I.R. and Wallbank, J. 1990. The effect of high-pressure coolant supply. *Lubricant Engineering*, **47**: 751–757.

Ezugwu, E.O. and Pashby, I.R. 1992. High speed milling of nickel-based superalloys. *Journal Material Processing Technology*, **3**: 429–437.

Ezugwu, E.O. and Tang, S.H. 1992. Surface abuse when machining cast iron and nickel base superalloy (Inconel 718) with ceramic tools. *Proceeding 9th Irish Manufacturing Conference, Dublin*, pp. 436–450.

Ezugwu, E.O. and Wang, Z.M. 1996. Performance of PVD and CVD coated tools when machining nickel-based, Inconel 718 alloy. *Progress of Cutting and Grinding*, **111**: 102–107.

Ezugwu, E.O., Bonney, J. and Olajire, K.A. 2004. The effect of coolant concentration on the machinability of nickel-base, nimonic C-263, alloy. *Tribology Letters*, **16(**4): 311–316.

Ezugwu, E.O., Bonney, J., Fadare, D.A. and Sales, W.F. 2005. Machining of nickel-base, Inconel 718, alloy with ceramic tools under machining conditions with various coolant supply pressures. *Journal Material Processing Technology*. **162–163**: 609–614.

Ezugwu, E.O., Olajire, K.A. and Wang,Z.M. 2000. Wear analysis of coated carbide tools when machining nickel base, Inconel 718 alloy. *Proceedings of the Fourteenth International Conference on Surface Modification Technologies, Paris, France*, pp. 279–286.

Ezugwu, E.O., Wang, Z.M. and Okeke, C.I. 1999. Tool life and surface integrity when machining Inconel 718 with PVD and CVD coated tools. *Tribology Transactions*, **42**(2): 353–360.

Ezugwu, E.O., Wang, Z.M. and Machado, A.R. 1998. The machinability of nickel-based alloys: a review. *Journal Material Processing Technology*, **86**: 1–16.

Fang, N. and Wu, Q. 2009. A comparative study of the cutting forces in high speed machining of Ti–6Al–4V and Inconel 718 with a round cutting edge tool. *Journal of Materials Processing Technology*, **209**: 4385–4389.

Farhat, Z.N. 2003. Wear mechanism of CBN cutting tool during high-speed machining of mould steel. *Material Science Engineering*, **A361**:100–110.

Feng, C.X. and Wang, X.F. 2003. Surface roughness predictive modelling: Neural networks versus regression. *IIE Transactions*, **35**: 11–27.

Ferreira, S.L.C., Bruns, R.E., Ferreira, H.S., Matos, G.D., David, J.M., Brandão, G.C., da Silva, E.G.P., Portugal, L.A.,dos Reis, P.S., Souza, A.S. and Dos Santos, W.N.L. 2007. Box-Behnken design: An alternative for the optimization of analytical methods**.** *Analytica Chimica Acta*, **597**(2): 179–186**.**

Field, M. and Kahles, J.F. 1971. Review of surface integrity of machined components. *Annals of the CIRP*, **20**(2): 153–163.

Field, M. and Kahles, J.F. 1964. The Surface Integrity of Machined and Ground High Strength Steels. *DMIC Report*, **210**: 54–77.

Fontaine, M., Devillez, A.,Moufki, A. and Dudzinski, D. 2007. Modelling of cutting forces in ball-end milling with tool–surface inclination: Part II. Influence of cutting conditions, run-out, ploughing and inclination angle. *Journal of Materials Processing Technology*, **189** (1–3): 85–96.

Gayton, N., Bourinet, J.M. and Lemaire, M. 2003. CQ2RS: a new statistical approach to the response surface method for reliability analysis. *Structure Safety*, **25**: 99–121.

.

Gelman, A. 2005. Analysis of variance: why it is more important than ever (with discussion). *Annals of Statistics*, **33**: 1–53.

Ghanem, F., Braham, C., Fitzpatrick, M.E. and Sidhom, H. 2002. Effect of near-surface residual stress and microstructure modification from machining on the fatigue endurance of a tool steel. *Journal of Materials Engineering and Performance*, **11**(6): 631–639.

Ginting A. and Nouari, M. 2009. Surface integrity of dry machined titanium alloys. *International Journal of Machine Tools and Manufacture*, **49**: 325–332.

Grabec, I. and Kuljanic, E. 1994. Characterization of manufacturing processes based upon acoustic emission analysis by neural networks. *Annals of the CIRP*, **3**: 77–80.

Gu, J., Barber, G., Tung, S. and Gu, R.J. 1999. Tool life and wear mechanism of uncoated and coated milling inserts. *Wear*. **225–229**: 273–284.

Guerville, L., Vigneau, J., Dudzinski, D., Molinari, A. and Schulz, H. 2002. Influence of machining conditions on residual stresses, metal cutting and high speed machining. *Kluwer Academic Plenum Publishers*, pp. 201–210.

Guo, Y.B. and Yen David, W.A. 2004. FEM study on mechanisms of discontinuous chip formation in hard machining. *Journal Material Processing Technology*, **155–156:** 1350–1356.

Gupta, A. 2005. Thermal modeling and analysis of carbide tool using finite element method. Master thesis. Deemed University, India.

Haber, R. E. and Alique, A. 2003. Intelligent process supervision for predicting tool wear in machining processes. *Mechatronics*, **13**(8–9): 825–849.

Hamann, J.C., Guillot, Dand Le, F. 1996. Maitre machinability improvement of steels at high cutting speeds-study of tool/work material. *Interaction Annals of the CIRP*, **45**(1): 87–92.

Hao, W., Zhu, X., Li, X. and Turyagyenda, G. 2006. Prediction of cutting force for self-propelled rotary tool using artificial neural networks. *Journal of Materials Processing Technology*, **180**(1–3): 23–29.

Ho, S.Y., Lee, K.C., Chen, S.S. and Ho, S.J. 2002. Accurate modeling and prediction of surface roughness by computer vision in turning operations using an adaptive neuro-fuzzy inference system. *International Journal of machine Tools and Manufacture*, **42**: 1441–1446.

Hua, J. and Shivpuri, R. 2004. Prediction of chip morphology and segmentation during the machining of titanium alloys. *Journal of Materials Processing Technology*, **150**: 124–133.

Ibaraki, S. and Shimizu, T. 2010. A long-term control scheme of cutting forces to regulate tool life in end milling processes. *Precision Engineering*, **34**: 675–682.

Ibraheem, A.F., Shather, S.K. and Khalaf, K.A. 2008. Prediction of cutting forces by using machine parameters in end milling process. *Engineering and Technology*, **26**:11.

Imani, B.M., Pour, M., Ghoddosian, M.A. and Fallah, M. 2012. Improved dynamic simulation of end-milling process using time series analysis. *Scientia Iranica*, **19**: 294-302

Isik, Y. 2007. Investigating the machinability of tool steels in turning operation. *Materials & Design*, **28**(5): 1417-1424.

Itakura, K., Kuroda, M., Omokawa, H., Itani, H., Yamamoto, K., and Ariura, Y. 1999. Wear mechanism of coated cemented carbide tool in cutting of Inconel 718 super-heat-resisting alloy. *International of Japan Society for precision Engineering*, **33**: 326–332.

Jang, D.Y., Choi, Y.G., Kim, H.G., and Hsiao, A. 1996. Study of the correlation between surface roughness and cutting vibrations to develop an on-line

roughness measuring technique in hard turning. *International Journal of Machine Tools and Manufacture*, **36**: 453–464.

Jawahir, I.S., Balaji, A.K., Rouch, K.E. and Baker, J.R. 2003.Towards integration of hybrid models for optimized machining performance in intelligent manufacturing systems. *Journal of Materials Processing Technology*, **139**(1–3): 488–498.

Jawaid, A., Koksal, S. and Sharif, S. 2001. Cutting performance and wear characteristics of PVD coated and uncoated carbide tools in face milling Inconel 718 aerospace alloy. *Journal Material Processing Technology*, **116**: 2–9.

Jeang, A. 2011. Robust cutting parameters optimization for production time via computer experiment. *Applied Mathematical Modelling*, **35(**3): 1354–1362.

Jianxin, D., Tongkun, C. and Lili, L. 2005. Self-lubricating behaviors of AlO/TiB ceramic tools in dry high-speed machining of hardened steel. *Journal of the European Ceramic Society*, **25**: 073–1079.

Jindal, P.C., Santhanam, A.T., Schleinkofer, U. and Shuster, A.F. 1999. Performance of PVD TiN, TiCN and TiAlN coated cemented carbide tools in turning. *International Journal Refractory Metals Hard Material*, **17**: 163–170.

Joshi, S.V., Vizhian, S.P., Sridhar, B.R. and Jayaram, K. 2008. Parametric study of machining effect on residual stress and surface roughness of nickel base super alloy UDIMET 720. *Advanced Materials Research*, **47-50**: 13-16.

Jung, Y.H., Kim, J.S. and Hwang, S.M. 2001. Chip load prediction in ball-end milling. *Journal Material Processing Technology*, **111**: 250–255.

Kadirgama, K. and Abou-El-Hossein, K.A. 2005. Force prediction model formilling 618 tool steel using response surface methodology. *American Journal of Applied Sciences*, **8**: 1222-1227.

Kadirgama, K., Abou-El-Hossein, K.A., Noor. M.M., Sharma. K.V. and Mohamad, B. 2011. Tool life and wear when machining Hastelloy C-22HS. *Wear*, **270**(4): 258-268.

Kalpakjian, S. and Schmid, S.R. 2007. Manufacturing Processes for Engineering Materials, (5th edition). New York: *Prentice-Hall.*

Kang, I.S., Kim, J.S., Kim, J.H., Kang, M.C. and Seo, Y.W. 2007. A mechanistic model of cutting force in the micro end milling process. *Journal of Materials Processing Technology*, **187-188**: 250–255.

Karayel, D. 2009. Prediction and control of surface roughness in CNC lathe using artificial neural network. *Journal Materials Processing Technology*. **7**: 3125-3137.

Kartalopoulos, S.V. 1996. Basic concepts and applications. *IEEE Press*.

Kaya, B., Oysu , C. and Ertunc, H.M. 2011. Force-torque based on-line tool wear estimation system for CNC milling of Inconel 718 using neural networks. *Advances in Engineering Software Advances in Engineering Software*, **42**: 76–84.

Khajeh, M. 2011. Response surface modelling of lead pre-concentration from food samples by miniaturised homogenous liquid–liquid solvent extraction: Box–Behnken design. *Food Chemistry*, **129**(4): 1832–1838.

Khidhir, B.A. and Mohamed, B. 2010. Machining of nickel based alloys using different cemented carbide tools. *Journal of Engineering Science and Technology*, **5**(3): 264 – 271.

Kim, G.M., Cho, P.J. and Chu, C.N. 2000. Cutting force prediction of sculptured surface ball-end milling using *Z*-map. *International Journal of Machine Tools and Manufacture*, **40**: 277–291.

Kincl, M., Turk, S. and Vrecer, F. 2005. Application of experimental design methodology in development and optimization of drug release method. *International Journal Pharm*, **291**: 39–49.

Kirby E.D., Zhang, Z. and Chen, J.C. 2004. Development of An Accelerometer based surface roughness Prediction System in Turning Operation Using Multiple Regression Techniques. *Journal of Industrial Technology*, **20**(4): 1-8.

Kishawy, H.A. and Elbestawi, M.A. 1999. Effects of process parameters on material side flow during hard turning. *International Journal of Machine Tools and Manufacture*, **39**: 1017–1030.

Kita, Y., Furuike, H., Kakino, Y., Nakagawa, H. and Hirogaki, T. 2001. Basic study of ball end milling on hardened steel. *Journal Material Processing Technology*, **111**: 240–243.

Kline, W.A., DeVor, R.E. and Lindberg, J.R. 1982.The Prediction of Cutting Forces in End Milling with Application to Cornering Cut. *International Journal Machine Tool Design and Research*, **22**: 7-22.

Ko, J.H. and Cho, D.W. 2004. Feed rate scheduling model considering transverse rupture strength of a tool for 3D ball-end milling. *International Journal of Machine Tools and Manufacture*, **44**: 1047–1059.

Korkut, I. and Donertas, M.A. 2007. The influence of feed rate and cutting speed on the cutting forces, surface roughness and tool–chip contact length during face milling**.** *Materials & Design*, **28**(1) : 308–312**.**

Krain, H.R., Sharman, A.R.C. and Ridgway, K. 2007. Optimisation of tool life and productivity when end milling Inconel 718. *Journal of Materials Processing Technology*, **189**(1–3): 153–161.

Kramer, B.M. and Hartung, P.D. 1980. Theoretical considerations in the machining of nickel-based alloys. *Proceeding International Conference of Cutting Tool Material*, Fort Mitchell, KY, pp. 57–74.

Kumar, M. and Yadav, N. 2011. Multilayer perceptrons and radial basis function neural network methods for the solution of differential equations: A survey. *Computers & Mathematics with Applications*, **62**: 3796–3811.

Kurt, A. 2009. Modelling of the cutting tool stresses in machining of Inconel 718 using artificial neural networks. *Expert Systems with Applications*, **36**: 9645–9657.

Kwak, J.S. 2005.Application of Taguchi and response surface methodologies for geometric error in surface grinding process. *International Journal of Machine Tools and Manufacture*, **45**: 327–334.

Lajis, M.A., Mustafizul Karim, A.N., Nurul amin, A.K.M., Hafiz, A.M.K. and Turnad, I.G. 2008. Prediction of tool life in end milling of hardened steel AISID2. *European Journal of Scientific Research*, **4**: 592 – 602.

Lamikiz, A., de Lacalle, L.N.L., Sanchez, J.A. and Salgado, M.A. 2004. Cutting force estimation in sculptured surface milling. *International Journal of Machine Tools and Manufacture*. **44**: 1511–1526.

Lee, S.C. and Ren, N. 1996. Behavior of elastic- plastic rough surface contact as affected by surface topography, loads, and material hardness. *Tribology Translations*, **39**(1): 67-74.

Lekkala, R., Bajpai, V., Ramesh, K., Suhas, S. and Joshi, S. 2011. Characterization and modeling of burr formation in micro-end milling. *Precision Engineering*, **35**(4): 625–637.

Li, S., Xie, Y. and Wu, X. 2010. Hardness and toughness investigations of deep cryogenic treated cold work die steel. *Cryogenics*, **50**: 89–92.

Li, H.Z.H., Zeng, X. and Chen, O. 2006. An Experimental study of tool wear and cutting force variation in the end-milling of Inconel 718 with coated carbide inserts. *Journal of Materials Processing Technology*, **180**(1-3): 294-304.

Li, H.Z. and Li, X.P. 2002. Milling force prediction using a dynamic shear length model. *International Journal Machine Tools and Manufacture*, **42**: 277–286.

Li, X.P., Iynkaran, K. and Nee, A.Y.C. 1999. A hybrid machining simulator based on predictive theory and neural network modeling. *Journal of Materials Processing Technology*, **89–90**: 224–230.

Liao, Y.S. and Shiue, R.H. 1996. Carbide tool wear mechanism in turning of Inconel 718 superalloy. *Wear*, **193**: 16–24.

Liao, Y.S., Lin, H.M. and Wang, J.H. 2008. Behaviors of end milling Inconel 718 superalloy by cemented carbide tools. *Journal of Materials Processing Technology*, **201**(1-3): 460-465.

Liew, W.Y.H. and Ding, X. 2008. Wear progression of carbide tool in low-speed end milling of stainless steel**.** *Wear*, **265**(1–2): 155–166.

Lin, H.M., Liao, Y.S. and Wei, C.C. 2008. Wear behavior in turning high hardness alloy steel by CBN tool. *Wear*, **264**(7–8): 679–684.

Lin, J.T., Bhattacharyya, D. and Kecman, V. 2003. Multiple regression and neural networks analyses in composites machining. *Composites Science and Technology*, **63**(3–4): 539–548.

Liu, G., He, N., Man, Z.L. and Li, L. 2004. Cutting Forces in the Milling of Inconel 718. *Key Engineering Materials*, **259–260**: 824–828.

Liu, Q. and Altintas, Y. 1999. On-line monitoring of flank wear in turning with multilayered feed-forward neural network. *International Journal Machine Tools Manufacture*, **39**: 1945–1959.

Liu, W., Jian, W.L., Chen , Z. and Li. W.S.F. 2010. Effect of Cutting Parameters on the Cutting Force in the End Milling of GH4169 Superalloy. *International Conference on E-Product E-Service and E-Entertainment (ICEEE) 2010*, pp. 1-4.

Li Ying, X., Hui, W. and Zhe-Zhao, Z. 2007. The algorithm of neural networks on the initial value problems in ordinary differential equations. *2nd IEEE Conference on Industrial Electronics and Applications*, pp. 813–816.

Lorentzon, J., Jarvstrat N. and Josefson, B.L. 2009. Modeling chip formation of alloy 718. *Journal of Materials Processing Technology*, **209**: 4645–4653.

Lou, J., Chen, J.C. and Li, C.M. 1999. Surface roughness prediction technique for CNC end-milling. *Journal of Industrial Technology*, **15**(1): 1–6.

Luo, F. and Unberhauen, R. 1998. Applied neural networks for signal processing. The University of Cambridge, New York, USA.

MacGinley, T. and Monaghan, J. 2001. Modelling the orthogonal machining process using coated cemented carbide tools. *Journal Material Processing Technology*, **118**: 293–300.

Machado, A.R., Wallbank, J., Pashby L.R. and Ezugwu, E.O. 1998. Tool performance and chip control when machining Ti6Al4V and Inconel 901 using high pressure coolant supply. *Machine Science Technology*, **2 (**1): 1–12.

Mansour, A. and Abdalla, H. 2002. Surface roughness model for end milling: a semi-free cutting carbon casehardening steel (EN32) in dry condition. *Journal of Materials Processing Technology*, **124**: 183–191.

Mantle, A.L. and Aspinwall, D.K. 2001. Surface Integrity of a High Speed Milled Gamma Titanium Aluminide. *Journal of Materials Processing Technology*, **118**: 143–150.

Maren, A.J., Harston, C.T. and Pap, R.M. 1990. *Hankbook Of Neural Computing Application.* USA: Academic Press Inc.

Marini, F., Magr, A.L. and Bucci, R. 2007. Multilayer feed-forward artificial neural networks for class modeling. *Chemometrics and Intelligent Laboratory System*, **88**(1): 118–124.

Mason, D.M., Huang, Y. and Luo, J. 2007. Chip morphology characterization and modeling in machining hardened 52100 steels. *Machining Science and Technology*, **11**: 335–354.

Mecomber, J.S., Hurd, D. and Limbach, P.A. 2005. Enhanced machining of micron-scale features in microchip molding masters by CNC milling. *International Journal of Machine Tools and Manufacture*, **45**(12–13): 1542–1550.

Milfelner, M., and Cus, F. 2003. Simulation of cutting forces in ball-end milling. *Robotics and Computer Integrated Manufacturing*, **19**(1–2): 99–106.

Miller, S. 1996. Advanced materials means advanced engines. *Interdisciplinary Science Reviews*, **21(**2):117–129.

Mohd Zain, A., Haron, H. and Sharif, S. 2010. Prediction of surface roughness in the end milling machining using Artificial Neural Network. *Expert Systems with Applications*, **37**(2): 1755–1768.

Montgomery, D.C. 1997. Design and analysis of experiments, fifth edition. *Publish by John Wiley and Sons.*

Montgomery, D.C. 2005. *Design and analysis of experiments: response surface method and designs.* New Jersey: John Wiley and Sons, Inc.

M'Saoubi, R., M'Saoubi, J.C., Outeiro, B., Changeux, L.J.L., and Morão Dias, A. 1999. Residual stress analysis in orthogonal machining of standard and resulfurized AISI 316L steels. *Journal of Materials Processing Technology*, **96**: 225–233.

M'Saoubi, R., Outeiro, J.C., Chandrasekaran, H., Dillon O.W. and Jawahir, I.S.A. 2008. Review of surface integrity in machining and its impact on functional performance and life of machined products. *International Journal of Sustainable Manufacturing*, **1(**1–2): 203–236.

Myers, R.H. 1971. Response surface methodology. New York: Allyn and Bacon.

Nachtman, E.S. 1995. Metal cutting and grinding fluids, metals handbook. Vol. 16, Machining. New York: ASM International.

Nakayama, K. and Arai, M. 1992. Comprehensive chip form classification based on the cutting mechanism. *Annals of CIRP*, **71**: 71-74.

Nalbant, M., Altm, A. and Gokkaya, H., 2007. The effect of cutting speed and cutting tool geometry on machinability properties of nickel-base Inconel 718 super alloys. *Material & Design*, **28**: 1334–1338.

Nalbant, M., Gokkaya, H., Toktas, I. and Sur, G. 2009. The experimental investigation of the effects of uncoated, PVD- and CVD-coated cemented carbide inserts and cutting parameters on surface roughness in CNC turning and its prediction using artificial neural networks. *Robotics and Computer-Integrated Manufacturing*, **25**: 211–223.

Negnevitsky, M. 2004. *Artificial intelligent: A guide to intelligent systems*. 2nd edition New York: Addison Wesley Publishing.

Niemi, R.M. 1971. Integrity prediction, SME Technical Paper, Dearbon, Michigan.

Noordin, M.Y., Venkatesh, V.C., Sharif, S., Elting, S. and Abdullah, A. 2004. Application of response surface methodology in describing the performance of coated carbide tools when turning AISI 1045 steel. *Journal Material Processing Technology*, **145**: 46–58.

Novovic, D., Dewes, R.C., Aspinwall, D.K., Voice, W. and Bowen, P. 2004. The effect of machined topography and integrity on fatigue life. *International Journal of Machine Tools and Manufacture*, **44**: 125–134.

Nurul Amin, A.K.M., Ismail, A.F. and Nor Khairusshima, M.K. 2007. Effectiveness of uncoated WC-Co and PCD inserts in end milling of titanium alloy—Ti–6Al–4V. *Journal of Materials Processing Technology*, **192–193**: 47–158.

Öktem, H., Erzurumlu, T. and Kurtaran, H. 2005. Application of response surface methodology in the optimization of cutting conditions for surface roughness. *Journal of Materials Processing Technology*, **170**(1–2): 11–16.

Oktem, H., Erzurumlu, T. and Erzincanl, F. 2006. Prediction of minimum surface roughness in end milling mold parts using neural network and genetic algorithm. *Materials & Design*, **27**: 735–744.

Olovsjö, S. and Nyborg, L. 2012. Influence of microstructure on wear behaviour of uncoated WC tools in turning of Alloy 718 and Waspaloy. *Wear*, **282–283**: 12–21.

Omirou, S.L. and Barouni, A.K. 2005. Integration of new programming capabilities into a CNC milling system. *Robotics and Computer-Integrated Manufacturing,* **21**(6): 518–527.

Onwubolu, G.C. 2006. Performance-based optimization of multi-pass face milling operations using tribes. *International Journal of Machine Tools & Manufacture,* **46**: 717–727.

Ostwald, K. 1995. Technology of machine tools. Fourth edition. New York: McGraw Hill.

Ostwald, P.F. and Munoz, J. 2002. Manufacturing process and systems. Ninth Edition. New York: John Wiley & Sons.

Outeiro, J.C., Pina, J.C., M'Saoubi, R., Pusavec ,F. and Jawahir, I.S. 2008. Analysis of residual stresses induced by dry turning of difficult-to-machine materials. *CIRP Annals—Manufacturing Technology*, **57**: 77–80.

Ozcelik, B. and Bayramoglu, M. 2006. The statistical modeling of surface roughness in high-speed flat end milling. *International Journal of Machine Tools and Manufacture* **46**(12–1): 1395–1402.

Ozel, T. and Karpat, Y., 2005. Predictive modeling of surface roughness and tool wear in turning using regression and neural networks. *International Journal Machine Tool Manufacture,* **45**: 467–479.

Pal, S.K. and Chakraborty, D. 2005. Surface roughness prediction in turning using artificial neural network. *Neural Computing and Application,* **14**: 319–324.

Palanisamy, S., McDonald, S.D. and Dargusch, M.S. 2009. Effects of coolant pressure on chip formation while turning Ti6Al4V alloy. *International Journal Machine Tool Manufacture,* **49**: 739–743.

Pawade, R.S., Joshi, S.S., Brahmankar, P.K. and Rahman, M. 2007.An investigation of cutting forces and surface damage in high-speed turning of Inconel 718. *Journal of Materials Processing Technology*, **192–193**: 139-146.

Peigne, G., Paris, H., Brissaud, D. and Gouskov, A. 2004. Impact of the cutting dynamics of small radial immersion milling operations on machined surface roughness. *International Journal of Machine Tools & Manufacture,* **44**: 1133–1142.

Prengel, H.G., Jindal, P.C., Wendt, K.H., Santhanam, A.T., Hegde, P.L. and Penich, R.M. 2001. A new class of high performance PVD coatings for carbide cutting tools. *Surface Coating Technology,* **139**: 25–34.

Prengel, H.G., Pfouts, W.R. and Santhanam, A.T. 1998. State of the art in hard coatings for carbide cutting tools. *Surface and Coatings Technology,* **102**: 183–190.

Qi, H.S. and Mills, B. 2000. Formation of a transfer layer at the tool–chip interface during machining, *Wear*, **245**: 136–147.

Radhakrishnan, V.R. and Mohamed, A.R. 2000. Neural networks for identification and control of blast furnace hot metal quality. *Journal of Process Control*, **10**: 509-524.

Rahman, M., Wong, Y.S. and Zareena, A.R. 2003. Machinability of titanium alloys. *JSME Series C*, **46**(1): 107–115.

Ranganath, S., Guo, C. and Holt, S. 2009. Experimental investigations into the carbide cracking phenomenon on Inconel 718 superalloy material. *ASME 2009 International Manufacturing Science and Engineering Conference*, pp. 33-39.

Rao, R.V. and Pawar, P.J. 2010. Parameter optimization of a multi-pass milling process using non-traditional optimization algorithms. *Applied Soft Computing*, **10**(2): 445–456.

Recht, R.F. 1964. Catastrophic thermoplastic shear. *Journal of Applied Mechanics—Transactions of the ASME*, **86**: 189–193.

Reddy,N. S.K. and Rao, P.V. 2006. Experimental investigation to study the effect of solid lubricants on cutting forces and surface quality in end milling, *International Journal of Machine Tools & Manufacture*, **46**: 189 – 198.

Sahin, Y. and Motorcu, A.R. 2008. Surface roughness model in machining hardened steel with cubic boron nitride cutting tools. *International Journal Metals Hard Material*, **26**: 84–90.

Seong, S.T., Jo, K.T. and Lee, Y.M. 2009. Cutting force signal pattern recognition using hybrid neural network in end milling. *Transactions of Nonferrous Metals Society of China*, **19(**1): 209–214.

Sharif, S., Mohruni, A.S., Noordin, M.Y. and Vencatesh, V.C. 2006. Optimization of surfaceroughness prediction model in end milling titanium alloy (Ti-6Al-4V). *Proceeding of ICOMAST*, pp. 55-59.

Sharman, A., Dewes, R.C. and Aspinwall, D.K. 2001.Tool life when high speed ball nose end milling Inconel 718. *Journal of materials Processing Technology*, **118**: 29-35.

Sharman, A., Hughes, J. and Ridgway, K. 2004. Workpiece surface integrity and tool life issues when turning Inconel 718. *Machining Science and Technology*, **8**(3): 399-414.

Shaw, D. and Ou, G.Y. 2008. Computer-aided design reducing *X*,*Y* and *Z* axes movement of a 5-axis AC type milling machine by changing the location of the work-piece. *Computer Aided Design*, **40**(10–11): 1033–1039.

Shetty, R., Pai, R., Kamath, V. and Rao, S.S. 2008. Study on surface roughness minimization in turning of dracs using surface roughness methodology and taguchi under pressured steam jet approach. *ARPN Journal of Engineering and Applied Sciences,* **3**(1): 59-67.

Shokrani, A., Dhokia, V. and Newman, S.T. 2012. Environmentally conscious machining of difficult-to-machine materials with regard to cutting fluids. *International Journal of Machine Tools and Manufacture,* **57**: 83-101.

Shunmugam, S.V., Bhaskara, R.T. and Narendran, T. 2000. Selection of Optimum Conditions in Multi-Pass Face Milling Using a Genetic Algorithm. *International Journal Machine Tool Manufacture,* **40**: 4014–4414 .

Skapura, D. 1996. Building neural networks. New York: ACM Press. Addison-Wesley.

Soo, S.L., Hood, R., Aspinwall, D.K. and Sage, W.E.V.C. 2011. Machinability and surface integrity of RR1000 nickel based superalloy. *CIRP Annals - Manufacturing Technology*, **60**(1): 89–92.

Sridhar, B.R., Devananda, G., Ramachandra, K. and Bhat, R. 2003. Effect of machining parameters and heat treatment on the residual stress distribution in titanium alloy IMI-834. *Journal of Materials Processing Technology*, **139**: 628–634.

Stephenson, D.A. and Agapiou, J.S. 1997. Metal cutting theory and practice. USA: Marcel Dekker, Inc.

Subhas, B.K., Bhat, R., Ramachandra K. and Balakrishna, H.K. 2000. Simultaneous optimization of machining parameters for dimensional instability control in aero gas turbine components made of Inconel 718 alloy, Transactions of ASME. *Journal of Manufacturing Science and Engineering*, **122**: 586–590.

Suresh, P.V.S., Rao, P.V. and Deshmukh, S.G. 2002. A genetic algorithmicapproach for optimization of surface roughness prediction model. *International Journal of Machine Tools and Manufacture*, **42**: 675–680.

Svozil, D., Kvasnicka, V. and Pospichal, J. 1997. Introduction to multilayer feed forward neural net. *Chemometrics and Intelligent Laboratory Systems,* **39**: 43–62.

Szeszulski, K.J., Thangaraj, A.R. and Weinmann, K.J. 1990. On the cutting performance of whisker-reinforced ceramics machining Inconel. *Winter Annual Meeting of ASME, Fundamental Issues in Machining ASME, Dallas, TX, USA,* pp. 97–113.

Takashi, I. 2000. Identification for axial force and boundary condition of an orthotropic rectangular plate using artificial neural networks. *Computer Engineering Using Methapors from nature,* pp. 7-13.

Tang, W.X., Song, Q.H,. Yu, S.Q., Sun, S.S., Li, B.B., Du, B. and Ai, X. 2009. Prediction of chatter stability in high-speed finishing end milling considering multi-mode dynamics. *Journal of Materials Processing Technology,* **209**(5): 2585–2591.

Thakur, D.G., Ramamoorthy, B. and Vijayaraghavan, L. 2009. Study on the machinability characteristics of superalloy Inconel 718 during high speed turning. *Materials & Design,* **30**: 1718–1725.

Thamizhmanii, S., Saparudin, S. and Hasan, S. 2007. Tool wear and surface roughness inn turning AISI 8620 using coated ceramic tool. *Proceedings of The World Congress on Engineering,* pp. 1-10.

Tong, L.I., Chang, Y.C. and Lin, S.H. 2011. Determining the optimal re-sampling strategy for a classification model with imbalanced data using design of experiments and response surface methodologies. *Expert Systems with Applications,* **38**(4): 4222–4227.

Tosun, N. and Ozler, L. 2002. A study of tool life in hot machining using artificial neural networks and regression analysis method. *Journal Material Processing Technology,* **124**: 99–104.

Trent, E.M. 1991. Metal cutting. London: Butterworths

Trent, E.M. and Wright, P.K. 2000. Metal cutting. 4th ed. London: Butterworth-Heinemann.

Tsai, K. and Wang, P. 2001. Predictions on surface finish in electrical discharge machining based upon neural network models. *International Journal of Machine Tools and Manufacture,* **41**: 1385–1403.

Tsao, C.C. and Hocheng, H. 2008. Evaluation of thrust force and surface roughness in drilling composite material using Taguchi analysis and neural network. *Journal Material Processing Technology,* **203**: 342-348.

Ulutan, D. and Ozel, T. 2011. Machining induced surface integrity in titanium and nickel alloys: A review. *International Journal of Machine Tools and Manufacture,* **51**(3): 250–280.

Uraikul, V., Chan, C.W. and Tontiwachwuthikul, P. 2007. Artificial intelligence for monitoring and supervisory control of process systems. *Engineering Applications of Artificial Intelligence,* **20**(2): 115–131.

Venugopal, K.A., Paul, S. and Chattopadhyay, A.B. 2007. Growth of tool wear in turning of Ti-6Al-4V alloy under cryogenic cooling. *Wear,* **262**: 1071–1078.

Vivancos, J., Luis, C.J. Ortiz J.A. and Gonzalez, H.A. 2005.Analysis of factors affecting the high speed side milling of hardened die steels. *Journal Material Processing Technology,* **162–163:** 696–701.

Vyas, A. and Shaw, M.C. 1999. Mechanics of saw-tooth chip formation in metal cutting. *ASME Journal Manufacturing Science Engineering*, **121**:163-172.

Wang, M.Y. and Chang, H.Y. 2004. Experimental study of surface roughness in slot end milling AL2014-T6. *International Journal of Machine Tools and Manufacture*, **44**(1): 51–57.

Wang, Z.G., Wong Y.S. and Rahman, M. 2005. High-speed milling of titanium alloys using binderless CBN tools. *International Journal Machine Tools Manufacture*, **45**: 105–114.

Wanigarathne, P.C., Kardekar, A.D., Dillon, O.W., Poulachon, G. and Jawahir, I.S. 2005. Progressive tool-wear in machining with coated grooved tools and its correlation with cutting temperature. *Wear*, **259(**7–12): 1215–1224.

Warburton, P. 1967. Problems of Machining Nickel-Based Alloys, Iron and Steel Institute. *Special Report*, **94**(1): 51–160.

Warren, A., Nylund, A. and Olefjord, I. 1996. Oxidation of tungsten and tungsten carbide in dry and humid atmospheres International. *Journal of Refractory Metals and Hard Materials*, **14** (5–6): 345–353.

Weinert, K. and Petzoldt, V. 2008. Machining NiTi micro-parts by micro-milling. *Materials Science and Engineering A*, **481–482**: 672–675.

Wright, P.K. and Chow, J.G. 1982. Deformation characteristics of nickel alloys during machining. *Journal of Engineering Materials and Technology, Transactions of the ASME*, **104**: 85–93.

Wu, L., Yick, K.L. Ng, S.P. and Yip, J. 2012. Application of the Box–Behnken design to the optimization of process parameters in foam cup molding. *Expert Systems with Applications*, **39**(9): 8059–8065.

Wu, Q. 2007. Serrated chip formation and tool-edge wear in high-speed machining of advanced aerospace materials. Utah State University, Logan, Utah.

Xue, C. and Chen, W. 2011. Adhering layer formation and its effect on the wear of coated carbide tools during turning of a nickel-based alloy. *Wear*, **270**(11–12): 895–902.

Yahya, I. 2007. Investigating the machinability of tool steels in turning operations. *Material & Design*, **28**: 1417–24.

Yamada, Y., Aoki, T., Tanaka, Y., Kitaura S. and Hayasaki, H. 1996. (Al, Ti) N coated carbide endmills for difficult-to-cut materials. *Proceedings of the Third International Conference on Progress Cutting and Grinding*, 211.

Yang, M.Y. and Lee, T.M. 2002. Hybrid adaptive control based on the characteristics of CNC end milling. *International Journal of Machine Tools and Manufacture,* **42**(4): 489–499.

Yih-fong, T. and Ming-der, J. 2005. Dimensional quality optimisation of high-speed CNC milling process with dynamic quality characteristic**.** *Robotics and Computer-Integrated Manufacturing,* **21(**6**)**: 506–517.

Yilmaz, O., Eyercioglu, O. and Gindy, N.N.Z. 2006. A user friendly fuzzy based system for the selection of electro discharge machining process parameters, *Journal Material Processing Technology*, **172**: 363–371.

Yuan, N., Rahman, M. and Wong, Y.S. 2001. Investigation of chip formation inhigh speed end milling. *Journal of Material Processing Technology*, **13**: 360 – 367.

Yue, H., Valle, S. and Qin, S.J. 1998. Comparison of several methods of multivariate soft sensor for emission monitoring. *Journal of Environmental Engineering,* **3(**6): 23-28.

Zhang, J.Z., Chen, J.C. and Daniel Kirby. E. 2007. Surface roughness optimization in an end-milling operation using the Taguchi design method. *Journal of Materials Processing Technology*, **184**(1–3): 233–239.

Zhang, M.Z., Liu, Y.B. and Zhou, H. 2001. Wear mechanism maps of uncoated HSS tools drilling die-cast aluminum alloy. *Tribology International*, **34**: 727–731.

Zhao, J., Yuan, X. and Zhou, Y. 2010. Cutting performance and failure mechanisms of an Al_2O_3/WC/TiC micro- nano-composite ceramic tool International. *Journal of Refractory Metals and Hard Materials*, **28**(3): 330–337.

Zhao, W., Wu, Z. and Wang, D. 2006. Ozone direct oxidation kinetics of Cationic Red X-GRL in aqueous solution. *Journal Hazard Material*, **137**: 1859–1865.

Zhu, R., Kapoor, S.G. and DeVor, R.E. 2001. Mechanistic modeling of the ball-end milling process for multi-axis machining of free form surfaces. *Journal Manufacturing Science Engineering*, **123**: 369–379.

Zou, B., Chen, M., Huang, C. and An, Q. 2009. Study on surface damages caused by turning $NiCr_{20}TiAl$ nickel-based alloy. *Journal of Materials Processing Technology*, **209**: 5802–5809.

LIST OF PUBLICATIONS

1. N. H. Razak, M. M. Rahman, and K. Kadirgama, Surface Roughness in End-Milling Operation When Machining of Hastelloy C-2000 using Uncoated Carbide. Journal Advanced Science Letters, 13, 300-305 (2012) (SCI,Q2, IF=1.253).

2. N. H. Razak, M. M. Rahman, M.M.Noor and K. Kadirgama, " A review of Minimum Quantity Lubricant on Machining Performance", 1st National Conference In Mechanical Engineering for Research & Postgraduate studies, (NCMER),26-27 May, 2010, Malaysia.

3. N. H. Razak, M. M. Rahman, and K. Kadirgama, "Artificial Neural Network for Machining Performance: A Review", 2nd National Conference In Mechanical Engineering for Research & Postgraduate studies(NCMER). UMP Pekan, Malaysia, 3-4 Dec, 2010.

4. N. H. Razak, M. M. Rahman, and K. Kadirgama, Tool Wear in End Milling Operation When Machining of Hastelloy C-2000 Using Uncoated Carbide Inserts. International Journal of Mechanical and Materials Engineering (Scopus Indexed), (in press)

5. N. H. Razak, M. M. Rahman, and K. Kadirgama, "Response Surface Design Model To Predict The Surface Roughness When Machining Hastelloy C-2000 using Uncoated Carbide. Journal of Materials Science and Engineering (in press).

6. N.H. Razak, M.M. Rahman and K. Kadirgama. 2012. Tool wear in end milling operation when machining Hastelloy C-2000. Wear (Under Review) (SCI, Q1, IF= 1.635).

7. N.H. Razak, M.M. Rahman and K. Kadirgama. 2012. Tool life prediction in end milling operation when machining of Hastelloy c-2000 by using artificial neural network. Journal of Intelligent Manufacturing. (Under Review) (SCI, Q2, IF= 1.081).

8. N.H. Razak, M.M. Rahman and K. Kadirgama. 2012. Prediction of Surface Roughness in Machining Hastelloy C-2000 using Response Surface Method and Artificial Neural Network. Journal of Intelligent Manufacturing. (Under Review) (SCI, Q2, IF= 1.081).

9. N.H. Razak, M.M. Rahman and K. Kadirgama. 2012. Cutting force and chip formation in end milling operation when machining of Hastelloy C-2000.

Journal of materials Processing Technology. (Under Review) (SCI, Q1, IF= 1.57).

10. N.H. Razak, M.M. Rahman and K. Kadirgama. 2012. Tool wear and chip formation in end milling operation when machining of Hastelloy C-2000 . Wear (Under Review) (SCI, Q1, IF= 1.635)